LOW TEMPERATURE PROPERTIES OF TRANSURANIC METALS

A study of the specific heat of plutonium, neptunium and plutonium monocarbide.

P.W. Sutcliffe, B.A.,
The Queen's College.

BODLEIAN LIBRARY OXFORD
DEPOSITED
THESIS
14. vii. 69.

A thesis submitted for the degree of Doctor of Philosophy in the University of Oxford.

August, 1968.

C O N T E N T S

		Page
Acknowledgements		
ABSTRACT	.....	1
INTRODUCTION		
CHAPTER 1.	A REVIEW OF THE THEORY OF SPECIFIC HEAT OF METALS	1.1
1.1	Lattice Specific Heat	1.2
1.2	Specific Heat of Conduction Electrons ..	1.11
1.3	Magnetic Contribution to the Specific Heat	1.17
	References	1.22
CHAPTER 2.	THE APPARATUS AND EXPERIMENTAL PROCEDURE	2.1
2.1	Relative merits of glove box and sealed capsule methods	2.1
2.2	Method of Specific Heat Determination ..	2.3
2.3	Choice of Thermometric Substance	2.6
2.4	Cryostat Design	2.10
2.5	Calorimeter and Specimen Design	2.21
2.6	Experimental Procedure	2.24
2.7	Temperature Measuring System	2.26
	The Back-off System	2.27

		Page
	Amplification of Difference Signal	2.31
	Measurement of Difference Signal	2.31
	Wiring Precautions	2.34
2.8	Adiabatic Control System	2.35
2.9	Additional Heat System	2.39
2.10	Thermocouple Calibration	2.43
2.11	Specimen Preparation, Canning and Decontamination Techniques	2.50
	References	2.56
CHAPTER 3.	ADDITIONAL DATA REQUIRED FOR CALCULATION AND ANALYSIS OF SPECIFIC HEAT	3.1
3.1	Self-Heat of Transuranic Specimens	3.1
	Plutonium 238	3.7
	Plutonium 239	3.8
	Plutonium 240	3.11
	Plutonium 241	3.12
	Plutonium 242	3.14
	Americium 241	3.15
	Neptunium 237	3.19
3.2	Thermal Capacity of the Calorimeters ...	3.21
3.3	Additional Data for Specific Heat Analysis	3.26
3.3. 1	Expansion Coefficient	3.29

		Page
3.3. 2	Elastic Constants	3.35
3.3. 3	Dilation Term	3.40
3.4	Estimation of Errors in Relation to Method of Evaluation	3.41
	References	3.46
CHAPTER 4.	EXPERIMENTAL RESULTS	4.1
4.1	Plutonium	4.2
4.1. 1	Pu3	4.2
4.1. 2	Pu4	4.6
4.1. 3	Pu6	4.15
4.2	Neptunium	4.25
4.3	Plutonium Monocarbide	4.31
	References	4.37
CHAPTER 5.	DISCUSSION OF RESULTS	5.1
5.1	Thorium	5.2
5.2	Uranium	5.5
5.3	Neptunium	5.10
5.4	Plutonium	5.15
5.5	Plutonium Monocarbide	5.34
	References	5.41

APPENDICES

Appendix I. Molar Thermodynamic Functions of α-Pu

Appendix II. Molar Thermodynamic Functions of α-Np

Appendix III. Thermodynamic Functions of $PuC_{0.87}$

Appendix IV. Thermodynamic Functions of $PuC_{0.96}$

ACKNOWLEDGEMENTS

I would like to express my gratitude to :-

Professor B. Bleaney for granting me the facilities of the Clarendon Laboratory.

Dr. K. Mendelssohn, my supervisor, for his constant interest, encouragement and advice.

Dr. M.B. Waldron and Dr. L.E. Russell for permitting my research to be carried out in the Plutonium physical properties group at A.E.R.E., Harwell.

Dr. J.A. Lee for his unstinted assistance and guidance in a thousand and one different ways, and for reading this thesis.

Mr. A. Hough for his assistance in thermal expansion measurements and in the preparation of specimens.

Mr. R.O.A. Hall and Mr. M.J. Mortimer for their help in the day to day running of the equipment and in the tedium of evaluation of early results and Mr. J.A.C. Marples for an introduction to computer programming.

Numerous people of the Instrument and Engineering

Service's sections at Harwell for construction of various parts of my apparatus.

Several people for allowing me to make use of unpublished work and many others for helpful discussions.

The authorities at A.E.R.E., Harwell for the award of a maintenance grant during the period of this research.

Mrs. E. Browne for typing this thesis.

Finally, to my wife without whose moral support during the period of this research, and assistance in final preparation, this thesis would not have been possible.

A B S T R A C T

The specific heat of the transuranic metals, plutonium and neptunium, has been measured below room temperature. Both these metals are strong α-emitters and are extremely toxic. As a consequence they have to be handled under special conditions, and the usual methods are either by containment in glove boxes or by encapsulation. The latter method has been adopted here and developed such that the calorimeter formed the encapsulation, and the canned specimens could then be handled in an inactive cryostat.

A further consequence of the high α-activity of these metals is their property of 'self-heating', which makes the determination of their specific heat by the conventional continuous-heating method impossible. The magnitude of the self-heat, particularly of plutonium, meant that a continuous heating method had to be evolved which could deal with the inevitable high rates of rise of temperature. A cryostat and measuring system were constructed and developed such that the specific heat could still be determined with reasonable accuracy. A control system was also developed in order that an adiabatic technique could be employed.

The self-heat is temperature independent and was

utilised as a constant power supply to the calorimeter. A review of the literature values of the half-lives and decay energies of the various radioactive isotopes present in any sample of a transuranic metal, is given since the calculation of the self heat is critically dependent of these quantities.

The specific heat (C_p) of α-plutonium was not found to exhibit the large and irreproducible peaks which characterised the early work of Sandenaw. C_p followed a smooth 'sigmoid' curve, except for a small 'excess' between 40 - 70°K, though the magnitude of the excess (~ 2.5 - 3%) was not sufficient to produce a maximum on C_p. C_p values were generally high, rising to a value of 7.86 cals./mole/deg. at 300°K, and analysis of the data gave an electronic coefficient (γ) of 38 x 10^{-4} cals./mole/deg.^{2} and Debye theta (θ_D) values between 150 and 170°K in the temperature range ~ 14 - 300°K. Further analysis and separation of the excess, yielded a contribution to the specific heat which had the typical λ -shape of a magnetic transition, though the energy and entropy involved were extremely small.

One of the main theories proposed to explain the unusual low temperature properties of plutonium is that there is a paramagnetic-antiferromagnetic transition at ~ 60°K, and the present specific heat work would indicate that this is not an unreasonable hypothesis. Lack of affirmative evidence

from neutron diffraction experiments however has necessitated a review and discussion of the alternative theories proposed, and also a comparison with the known antiferromagnetic α-manganese, to which many parallels exist.

Short term self-irradiation experiments were carried out on α-plutonium. The magnitude of the energy stored by the defects produced by storage at low temperatures, and the temperature range in which this annealed out, were found to give satisfactory agreement with the theoretical estimates and the self-irradiation damage effects previously observed on the electrical resistivity.

The specific heat of α-neptunium was found to be a smooth curve throughout the range of measurement of $\sim$ 7.5 - 300°K, and the values of $\gamma = 34 \times 10^{-4}$ cals./mole/deg.^{2} and $\theta_o = 187.5$°K resulted from analysis of the low temperature region. No evidence of any magnetic phenomena, which must always be in mind in view of the close similarities between the actinide and lanthanide series of metals, was seen on α-neptunium in keeping with the bulk of the other known properties. Neptunium however is still only available in very limited quantities and in a state of purity that is by no means high ($\sim$ 99%).

In view of the large electronic coefficients observed

in plutonium and neptunium, a discussion is given on the band structures of the actinides in relation to their electronic properties.

The analyses of the specific heat dats are dependent in the first place on a reduction of C_p to C_v. Lack of sufficient data on the expansion coefficients (a_L) of plutonium and neptunium, led to the measurement of a_L for these two metals in the temperature range 20 - 300°K. A simple push-rod dilatometer technique was used, and expansion coefficients of ~ 45 x 10^{-6}/deg. for α-Pu and ~ 20 x 10^{-6}/deg. for α-Np were found. The Grüneisen gamma values were ~ 2.6 for α-Pu and ~ 1.8 for α-Np respectively.

The development of reactor fuel materials has caused a great deal of interest to be centred on the carbides of uranium and plutonium. Since no previous specific heat determination had been carried out below room temperature on PuC, this was investigated down to ~ 12.5°K. Other low temperature properties of this metallic carbide had again suggested antiferromagnetic behaviour below 100°K. No evidence in support of this was found on the specific heat results though an extremely high density of states at the Fermi surface is suggested.

The standard thermodynamic functions of plutonium, neptunium and plutonium monocarbide have been calculated and are tabulated in the appendices.

INTRODUCTION

Following the formulation of the Periodic System of the elements in order of ascending atomic weight, and the discovery of the naturally occurring radioactive elements in the latter half of the nineteenth century, many scientists had speculated upon the existence of further members of the series beyond the heaviest then known, uranium. The discovery of such 'trans-uranium' elements had however to wait until 1940-1 when Seaborg and his co-workers, as part of the wartime Manhattan Project, by means of neutron bombardment of uranium, first produced and identified the new element of atomic number 93, neptunium and that of the succeeding element number 94, plutonium.

However it was not the production of these new transuranic elements, but the discovery of the new phenomenon 'nuclear fission', with its subsequent exploitation as a source of energy for both constructive and destructive purposes that provided the impetus for the rapid development in this completely new field. Within ten years the following elements of still higher atomic number, curium (96), americium (95), berkelium (97) and californium (98), were discovered in that order, and there was no doubt that a new series of elements

with distinctive properties had been produced.

Several factors however hampered the studies of these transuranic elements. Firstly, because of the neutron irradiation methods by which they were produced, the initial work on all of them had to be carried out on a very small scale, the order of microgm. or less. Even now it has been possible to isolate such elements as neptunium and americium only on a gm. scale. Plutonium however because of its civil and military uses has been produced in multi-kilogram quantities. Secondly the radioactivities associated with all these transuranic elements leads to hazards and difficulties.

The α-activity of such isotopes as Np^{237}, Pu^{239} and Am^{241}, produce α-particles of a range in air of a few centimeters, or $\sim$ 50 μcrons in skin tissue, and provided they remain outside the human body their effect is minimal. Internally however they produce severe biological damage in the region surrounding the α-emitting nucleus. This toxic effect in the case of Pu^{239} for instance is such that the maximum total body-burden permitted is set at the low level of 0.6 μgm., and to prevent such levels accumulating in those working regularly with plutonium, the maximum level of airborne contamination is set at 10^{-11} μgm/c.c..

Such levels can be quickly exceeded if plutonium is

exposed to the atmosphere, particularly in the presence of moisture. The nonadherent oxide consists of very fine particles which can rapidly disperse and contaminate the surrounding atmosphere. Although for small quantities, $\sim$ mgm. of plutonium, a fumehood may provide sufficient protection, in all other cases the policy of complete containment has been generally adopted. Thus most of the work on plutonium has been carried out in hermetically sealed enclosures with perspex fronts to provide visibility, and with long rubber gloves sealed into special glove ports to provide access. Such enclosures known as glove boxes usually have an inert atmosphere of argon or nitrogen, since plutonium in finally divided form is pyrophoric.

The requirement of such handling facilities had thus restricted the study of the transuranic elements to a dozen or so laboratories in the world. One of these is A.E.R.E., Harwell, and for several years the facilities there, in what was the Plutonium Metallurgy Division have been made available to a few members of the Clarendon Laboratory, in order that a joint programme of research on the low temperature properties of the transuranic elements could be carried out. The first results of this collaboration were the investigation of the low temperature resistivity and thermo-electric power of

thorium, uranium, neptunium and plutonium by Meaden (thesis, 1961), and were followed by a study of the effects of self-irradiation damage on the electrical resistivity of U, Np and Pu by Wigley (thesis, 1963).

Prior to the work of Meaden, very few properties had been studied below room temperature, and for this reason, together with the handling difficulties described which complicate the experimental problem, the transport properties investigated were of the more straightforward ones from the experimental point of view. Nevertheless a great deal of information was obtained on the electronic properties of the transuranics available, in particular plutonium. One of the suggestions put forward was the possibility of a magnetic transition in α-Pu in the region of $60^{\circ}K$.

It was in order to throw further light on the existence of such a transition, and to provide further information on the electronic, lattice and thermodynamic properties, that the work presented here on the low temperature specific heat was commenced. The investigation was concentrated on α-Pu, but results on α-Np, the only other transuranic element available in sufficient quantities for a specific heat determination, are also presented. Because of the possible use of the metallic compound plutonium carbide as a nuclear

fuel, a knowledge of its physical and thermodynamic properties were of vital interest to the Ceramics Division at A.E.R.E. Harwell, which during the course of this research had taken over the Plutonium Physical Properties Group. The specific heat of plutonium carbide is also presented.

A cryostat suitable for the determination of the specific heat of these radioactive materials was therefore designed and this is described in Chapter 2 together with full experimental details. This is followed in Chapter 3 by a discussion of the additional data required for the determination and analysis of the specific heat results. A full presentation of the results is given in Chapter 4, together with some discussion and analysis. Further analysis and a more detailed discussion is contained in Chapter 5. First however in Chapter 1, a review of the theories of lattice and electronic specific heats is given together with an appraisal of some of their limitations.

C H A P T E R 1

A REVIEW OF THE THEORY OF SPECIFIC HEAT OF METALS

A comprehensive study of the theory of the low temperature specific heats of metals must inevitably cover a very wide field, since any temperature dependent phenomenon can contribute to the specific heat. The total specific heat of a metal is governed by the way in which the total internal energy is distributed among its constituents. Two such constituents in a metal are the lattice and conduction electrons, whose contributions are present at all temperatures, and an understanding of these two is vital to the interpretation of the specific heat of any metal. Some of the more important steps towards our modern theoretical understanding of these two are discussed in the first two sections of this chapter.

Further contributions which are significant over only a restricted temperature range, such as those due to magnetic and superconducting transitions, spin excitations, order-disorder transformations, molecular rotations and so on, could not possibly be covered in this chapter even in review. Only the particular case of that contribution due to an antiferromagnetic transition will be mentioned in Section 1.3, because

of its possible relevance to the case of α-plutonium.

1.1 Lattice Specific Heat

The limitations of the earliest theoretical application of classical statistical mechanics by Boltzman in 1871, leading to a temperature independent value of 3R cals./mole/deg. for the lattice specific heat, are well known.

The first major step in understanding the marked drop in specific heat at low temperature was made by Einstein in 1907. He suggested on the basis of the [then] new quantum theory of Planck that the thermal oscillations of the atoms of frequency ν_E could only have discrete energy levels given by

$$\epsilon = (n + \tfrac{1}{2})\, h\nu_E$$

where n is zero or any integer. Further there is a statistical probability of any atom existing in an excited state propertional to $e^{(-\epsilon/kT)}$. The resulting mean energy for each atom is

$$\bar{U} = \tfrac{1}{2} h\nu_E + \frac{h\nu_E}{e^{(\frac{h\nu_E}{kT})} - 1} \qquad 1.1$$

and molar specific heat at constant volume

$$C_V = 3R \frac{x^2 e^x}{(e^x - 1)^2} \qquad 1.2$$

where $$x = \frac{h\nu_E}{kT} = \frac{\theta_E}{T} .$$

At high temperatures ($T \gg \theta_E$), the above Einstein function leads to the classical value of 3R, and at low temperatures $T \ll \theta_E$, the exponential decrease of

$$C_V = 3R \left(\frac{\theta_E}{T} \right)^2 \cdot e^{(-\theta_E/T)} .$$

Although the Einstein theory provided qualitative agreement for the temperature dependence of the specific heat, it was found to be inadequate quantitatively at the lower temperatures ($\sim \theta_E/5$). The assumption that all the atoms vibrated at the same frequency and were independent of each other was an oversimplification in a tightly coupled system such as the atoms of a lattice.

Following Einstein's original paper the idea that there was a spectrum of lattice vibrational frequencies, $g(\nu)$, began to take shape, $g(\nu)$ being defined such that the number of modes of oscillation between frequencies ν and $\nu + d\nu$

is given by $g(\nu)d\nu$. In terms of $g(\nu)$, the specific heat becomes :-

$$C_V = 3R \int_0^{\nu_m} \left(\frac{h\nu}{kT}\right)^2 \frac{e^{\left(\frac{h\nu}{kT}\right)}}{\left(e^{\left(\frac{h\nu}{kT}\right)} - 1\right)^2} \, d\nu \qquad 1.3$$

where the maximum frequency ν_m is defined such that the total number of modes must be 3N per mole where N is the number of atoms per mole, i.e.,

$$\int_0^{\nu_m} g(\nu)d\nu = 3N . \qquad 1.4$$

Further theoretical advances were dependent upon the particular choice of $g(\nu)$, and were made by Debye, and Born and Von Karman at about the same time, 1912.

Debye showed that $g(\nu)$ was proportional to ν^2 in the region of low frequencies, where the theory of solids could be replaced by that of an isotropic elastic continuum. An approximation for the total spectrum was then made by continuing the ν^2 function up to a maximum frequency (ν_D) and cutting off the spectrum sharply at this point.

Thus

$$g(\nu) = a\nu^2 = \frac{4\pi V}{3} \cdot \left(\frac{1}{c_L^3} + \frac{2}{c_T^3} \right) \cdot \nu^2$$

where c_L and c_T are the acoustic velocities.

Equation 1.4 then gives :-

$$\nu_D = \left(\frac{9N}{4\pi V}\right)^{1/3} \left(\frac{1}{c_L^3} + \frac{2}{c_T^3} \right)^{-1/3} \qquad 1.5$$

Defining a characteristic temperature, θ_D, known as the Debye temperature, by the relation $\frac{h\nu_D}{k} = \theta_D$, leads to a specific heat relation from equation 1.3 of the form :-

$$C_V = 3R \left[12 \left(\frac{T}{\theta_D}\right)^3 \int_0^{\theta_D/T} \frac{x^3}{e^x - 1}\, dx - \frac{\theta_D/T}{e^{\theta_D/T} - 1} \right] \qquad 1.6$$

The Debye function has the properties that C_V is determined by one parameter, θ_D/T ; that C_V approaches the classical 3R value at high temperatures, $T \gg \theta_D$, and that at low temperatures, $T \ll \theta_D/12$, C_V is given by :

$$C_V = \left(\frac{12R\pi^4}{5} \right) \left(\frac{T}{\theta_D} \right)^3 \qquad 1.7$$

The Debye model was extremely successful in correlating the specific heats of a large number of solids. The fact that C_V depended on the single parameter, meant that by suitable normalisation of the temperature scale (T/θ_D), the specific heats were found to fall on the same curve. Schrödinger and later Eucken in a review of the specific heat data available prior to 1928, found remarkably good agreement with Debye's theory over a wide temperature range.

A fundamental feature of Debye's theory is the connection between elastic and thermal properties of a solid. From equation 1.5, the characteristic temperature θ should be calculable from the longitudinal and transverse acoustic velocities. Even in the case of an anisotropic medium, θ could still be determined from a mean velocity dependent upon the various elastic constants. Comparison of the θ values so obtained with the calorimetric θ_D's revealed a surprisingly good agreement at moderate temperatures (see e.g., Blackman (1941)). The first signs of the limitations of Debye's theory however came from early observations of Eucken, Grüneisen and others, that as low temperature elastic constants became available, the agreement became worse.

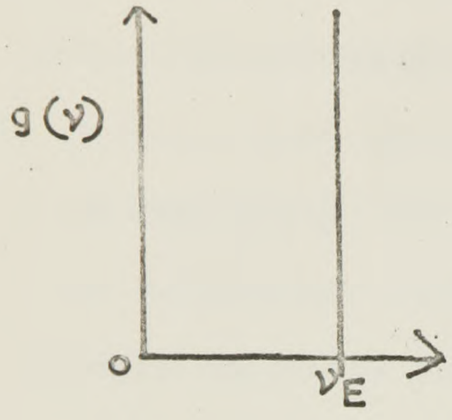
In addition as accurate specific heat values at low temperatures became available with improved calorimetric techniques, it was found that equation 1.6 for C_V did not

fit the experimental values exactly. By calculating the effective values of θ_D necessary to fit the experimental data at each temperature, instead of the constant θ_D that exact agreement with Debye's model would produce, the effective θ_D values were found to be temperature dependent. Typically θ_D began to decrease around $\theta_D/2$ from a constant value at higher temperatures, reach a minimum $\sim \theta_D/10$ and then increase to attain a constant value again around $\theta_D/50$. Agreement with the low temperature elastic constants θ was only achieved in the $\theta/50$ region and not in the 'pseudo-T^3' region of $\theta_D/10$ as predicted by Debye from equation 1.7.

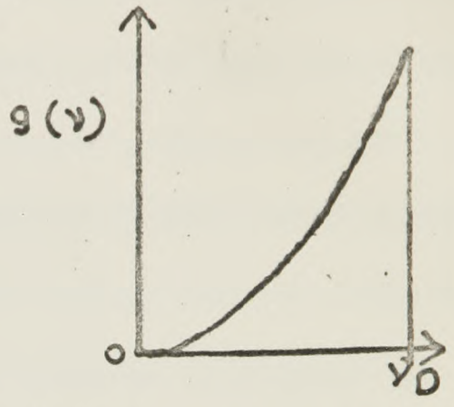
It was soon realised that such θ_D variation was due to a fundamental deficiency in the extremely simple Debye model in that inadequate treatment of the effects arising from the discrete nature of the crystal lattice.

The periodicity of the lattice, leading to phonon dispersion, had been taken into account by Born and Von Karman in their treatment of a simple cubic lattice, but cumbersome mathematics and certain approximations led to an inferior fit to the experimental specific heat value than the extremely simple Debye function.

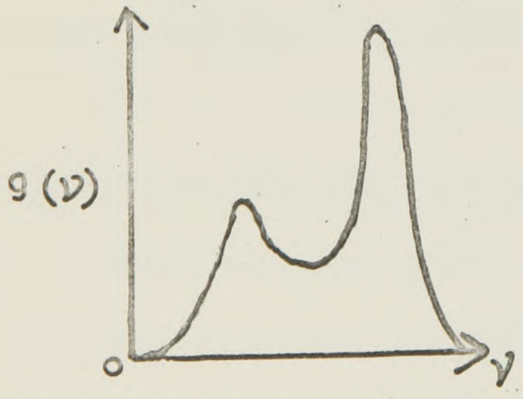
The development of lattice dynamics by Born in 1923, led to a more complicated dispersion relation than the simple elastic continuum case of $\omega = 2h\gamma = cq$ where q is the wave



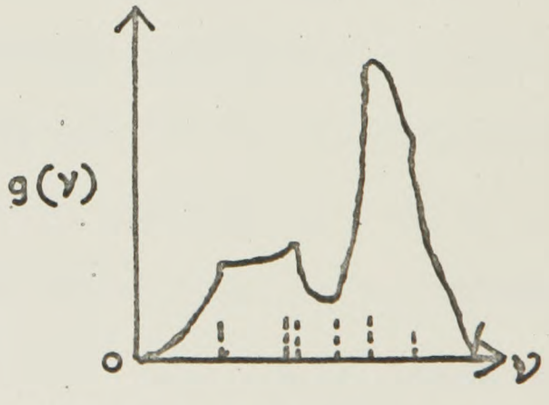
(a) EINSTEIN MODEL



(b) DEBYE MODEL



(c) BLACKMAN'S APPROX. OF CUBIC LATTICE.



(d) SPECTRUM WITH SINGULARITIES.

FIG 1.1 FREQUENCY SPECTRA OF LATTICE VIBRATIONS.

vector. In a diatomic linear chain or monatomic lattice, the acoustical branch of the ω-q relation now deviates from a straight line and further optical branches appear to higher frequencies. Extension to a cubic lattice was performed in a series of papers by Blackman from 1935 - 1937.

In any direction a cubic lattice $g(\nu)$ is proportional to $q^2\, dq/d\omega$. It starts as ν^2 due to a linear portion of the acoustical branch of the ω-q relation at low q values; as the frequency reaches the limit of the acoustic mode $dq/d\omega$ increases and hence $g(\nu)$ becomes large; with further increase in ν, there is a gap in $g(\nu)$ followed by another peak due to the lower limiting value of the optical branch where $dq/d\omega$ is again large; this is then followed by the contribution of the remainder of the optical branch. When summed over all directions of the lattice, the characteristic presence of two peaks in the frequency spectrum results, with the gap between being smeared out into a shallow minimum. This $g(\nu)$ spectrum is shown in Fig. 1.1(c) together with those of the Einstein (a) and Debye (b) models for comparison.

Such a frequency distribution has the following consequences At low frequencies the ν^2 Debye spectrum is confirmed, resulting in $C_V \propto T^3$, though now at a much lower temperature ($\sim \theta_D/50$), than Debye's original $\theta_D/10$; as the temperature is raised more modes are excited than the Debye model, due to

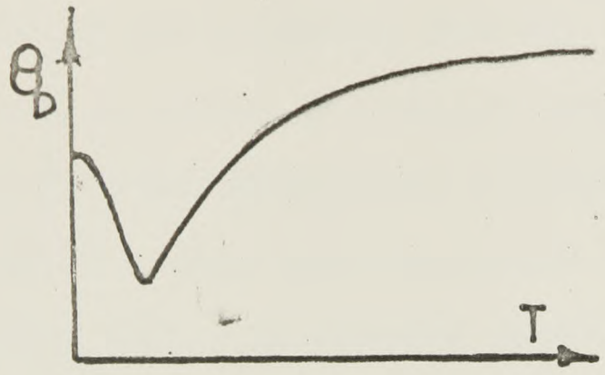


FIG.1.2(a) VARIATION IN θ_D FOR BLACKMAN'S SIMPLE CUBIC LATTICE (SCALES ARBITRARY).

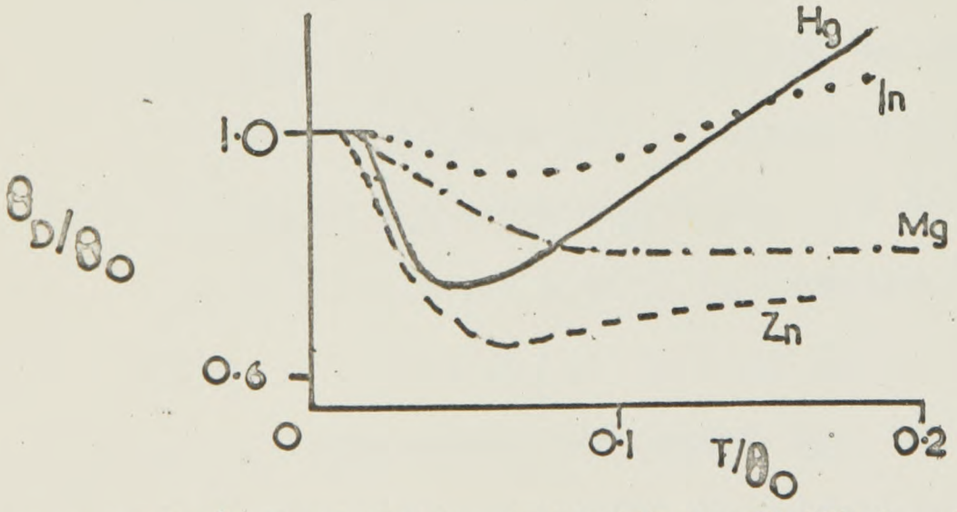


FIG.1.2(b) TYPICAL EXPERIMENTAL VARIATION OF θ_D.

the rise in $g(\nu)$ and C_v is increased or a fall in θ_D occurs; the presence of the maximum in $g(\nu)$ followed by a minimum ensures that the effective θ_D goes through a minimum and then levels off. The resulting θ_D variation is shown in Fig. 1.2(a) and resembles many that have been found experimentally (Fig. 1.2(b)). It also provides evidence that θ_D can vary quite considerably ($\sim$ 25%) purely from the inadequacy of the Debye model to represent the true lattice conditions without invoking any additional phenomenon.

The simple cubic model of Blackman considered quasi-elastic forces for nearest and next-nearest neighbour interactions. Despite an arbitrary choice of the ratio of these two force constants, resulting in high anisotropy, considerable success was achieved in predicting the expected θ_D variation. For the result to be of practical value for an actual crystal, the computation of $g(\nu)$ requires that the interatomic forces extending over several neighbours are known, and that the equations of motion for a large number of wave vectors along many crystal directions are solved. The frequency spectrum can then be mapped out accurately. Such a formidable computational solution has been eased in recent years by the use of modern computers, and our knowledge of $g(\nu)$ is now more limited by the incomplete knowledge of the interatomic forces.

The practice has been to assume simple models of forces for example, central bond-stretching forces, non-central bond-bending forces, and volume forces of the electronic clouds (due in a first approximation to the elasticity of the electron gas). The magnitude of the force constants is then chosen such that agreement is achieved with the experimentally determined macroscopic elastic constants in the limit of $q \to 0$.

More recently use has been made of inelastic neutron and diffuse X-ray scattering experiments to provide ω-q dispersion relations along several directions in many crystals. By fitting the theoretical dispersion curves with the experimental ones, numerical values of the force constants may be obtained. Topological arguments have also helped by showing that the periodicity of the lattice implies the existence of various kinds of singularities in $g(\nu)$. In a three dimensional lattice, infinite discontinuities in $\partial g/\partial \nu$ must occur at certain critical points, and the $g(\nu)$ curve must have certain well-defined shapes near the singularities. Figure 1.1(d) shows such a spectrum with the singularities.

The logical necessity of knowing $g(\nu)$ to calculate C_V and many other properties of solids is well established and has resulted in a great deal of effort being put into the

problem of evaluating $g(\nu)$. There are many excellent reviews of such evaluations for real crystals namely by Blackman (1955), de Launay (1956), Maradudin, Montroll and Weiss (1963) and Cochran (1963).

Lattice theory is therefore well established and where detailed information on the interatomic forces is available, the experimental variation of θ_D with temperature has been satisfactorily explained. This however is mainly restricted to the three common structures of metals, body-centred cubic, face-centred cubic and hexagonal close-packed.

As a consequence the interpretation of experimentally determined C_V in terms of θ_D has been adopted universally. Despite the fact that virtually no work has been done on the lattice theory of the structurally more complex and little known materials investigated in this thesis, we have dealt in some detail with the type of θ_D variation that can probably also be expected to exist with these materials.

1.2 Specific Heat of Conduction Electrons.

The theoretical treatment of the contribution of the conduction electrons in a metal has many parallels to that of the lattice vibrational contribution already outlined. Classical theory is again inadequate and leads to a contribution

of $3/2$ R per mole. This is much too large even at room temperature since the experimental 6 cals./mole/deg. can be almost entirely accounted for by the lattice contribution.

It was only after the application of quantum statistics that the reason for the small electronic specific heat became evident. Defining a density of states $n(\epsilon)$, such that the number of energy states per unit volume available to the conduction electrons between energy ϵ and $\epsilon + d\epsilon$ is $n(\epsilon)d\epsilon$ and introducing a Fermi-Dirac probability function

$$f(\epsilon) = \frac{1}{1 + e^{(\epsilon - \epsilon_F/kT)}}$$

leads to the number of states occupied, dn

$$dn = \frac{n(\epsilon)}{e^{(\epsilon - \epsilon_F/kT)} + 1} = n(\epsilon)\, f(\epsilon)\, d\epsilon$$

where the parameter ϵ_F, the Fermi energy is defined in terms of the total number of conduction electrons per unit volume, N, by

$$N = \int_0^\infty n(\epsilon)\, f(\epsilon)\, d\epsilon \,.$$

The total mean energy per mole then becomes

$$\overline{\epsilon} = V \int_0^\infty \epsilon . n(\epsilon) . f(\epsilon) . d\epsilon .$$

Such an integral can be evaluated for $T \ll \epsilon_{F_o}$ where ϵ_{F_o} is the value of ϵ_F at absolute zero, and gives a mean energy expression that on differentiation leads to the electronic specific heat, C_e of

$$C_e = \frac{2}{3} \pi^2 k^2 V n(\epsilon_F) T \qquad 1.8$$

Since $n(\epsilon_F)$ determines the coefficient of T in this expression, the theoretical problem is to find the form of $n(\epsilon)$ and in particular its value $n(\epsilon_F)$ in the vicinity of the Fermi surface.

Sommerfeld in 1928 considered the electrons in terms of the model of a free electron gas. The electrons move within a rectangular potential well of the dimensions of the crystal and results in a parabolic energy-wave vector relation. This gives a density of states distribution of

$$n(\epsilon) = 2\pi (2m)^{3/2} \frac{V}{h^3} \epsilon^{1/2} \qquad 1.9$$

and a value of ϵ at the Fermi surface of

$$\epsilon_F = \frac{1}{2m} \left(\frac{3Nh}{8\pi V} \right)^{2/3} . \qquad 1.10$$

From equation 1.8, the specific heat then becomes

$$C_e = \frac{4\pi^3 mk^2}{3h^2} \left(\frac{3NV^2}{w} \right)^{1/3} . T \qquad 1.11$$

or

$$C_e = 3.26 \times 10^{-5} V^{2/3} n_a^{1/3} . T \qquad 1.12$$

where n_a is the number of free electrons per atom.

Because of the high degeneracy of the electrons the condition $kT \ll \epsilon_{F_o}$ is valid even at room temperatures, and equation 1.12 gives for a typical metal such as copper, where $n_a = 1$, $V \sim 7$ cm^3/mole, a value of $C \sim .04$ cals./mole/deg. at $\sim 300^oK$. This is less than 1% of the lattice contribution and the dilemma of the classical contribution of the electrons of 3 cals./mole/deg. was therefore satisfactorily explained and was indeed a triumph for the Sommerfeld free electron model.

Although at room temperature the electronic contribution is small, at low temperatures it becomes comparable with the lattice contribution. In the region of $\theta/50$, the total specific heat is of the form of

$$C_V = C_L + C_e = \beta T^3 + \gamma T \qquad 1.13$$

and a plot of C_V/T against T^2 should be a straight line, the intercept and gradient yielding γ and β. Keesom and co-workers in the early 1930's were the first to test the linear electronic prediction of Sommerfeld, and indeed determined γ values for many metals which were of the right order of magnitude. Comparison with the free-electron model is conveniently made in the case of the monovalent metals ($n_a = 1$), by the introduction of an effective electron mass m^* such that

$$\frac{\gamma_{exp.}}{\gamma_{theor.}} = \frac{m^*}{m} .$$

Similarly for divalent metals, comparison is made by using the ratio of n_a values resulting from experiment and theory. Excellent reviews of such comparisons exist, two of which were made by Parkinson (1958) and Keesom and Pearlman (1956).

In general there is a difference between experiment and free-electron theory, of anything up to a factor of 2-3 for the metals mentioned, which is due to the oversimplification of the free electron model. Improvements were made by inclusion of the effect of the periodic potential field associated with the atoms of the lattice. The resulting solutions of Schrödinger's wave equation, include a factor exhibiting the periodicity of the lattice of the form

developed by Bloch. The net result is to alter the parabolic E - k relation, particularly in the region of the well-known Brillouin zone boundaries, and to divide the E - k relation into energy bands.

The extent of the deviation from the free electron model thus depends on the position of the Fermi surface, whether it occurs in the centre of an allowed band where the E - k relation is still almost parabolic, or near the extremes of a band. Further complications arise from the dependence of the E - k relation upon the crystallographic direction, and from the overlapping of the energy bands particularly in the more complex transition and rare-earth metals.

Solution of the wave equation becomes exceedingly difficult as the model assumed for the solid becomes more complex. Despite such mathematical problems a great deal of effort has been applied to the problem of the shape of the Fermi surface and of the band structure, and hence the value of the electronic coefficient γ.

Even with the inclusion of electron-phonon and electron-electron interactions, good quantitative agreement in γ values does not extend much beyond the mono-valent and noble metals. The dependence of axial ratio among the hexagonal structured divalent metals has been investigated and the work of Mott (1962 and 1964) on the transition metals must be mentioned.

In general incomplete knowledge of the highly complex band structures of the transition and rare-earth metals is the limiting factor. In fact the reversal has taken place in that the specific heat determination of γ has been used to provide information on the band structure, though such knowledge is limited from the fact that γ measures only an averaged density of states.

1.3 Magnetic Contribution to the Specific Heat

It was Weiss who in 1907 first gave a simple explanation for ferro-magnetism by postulating an internal field (H_i) proportional to the net magnetization (M). In the absence of an external magnetic field, the effective field is thus

$$H_i = \lambda . M$$

and the energy of magnetisation E_M is

$$E_M = - \int_0^M H_i \, d M = - \frac{\lambda^2}{2} M^2 .$$

The magnetic contribution to the specific heat then becomes

$$C_M = - \frac{1}{2} a \frac{d(M^2)}{dT} . \qquad 1.14$$

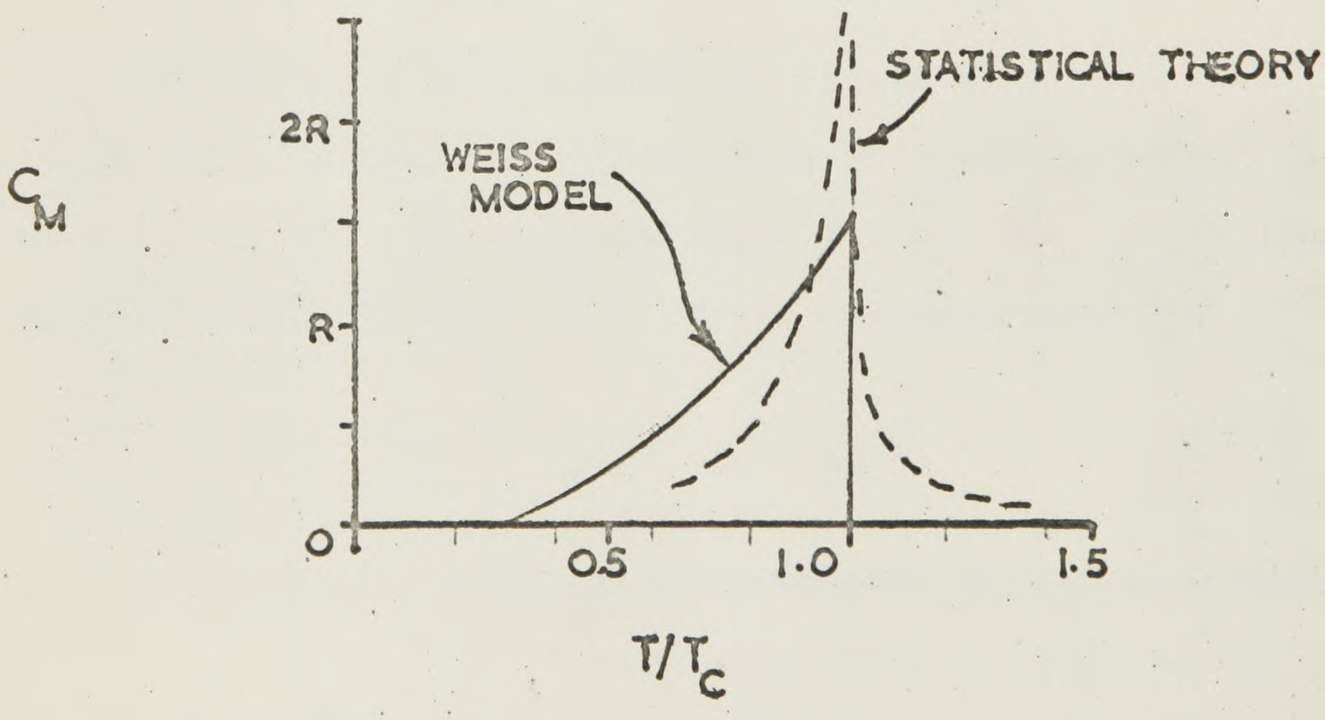


FIG. 1.3 SCHEMATIC VARIATION OF C_M.

The magnetisation M is a complex function of temperature, being the solution of the equations

$$\frac{M}{M_S} = \emptyset(y) \quad \text{and} \quad \frac{M}{M_S} = y\left(\frac{nkT}{M_S^2}\right)$$

where $\emptyset(y)$ is the Brillouin function.

M_S the saturation magnetisation and

n the number of atomic dipoles.

M however has the properties that it decreases with increasing temperature; its derivative is zero at absolute zero, and increases to a maximum negative value at the Curie point. The resulting C_M from equation 1.14 does not therefore have a simple temperature dependence, but increases from zero at $T = 0$ to a maximum at $T = T_c$, followed by a discontinuous drop to $C_M = 0$ in the paramagnetic state when $T > T_c$. The shape of C_M given by the Weiss model is shown in Fig. 1.3.

The experimentally determined values of C_M follow this general trend, but near T_c there is not even qualitative agreement. The value of the maximum is considerably different from $^3/_2R$ and a high temperature tail is evident above the transition.

The simple molecular field theory of Weiss was followed inevitably by the application of quantum mechanics and more recently by spin-wave theory. Space does not allow more than

a brief mention of some of the results of these theories.

Heisenberg in 1928 gave an explanation of the large magnitude of the Weiss internal field ($\sim 10^7$ oersted). Electrons of spins $\bar{s}_1$ and $\bar{s}_2$ have an exchange interaction of the form $-2J\ \bar{s}_1.\bar{s}_2$, where the exchange integral J is a function of distance, and can become the same order as the chemical binding energies for separations of a few Angstroms.

Calculations of the resulting partition functions despite simplifying assumptions that J decreases rapidly with increasing distance, leads to reasonably successful estimates of the ferromagnetic transition temperature (T_c), and the magnetic entropy (S_M) and energy (W_M) involved in the transition, as well as confirming the spin-wave theory. Van Vleck (1941) extended Heisenberg's work to antiferromagnetic materials and the following relationships result :-

$$\frac{W_M}{NkT_c} = \frac{3s}{2(s+1)} \qquad 1.15$$

where N is the number of magnetic atoms per mole and s is the atomic spin, and

$$S_M = R \log_e(2s+1). \qquad 1.16$$

More recent 'cluster' calculations of Brown and Luttinger

(1955) include the effect of short-range order and slightly modify equation 1.15. They also provide evidence of an approximate $1/T^2$ tail to the specific heat curve above the transition temperature shown by the dotted line in Fig. 1.3.

The above results have been reasonably verified (see Hofman, Paskin, Tauer and Weiss (1965)) for a number of ferromagnetic metals and non-metallic binary compounds.

In spin-wave theory, the excitation of spins from their perfectly aligned state at absolute zero may be described by a sinusoidal disturbance, or spin wave, of the spin system. Such spin waves can be shown (see Van Kronendonk and Van Vleck (1958)) to obey the following dispersion relations :-

$$\omega = a_f \frac{2Jsa^2}{\hbar} q^2$$

in the ferromagnetic case, where

a_f is a constant dependent upon crystal structure.

a lattice constant

J Quantum mechanical exchange constant,

and

$$\omega = a_a \frac{2J'sa^2}{\hbar} q$$

in the antiferromagnetic case where J' is the magnitude of

exchange constant.

Spin waves may be quantised into magnons and application of Bose-Einstein statistics leads to complex energy and therefore specific heat functions in both cases. In the limit of moderately low temperatures C_M can be reduced to

$$C_M = c_f Nk \left(\frac{kT}{2Js} \right)^{3/2} \qquad \text{(ferromagnetic)}$$

and

$$C_M = c_a Nk \left(\frac{kT}{2J's} \right)^{3} \qquad \text{(antiferromagnetic)}$$

where the constants c_f and c_a are dependent upon crystal structure.

The temperature dependences are strikingly different but in metals, the separation from the not too different electronic term ($\propto T$) in ferromagnets and the lattice term ($\propto T^3$) in antiferromagnets make confirmation experimentally exceedingly difficult. Further discussion of such a separation of the latter kind is discussed in Chapter 5.

REFERENCES

All historical references are not given but can be found from :

J.R. Partington (1952): Advanced Treatise on Physical Chemistry, Vol. III, Longmans-Green, London.

Blackman, M., (1935a): Proc. Roy. Soc., 148A, 365 and 386.

Blackman, M., (1935b): Proc. Roy. Soc., 149A, 117 and 126.

Blackman, M., (1937a): Proc. Roy. Soc., 159A, 416.

Blackman, M., (1937b): Proc. Camb. Phil. Soc., 33, 94.

Blackman, M., (1941): Rept. Progr. Phys., 8, 11.

Blackman, M., (1955): Handbuch der Physik, VII, (1), 325.

Brown, H.A. and Luttinger, J.M., (1955): Phys. Rev., 100, 685.

Cochran, W., (1963): Rept. Progr. Phys., 26, 1.

Hofman, J.A., Paskin, A., Tauer, K.J. and Weiss, R.J., (1956): J. Phys. Chem. Solids, 1, 45.

Keesom, P.H. and Pearlman, N., (1956): Handbuch der Physik, XIV, (1), 282.

Van Kronendonk, J. and Van Vleck, J.H., (1958): Rev. Mod. Phys., 30, 1.

de Launay, J., (1956): Solid State Physics., 2, 219.

Maradudin, A.A., Montroll, E.W. and Weiss, G.H., (1963): Theory of Lattice Dynamics in the Harmonic Approximation, Academic Press, N.Y..

Mott, N.F., (1962): Rept. Progr. Phys., 25, 218.

Mott, N.F., (1964): Advan. Phys., 13, 325.

Parkinson, D.H., (1958): Rept. Progr. Phys., 21, 226.

Van Vleck, J.H., (1941): J. Chem. Phys. 9, 85.

C H A P T E R 2

THE APPARATUS AND EXPERIMENTAL PROCEDURE

2.1 Relative merits of glove box and sealed capsule methods

The accepted methods of complete containment of extremely toxic materials, such as plutonium, in order to avoid the spread of radioactive contamination, are by the use of glove boxes or the sealed capsule technique.

The use of free standing glove boxes has been fully described by Lord and Waldron (1957), and in papers read at the Glove Box Symposium (Walton, 1958, Ed.). The use of glove boxes necessarily requires that the equipment being used can be contained inside a leak free box, access being achieved by means of neoprene gloves mounted into a transparent perspex front panel.

The development of a standard glove box to enable work at low temperatures to be carried out has been described by Meadon and Lee (1960). This was achieved by means of an extension tube from the floor of the box, which can be surrounded by cryogenic fluids. The extension tube thus forms the outer boundary of the 'cryostat', into which a specimen on its mounting can be lowered. Heat exchange between specimen and

cryogenic fluid can be achieved by filling the tube with exchange gas from inside the box or by condensing liquid inside the tube by pumping on the external liquid refrigerant. The inside of the extension tube is thus active in common with the inside of the glove box, but completely separated from the external inactive cryogenic fluids. The difficulty of handling cryogenic fluids inside an active glove box is thus overcome.

The cryogenic glove box has the advantages that a highly toxic specimen can be used in a bare condition, uncanned or uncoated, and that the specimen is readily accessible for repairs or alterations by raising with its associated mounting out of the extension tube into the glove box proper.

It suffers however from the disadvantages that work at all times on the specimen and mounting is through neoprene gloves which can be extremely cumbersome for delicate work; that one is considerably limited to the temperature ranges covered by liquids boiling under normal or reduced pressures, if constant temperatures are required; and that one is limited in the properties that can be investigated with a relatively simple specimen and mounting because of the need for raising and lowering into the extension tube.

The alternative technique is to encapsulate the specimen inside a sealed container, decontaminate the exterior of the

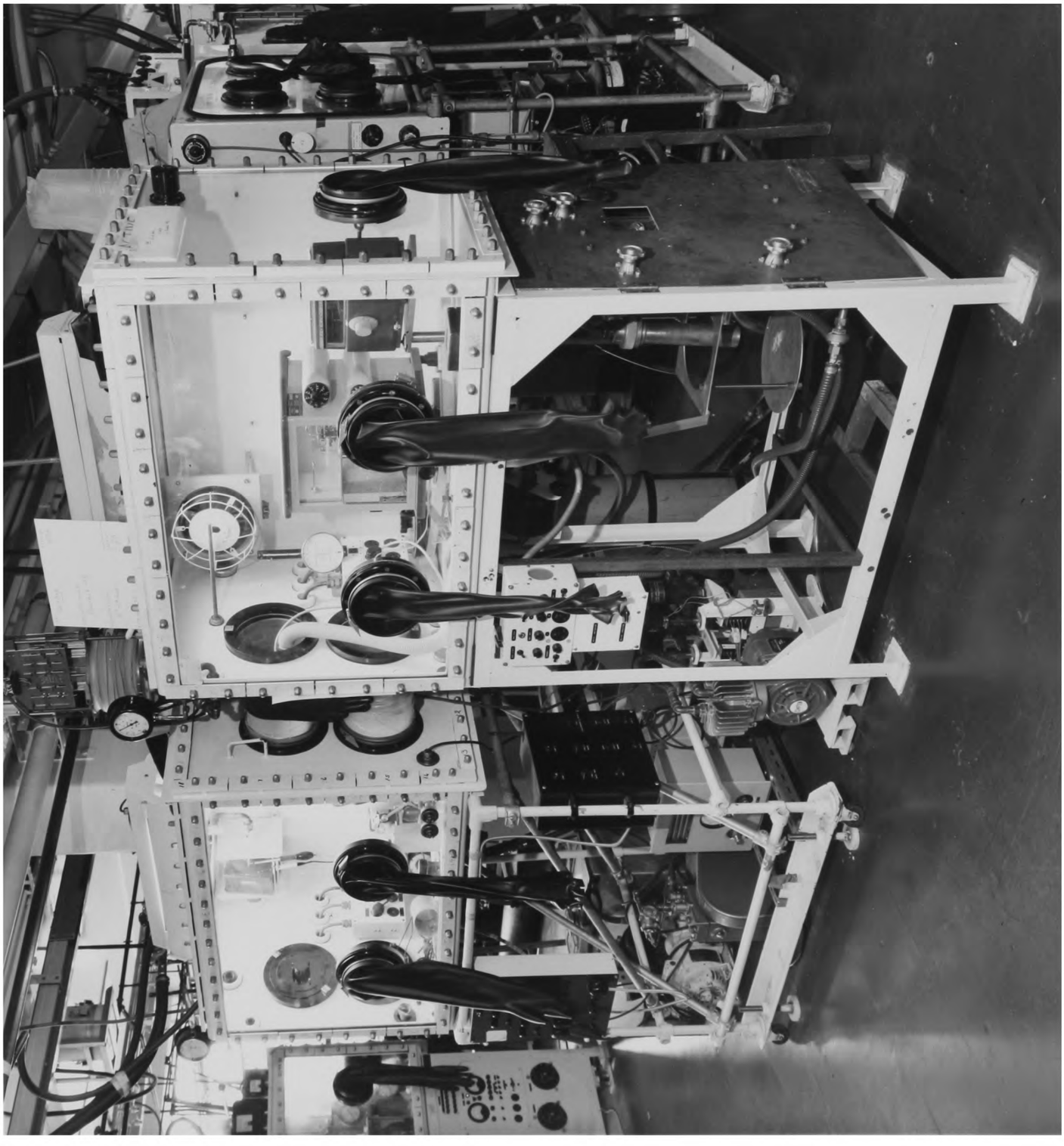


FIG. 2·1.

container and thenceforth use the encapsulated specimen in the conventional manner. Conventional equipment can be used without the inherent handling and operating difficulties associated with containment inside a glove box. Both Meadon (1961) and Wigley (1964) have described methods of encapsulation.

Obviously the relative merits of these two methods are dependent upon the properties being studied. In our particular case, the determination of specific heat, which requires a relatively sophisticated mounting of the specimen, and which does not require any electrical connections directly onto the surface of the specimen, lends itself to the sealed capsule technique, in which the capsule takes the form of the calorimeter.

Glove boxes were however used in the various stages of specimen preparation and in the encapsulation of the specimens. Fig. 2.1 shows the helium-atmosphered canning box with adjoining balance box.

2.2 Method of Specific Heat Determination

The radioactive decay of the predominantly α-active transuranic elements produces an energy release per disintegration in the form of kinetic energy of the α-particle

produced and of the recoiling resultant nucleus. Their kinetic energy is transferred to the remaining lattice atoms by a series of collisions and so eventually appears in the form of heat. In the case of Pu^{239} this 'self heat', as it is called, is $\sim$ 2 milliwatts per gram which is sufficient for a 50 gm. mass of Pu^{239} metal to maintain itself at a temperature of 10°C or so above its surroundings if these are gaseous.

In relation to specific heat determinations, the existence of the self heat eliminates any discontinuous heating method. Also the magnitude of this self heat not only limits the lowest temperature at which specific heat measurements can be made, but also means that equipment capable of dealing with rapidly rising temperatures had to be developed. For instance after cooling to $\sim$ 10°K using liquid helium, the initial rate of rise of temperature on isolating a specimen of Pu thermally is of the order of 0.5 deg./sec..

There are consolations however in that despite its magnitude, the self heat is a volume generated source of heat providing uniform heating throughout the specimen. Also the self heat is dependent only upon the isotopic content of the specimen and thus forms a conveniently temperature independent

source of heat which can be calculated from an isotopic analysis and the known disintegration energies of the isotopes present.

If the self heat of the specimen is dQ/dt then :-

$$\frac{dQ}{dt} = \left(\sum mC_p \right) \frac{dT}{dt} + \frac{dH}{dt} \qquad 2.1$$

where $\sum mC_p$ is the sum of the thermal capacities of specimen and calorimeter at the temperature T,

dT/dt is the rate of rise of temperature,

and dH/dt is the rate of heat loss to the surroundings.

In the temperature range of 10 - 300 ^{o}K to be covered by the continuous heating method, above about 100^{o}K, dH/dt, if the surroundings were say an isothermal enclosure, would obviously be appreciable and determination of this heat loss would be crucially dependent upon the emissivity of the surface of the calorimeter. We therefore decided to employ an adiabatic method, in which dH/dt is eliminated, despite the difficulties envisaged in controlling the temperature of the adiabatic enclosure to follow the rapidly rising calorimeter temperature.

From Equation 2.1 then under adiabatic conditions, knowing the self heat of the specimen and the thermal capacity of the calorimeter, the only measurement required to determine

the specific heat of the specimen is a measurement of the rate of rise of temperature.

2.3 Choice of Thermometric Substance

In the selection of a suitable thermometer for our particular specific heat determinations, regard must be made to the following :-

a) the high rates of rise of temperature involved place particular emphasis on the low thermal mass of the thermometer and of its time response

b) the somewhat limited quantities of the transuranic elements available also places a limitation on the magnitude of the thermal mass of the thermometer

c) the temperature range to be studied from $\sim 10 - 300\ ^{\circ}K$

d) the accuracy required in the measurement of temperature in relation to the sensitivity and reproducibility of the thermometer.

In the range $10 - 300\ ^{\circ}K$ the thermometers normally used for temperature measurement are either resistance thermometers or thermoelectric devices. While the considerable advantages in accuracy and reproducibility of such resistance thermometers

as say platinum are well known, their thermal mass and time response are unfortunately too large to be practicable in our case. We were therefore virtually forced to rely on a suitable low temperature thermocouple, particularly as they readily lend themselves to conditions a) and b) above.

The particular thermocouples which have been commonly used in the required temperature range are constantan versus copper and gold - 2.1 atomic per cent cobalt versus copper or 'normal' silver (i.e., silver - 0.37 at % gold). Although constantan v. copper thermocouples have been used extensively including calorimetry, because of their good reproducibility and long term stability, they have considerably lower sensitivity - the thermoelectric power being less than half that of gold-cobalt v. copper below 100°K.

Previously published data on the thermoelectric properties of Au-Co v. Cu or normal silver by Borelius et al. (1932), Fuschillo (1957), Powell, Bunch and Corruccini (1961), Powell, Caywood and Bunch (1962) and Wigley (1964), have shown differences in total thermoelectric force of up to $\sim 15\%$, and in general, differences between wires from different lots are greater than deviations within one lot.

Similarly constantan v. copper reported values by Scott (1941), Giaque, Buffington and Schulze (1927), Aston,

Willihnganz and Messerly (1941), and Meadon (1964) also show considerable differences.

Such differences are important in that they probably reflect the difference in the stated composition of the various samples of dominant element of the thermocouples used by the different workers but they are not detrimental to the use of either thermocouple provided each couple made up is carefully calibrated and thereafter remains stable and reproducible.

Large deviations from a given reference table can affect the accuracy of the much used method of calibration at a few fixed points and construction of a deviation curve (often an approximate straight line) from the reference table. Whichever low temperature couple was selected for measurement of a property such as specific heat, dependent directly upon measuring a change in temperature, then careful calibration over the whole temperature range with reference to say a platinum resistance thermometer was going to be necessary.

Previous works viz. Fuschillo (1957) and Powell, Bunch and Corruccini (1961) (hereafter referred to as P.B. and C.) suggested that the limiting factor in the stability of gold-cobalt v. copper thermocouples is the reproducibility and stability of the temperature gradients which give rise to

inhomogeneity e.m.f.'s rather than any intrinsic instability in the thermometer. Improvement in the reproducibility of this thermocouple is principally the metallurgical problem of producing more homogeneous alloy wire.

However, provided that certain precautions are observed to reduce the effects of inhomogeneities, we have found that gold-cobalt v. copper can be used for reasonably precise work. These precautions are described in Sections 2.4 and 2.10. Thus the advantage of the higher sensitivity of this pair in comparison with constantan v. copper can be utilised. This has slightly eased the problem of development of a system of continuous measurement of the thermocouple output with sufficient precision to enable a reasonable accuracy in the specific heat to be achieved.

The relative merits of copper and normal silver as the passive element of a couple with gold-cobalt has also been discussed in the literature. P.B. and C. prefer copper because of its greater homogeneity except for applications below 60°K where the considerably lower thermal conductivity is important. Crisp and Henry (1964) criticize both; copper because its thermoelectric power is very sensitive to iron impurities (see Gold, MacDonald, Pearson and Templeton (1960)); normal silver because its gold concentration dependence is large.

They would appear to favour normal silver at the lower temperatures.

At the time our measurements were started, thermocouple grade copper which had been used and calibrated by Headon (1961) for low temperature thermoelectric power measurements, was at hand and was used.

More recently gold - 0.03 $^{at}/_{0}$ iron versus chromel as a low temperature thermocouple has been reported by Berman and Huntley (1963) and Berman, Brock and Huntley (1964). The outstanding advantage of this thermocouple is in its large thermoelectric power below 10°K. For temperatures up to 300°K it has a lower thermoelectric power over most of this temperature range than gold-cobalt v. copper. Its unusual thermoelectric power versus temperature curve with a maximum at $\sim$ 10°K and minimum at $\sim$ 60°K makes accurate calibration essential and produces difficulties in smoothing techniques.

2.4 Cryostat Design

The essential requirements of the cryostat were :-

a) to cool the specimen from room temperature to a temperature approaching that of liquid helium

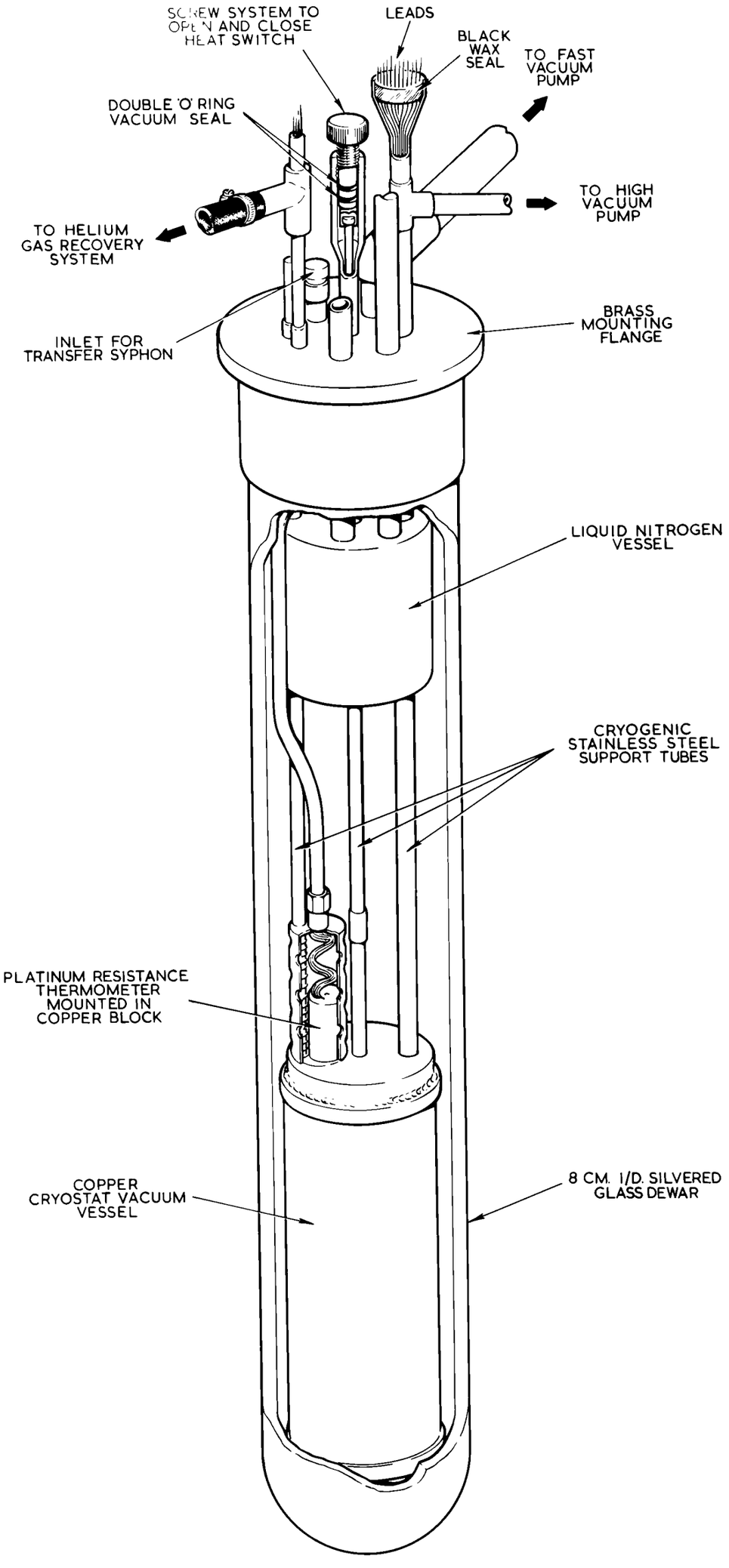


FIG. 2·2a SPECIFIC HEAT CRYOSTAT

b) to contain the refrigerants required to achieve this cooling

c) to isolate the specimen thermally after cooling to the lowest temperature attainable

d) to maintain adiabatic conditions surrounding the specimen as it warms back up to room temperature.

A drawing of the cryostat is shown in Fig. 2.2(a). It consisted basically of a copper vacuum chamber containing calorimeter and adiabatic shield etc., supported on three thin-walled cryogenic stainless steel tubes, from a brass mounting flange. The vacuum chamber was surrounded by a silvered glass dewar filled with the required refrigerant. When using liquid helium, an outer glass dewar of liquid nitrogen was employed, and the nitrogen can through which the three support tubes passed was filled with liquid nitrogen.

The vacuum chamber was evacuated via the right-hand side support tube to a pressure of $< 5 \times 10^{-6}$ by means of an Edwards Oil Diffusion Pump type F203 complete with liquid nitrogen trap and backed by a Metrovac Rotary Pump type DR1. Pressures were measured with Ionisation and Penning gauges situated as near the cryostat top as possible.

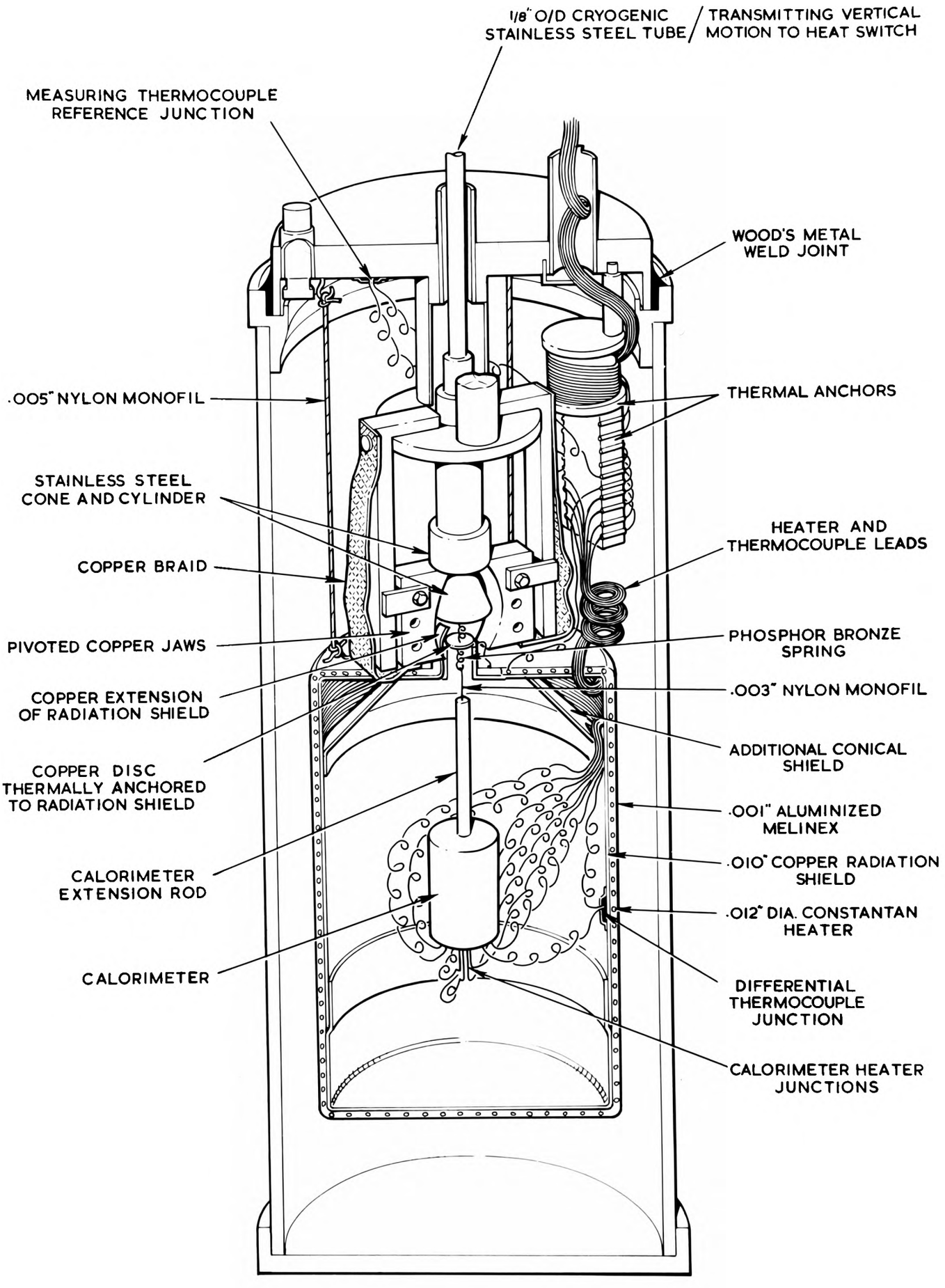


FIG. 2·2b ENLARGEMENT OF CRYOSTAT VACUUM VESSEL

A separate fast pumping system to reduce the pressure above the liquid helium was originally built at the same time as the high vacuum system. It was hoped that the range of temperature at which specific heat measurements were made, could be extended to a lower temperature. In practice the rate of rise of temperature was so large at these low temperatures that adiabatic conditions could not be achieved at any significantly lower temperature whether the helium was pumped or not.

Another feature of the high initial rate of rise of temperature was that helium exchange gas could not be used as a means of cooling, since in the time taken to pump out the exchange gas the calorimeter would have risen some 30 - 40°K or more. A mechanical heat switch was therefore used of the type described by Webb and Wilks (1955).

As shown in Fig. 2.2(b), a pair of copper jaws were pivoted such that vertical movement of the stainless steel cone and cylinder caused the jaws to clamp or unclamp onto an extension rod of the calorimeter. Vertical movement of the cone was achieved by the screw mechanism mounted at the top of the cryostat, movement being transmitted to the cone and cylinder by an 1/8" diam. stainless steel cryogenic tube. The tubing was found preferable to a piano wire since positive opening

of the jaws with the shoulder of the cylinder could be achieved without relying on a spring mechanism. The threaded piston of the screw mechanism was separated from the point of attachment of the transmitting tube by a freely pivoted joint, allowing relative rotational motion. The cylinder of the cone and cylinder at the heat switch end was keyed to prevent rotation of the cone. In this way only the vertical movement of the screw mechanism was transmitted to the cone. The piston of the screw mechanism possesses a double O-ring high vacuum seal. A jaw separation of $\sim$ 1 cm in the fully open position could be achieved for a vertical movement of the screw mechanism of $\sim$ 1.5 cm.. Good thermal contact between jaws and refrigerant was obtained by flexible copper braid soldered between each of the jaws and the supporting framework which was silver soldered to the lid of the vacuum can.

The calorimeter was suspended with 0.003" diam. nylon monofil between the end of the extension rod and a Teflon insulated hook inset into the base of the cone. In the centre of the nylon suspension a small phosphor bronze spring and copper disc were mounted, the disc being connected to the adiabatic shield by flexible copper wires.

The lengths of nylon both above and below the disc and spring arrangement were adjusted such that as the heat switch

was closed the calorimeter was raised until the top end of the extension rod was clamped between the jaws. Further tightening of the heat switch to achieve good thermal conductance, moved the cone up further and without the phosphor bronze spring would result in breakage of the fine nylon thread. On opening the heat switch the calorimeter then dropped completely inside the shield and the copper disc was positioned such that in the position of the jaws fully open, the disc just sat on top of the hole in the adiabatic shield. The flexible copper wires formed a thermal connection to the shield and the disc temperature thus approximated to that of the shield. In this way the disc at shield temperature prevented any part of the calorimeter from seeing the relatively cold heat switch components and also reduced the temperature gradient along the nylon suspension.

The adiabatic shield was also suspended on nylon threads, tied to three small eyelets on its top face, from the underside of the vacuum can lid. The length of these threads was adjusted such that the shield was clear of the movement of the jaws but a 0.010" thick copper foil extension of the top surface of the shield was also clamped between the jaws of the heat switch at the same time as the calorimeter extension rod.

The shield was constructed of 0.010" thick O.F.H.C. copper foil and was in the shape of two interfitting cylinders complete with top and bottom. An enamel insulated constantan heater 0.012" diam. was wound non-inductively on the cylindrical surfaces of both halves, and on the top and bottom, to provide approximately uniform heating. The heater windings were held in place by Araldite* and electrical insulation was assisted with cigarette paper between heater windings and copper shield.

Thermocouple junctions were attached in the following manner. A small 0.005" thick disc of copper foil, tinned at its centre with Woods Metal was glued with Araldite again with cigarette paper between, to the inside of the copper shield. The thermocouple junction was then soldered with Woods Metal to the tinned centre of the disc. Electrical insulation of the order of 20 x 10^6 ohms, could be achieved without sacrificing thermal contact (response times were of the order of 1 sec.) provided the thickness of the Araldite layer was kept to a minimum, approximately not much in excess of the thickness of the cigarette paper. Pressure was exerted if

---

* The Araldite referred to in the text was AY103 with hardener X83/193 cured at 100°C for 20 minutes. When used on copper a primer X83/65 was also used.

necessary during the curing of the Araldite to keep its thickness as small as possible. Several of these attachment points were cured onto the inside of the shield during its construction. Only a single differential couple was used in fact, but the effect of a three stage thermo pile was investigated.

The outer surface of the adiabatic shield was covered with 0.001" thick aluminised Melinex to minimize the heat exchange by radiation to the surrounding silver plated inside of the vacuum can.

More detailed diagrams of the calorimeters used are shown in Fig. 2.4(a) and (b) and their design is discussed in Section 2.5.

Both temperature measuring and differential gold-cobalt v. copper thermocouple junctions were connected to and electrically insulated from the calorimeter in a similar manner to the junctions on the shield described above. So also was the reference junction of the measuring thermocouple which was situated on the under side of the copper lid of the vacuum can, and was therefore at refrigerant temperature. For the temperature range 100°K to 300°K, the refrigerants employed were liquid nitrogen, solid carbon dioxide in acetone

and melting ice. Since the temperature of these baths, particularly with liquid nitrogen, can vary, a platinum resistance thermometer mounted in a copper block was placed just above the vacuum can to monitor the refrigerant bath temperature.

The thermocouple and heater wires (five 0.005" diam. enamelled copper and eight 0.005" diam. diamel coated manganin) entered the cryostat from the measuring circuits through a room temperature black wax seal at the top of the high vacuum pumping tube. They were shellaced together as a harness and coiled as they pass down the high vacuum tube, into the vacuum can. There they were wrapped, and fixed in place with shellac, round the cylindrical copper thermal anchor, before being separated through individual slits in the extension of the thermal anchor.

Leads to the shield heater and to the reference junction of the measuring thermocouple were coiled to increase their length before being soldered with Woods Metal to their respective connections. The remainder were recombined into a harness and also coiled before entering the adiabatic shield through a small hole in its top surface. They were then wrapped 5 or 6 times round the inside of the shield and fixed with shellac. A conical inner liner to the adiabatic shield

soldered with Woods Metal to the shield itself at both top and bottom edges, screened these leads from the calorimeter until they have achieved the temperature of the shield. They emerge from the bottom edge of this conical shield before being coiled again and soldered to their corresponding points of connection. An extension of the shield heater was wrapped several times round the lead harness just before it enters the shield to aid the attainment of shield temperature.

Removal of the calorimeter required only the unsoldering of the four heater leads and both thermocouple junctions and the cutting of the nylon suspension. The unsoldering of all Woods Metal connections was carried out with a temperature controlled miniature Soldering iron to prevent excessive temperatures in any of the wires.

The recommendations of P.B. and C. (1961) with respect to the reduction of the effect of inhomogeneities when using gold-cobalt as a thermocouple element have been followed.

Temperature gradients along the gold-cobalt wires were made as small as possible by using the reference junctions as close to the measuring temperature as possible, i.e., by using several refrigerant baths to cover the whole 10 - 300^{o}K

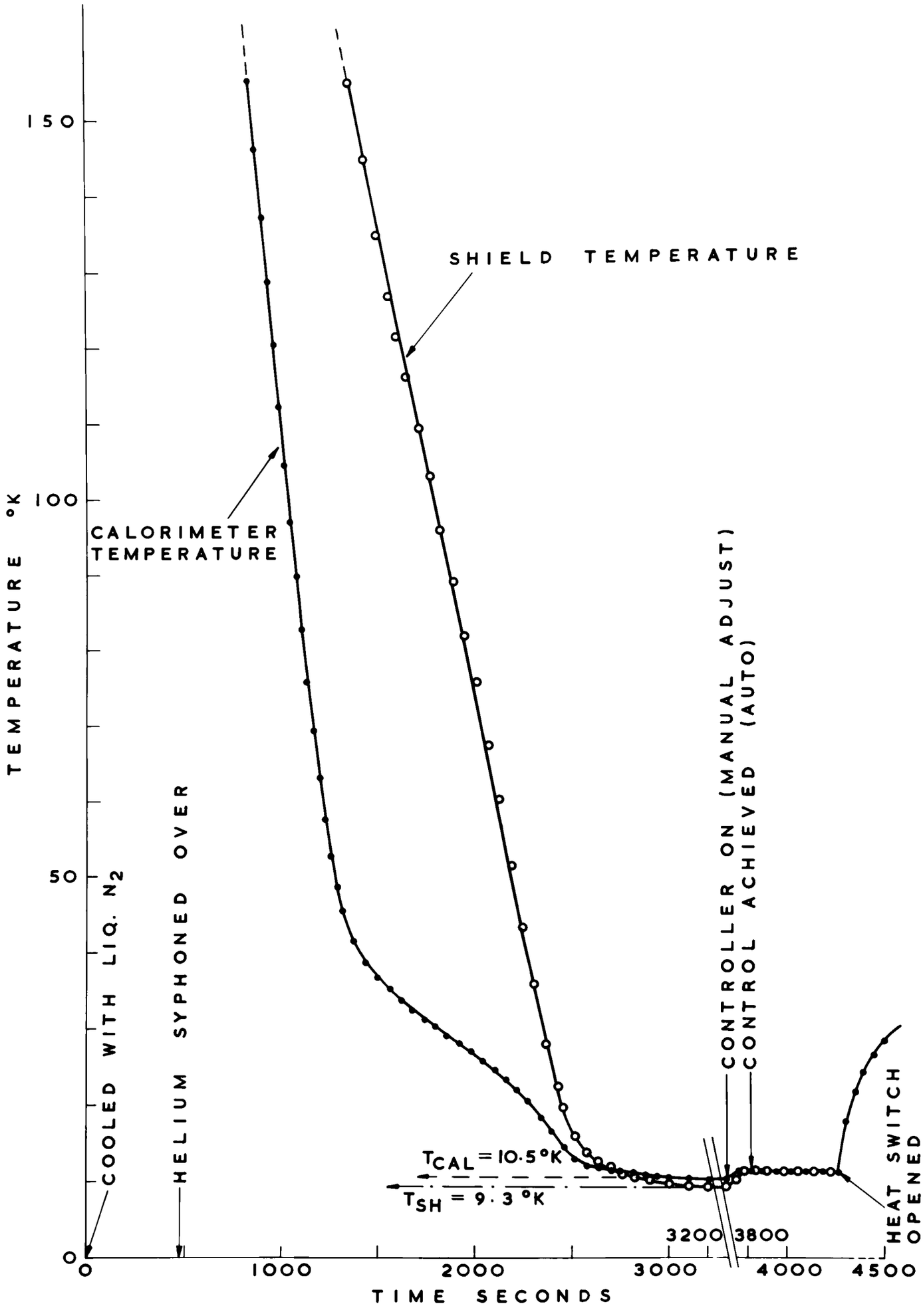


FIG. 2·3. COOLING ACHIEVED WITH MECHANICAL HEAT SWITCH

temperature range. The gold-cobalt wires were made as long as possible and the situation of the reference junction inside the vacuum can meant that they did not pass through any region of high temperature gradient such as the surface of a liquid refrigerant.

P.B. and C. also found that annealing at temperatures in excess of 90°C produced changes in the thermocouple calibration. All soldering with Woods Metal was carried out just above the melting point of $\sim 67^{\circ}C$.

Cold work has also been found to effect the calibration of gold-cobalt. In this light coiling of the gold-cobalt wire between calorimeter and reference function was kept to a minimum and once the thermocouple leads had been mounted in the cryostat, the only treatment they received after calibration was the small movement required to unsolder their junctions from the calorimeter and remove the calorimeter.

The performance of the heat switch is illustrated by the typical cooling curves for both calorimeter and shield shown in Fig. 2.3. Temperature measurements of calorimeter and difference between shield and calorimeter (assuming the differential thermocouple has the same calibration as that of the measuring thermocouple) were taken during a cool with

liquid helium following a short precool with liquid nitrogen. The precool was such that the bulk of the cryostat (but not the calorimeter) cooled to $\sim 77^{\circ}K$ before syphoning in helium.

The faster cooling of the calorimeter as compared with the shield, together with the knee in the calorimeter cooling curve at $\sim 25^{\circ}K$ was due to the copper foil extension of the shield, which was clamped between the heat switch jaws, having too high a thermal resistance. This was not altered as it would have been difficult to replace and also since cooling times were not increased excessively. Ultimately it can be seen that after approximately one hour the shield cools to $\sim 9^{\circ}K$ and the calorimeter to $\sim 10.5^{\circ}K$.

Typical thermal conductances of the heat switch based on the cooling curve of the calorimeter are between 2 and 15 mw/deg. in the temperature range 15 - $100^{\circ}K$. The additional cooling of the shield (of unknown thermal capacity) and the interdependence of the shield and calorimeter cooling obviously makes these figures only approximate. The T^2 temperature variation in thermal conductance found by Berman (1956) below $10^{\circ}K$, was not reached in this work, but the general variation of thermal conductance becoming less temperature dependent than T^2 above $10^{\circ}K$, and almost temperature independent at liquid nitrogen temperatures (illustrated for instance by

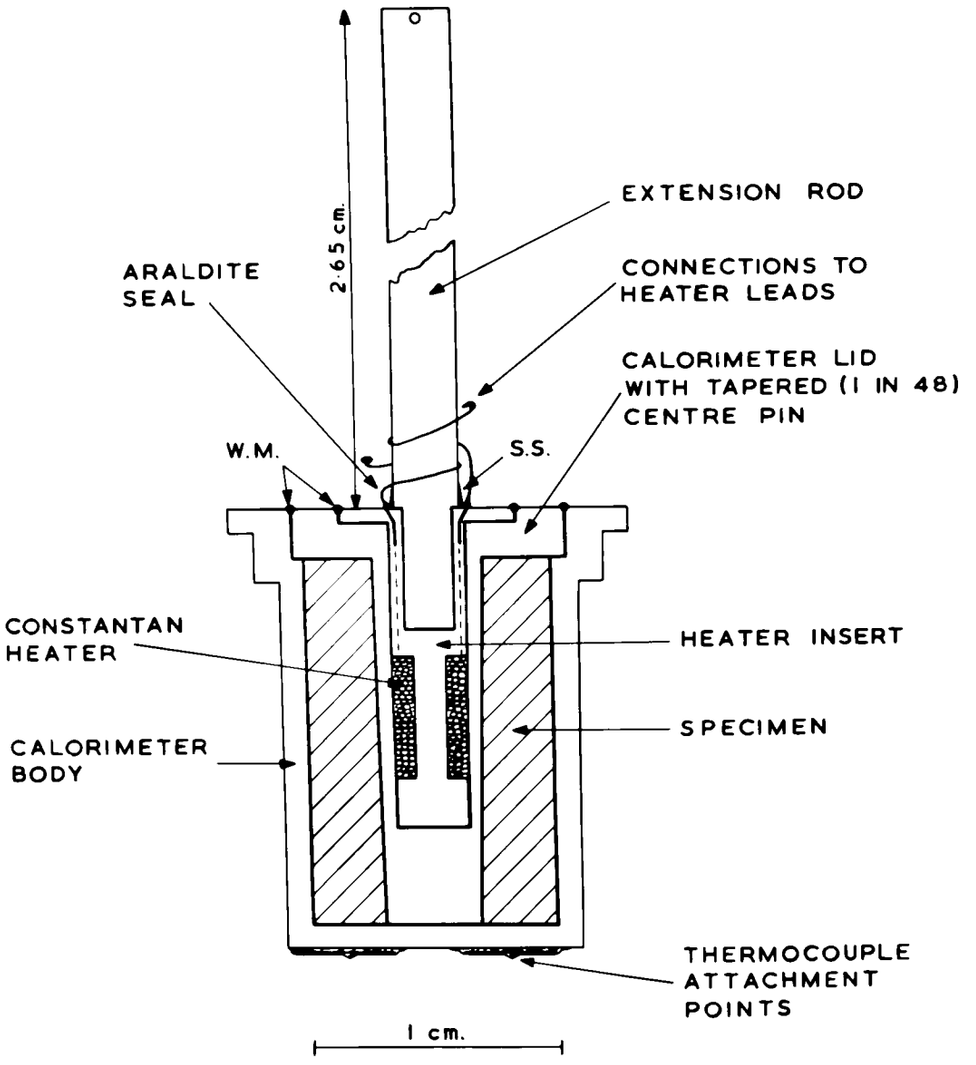


FIG. 2.4(a) Pu4 COPPER CALORIMETER

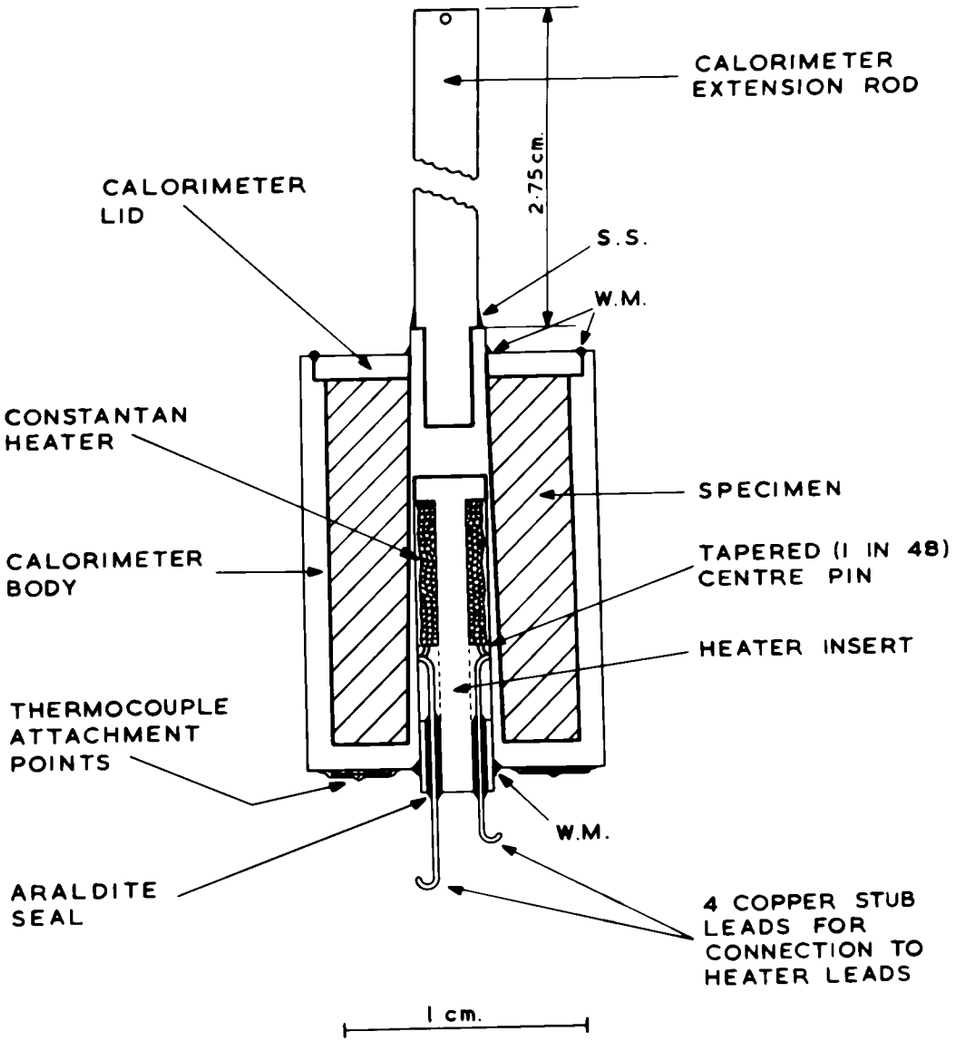


FIG. 2.4(b) Pu6 SILVER CALORIMETER

Gonelin (1967)) was observed.

Also shown in Fig. 2.3 is the change in temperature which occurs during attainment of adiabatic control of the shield, described in Section 2.8 and the typical rate of rise of temperature after opening the heat switch.

2.5 Calorimeter and Specimen Design

The size of the specimens used was determined by both the limited availability of, for instance, the very high purity plutonium investigated and by its high self heat.

The shape of the specimen was chosen in order to utilise the high expansion coefficient of plutonium relative to copper or silver. The annular cross section of the specimen caused the specimen to shrink on to the tapered centre pin on cooling, thus providing good thermal contact between specimen and calorimeter. See Fig. 2.4(a) and (b) for detailed diagrams of two of the calorimeters used. The specimens were machined such that they were a force fit at room temperature and were canned in a helium atmosphere to further improve thermal contact.

Despite the low thermal conductivity of plutonium the volume generated self heat of the specimen means that provided

heat loss away from the surface of the calorimeter can be reduced to a minimum, uniform temperatures throughout specimen and calorimeter should exist.

The calorimeter was designed to contain the chosen specimen shape completely both as a radioactivity seal and as a containment of the helium exchange gas. It was essential to keep the design of the calorimeter as simple and robust as possible for reasons of handling inside a glove box and of its subsequent decontamination.

The heater for the supply of heat in addition to the self heat when necessary was submerged in the tapered centre pin since this was the region of best thermal contact with the specimen. It also enabled the outer surface to be as smooth (thus aiding decontamination) and as polished (thus minimising heat exchange to the surroundings) as possible, when compared with a heater wound on the outside. The heater was wound of 0.005" diam. diamel coated manganin wire on the centre bobbin of the insert. In the case of Fig. 2.4(a) the heater wires passed out through an Araldite seal before being soldered with Woods Metal to a single turn of 0.010" diam. manganin glued to the base of the extension rod, for strength and robustness when connecting and disconnecting the heater leads. In Fig. 2.4(b) the heater windings were connected to

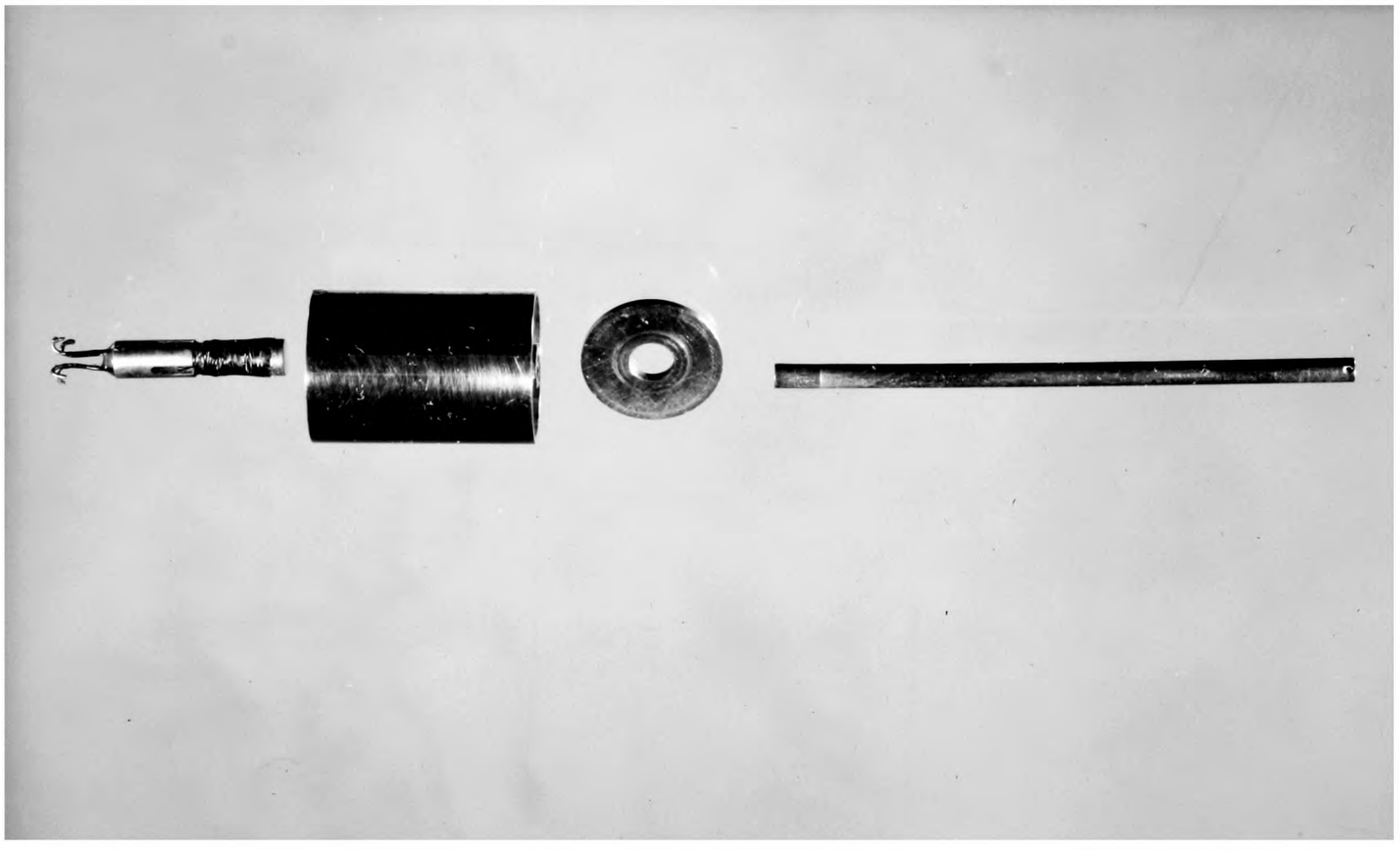




FIG. 2·5.

short copper (0.012" diam.) stub leads which pass through an Araldite seal before being connected to the heater leads.

The calorimeter shown in Fig. 2.4(a) was used for early α-Pu specimens and was machined from O.F.H.C. copper. Later work employed 99.99% silver calorimeters (Fig. 2.4(b)) where it was found more convenient to insert the heater bobbin from the bottom. Figure 2.5 shows a photograph of the silver calorimeter used for later α-Pu specimens, with alongside an exploded replica showing the various components (these are untinned on soldered joints).

The extension rod was soft soldered to the calorimeter and Woods Metal was used for calorimeter lid joint and heater bobbin insert joint. The components, e.g., can, lid, insert and extension rod were accurately weighed, together with the amounts of Araldite, manganin, copper, soft solder and Woods Metal added during the various stages of assembly.

The thermocouple junction connections were made as described in the previous section. There was a source of uncertainty in the weight of Woods Metal remaining on the tinned thermocouple disc araldited to the calorimeter, after connecting the thermocouple junction <u>in situ</u>. This was found to be negligible (~ 0.001 gms.) when a 0.040" diam. miniature Soldering iron bit was used. The bit was tinned but wiped

clean of excess Woods Metal and the iron was temperature controlled to raise the disc just above $\sim 67^{\circ}C$. No appreciable amounts of Woods Metal were removed on the iron from the known weight of bead already on the thermocouple disc.

2.6 Experimental Procedure

The specific heat measurements in the range 10 - 300°K were divided up into four overlapping temperature regions, employing four different refrigerants. Liquid helium was used for 10 - 100°K, liquid nitrogen from 80 - 200°K, solid CO_2 in acetone from 195°K - 280°K and melting ice from 275 - 300°K.

Cooling of the calorimeter and shield with all the refrigerants was achieved by use of the mechanical heat switch, the jaws being closed at room temperature and further tightened after cooling of the cryostat to counteract the inevitable slackening due to differential contraction.

A liquid nitrogen precool was employed when further cooling to liquid helium was required. Approximately 2.5 litres of liquid helium were required for cooling to $\sim 10^{\circ}K$ and with a further top up of $\sim$ 1 litre a length of run from 10 - 100°K of $\sim$ 2 hours could easily be achieved without further refilling. Similarly with other refrigerants initial filling of the single dewar used at room temperature, and

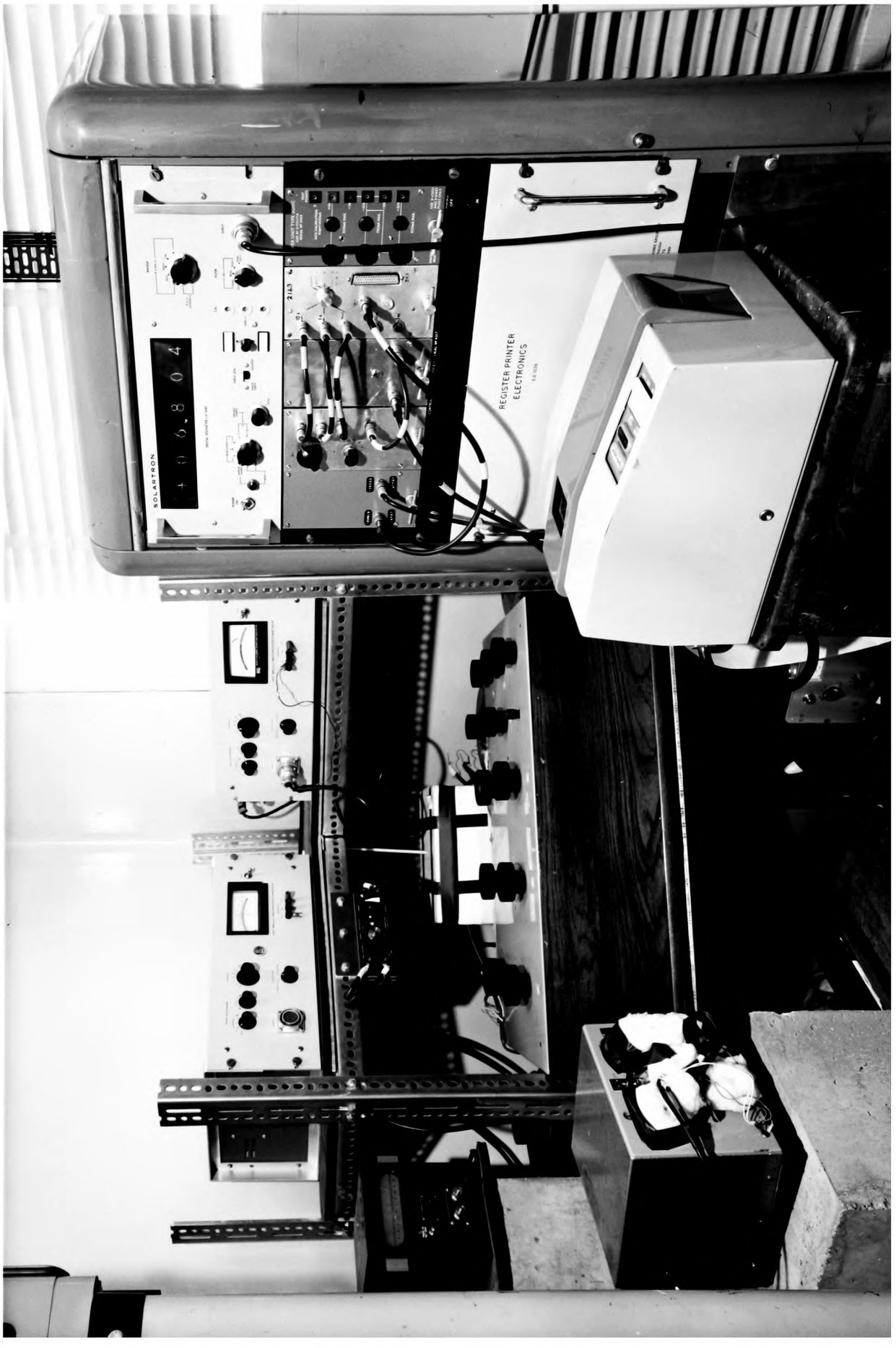


FIG. 2·6(a).

topping up when the calorimeter had cooled to the required temperature was sufficient, such that no further refilling during the length of run was necessary.

Typical cooling of calorimeter containing an α-Pu specimen of total self heat ~ 40 mwatts and shield were shown in Fig. 2.3. Cooling and control of the shield temperature to be the same as the calorimeter at ~ 11°K could be attained within 1½ hours.

Calibration procedures for the temperature measuring circuit, described in Section 2.8 and for the additional heat circuit (when used) in Section 2.10 were then carried out, and the printer recording the temperature of the calorimeter was started, prior to opening the heat switch.

Periodic increments in 100 μV steps of the backing off voltage of the measuring thermocouple circuit at intervals of 1 to 5 mins. and a less frequent reduction of the time interval between temperature measurements from 1/10 sec. initially to 1 sec. at the end of a helium run, were the only adjustments required.

A repeat of the calibration procedures in the temperature measuring, control and additional heat (when used) circuits was repeated at the end of a run. The stability of the measuring circuits was such that during a run lasting several



FIG. 2·6(b).

hours intermediate calibrations or adjustments were not required.

Use of other refrigerants requires the additional measurement of the resistance of the platinum resistance thermometer, measuring the bath temperature at intervals of 10 - 15 mins. throughout a run.

Two views of the equipment used are shown in Figs. 2.6(a) and 2.6(b). Figure 2.6(a) is a general view of the temperature measuring system to be described in the next section and Fig. 2.6(b) shows the additional heat equipment (Section 2.9) in the foreground and behind the control system (Section 2.8) and vacuum controls. The positions of the measuring systems in relation to the cryostat can be assessed from both photographs.

2.7 Temperature Measuring System

The output of the gold-cobalt v. copper measuring thermocouple with reference junction at liquid helium can vary between $\sim 50\ \mu V$ at $10^{\circ}K$ to $\sim 11{,}500\ \mu V$ at $300^{\circ}K$ with a corresponding thermoelectric power of between $\sim 10\ \mu V/^{\circ}K$ and $\sim 45\ \mu V/^{\circ}K$. Thus a precision of say $\pm 0.05\ \mu V$ in the measurement of the thermocouple output corresponds to $\pm 0.005^{\circ}K$ at $10^{\circ}K$ and $\pm 0.001^{\circ}K$ at $300^{\circ}K$. A temperature interval of say $1^{\circ}K$ over which it is required to calculate

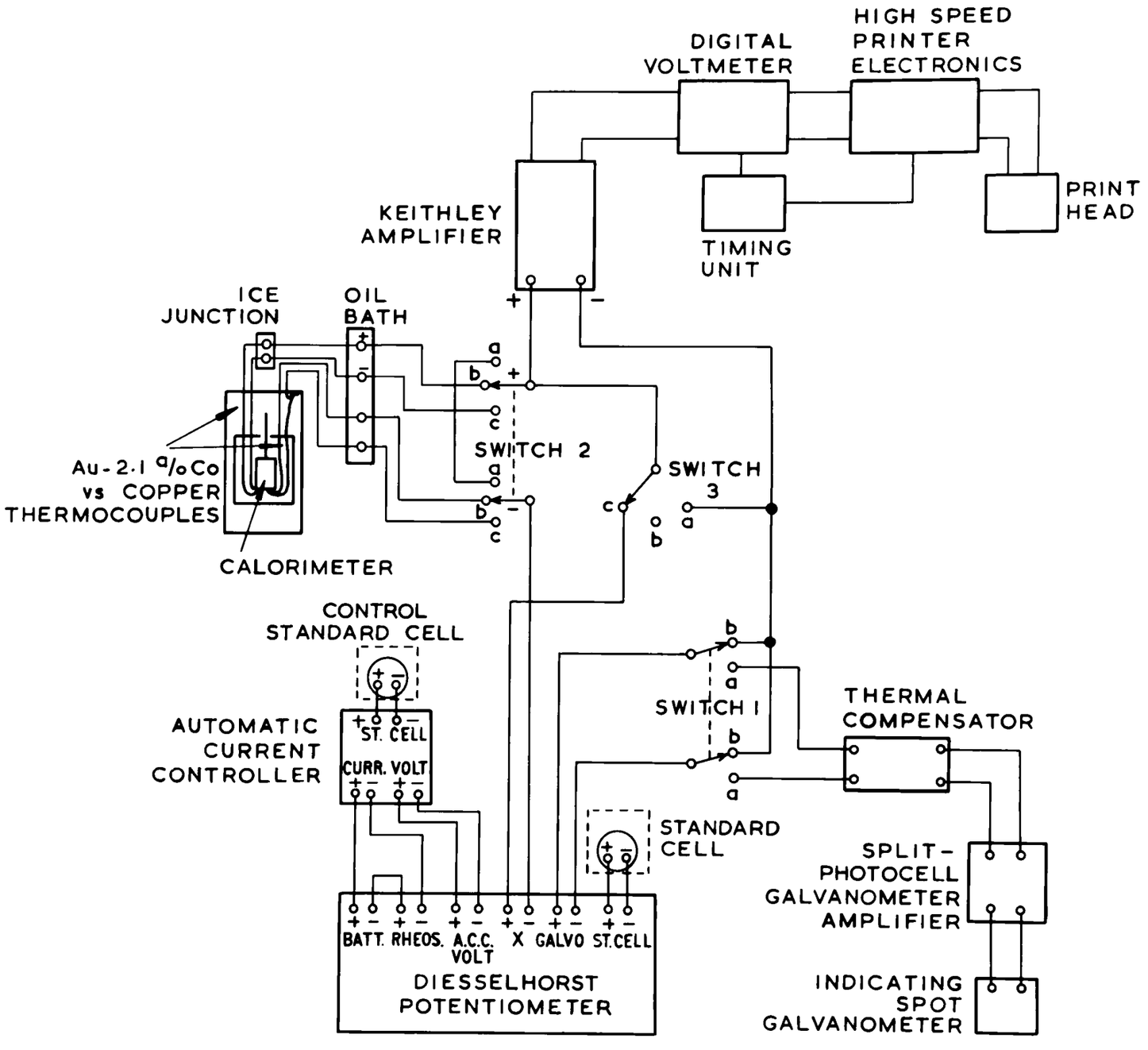


FIG. 2.7 TEMPERATURE MEASURING CIRCUIT.

the rate of rise of temperature and hence the mean specific heat in that interval could thus be measured to a precision of ± 0.01°K at 10°K and ± 0.002°K at 300°K, i.e., 1% and 0.2% respectively. Measurement of the thermocouple output to achieve a reasonable accuracy in the specific heat must therefore be carried out with considerable precision over the whole temperature range.

The circuit devised to obtain such precision is shown in Fig. 2.7. It consists of a stable back-off system which backs of all except 0 - 100 μV of the thermocouple signal and amplification and measurement of this 100 μV difference.

The Back-off System

The back-off system consisted of a Tinsley Thermo-electric-free Diesselhorst Potentiometer Model 3589-R/AVTO automatically standardised by means of a Tinsley Automatic Current Controller Model 5388.

The controller compared the potential drop across a resistor in the potentiometer current circuit with the e.m.f. of a control standard cell. The difference, or error, was fed into a d.c. amplifier which caused the current to change in the direction which reduced the error. The source of potentiometer current was also provided by the unit by means

of a rechargeable nickel-cadmium accumulator. Under steady state conditions the potentiometer current could be controlled to 1 part in 10^6.

The temperature dependence of the control standard cell ($\sim$ 40 parts in 10^6 per $^{\circ}C$) was the major source of error. For accurate control over the duration of a specific heat run of several hours it was thus necessary to immerse the standard cell in a constant temperature bath. An oil-filled mercury regulator controlled bath (Townsend and Mercer Model X27 Major) was used. With cold water cooling, control at $30^{\circ}C$ to better than $\pm$ $0.1^{\circ}C$ was easily achieved and thus control of the Diesselhorst current could be maintained to better than 5 parts in 10^6.

Initial standardisation of the potentiometer current against a reference standard cell was carried out in the usual manner using as a null detector a Tinsley Photocell-Galvanometer Amplifier type 5214 with indicating spot galvanometer type SS2.45E. The sensitivity of this null detector was such that even on a feedback setting midway between maximum and minimum sensitivity, a deflection of 5 mm was equivalent to a change in potentioneter current of 5 parts of 10^6.

The current controller, galvanometer amplifier and indicating galvo were all mounted on concrete pillars to

reduce the effect of building vibrations, and fluctuations of the indicating galvo were $\leq \pm 0.5$ mm. Use of the Thermal Compensator type 5214A to eliminate small parasitic e.m.f's had a negligible effect (< 1 mm) on the position of the standardisation zero.

Care was taken in the choice of reference standard cell (also immersed in the constant temperature bath) such that its e.m.f. at 30°C corresponded exactly to the minimum setting (1.01812) on the standard cell dial of the potentiometer. The potentiometer could thus be standardised to an accuracy of < 5 parts in 10^6, and would remain standardised to this accuracy for periods of several hours.

The resistance elements used in a Diesselhorst potentiometer including the reduction ratio of x 1/10 were such that an absolute accuracy of ~ 1 part in 10^6 could be attained, i.e., well within the above standardisation error. Thus since the thermocouple voltage could vary up to $\sim 10{,}000$ μV, the back-off system was capable of providing a back-off voltage of this magnitude accurate to 0.05 μV.

Referring again to the measuring circuit (Fig. 2.7), the oil-filled multiposition thermoelectric-free switches 1, 2 and 3 were arranged such that :-

Switch 1 either (position a) allowed the galvo system to be used as a null detector during standardisation

or (position b) short circuited the galvo when using the potentiometer as a back-off source.

Switch 2 either (position a) short circuited the various thermocouples to eliminate zero errors in the back-off circuit

or (position b) selected the appropriate thermocouple.

etc.

Switch 3 either (position a) allowed the Keithley amplifier (see below) to be short circuited while standardising potentiometer

or (position b) broke that link in the circuit during back-off

or (position c) allowed the potentiometer to measure the thermocouple voltages directly in the conventional manner using galvo as a null detector.

This last case was an added check on the accuracy of the

back off and difference measuring system and a sensitivity of between 50 and 100 mm. deflection per 0.1 μV change was obtained on the same feed back setting described above.

Amplification of Difference Signal

The difference voltage of 0 - 100 μV was fed into a Keithley D.C. amplifier Model 149. This chopper amplifier offered high zero stability (typically on the - 0.1 - 0 - + 0.1mV range with source resistances of between 10Ω and 1kΩ, zero stability was $< \pm$ 0.03 μV in an 8 hour period) and low noise level ($< \pm$ 0.03 μV). Input resistance of the amplifier was $\sim$ 10 megohms and response time was within 0.5 sec. for 10 - 90% of full scale deflection. The gain on the range used was 10^5 providing an output of $\pm$ 10 volts at 5 milliamps.

The important additional feature of this amplifier was the zero suppression which was of sufficient stability to back off up to 100 times full scale deflection. Suppressions of this magnitude were not used, but any small e.m.f.'s that existed in the measuring circuit could be eliminated (with thermocouple input shorted) by adjustment of this zero suppression.

Measurement of Difference Signal

The output of the Keithley amplifier was then fed into

a Solartron Digital Voltmeter Model LM1440. This was a five figure digital voltmeter with maximum resolution of 1 part in 30,000 and an accuracy of 0.01% of reading ± 1 digit. Thus a 0 - 100 μV difference between thermocouple signal and back-off system, which was amplified to 0 - 10 volts could theoretically be measured by the voltmeter to an accuracy of 0.01% ± 1 digit i.e., 0.002 volts on 10 V signal or ± 0.02 μV on 100 μV difference. In practice the noise generated by the Keithley limits such accuracy to ± 0.03 - 0.04 μV.

Calibration of the voltmeter was normally carried out using the Weston standard cells incorporated in the voltmeter with adjustable variable potentiometers for accurate setting. In our case, the back-off system was used to supply ± 100 μV signals (with thermocouple shorted) which when amplified gave ± 9.963$_0$ volts instead of 10. The gain of the Keithley though stable and linear was not accurately 1.000 x 10^5. The adjustable potentiometers of the voltmeter were therefore used to correct this error in the gain of the Keithley such that ± 100.00 μV from the potentiometer reads ± 10.000 volts on the voltmeter.

The voltage measured by the voltmeter was printed out by means of a Solartron High Speed Register Printer type ED1176. B.C.D. voltage signals, polarity and decimal point information

were available from a 50-way output socket of the voltmeter, and were printed out in seven columns of the printer.

Since the rate of change of thermocouple voltage was needed, then voltage readings at accurately known intervals of time were required. A clock pulse generator (A.E.R.E. Model 2143) based on a 10 Kc/s quartz crystal was modified to provide a suitable command pulse to trigger the voltmeter to read the output of the amplifier. The voltmeter reading remains constant until the next command pulse was received. Each time the voltmeter takes a reading this was automatically printed out on the strip printer.

The selector switch of the timing unit determining the length of time between pulses was wired directly to two additional channels of the printer to provide a record of which time interval was being used. Intervals of 1/10, 1 and 10 secs. with factors of x 1, 2, 4, 6 or 8 on each range were available.

Measurement by the voltmeter was achieved in $\sim$ 20 msecs., and by the printer in less than 85 msecs.. Thus a printing rate of 10 lines or voltage readings per second corresponding to the shortest timing interval available was easily achieved. In practice this fast rate was only used in the first few minutes of the specimen warming from helium temperatures.

Wiring Precautions

Several precautions were taken to reduce thermals, noise and pick-up from external sources.

Screened leads with untinned copper core were used throughout the measuring system. Since the terminals of the potentiometer, current controller and galvanometer system are all copper - connections to these elements were thus all copper to copper. All exposed terminals were shielded with cotton wool as an additional precaution. Soldered connections to the three selector switches were all immersed in oil and therefore at uniform temperature. The only other connection was inside the input socket of the Keithley amplifier, where a special thermal free solder (cadmium-tin) was used. Beyond the amplifier the magnitude of the voltages (~ volts) involved was sufficient not to be influenced by thermals of the order of microvolts or less.

Screening of all leads was carried out with great care. The screening of a copper lead connecting two components of the system was connected at both ends to the case of these components. In this way the screening of the whole system was built up into one continuous line, provided the screening of any copper wire forming a loop in the system was left

unconnected at one end. The mains earth of the various components was disconnected and the continuous screened line was then earthed at one point to a special earth mat sunk in the ground outside the laboratory. The cryostat was also isolated from mains earth by an insulated mounting and glass-fibre inserts in the pumping tubes. Thus the whole system was free of any possibility of extraneous pick-up from mains earth.

The limiting factor in this measuring system was the noise generated in the Keithley amplifier. This was larger than the noise levels claimed by the manufacturer, and was found to be due to the particularly dirty mains voltage present at A.E.R.E., Harwell. Various types of mains stabilisers were tried, in an attempt to get rid of the offending rapid fluctuations in mains voltage, and although their effect was reduced, they were by no means eliminated.

2.8 Adiabatic Control System

With the rates of rise of temperature involved it was essential that in the first place control of the radiation shield surrounding the specimen, to the same temperature as the specimen could be achieved as quickly as possible after the specimen started to warm up, in order not to restrict the

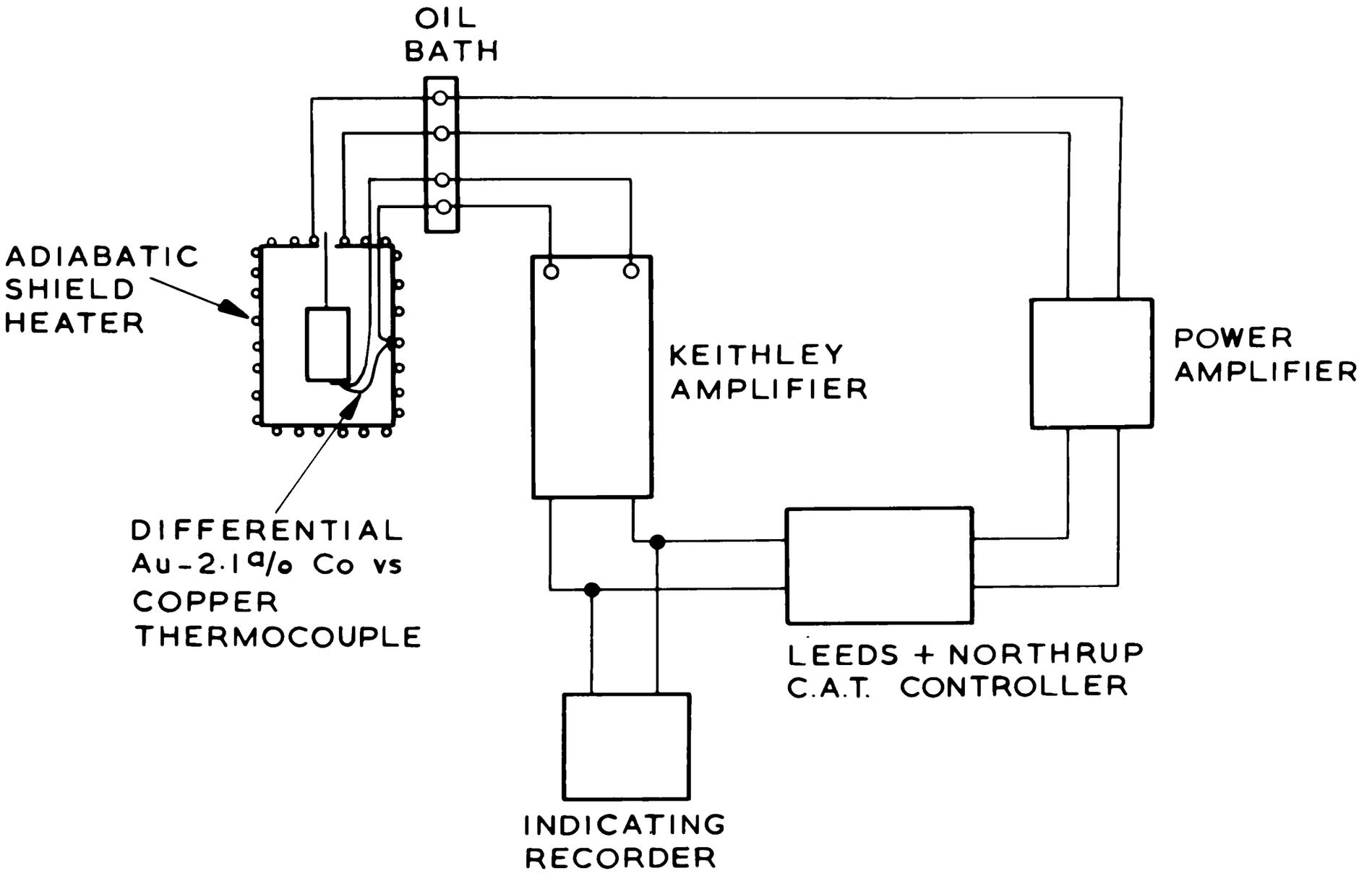


FIG. 2.8 ADIABATIC CONTROL CIRCUIT

range of measurement further; and in the second place once control had been achieved that it was maintained with sufficient accuracy and uniformity to enable true adiabatic conditions to exist up to room temperature.

The high speed of response of the temperature of the shield placed a limitation on the thermal mass of the shield which was therefore constructed of a comparatively thin gauge copper sheet. A compromise between the high speed of response of such a thin shield and the greater temperature uniformity of a more massive shield had to be made.

The thermometric device sensing the temperature difference between calorimeter and shield must also have a low thermal mass and high speed of response and a gold - 2.1 atomic per cent cobalt versus copper differential thermocouple was used. Since on control there was zero thermocouple output, there are no problems of accurate calibration required.

As shown in Fig. 2.8, the output of the differential thermocouple or error signal was fed into a Keithley amplifier Model 150 used on the - 10 — 0 — + 10 μV range (or when mains conditions allowed - 3 — 0 — + 3 μV range). The Model 150 was a slightly less sensitive version of the Model 149 described in the previous section. Typical zero stability was of the order of ± 0.1 μV per day. Again the zero suppression

facility was used to establish a true zero in the system with the thermocouple shorted out.

The output of the Keithley (± 10 volts for full scale deflection) was monitored by a Leeds and Northrup centre zero chart recorder such that a permanent record of the thermocouple output, i.e., the temperature difference was made at all times. It was then fed into a Leeds and Northrup Series 60 C.A.T. Control Unit. A faster time response was achieved by feeding the Keithley output directly into the C.A.T., and using the recorder only as a monitor, than the more usual method of using the out of balance signal provided by the recorder slidewire as the error signal to be fed into the C.A.T..

The C.A.T. unit was a 3-action (proportional, reset and rate) controller which produced an output correcting current whenever the input error signal deviated from zero automatically. Manual control was also available. Proportional control was a control action which determined the amount of correcting current developed for a given change in error signal. Reset action provided a further amount of correcting output current at a rate proportional to the magnitude of the error signal. Rate action produced a correction current which was proportional to the rate of change of the error signal. Thus proportional control was thus essentially a

sensitivity control; reset control was the basic control returning the error signal to zero and rate control was that which controlled the speed at which the error signal returned to zero.

The settings of these three controls was determined by the time constant of the whole servo-loop which included both the temperature sensing device and the radiation shield. Trial and error, together with certain guiding principles, enabled the correct settings to be attained which gave stable non-oscillatory control, which did not become unstable under small changes in error signal (i.e., noise or mains fluctuations) and which reacted to a large change in error signal (i.e., initial warming of the specimen after isolation) such that control was regained with the minimum deviation and in the minimum time (i.e., corresponding to the 'critical damping' situation).

The correcting output provided by the C.A.T. unit was only 0 - 5 mA insufficient to provide the power of 1 - 2 watts required by the shield. A single stage transistorised power amplifier was included. This used the 0 - 5 mA output of the C.A.T. as a control of the impedance of a silicon transistor which was in series with the load (shield heater) and a 30 volt D.C. power supply.

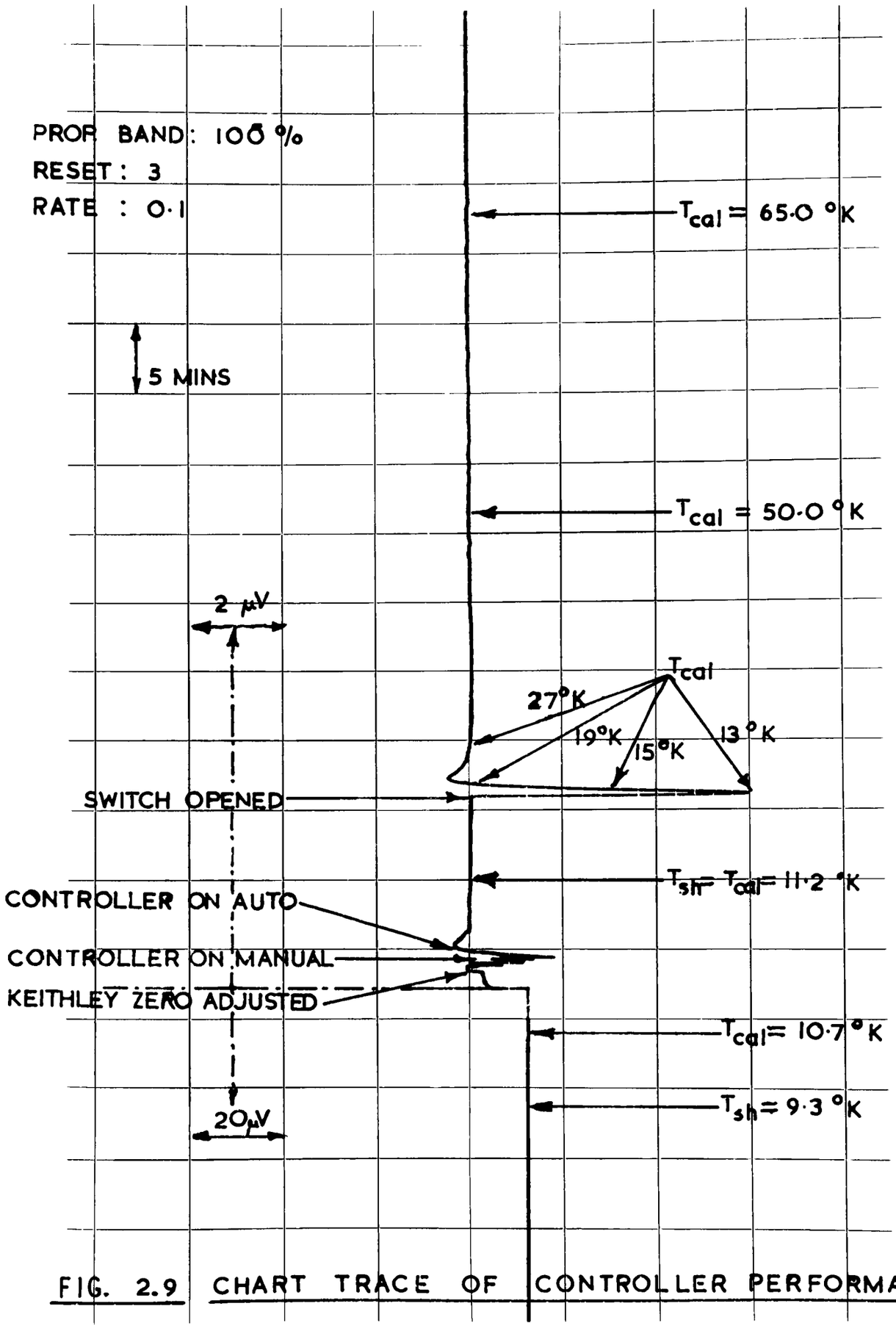


FIG. 2.9 CHART TRACE OF CONTROLLER PERFORMANCE

A typical recorder trace showing the differential thermocouple output during the initial part of a warm up from near helium temperatures is shown in Figure 2.9. Maximum deviations from control immediately after opening the heat switch was ~ 6 μV volts occurred when the calorimeter temperature was 13°K. Thus the maximum temperature difference was ~ 0.5 degK. At 20°K, this had fallen to $\sim \pm 0.025$°K and at 30°K to $\pm$ 0.002 degK, which was maintained throughout the remainder of the run. The limiting factor of this general control of $\pm$ 0.002°K was again due to the noise developed by the Keithley amplifier which was $\sim \pm 0.05$ μV.

2.9 Additional Heat System

Despite the self heat of the specimens investigated providing a constant, temperature independent power source, it was necessary to be able to supply additional power to the calorimeter. Investigations into the possible temperature gradients within the calorimeter, additional information upon the validity of the calculated self-heat values and determination of the thermal capacity of the empty calorimeter all require the supply of power to the calorimeter.

A system which could be used in conjunction with the continuous heating method was essential and a constant power

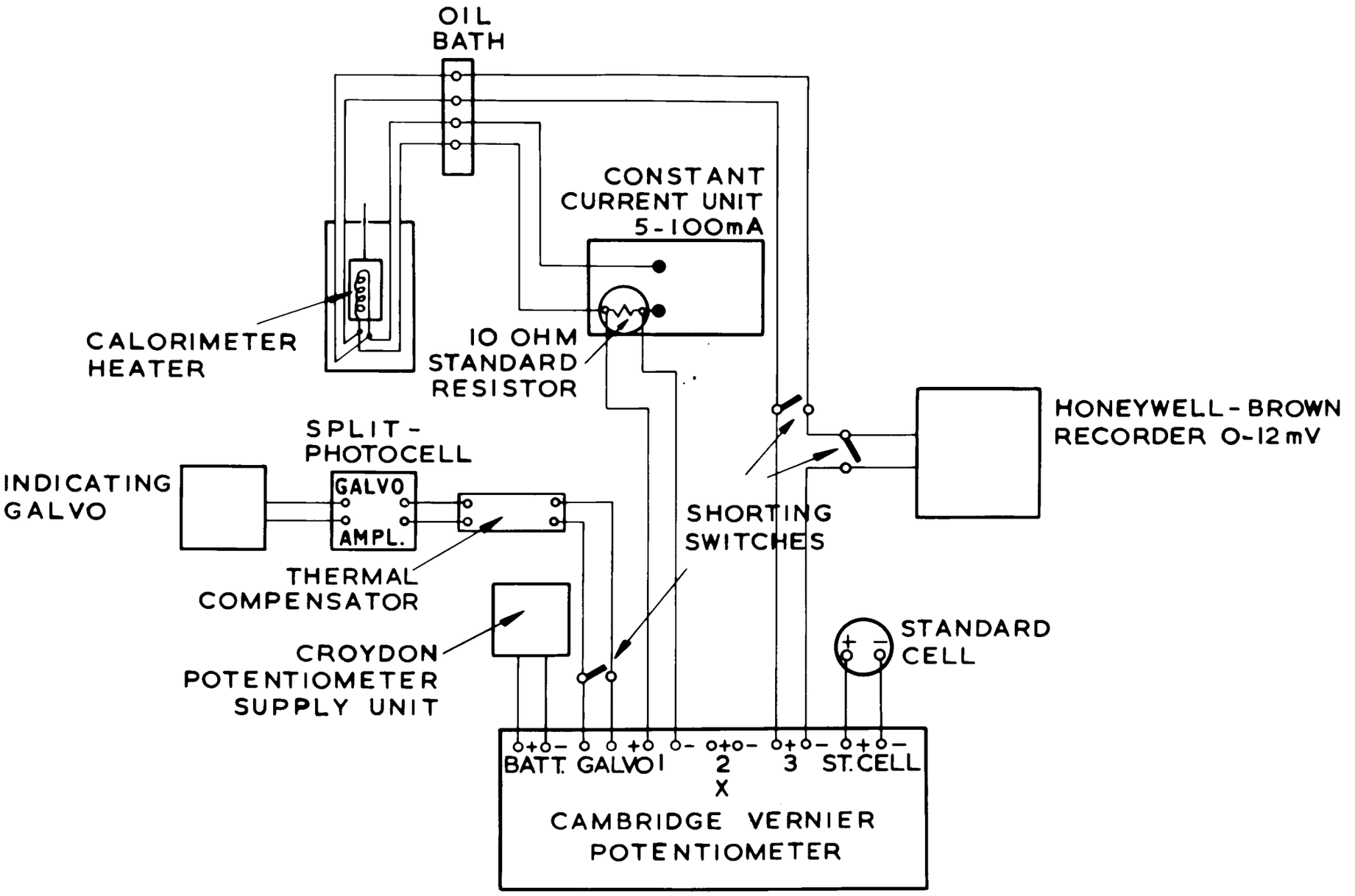


FIG 2.10 ADDITIONAL POWER CIRCUIT

source supplying a temperature independent power to the calorimeter heater would obviously lend itself to such a situation. However such a constant power source of sufficient accuracy was not obtainable. It was therefore decided to use a constant current source with a suitable measuring system to continuously monitor the voltage developed across the calorimeter heater, and a means of correlating this with the temperature measuring system.

The system used is shown in Fig. 2.10. It consisted of an adjustable constant current supply capable of supplying currents in the range 5 - 100 mamps to a constancy of 1 part in 10^4, into a total load of $\sim$ 250 ohms. Supply for the constant current unit was from a rectified A.C. source, heavily smoothed. The current supply was developed from a series regulated transistor control circuit, in which a differential comparator compared the actual output through a stable resistor with a stable reference derived from cascaded Zener diodes. The unit also incorporated a 10 ohm standard resistor in series with the output.

The remainder of the circuit provided a means of relatively infrequent measurement ($\sim$ 30 min. intervals) of the current supplied to the calorimeter heater and a continuous measurement (except when checking the current) of the voltage

across the heater. Essentially it was a less accurate version of the temperature measuring circuit. A 3-range Cambridge Vernier Potentiometer used on the X 1 i.e., 1.9 volt range was supplied by a Croydon Potentiometer Supply unit which maintained the potentiometer current constant to 1 part in 10^5. Initial standardisation by comparison with a standard cell (again immersed in the constant temperature bath) used a similar photocell galvo. amplifier and indicating galvo. as before as a null detector though on a less sensitive setting.

Once standardised, and the galvo. shorted the potentiometer was used to back off the majority of the voltage across the heater, the difference being recorded by a Honeywell-Brown 0 - 12 mvolts recorder. A continuous recording of the voltage was thus obtained from the chart reading (plus back off voltage) and was correlated to the temperature measurements by means of a 10 secs. interval event marker on one edge of the chart. The event marker was driven by the same timing unit, and the 10 secs. interval was thus an exact multiple of whatever timing interval was being used in the temperature measuring circuit.

Infrequently noting the thermocouple voltage corresponding to the beginning of any 10 secs. interval allowed the

additional power to be found at that thermocouple reading. From the printer output the time interval between the thermocouple reading at the centre of any temperature interval over which a specific heat value was to be calculated, and the nearest noted thermocouple reading was easily determined. The additional power voltage at the centre of that temperature interval could then be found.

Infrequent checks on the current were made by using the potentiometer in the conventional manner on a different input channel of the potentiometer.

Shorting links across the recorder input or voltage leads enabled the additional power voltage to be measured directly by the potentiometer or a calibration voltage to be fed into the recorder.

Currents in the range 5 - 100 mA produced voltages from the standard resistor and calorimeter heater in the ranges 50 - 1,000 mV and 250 - 5,000 mV respectively, corresponding to power dissipations in the calorimeter heater of 1 - 500 mwatts. Standard resistor voltages could be measured at worst to ± 0.02% directly by the potentiometer. Additional power voltages could be measured to 0.05% at worst on the lowest power level using the back off and recorder system. The additional power could thus be measured continuously to an

accuracy better than 0.1% even for the smallest power levels available.

A small correction ($\sim$ 0.1%) to the total power dissipated in the calorimeter was made for the joule heating in the 0.005" diam. copper current leads between calorimeter and shield. Half of this joule heating flowed into the calorimeter and half to the shield.

2.10 Thermocouple Calibration

The precautions observed in the environmental treatment and selection of the reference junction of the gold-cobalt v. copper thermocouples used have been described in Section 2.4.

In the initial selection of the particular sections of wire used from the reels of 0.005" diam. gold - 2.11 $^{at}/_{o}$ cobalt wire obtained from Johnson and Matthey and Company, Limited, London, and the reel of thermocouple grade 0.005" diam. copper from the Clarendon Laboratory, tests were made for local inhomogeneities. This was done by passing a length of wire, whose ends were connected to a potentiometer, through a thin plastic tube bent into a U-shape and immersed in liquid helium. The potentiometer null point galvanometer deflections indicate the potential differences between different sections of the wire in the two sides of the U-tube in the region of

the liquid surface subjected to the same temperature gradient.

Voltages of the order of 5 μV were obtained with some sections of the gold-cobalt wire, although the relatively short length required for the couple with reference junction at refrigerant temperature enabled a section to be chosen which gave inhomogeneity voltages of only 1 - 2 μV. Copper gave considerably smaller voltages ~ 0.5 μV.

Calibration of the thermocouple selected was carried out after it had been made up and wired into the cryostat, i.e., in situ, with reference to a N.P.L. calibrated platinum resistance thermometer type 5187L from H. Tinsley and Company. A massive cylindrical copper block was suspended in place of the specific heat calorimeter in the centre of the adiabatic shield. The platinum sheathed platinum resistance thermometer (p.r.t.) was a sliding fit, with Apiezon T grease as conducting medium, into a vertical re-entrant well in the centre of the block. The junctions of the measuring and differential thermocouples were soldered with Woods Metal to small copper plates glued with Araldite to the bottom of a deep grove around the copper block approximately level with the centre of the p.r.t.. For the higher temperatures the junctions were shielded by means of a copper band covering the groove and clamping around the block.

The block was cooled by means of an extension rod soft soldered to its top surface, and clamped between the jaws of the heat switch. Using liquid helium the block could be cooled to less than 6°K in ~ 2 hours. On opening the heat switch control of the adiabatic shield to the same temperature as the block was achieved by ~ 8°K. The temperature of the shield and block were then held constant by the control system of the shield. Measurements of p.r.t. resistance and thermocouple output were then made and repeated to ensure thermal equilibrium. Additional heat was then put into a heater wound on the upper part of the block to raise its temperature to the next required temperature. The additional heat was then switched off and control of the shield followed automatically. After equilibrium was attained the measurements were again taken.

In this way the cryostat was used as a constant temperature enclosure in which any temperature from ~ 8°K upwards could be achieved to a constancy of a few millidegrees in a period of ~ 30 minutes. Elevation to the next temperature took ~ 5 mins. and attainment of equilibrium ~ 25 - 30 minutes. The temperature range 8 - 100°K was covered using liquid helium, 85 - 210°K using liquid nitrogen, 200 - 290°K using solid CO_2 in acetone and 280 - 300°K using melting ice.

The temperatures of the liquid nitrogen, CO_2 and ice baths were measured by means of a second platinum resistance thermometer and all thermocouple readings were corrected with reference to liquid helium at 760 mm. of Hg pressure.

Thermocouple voltages were measured (as described in Section 2.8) to ± 0.05 μV continuously at 1 - 2 sec. intervals while the p.r.t. resistances were measured on an additional Diesselhorst potentiometer system borrowed temporarily for the calibration. Currents of 1 mamp. was delivered to both p.r.t.'s from a lead accumulator and measured in a forward and reverse direction by means of a 1Ω or 10Ω standard resistor. The bath temperature p.r.t. was measured on the same potentiometer immediately before and after the calibration p.r.t. measurement.

A precision of ± 0.05 μV was achieved by interpolation between the smallest potentiometer dial of 0.1 μV using the deflection of the galvo. spot, when on the X 0.1 range. Using a current of 1 mA, the p.r.t. voltage output exceeds 11 mV at ~ 140°K and thereafter a precision of ± 0.5 μV on X 1 range was attainable. Such errors in voltage and current allowed temperatures to be measured to better than ± 0.01°K from 12°K to 300°K and to better than ± 0.02°K from 9 - 12°K where the N.P.L. calibration was extended. Accuracies of calibration

quoted by N.P.L. in terms of the thermodynamic scale are estimated to be ± 0.02 from 12 - 20°K and ± 0.01°K from 20°K upwards.

Below 90°K linear interpolation of the tables of W ($= R_t/R_{273.15}$) together with a correction table for ΔW supplied by N.P.L. were used. Above 90°K the Callendar-Van Dusen equation

$$t = \frac{1}{a}\left(\frac{R_t}{R_0} - 1\right) + \delta\left(\frac{t}{100} - 1\right)\frac{t}{100} + \beta\left(\frac{t}{100} - 1\right)\left(\frac{t}{100}\right)^3$$

was used, where t = temperature in °C, R_t is the observed resistance at t °C, R_0 that at 0°C and a, β and δ are the constants of the thermometer, determined by N.P.L.. Since it was inconvenient to solve the explicitly for t use was made of the relatively simple method of Werner and Frazer (1952) for conversion of R_t into t.

Calibration of the thermocouple used in the specific heat determinations was initially carried out immediately prior to investigating the first plutonium sample. Some 51 calibration points were taken in the range 9°K to 300°K using liquid helium and nitrogen as refrigerants. The resulting temperatures and thermocouple readings were computer fitted

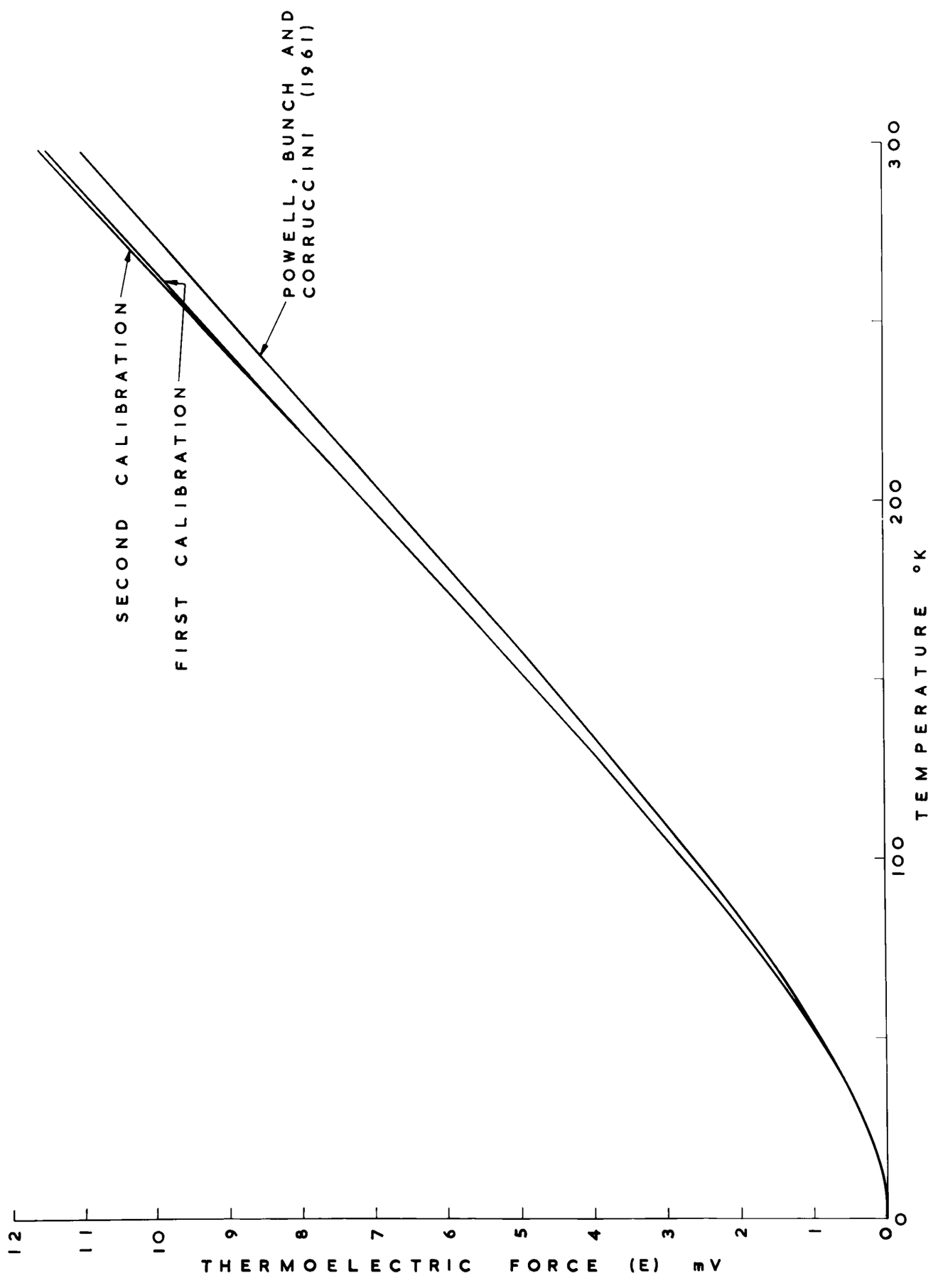


FIG. 2·11. THERMOCOUPLE CALIBRATION REF. JUNCTION AT 4·2 °K.

to a polynomial of degree 8 of the form :-

$$E = \sum_{n=0}^{9} a_n T^n$$

the coefficients being chosen to produce a least squares fit. The thermocouple output (E μV) with reference to helium (4.21_4 °K) was tabulated at $\frac{1}{2}$° intervals together with its first derivative the thermoelectric power (dE/dT μV/degree). The results of this calibration showed a drop in dE/dT above about 200°K which also corresponded to increasing difficulty in maintaining constant temperatures during measurements in that region.

Subsequent specific heat runs made it increasingly obvious that adiabatic conditions did not obtain in the higher temperature region. It was considered probable that non-thermal equilibrium conditions during this initial calibration produced erronous thermocouple outputs and hence incorrect dE/dT values.

Considerable modifications were carried out to improve adiabatic conditions and following these the thermocouple was recalibrated. A further 32 calibration points were taken this time (~ 1 year later) employing CO_2 and ice refrigerants for the higher temperatures. A similar smoothing technique by power series fitting was employed to derive tabulated

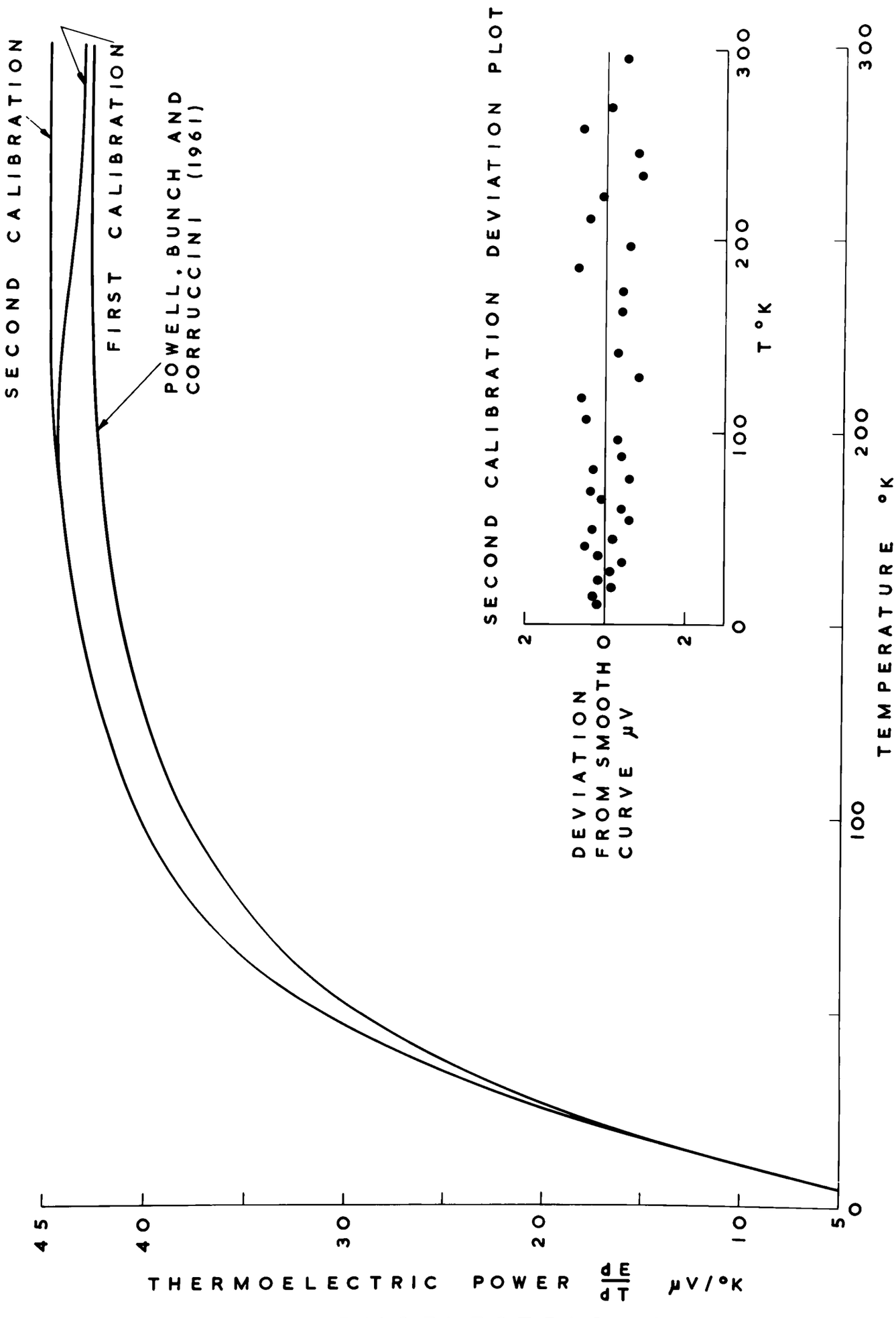


FIG. 2·12. THERMOELECTRIC POWER OF GOLD – 2·1 AT/o COBALT vs. COPPER

values of thermoelectric force (E) and power (dE/dT) at $\frac{1}{2}^{\circ}K$ intervals.

The results of both calibrations are shown in Fig. 2.11 for E and Fig. 2.12 for dE/dT values, together with the values quoted by P.B. and C. (1961). The thermoelectric force for the two calibrations agreed within 4 μV at $\sim 150^{\circ}K$, i.e., < 0.1% or $< 0.1^{\circ}K$ at $150^{\circ}K$, with correspondingly smaller differences at lower temperatures. At room temperature the difference was apparently 98μV due to non-equilibrium conditions. dE/dT values were virtually coincident up to $\sim 180^{\circ}K$ the values of the first calibration falling off above this temperature.

The difference between our values and P.B. and C. were about 5% or 562 μV at $300^{\circ}K$, the actual difference being approximately linear with temperature as found by P.B. and C. for various thermocouples tested.

As a final check that the drop in dE/dT was entirely due to non-equilibrium conditions and was not some abnormal behaviour of the thermocouple itself, on completion of the present work spot calibrations at a few temperatures were carried out. Again deviations from the second calibration were at worst ~ 3 μV at the highest temperature checked of $\sim 273^{\circ}K$.

Also shown inserted in Fig. 2.12 are the typical deviation plots for the calibration points of the second calibration from the smooth computer fitted curve. Deviations on average are approximately ± 0.5 μV corresponding to ± 0.05°K under the worst conditions of dE/dT at 10°K and ± 0.01°K at 300°K. As suggested by P.B. and C. these deviations were representative of local inhomogeneities in the gold-cobalt wire. The deviations were smaller than during the initial dip tests as the wires were under considerably less severe temperature gradients.

In summary we have found gold-cobalt v. copper to be a satisfactory low temperature thermocouple with which temperatures in the range 10 - 300°K could be measured to an accuracy of a few hundreths of a degree, with the strong proviso that great care was taken in selection, treatment and calibration.

2.11 Specimen Preparation, Canning and Decontamination Techniques

The source, dimensions, density, treatment and spectrographic and chemical analyses of the specimens will be given in Chapter 5 when presenting the results.

As discussed in Section 2.5, the specimen shape was a

right cylinder with annular cross section, the axial centre hole having a taper of 1 in 48. The two plutonium samples (Pu3 and Pu4) were machined from as-received 1 cm. diam. bar. Pu6 was received in a smaller diam. bar. Recasting was carried out in an argon arc furnace, with zirconium as getter, gravity casting in a split copper mould complete with centre pin, in contact with the water-cooled copper hearth. Use of such a mould enabled the minimum wastage of relatively limited high-purity plutonium, in the final machining to size.

In the case of neptunium only $\sim$ 6 gms. were available, and a similar shape though smaller with tapered centre hole was required. Arc casting into a similar copper mould as above with solid centre pin was not successful. Due possibly to the higher surface tension of molten neptunium and to a smaller mass of specimen, the neptunium solidified over the top of the centre pin before it could run down to fill the annular space of the mould. Reduction of the heat conducted away to the hearth by the centre pin, by using a hollow pin eliminated the problem of filling the mould. However several small radial cracks were seen to develop on the removal from the split mould. Arc-casting was repeated to eliminate the possibility of a defective casting causing the cracking but without success. The relative contraction of Np (the density

of Np changes from 17.9 gms./c.c. to 20.5 from melting point to α-phase) with respect to the copper centre-pin being presumably too large for a material as brittle as Np.

The centre pin mould was therefore abandoned and casting in the form of a solid cylinder was achieved successfully, without cracking. As a precaution against cracking during the subsequent drilling and machining the cast cylinder was annealed for 2 - 3 hours in the high α-phase region of ~250°C, followed by slow cooling to room temperature.

The plutonium monocarbide specimen was made by arc-melting together plutonium metal and high purity graphite. Arc-melting was repeated several times, turning the button over between melts, in order to achieve an homogeneous product, before casting into a solid cylindrical mould. Plutonium monocarbide is a very hard and brittle material and can only be machined with difficulty and a high failure rate. The solid cylindrical cast was therefore ultra-sonically drilled for the centre hole and ground to size on external faces.

All specimens were machined to be a force fit into the calorimeters such that optimum thermal contact was achieved. Canning of the specimens was carried out immediately after machining, before any surface oxidation formed, in a helium

filled glovebox. Some of the gas produced by the low-temperature group's helium recovery system was used to supply the atmosphere after purification of the pair of boxes shown in Fig. 2.1. We were indebted to R.O.A. Hall for the use of these boxes, which he successfully designed and developed to produce a helium atmosphere of the order of 500 - 1,000 pp.m. total gaseous impurities.

The specimen was weighed on the Sartorius Microbalance in the adjoining box (R.H.S. of Fig. 2.1), before being forced into the previously prepared calorimeter. The lid to calorimeter Woods Metal joints were then run with a temperature controlled soldering iron, such that the joint temperature was just above the melting point of Woods Metal. The heater insert Woods Metal joint was also re-made to ensure a helium atmosphere in the heater space.

The calorimeter prior to posting into the helium canning box was coated with shellac on all external surfaces except the two joints mentioned above. On removal of the canned specimen from the helium box to a fume hood, most of the radioactivity picked up on the surface of the calorimeter, from being handled inside an active box, could be easily removed by dissolving off the shellac in several baths of clean methyl alcohol. The only activity usually remaining was on the Woods

Metal joints. Care was taken during canning to keep this to a minimum by using a new soldering iron bit and fresh Woods Metal posted in with the calorimeter. Most loose activity on the joints could be removed by rubbing with meths.-soaked tissues, this being continued until smear monitoring produced an acceptable level of activity ($\sim$ 5 - 10 counts per sec.). Direct monitoring produced a larger count as some activity was inevitably fixed in the Woods Metal itself, while the joint was being made. Any small areas of the joint which gave an excessive count on direct monitoring were covered with a thin coat of dilute shellac.

Additional protection during canning to prevent the shellac coat and/or calorimeter from being scratched was achieved by either a protective brass can or using thermo-shrinking plastic tubing. The earlier calorimeter with heater insert entering from the top was protected by a brass can over all but the top surface of the calorimeter. Later calorimeters were covered over most of the length of the calorimeter body by the heat-shrinkable plastic tubing. The soldering iron used during canning was temperature controlled such that damage did not occur to the electrical insulating properties of the Araldite; the shellac coating was not burnt; and the plastic tubing, when used, was not softened excessively.

After decontamination the calorimeter was re-weighed on an inactive balance to determine the weight of Woods Metal used. Thereafter the canned specimen could be handled in the open laboratory and was mounted in the specific heat cryostat. No activity whatsoever was detected at any time on any part of the cryostat, and all joints provided a perfect activity seal despite frequent cycling from room temperature to 10°K. Evidence of complete containment of the helium exchange gas was provided by the dull but unoxidised state of the specimens on decanning.

REFERENCES

Aston, J.G., Willihnganz, E. and Messerly, G.H., (1941): Temperature. Its Measurement and Control in Science and Industry. Vol. 1, 219 (Rheinhold, New York).

Berman, R., (1956): J. Appl. Phys., 27, 318.

Berman, R., Brock, J.C.F. and Huntley, D.J., (1964): Cryogenics 4, 233.

Berman, R. and Huntley, D.J., (1963): Cryogenics 3, 70.

Borelius, G., Keesom, W.H., Johansson, C.H. and Linde, J.O., (1932): Leiden Comm. 217d.

Crisp, R.S. and Henry, W.G., (1964): Cryogenics 4, 361.

Fuschillo, N.J., (1957): J. Phys. Chem. 61, 644.

Giaque, W.F., Buffington, R.M. and Schulze, W.A., (1927): J. Amer. Chem. Soc. 49, 2343.

Gmelin, E., (1967): Cryogenics 7, 225.

Gold, A.V., MacDonald, D.K.C., Pearson, N.B. and Templeton, I.M., (1960): Phil. Mag. 5, 765.

Lord, W.B.H. and Waldron, M.B., (1957): J. Inst. Metals 86, 385.

Meaden, G.T., (1961): Thesis, Oxford University.

Meaden, G.T. and Lee, J.A., (1960): Cryogenics 1, 33.

Powell, R.L., Bunch, M.D. and Corruccini, R.J., (1961): Cryogenics 1, 139.

Powell, R.L., Caywood, L.P. and Bunch, M.D., (1962): Temperature. Its Measurement and Control in Science and Industry. Vol. 3., p. 65, (Rheinhold, New York).

Scott, R.B., (1941): Temperature. Its Measurement and Control in Science and Industry. Vol. 1, p. 206, (Rheinhold, New York).

Walton, G.N., (1958 ed.) Glove Boxes and Shielded Cells for handling Radioactive Materials.

Webb, F.J. and Wilks, J., (1955): Proc. Roy. Soc., 230A, 549.

Werner, F.D. and Frazer, A.C., (1952): Rev. Sci. Instru. 23, 163.

Wigley, D.A., (1963): Thesis, Oxford University.

C H A P T E R 3

ADDITIONAL DATA REQUIRED FOR CALCULATION AND ANALYSIS OF SPECIFIC HEAT

As indicated in Section 2.2, the measurement of the rate of rise of temperature of the calorimeter under adiabatic conditions, relies on a knowledge of the self-heat of the specimen to derive the total thermal capacity of the calorimeter and specimen. Further, a knowledge of the thermal capacity of the calorimeter is then required to derive the specific heat of the specimen.

3.1 Self-Heat of Transuranic Specimens

The following discussion on the calculation of the self heat is mainly concerned with that of plutonium since this is immediately relevant to the plutonium metal and compounds studied. A particular sample of plutonium contains an isotopic mixture of Pu^{238}, Pu^{239}, Pu^{240}, Pu^{241}, Pu^{242} together with trace amounts of Am^{241}. The total self-heat of such a sample depends upon the knowledge of the respective weight percentages of the isotopes present as well as their individual self-heats. A typical analysis of 'high purity'

plutonium metal used in the present work is shown in Table 3.1 together with selected values of the self-heats of the various isotopes and their relative contributions to the total self-heat.

The selected power outputs shown in Table 3.1 were calculated from the half-lives and disintegration energies appearing in the literature. It will be seen that the spread of the values quoted for the half lives, in particular for Pu^{239}, produces a major source of uncertainty in the calculated total self-heat, and therefore in the resulting specific heat values. A careful search of the literature was undertaken to attempt to establish the relative merits of the published data and their effect on the calculation of the total self-heat. In this respect the review articles of Strominger, Hollander and Seaborg (1958) and of Lederer, Hollander and Perlman (1967) were found very helpful.

The isotopes shown above are predominantly α-active, with the exception of Pu^{241} which decays by β-emission. The literature contains values of the energies of the α-particles emitted by each isotope together with the relative abundances of the α-particle groups within the α-spectrum of each isotope. For all the above isotopes except Am^{241}, $\sim$ 70 - 75% of the α-particles emitted ($\sim$ 5 - 6 MeV) correspond to the

TABLE 3.1

ISOTOPIC ANALYSIS OF Pu6

Isotope	Weight per cent	Self Heat mwatts/gm. of isotope	Self Heat mwatts/gm. of specimen	% of total Self Heat
Pu^{238}	0.005	568.8	0.028	1.39
Pu^{239}	98.02_2	1.92_3	1.885_0	91.83
Pu^{240}	1.93_8	7.03_0	0.136_2	6.64
Pu^{241}	0.033_6	4.49	0.001_5	0.07
Pu^{242}	0.001	0.11_3	1.2×10^{-6}	0.00
Am^{241}	0.001_4	114.5	0.001_6	0.07
			Total 2.052_8 mwatts/gm.	

transition from the ground state of the parent nuclide to the ground state of the daughter. The remaining 25 - 30% of the α-particles correspond to α-decay to an excited state of the daughter nuclide followed by γ-ray emission (typically $\sim$ 50 keV) as the daughter nuclide falls to its ground state. Thus $\sim$ 0.25% of the total disintegration energy is in the form of γ-rays.

Rothschild (1958) has calculated in the case of Pu^{239} that 99.6% of the γ-rays emitted are absorbed by 0.5 mm. of platinum-irridium alloy. Similar γ-absorption must be the case with our 1 mm. thick silver or copper calorimeters, but even a 5% error in the % absorbed would only cause a 0.01% error in the disintegration energy. It is therefore justifiable to assume that the total energy produced per disintegration which appears as heat in the specimen can be calculated using the α-particle energy corresponding to the ground state to ground state transition, plus the recoil energy of the daughter nuclide.

The disintegration energy (Q_α) is thus given by :-

$$Q_\alpha = E_{\alpha_o} \left(1 + \frac{m_\alpha}{M_D}\right)$$

where E_{α_o} is the α-particle energy corresponding to the

ground state to ground state transition

m_α is the mass of an α-particle

M_D is the mass of the daughter nuclide

Thus

$$Q_\alpha = E_{\alpha_o} \left(1 + \frac{A_\alpha}{A_D}\right) \qquad 3.1$$

where A_α and A_D are the corresponding atomic weights.

The number of such disintegrations per second can be derived from the basic exponential law of radioactive decay :-

$$N(t) = N(0)e^{-\lambda t} \qquad 3.2$$

where N(t) is the number of parent atoms present at time t

N(0) is the number of parent atoms initially

and λ is the disintegration constant which is related to the half-life ($T_{\frac{1}{2}}$) by :-

$$\lambda = \frac{1}{T_{\frac{1}{2}}} \log_e 2$$

The number of disintegrations per second is thus :-

$$\frac{d(N(t))}{dt} = -\lambda N(0)e^{-\lambda t} = -\lambda N(t)$$

$$\text{or} \quad \frac{d(N(t))}{dt} = \frac{1}{T_{\frac{1}{2}}} \cdot \log_e 2 \cdot N(t) \qquad 3.3$$

The number of disintegrations per second per gm

$$= \frac{1}{T_{\frac{1}{2}}} \log_e 2 \times \frac{6.0225 \times 10^{23}}{A_p}$$

where A_p is the atomic weight of the parent nuclide.

The self-heat ($\dot{Q}$) is given by :-

$$\dot{Q} = \left(\frac{1}{T_{\frac{1}{2}}} \right) \log_e 2 \times \frac{6.0225 \times 10^{23}}{A_p} \times Q_a$$

$T_{\frac{1}{2}}$ is usually quoted in years and Q_a in MeV. Since 1 year $= 3.1557 \times 10^7$ secs. and 1 MeV $= 1.6020 \times 10^{-13}$ joules then $\dot{Q}$ in watts/gm is given by :-

$$\dot{Q} = \frac{0.6931_5 \times 6.0225 \times 10^{23} \times 1.6020 \times 10^{-13}}{3.1557 \times 10^7} \times \frac{Q_a}{T_{\frac{1}{2}} \times A_p} \text{ watts/gm}$$

or

$$\dot{Q} = 2.1192 \times 10^6 \times \frac{Q_a}{T_{\frac{1}{2}} \times A_p} \text{ mwatts/gm} \qquad 3.4$$

Thus from equation 3.1, substituting for Q_a gives

$$\dot{Q} = 2.1192 \times 10^{6} \times \frac{E_\alpha}{T_{\frac{1}{2}} \times A_P} \left(1 + \frac{A_\alpha}{A_D}\right) \qquad 3.5$$

The dependence of the self heat of an isotope upon the α-particle energy and half-life is thus obvious, and a review of these values for the isotopes shown in Table 3.1 now follows. The atomic weights used are on the C_{12} scale.

Plutonium 238

Pu^{238} decays to U^{234} by α-particle emission. Since U^{234} has a half-life of $\sim 2.5 \times 10^{5}$ years, the power output from its α-decay is insignificant. The following half-lives of Pu^{238} can be found in the literature :-

77 yrs - Jaffey and Magnusson (1949),
86.4 (± 0.3) yrs - Hoffman, Ford and Lawrence (1957),
87.5 (± 0.3) yrs - Eicheberger, Grove and Jones (1963),
89.59 (± 0.37) yrs - Jaffey and Lerner (1950),
92 (± 2) yrs - Seaborg, James and Ghiorso (1949).

The first and last are early inaccurate values, and the remaining three lie within (± 1.8%) of each other. The value of 87.5 (± 1.8%) was selected for three reasons; it was the most recent, it was determined calorimetrically and it lies

within 0.5% of the average value of the three more accurate values.

Quoted ground state α-particle energies (E_{α_o}) are :-

5.491 (± 0.0005)MeV - Goldin, Tretyakov and Novikova (1955),

5.495 (± ~ 0.003)MEV - Asaro and Perlman (1954),

5.499 (± 0.0008)MeV - Chin-Fan Leang (1962).

The first value was determined by comparison with Po^{210} as standard using a value of 5.298_4 MeV. Rytz (1960) has suggested that the Po^{210} standard should be 5.304_8 (± .0006) which would increase the first value above to 5.497_5 MeV. A reasonable mean value for E_{α_o} of Pu^{238} would thus be 5.497 MeV (± 0.02%).

Using the best values for Pu^{238} of 87.5 yrs (± 1.8%) for $T_{\frac{1}{2}}$ and 5.497 MeV (± 0.02%) for E_{α_o} in equation 3.5 gives a self-heat of 568.8 mw/gm (± 2.0%). Since from column 4 of Table 3.1, the contribution to the total self heat of our typical sample is ~ 1.4%, then the error in the total self-heat from the uncertainty in Pu^{238} values is $< \pm$ 0.03%.

Plutonium 239

Pu^{239} transforms to U^{235} by α-decay. Since U^{235} has a half-life of ~ 7.1×10^8 years, the power output of this

daughter nuclide is negligible. The literature gives the following half-lives for Pu^{239} :-

24,110 (± 100) yrs - Stout and Jones (1947),

24,181 (± 25) yrs - Oetting (1965),

24,390 (± 30) yrs - Dokuchaev (1959),

24,400 (± 500) yrs - Farwell, Roberts and Wahl (1954),

24,400 (± 70) yrs - Westrum, Hindman and Greenlee (1949),

24,413 (± 30) yrs - Markin (1959).

The first two were determined calorimetrically and in fact result from the same self-heat value of 1.923 mwatts/gm., a different α-particle energy being used in the conversion to $T_{\frac{1}{2}}$ in the two cases (see Oetting (1965)). The remaining four values of $T_{\frac{1}{2}}$ all determined by specific activity methods also show excellent agreement within themselves. An average value of these four of 24,400 (± 0.1%) leads to a self-heat value of 1.906 mwatts/gm., which is ~ 0.9% different from the calorimetric value. Since Pu^{239} contributes ~ 92% to the total self-heat, then such a discrepancy forms a major contribution to the error in calculating the total self-heat. The value of 1.923 mw/gm. has been chosen because it was determined calorimetrically and because the present work supports the choice of this value as compared with 1.906 mw./gm.

It will be seen in the next chapter that during specific heat runs on plutonium metal samples with electrical heat in addition to the self-heat, better agreement was obtained between the specific heat values obtained for runs with and without additional heat, when the higher Pu^{239} contribution was used.

The α-particle energies (E_{α_0}) of Pu^{239} in the literature are :-

5.144 MeV - Chamberlain, Gofman, Segre and Wahl (1947),

5.147 (± 0.0005)MeV - Goldin, Tretyakov and Novikova (1955),

5.150 (± 0.002)MeV - Asaro and Perlman (1952),

5.156 (± 0.0006)MeV - Chin-Fan Leang (1962),

5.157 (± 0.001)MeV - Baranov, Kulakov and Belenky (1963).

The first three are only a selection of the pre-1958 published data which all give values in the range 5.144 - 5.150 MeV. Most are determined relative to Po^{210} and so if the revised value of this standard is used they should be increased by $\sim$ 6.4 keV. The last two are more recent, probably the most accurate, and are not dependent upon the Po^{210} value. Taking a mean of these last two of 5.156_5 MeV with an error of ± 0.12% to take in the corrected earlier values, still gives a small error compared with the spread in $T_{\frac{1}{2}}$ values.

Plutonium 240

Pu^{240} decays to U^{236} by α-emission and again the daughter nuclide has a long half-life ($\sim 2.4 \times 10^7$ yrs) and contributes no appreciable power by its decay. The reported values of $T_{\frac{1}{2}}$ for Pu^{240} are :-

6240 (± 120) yrs - Westrum (1951),

6300 (± 600) yrs - Farwell, Roberts and Wahl (1954),

6580 (± 40) yrs - Inghram, Hess, Fields and Pyle (1951),

6600 (± 100) yrs - Butler, Eastwood, Collins et al.(1956),

6620 (± 50) yrs - Dokuchaev (1959).

Since the last four all agree within their respective quoted accuracies, it was considered reasonable to neglect the first unsupported value and take the mean of the more precise last three values. Thus for Pu^{240}, $T_{\frac{1}{2}}$ = 6600 yrs (± 0.3%).

The ground state α-particle energies (E_{α_o}) for Pu^{240} quoted are :-

5.159 (± 0.0005)MeV - Goldin, Tretyakov and Novikova (1955),

5.162 (± 0.004)MeV - Asaro and Perlman (1952),

5.168 (± 0.0007)MeV - Chin-Fan Leang (1962),

5.169_5(± 0.001)MeV - Baranov, Kulakov and Belenky (1963).

Again corrections of + 6.4 keV are necessary to the first two. Taking the mean of the last two of 5.168_5MeV with an error of ± .06% to include the corrected first two, with the above half-life of 6600 yrs (± 0.3%) leads to a self-heat for Pu^{240} of 7.03_0 mwatts/gm. Since Pu^{240} contributes ~ 6.64% to the total self-heat, then the error in the total self heat from the uncertainties in the Pu^{240} values is < ± 0.03%.

Plutonium 241

Pu^{241} decays by β-emission to Am^{241} for > 99% of its disintegrations. A small percentage (~ 4×10^{-3}%) of Pu^{241} decays by α-emission to U^{237}. Contrary to the previous decay schemes the daughter of the predominant β-decay, namely Am^{241}, is a comparatively powerful heat source.

The β half-life of Pu^{241} has been determined by observing the growth of Am^{241} activity from a plutonium sample of known Pu^{241} content. The β half-life of Pu^{241} is consequently inversely dependent on the half-life assumed for Am^{241}. Correcting the literature values to a common $T_{\frac{1}{2}}$ for Am^{241} of

457.9 yrs (see Section on Am^{241}) produces the following values for $T_{\frac{1}{2}}$ of Pu^{241} :-

13.05 (± 0.3) yrs - Rose and Milstead (1956),

13.3 (± 0.3) yrs - Smith (1961),

13.34 (± 0.24) yrs - Brown, George, Green and Watt (1960),

13.35 (± 0.12) yrs - MacKenzie, Lounsbury and Boyd (1953).

A mean value of these is 13.26 yrs (± 1.1%). However a recent paper by Oetting and Gunn (1967) suggest that the half-life of Am^{241} is 432.7 (± 0.7) yrs, some 5% different from the value used to calculate the above half-lives of Pu^{241}. The resulting mean value is 14.03 yrs for $T_{\frac{1}{2}}$ of Pu^{241}.

The quoted β-spectrum end point energies are :-

20.8 (± 0.2)keV - Shliagin (1956) and (1956a),

20.5 $(^{+1.2}_{-0.3})$keV - Freedman, Wagner and Engelkemeir (1952).

Using the first and a value for the second in the centre of the error band leads to an average value of 20.8$_7$keV (± .75%) for the β end point energy. For calorimetric work the relevant energy of the β-spectrum is the mean energy which is assumed to be 1/3 (end point energy). Thus a mean energy of 6.9$_6$ keV (± .75%) needs a small correction for the 4 x 10^{-3}% of the disintegrations which decay by α-decay of + 0.20$_5$ keV from

E_{a_o} value of 5.051 (Baranov, Gadzhiev, Kulakov et al. (1965)). With the more recent americium half-life giving a Pu^{241} half-life of 14.03 yrs with an error band of ± 5% to include the lower $T_{\frac{1}{2}}$ value, and the above average energy per disintegration of 7.16_5 keV (± 1%) leads to a self-heat value of Pu^{241} of 4.4_9 mwatts/gm (± 6%). Since Pu^{241} only contributes 0.07% to the total self heat of our typical specimen, the error in the total self heat is $< \pm .005\%$ despite the ± 5% uncertainty in the Pu^{241} half life.

Plutonium 242

Pu^{242} decays to U^{238} by α-emission. The daughter nuclide having a half-life $\sim 4.5 \times 10^9$ yrs makes no contribution to the total self-heat. Pu^{242} half-lives given in the literature are :-

3.79 (± 0.05)x10^5 yrs - Butler, Eastwood, Collins et al. (1956a),

3.73 (± .05) x 10^5 yrs - Butler, Lounsbury and Merritt (1956),

3.87 (± .15) x 10^5 yrs - Mech, Diamond, Studier et al. (1956).

All agree reasonably well giving a mean value of 3.80 x 10^5 yrs (± 1.8%).

The ground state α-particle energies for Pu^{242} quoted are :-

4.898 (± .003) MeV - Asaro (1953),

4.898 (± .002) MeV - Hummel (1956),

4.88 (± .02) MeV - Thompson, Street, Ghiorso et al. (1950).

Using the first two more accurate values of 4.898 MeV (± .03%) and the above mean $T_{\frac{1}{2}}$ value of 3.80×10^5 yrs (± 1.8%) gives the self-heat of Pu^{242} as 0.11_3 mwatts/gm (± ~2%). As can be seen from Table 3.1 the small self-heat and low per cent concentration of Pu^{242} make its contribution to the total self heat negligible.

Americium 241

Am^{241} decays by α- emission to Np^{237} which again is a comparatively stable nuclide of half-life ~ 2.2×10^6 yrs, and contributes no appreciable power. The following half-lives of Am^{241} appeared in the literature prior to 1967 :-

457.7 (± 1.8) yrs - Wallman, Graf and Coda (1958),

458.1 (± 0.5) yrs - Hall and Markin (1957),

461.3 (± 1.7) yrs - Hall and Markin (1956),

470 $(^{+5}_{-10})$ yrs - Harvey (1952).

Within themselves these four are in reasonable agreement and a best value would seem to be taken from the average of the first two, i.e., by neglecting the inaccurate 470 yr. value, and preferring the more recent and precise value of the two published by Hall and Markin. Thus 457.9 yrs would appear reasonable.

However the following values were published in 1967 :-

432.7 ($\pm$ 0.7) yrs - Oetting and Gunn (1967),
436.7 ($\pm$ 2.0) yrs - Stone and Hulet (1967).

The former is from accurate calorimetry and the latter from specific activity on part of the same sample. The value of 432.7 years is some 5% lower than the previously accepted value and such a difference seems difficult to resolve (see Oetting and Gunn (1967)).

The majority ($\sim$ 85%) of the α-disintegrations of Am^{241} are to a 59 keV excited state of the daughter, with the result that Am^{241} is considerably more γ-active than the other isotopes discussed. All the γ-radiation is not absorbed by our calorimeters but it is considered, with the low levels of Am^{241} present in our samples, that the fraction not absorbed has a negligible effect on the total self-heat.

The following are the published ground state α-particle

energies (corrected by addition of 59 keV where the E_{α_o} state was not determined) :-

5.534 MeV - Rosenblum, Valaderes and Milstead (1957),
5.535 (± .001)MeV - Asaro and Perlman (1954a),
5.541 (± .0006)MeV - Goldin, Tretyakov and Novikova (1955),
5.545 (± .001)MeV - Baranov, Kulakov and Shatinsky (1964),
(Corrected)5.545 (± .001)MeV - Chin-Fan Leang (1962).

The second and third of these were determined by comparison with Po^{210} and should be increased by 6.4 keV for the revised value of the Po^{210} standard α-energy. The last four will then give an average value of 5.545 MeV (± 0.1%). Using this E_{α_o} value and the half-life of 432.7 yrs (± 5% to include the higher $T_{\frac{1}{2}}$ value of 457.9 years) gives a self-heat value of 114.5 mwatts/gm (± 5.1%) for Am^{241}. Since its contribution to the total self-heat is only ~ 0.07% even the ± 5.1% uncertainty leads to an uncertainty in the total self heat of < ± 0.005%.

The Am^{241} content of a sample results not only from the initial americium impurity level but also from the Pu^{241} β-decay. Since Am^{241} has a comparatively high self-heat, the total self heat of a sample will change as the Pu^{241} content decreases and the Am^{241} content builds up. The Pu^{241} and

Am^{241} percentage contents must be accompanied by a date on which the analysis was carried out, such that corrections may be applied for the change in relative contents that occur between the times of analysis and specific heat determination. In the case of Pu6 the Am^{241} build up is $\sim$ 1.4 ppm/month; for comparison the corresponding build up for Pu3 and Pu4 are 3.3 and 4.7 ppm/month respectively due to the slightly higher Pu^{241} content of these samples.

On the question of analysis the accuracy of determination of the percentage contents of the radio-active isotopes present is obviously a source of error in totalling the individual self-heats. Accuracy limits from the mass and α-kick spectrometry and radiochemical analyses carried out at A.E.R.E. Harwell on the plutonium metal samples are quite wide, viz., $< \pm$ 1% for Pu^{239}, a few per cent for Pu^{240} and Pu^{241} and $\sim$ 10 - 20% for Am^{241} and Pu^{238}. Similar analyses were also carried out in the U.S.A. before shipment of the plutonium metal. Agreement between these two completely independent analyses was in fact considerably better than the conservative accuracies quoted above, e.g., $\sim$ 0.01% for Pu^{239}, $\sim$ 0.4% for Pu^{240}. If one takes such agreement as representative of the accuracy of the analyses then the effect

on the calculation of the total self heat of a typical sample is within ± 0.1%.

In summary therefore in so far as the literature values of $T_{\frac{1}{2}}$ and E_{α_0} allow one to calculate the total self-heat of our typical sample of plutonium, all the isotopes considered except Pu^{239} lead to a maximum error of $< \pm 0.1\%$. This is small in comparison with the 0.9% difference between the two possible values of the self-heat of Pu^{239}. Although our work would seem to favour the higher self-heat value of Pu^{239}, this remains the largest uncertainty in the calculation of the total self-heat.

The previous discussion in this section has been concerned with the self-heats of the various plutonium isotopes together with the radio-active impurity Am^{241}. These are directly relevant to the calculation of the total self heat of the plutonium metal samples and plutonium compounds studied. The remaining sample studied was neptunium metal.

Neptunium 237

The only isotope of neptunium which contributes to the total self-heat of a neptunium sample is Np^{237}, which decays

by a-emission to Pa^{233}.

The literature quotes for the half-life of Np^{237} :-

2.20×10^6 yrs (± 0.4%) - Magnusson and La Chappelle (1948),

2.14×10^6 yrs - Brauer, Stromatt, Ludwick et al. (1960),

and for the ground state a-particle energy (E_{a_o}) :-

4.871 MeV - Asaro, Stephens and Perlman (1957) (unpublished, reported in Lederer, Hollander and Perlman (1967)),

4.867 (± .002)MeV - Kondratev, Novikova, Vorobev et al. (1956),

4.872 MeV - Magnusson, Engelkemeir, Freedman et al.(1955),

4.872 (± .001)MeV - Baranov, Kulakov, Samoilov et al. (1962).

Using an average value of 4.871 MeV (± .08%) and the average $T_{\frac{1}{2}}$ value(of 2.17×10^6 yrs (± 0.7%)) leads to a self heat value of 0.0204_1 mwatts/gm (± 0.8%).

With such a small self heat value obviously small percentages of plutonium isotopes present as impurities will make a significant contribution to the total self-heat. The analysis and total self-heat of the neptunium sample studied is given in the next chapter when presenting the specific heat results.

3.2 Thermal Capacity of the Calorimeters

Several calorimeters were used in the specific heat determinations presented in the next chapter. Early work on plutonium metal, viz, Pu3 and Pu4 employed calorimeters constructed from oxygen-free, high-conductivity copper, whereas the later work on Pu6 and plutonium carbide employed a 99.99% silver calorimeter. The small amount of neptunium available necessitated the use of a silver calorimeter of smaller scale than the above. Great care was taken throughout the assembly of the calorimeters to determine the weights, to an accuracy of $\pm$ 0.1 mgm., of not only the parts made from copper or silver, but also the small amounts of additional materials used such as Wood's Metal, Soft Solder, Araldite and manganin (or in some cases, constantan).

The relative weights of these materials in a typical calorimeter are shown in Table 3.2, together with the relative percentage contribution to the total weight (third column). The simplicity of the calorimeters, combined with the use of thermocouples as temperature measuring elements, allow the total weight of additional materials to be kept small ($\sim$ 3.2%) in comparison with the major constituent, silver. Also the weights of all the additional materials can be

TABLE 3.2

WEIGHTS OF COMPONENT MATERIALS OF Pu6 SILVER CALORIMETER

Material	Weights gms.	% of total weight	% of total thermal capacity at temperatures of :- 20°K	50°K	100°K	300°K
Silver	12.051_9	96.76	93.22	96.95	97.06	96.63
Copper	0.060_2	0.48	0.23	0.45	0.66	0.79
Manganin	0.034_7	0.28	0.06	0.11	0.31	0.54
Araldite	0.015_3	0.12	0.53	0.22	0.24	0.49
Woods Metal	0.2938	2.36	5.96	2.27	1.73	1.55

assigned accurately and therefore accounted for in the calculated total thermal capacity of the calorimeter, since it is reasonable to neglect the weight of the thermocouple leads themselves, provided the small beads of Wood's Metal, to which the thermocouple junctions are soldered, is included.

The literature was again consulted for values of the specific heat of the component materials and the reviews of Landholt and Börnstein (1961), Johnson (1961, Ed.) and Corruccini and Gniewek (1960) were found useful in this respect. The specific heat values of the major component, silver, (and copper for the earlier calorimeters) which corresponded to the purity of the materials used, were selected from the literature. These turned out to be virtually identical, over the temperature range 10 - 300°K, to the values recommended by Corruccini and Gniewek (1960). The alloys of manganin and Wood's Metal (and of constantan and Soft Solder, when used) were taken from the literature, where available, or estimated by the Kopp-Neumann rule from their constituents over the temperature ranges that values were not available. The specific heat values for the Araldite used were estimated from the literature data below 20°K, and from its room temperature value; the shape of the curve between these two temperatures was made similar to that of another

organic material PTFE, whose low temperature and room temperature values are very similar.

Using these specific heat values, the contributions of the various components to the total thermal capacity was calculated. The relative percentages at temperatures of 20, 50, 100 and 300 ^{o}K are shown in columns 4 - 7 of Table 3.2. Only at the lower temperature of 20^{o}K are the percentage contributions to the total thermal capacity significantly different from the weight percentages, due to the larger specific heat values of Araldite and Wood's Metal.

The above method of estimation of specific heat values of the additional materials should be accurate to within $\pm$ 5%, probably within $\pm$ 2.5%. With the small amounts of these substances present, the contribution to the accuracy of the total thermal capacity even with an error of $\pm$ 5% is still within the accuracy of the quoted values for the major component, silver. This is $\pm$ 0.5% below 40^{o}K and $\pm$ 0.2% above 40^{o}K, which thus determines the accuracy with which the total thermal capacity can be calculated.

To check the validity of such calculated thermal capacities, the calorimeter considered above, Pu6 silver calorimeter, was determined experimentally. The weight of Wood's Metal was made exactly the same as during the specific heat runs on Pu6, by addition or subtraction of a small amount

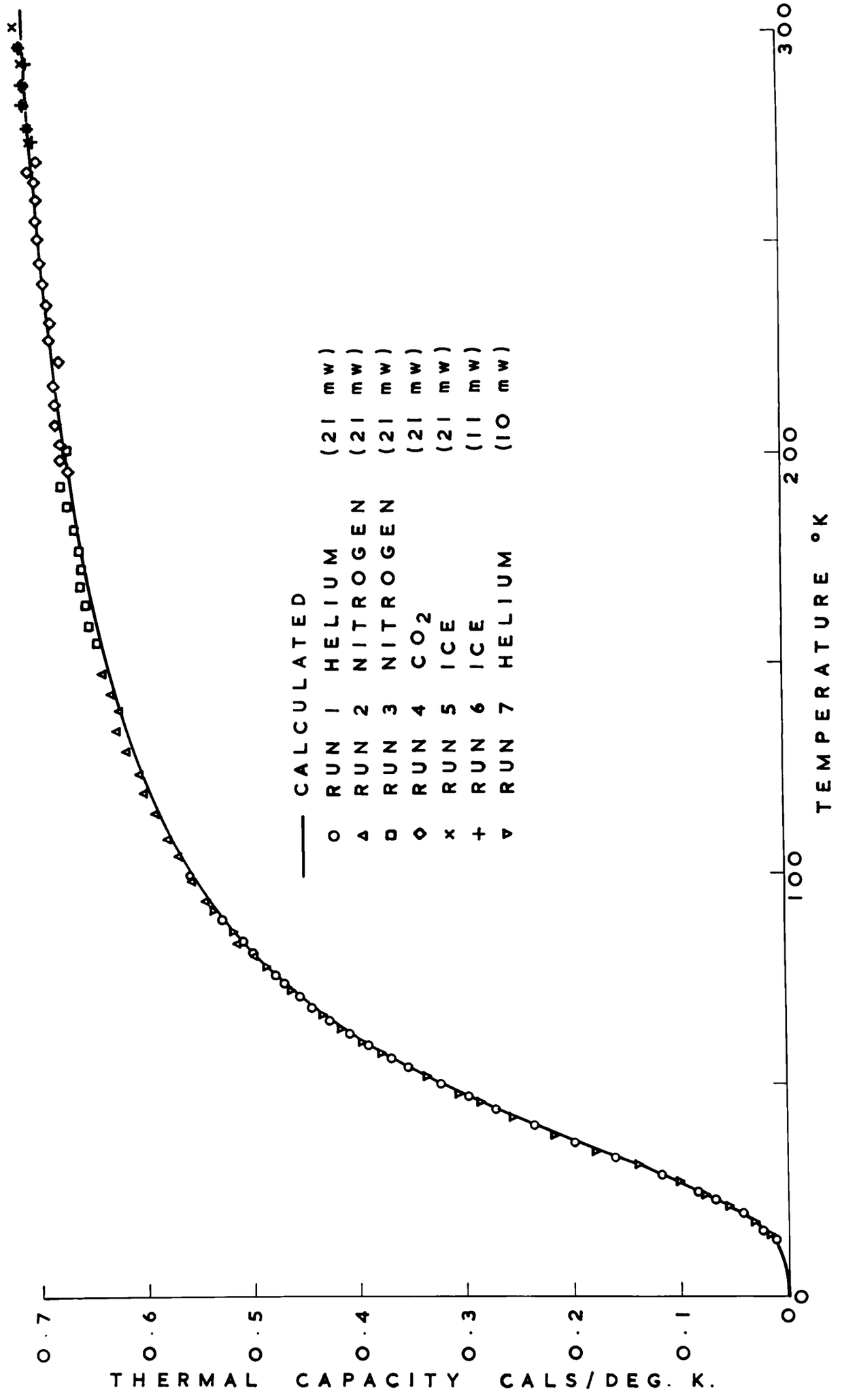


FIG. 3.1 THERMAL CAPACITY OF Pu 6 SILVER CALORIMETER

of Wood's Metal to the calorimeter lid joint, which was remade during de-canning of the specimen. Helium, nitrogen, CO_2 and ice runs were carried out on the empty calorimeter with power inputs of $\sim$ 21 mwatts to the calorimeter heater. Such power levels produced rates of rise of temperature, which were comparable to those used in the plutonium metal specific heat runs. Power inputs of $\sim$ 21 mwatts corresponded to rates of rise of temperature of :-

$\sim$ 3.22, 0.86, 0.55, 0.43 degrees/min.

at temperatures of :-

$\sim$ 25, 50, 90, 300 ^{o}K.

Further helium and ice runs were carried out with power levels of $\sim$ 10.5 mwatts, i.e., half the above rates.

The results of these runs are shown in Figure 3.1, in which the curve drawn is that corresponding to the calculated thermal capacity as described above. The good agreement between helium and ice runs, with rates of rise of temperature differing by a factor of $\sim$ 2, can clearly be seen, as well as the overall agreement between calculated and experimental values within an average of $\pm$ 1% up to 40^{o}K and $\pm$ 0.5% above 40^{o}K.

In view of the fact that in the earlier calorimeters the major component, copper, similarly formed $\sim$ 96.3 and 95.2% of the total weight, (even in the smaller neptunium calorimeter the silver still formed $\sim$ 93.3% of the total weight) it is considered justifiable to use the calculated total thermal capacity for all the other calorimeters without introducing any errors in excess of the above accuracies.

3.3 Additional Data for Specific Heat Analysis

The first stage in the analysis of the experimentally determined molar specific heat at constant pressure (C_p) is the reduction to the molar specific heat at constant volume (C_V), by subtraction of the dilation term ($C_p - C_V$).

The dilation term can be derived from the following thermodynamic formulae :-

$$C_p = \left(\frac{dQ}{dT}\right)_p = T\left(\frac{\partial S}{\partial T}\right)_p ,$$

$$C_V = \left(\frac{dQ}{dT}\right)_V = T\left(\frac{\partial S}{\partial T}\right)_V ,$$

and Maxwell's relations. The result is that :-

$$C_P - C_V = - T \left(\frac{\partial V}{\partial T} \right)_P^2 \left(\frac{\partial P}{\partial V} \right)_T \qquad 3.6$$

The volume coefficient of expansion, β, is given by :-

$$\beta = \frac{1}{V} \left(\frac{\partial V}{\partial T} \right)_P$$

and for a polycrystalline substance

$$\beta = 3\alpha_L$$

where α_L is the mean linear coefficient of expansion. Further the isothermal bulk modulus, K_T, is given by

$$K_T = - V \left(\frac{\partial P}{\partial V} \right)_T .$$

Thus substituting α_L and K_T in equation 3.6 gives

$$C_P - C_V = 9\alpha_L^2 K_T T V \qquad 3.7$$

The bulk modulus normally measured by velocity of sound measurements is the adiabatic bulk modulus, K_S. The correction

of K_S to K_T can be derived using the further thermodynamic result that

$$\frac{C_P}{C_V} = \frac{K_S}{K_T} \qquad 3.8$$

Eliminating C_V from equations 3.7 and 3.8 leads to :-

$$K_T = \left[\frac{1}{K_S} + \frac{9\alpha_L^2 T V}{C_P} \right]^{-1} \qquad 3.9$$

from which the isothermal bulk modulus can be calculated.

It can be seen from equations 3.7 and 3.9 that in order to calculate $(C_P - C_V)$ exactly a tremendous amount of data is needed. The complete temperature dependence of the molar volume, linear expansion coefficient and adiabatic bulk modulus are required besides C_P, and this data is not always available. Under such conditions, approximate relations are used and the most successful one is the Nernst-Lindemann relation based on Grüneisen's equation of state. From equation 3.7

$$C_P - C_V = \frac{9\alpha_L^2 K_T V}{C_P^2} \cdot C_P^2 T$$

Denoting $\frac{9\alpha_L^2 K_T V}{C_P^2}$ by the parameter, A, leads to

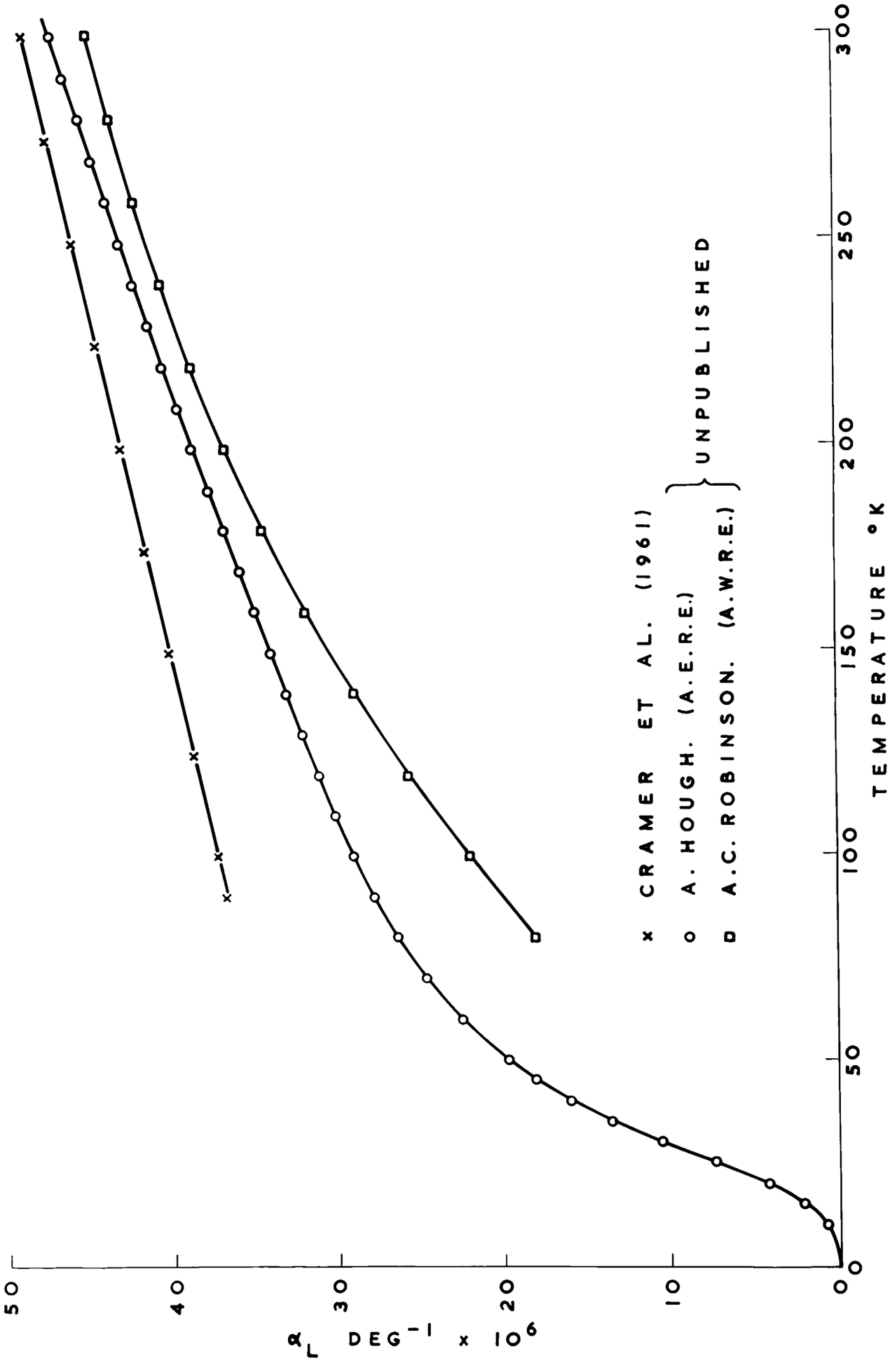


FIG. 3.2 LINEAR EXPANSION COEFFICIENT (α_L) OF α – Pu

$$C_P - C_V = A\,T\,C_P^2 \qquad 3.10$$

The parameter, A, has been found experimentally to be nearly constant over a wide range of temperature for a large number of substances. If A is calculated from the values V, α_L, K_T at any one temperature, usually room temperature, it may be used to calculate $C_P - C_V$ over a wide range of temperature without serious error.

A summary of the data available, from which $(C_P - C_V)$ for the specimens investigated can be calculated, will now follow.

3.3. 1 Expansion Coefficient

For α-plutonium several authors have reported work on the length changes below room temperature but only two quote values of the linear expansion coefficient (α_L), which are not averaged over appreciable temperature intervals. Cramer, Hawes, Miner et al. (1961) quote α_L from 90°K to room temperature and Robinson (1964) from 80 to 300°K. These are shown in Figure 3.2 and can be seen to differ quite markedly, the difference being ± 5% about a mean value at 300°K and ± 25% at 100°K. Considerable differences were also found in the length change determinations by earlier workers on different samples of somewhat impure plutonium.

Since the values of α_L for α-Pu are large being $\sim 47 \times 10^{-6}$ per deg. at 300°K, compared with copper of $\sim 17 \times 10^{-6}$ and silver of $\sim 19 \times 10^{-6}$, the magnitude of $(C_p - C_v)$ which is dependent upon α_L^2 is also going to be large ($\sim$ 1 cal/mole/deg. at 300°K). Thus discrepancies of the order mentioned above will effect the accuracy of the derived C_v considerably.

It was therefore decided that the measurement of α_L of α-Pu of a similar purity to that used in the specific heat work, ought to be attempted. Members of the physical properties group at A.E.R.E. Harwell had recently been investigating the low temperature thermal expansion of α-U (see Hough, Marples, Mortimer and Lee (1968)), and we are indebted to the assistance of A. Hough in extending these measurements to α-Pu.

The method involved a simple push-rod dilatometer. The specimen in the form of a hollow cylinder $\sim$ 1" long and 0.15" outer diameter rested in the bottom of a closed-ended silica tube 20" long. A silica push rod resting on top of the specimen communicated its expansion to a Sogenique variable-capacitance transducer clamped to the top of the silica tube. The transducer was sensitive to $\sim \pm$ 1 μin. The silica tube was surrounded by a cryogenic stainless-steel tube with copper end cap, in the specimen region. The outer

tube formed a vacuum-tight enclosure around the silica tube. It thus not only formed an activity seal but also enabled the enclosure to be evacuated and then filled with helium exchange gas, which was maintained at a slight over-pressure by means of a football bladder. Slots were cut in the sides of the silica tube opposite the specimen to allow access of the exchange gas. The lower part of the assembly was surrounded by the normal double glass-dewar system.

By controlled syphoning of cold helium gas or liquid into the inner dewar, or, after filling with liquid helium such that equilibrium was attained, by allowing the specimen to warm back up to room temperature as the liquid evaporates away, dynamic measurements of the length change, during both cooling and warming between 4.2°K and 300°K, could be achieved.

Temperatures were measured with a Au - 2.1 $^{at}/_{o}$ Co v. 'normal silver' thermocouple with its measuring junction pressed against the centre of the inside of the hollow specimen.

Large scale graphical plots of the length change against temperature were made for both cooling and warming runs. From the best smooth curve through such plots for each run, length increments (Δl) for 5°K temperature intervals were taken and the expansion coefficient (α_L) calculated from :-

$$\alpha_L = \frac{1}{\ell_{300}} \left(\frac{\Delta \ell}{\Delta T} \right)$$

where ℓ_{300} is the length of the specimen at room temperature. The best smooth curve through the α_L v. T plots, for a specimen of high purity α-Pu from the same stock as Pu4, are shown in Figure 3.2.

The expansion coefficient of α-Pu from the present work lies between the other published data shown, and has a value of $\sim 47 \times 10^{-6}$ per deg. at 300°K, $\sim 29 \times 10^{-6}$ per deg. at 100°K and falls rapidly to zero below ~ 50°K. The overall accuracy of these measurements based on the sensitivity of detection of length changes, the scatter of α_L values resulting from the several runs and the small but finite expansion coefficient of the silica (within $\sim \pm 0.5 \times 10^{-6}$ per deg.) is estimated to be within ± 10% below 40°K, ± 5% between 40°K and 100°K and ± 2.5% above 100°K.

The expansion coefficient, α_L, is related to C_V by the Grüneisen expression (see for example, Mott and Jones (1936)):-

$$3\alpha_L = \frac{\gamma \ C_V}{K_T \ V}$$

where the proportionality constant, γ, is known as Grüneisen's constant. The Grüneisen relation is derived on the basis of

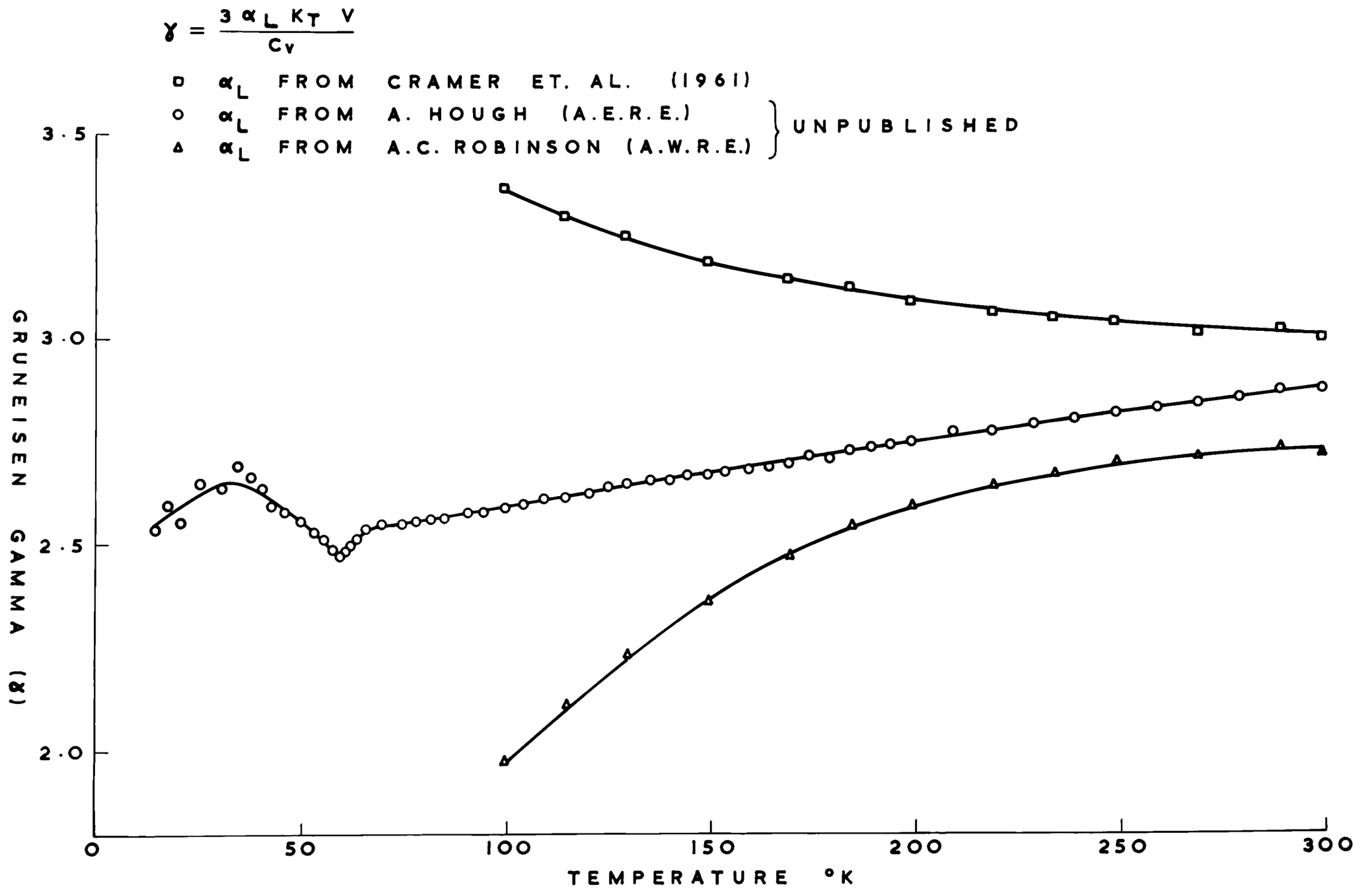


FIG. 3.3 GRUNEISEN GAMMA VARIATION FOR EXPANSION DATA

certain assumptions and is not necessarily valid at all temperatures (see Bijl and Pullan (1955) and Barron (1957)). At normal temperatures ($> 0.3\ \theta_E$) however γ is sensibly constant, and the value for many elements is in the range 1.5 - 2.5.

In Figure 3.3, the values of Grüneisen's constant γ as given by :-

$$\gamma = \frac{3\alpha_L K_T V}{C_V}$$

are plotted for the three sets of data of α_L shown in Figure 3.2, using C_V values of Pu6 and K_T values described in the next section. Justification for the α_L values determined as described above, in comparison with the other published α_L data, is clearly shown in that they produce a reasonably temperature-independent γ, which varies from ~ 2.5 at $70^{\circ}K$ to 2.75 at $300^{\circ}K$. The dip in γ centred at $\sim 60^{\circ}K$ is due to the small 'excess' found in the specific heat values (see next chapter) and the maximum below $50^{\circ}K$ is not considered genuine being well within the high experimental error ($\sim \pm 12\%$) in this region.

In the case of neptunium, the published data is very limited, only average values of α_L over the temperature

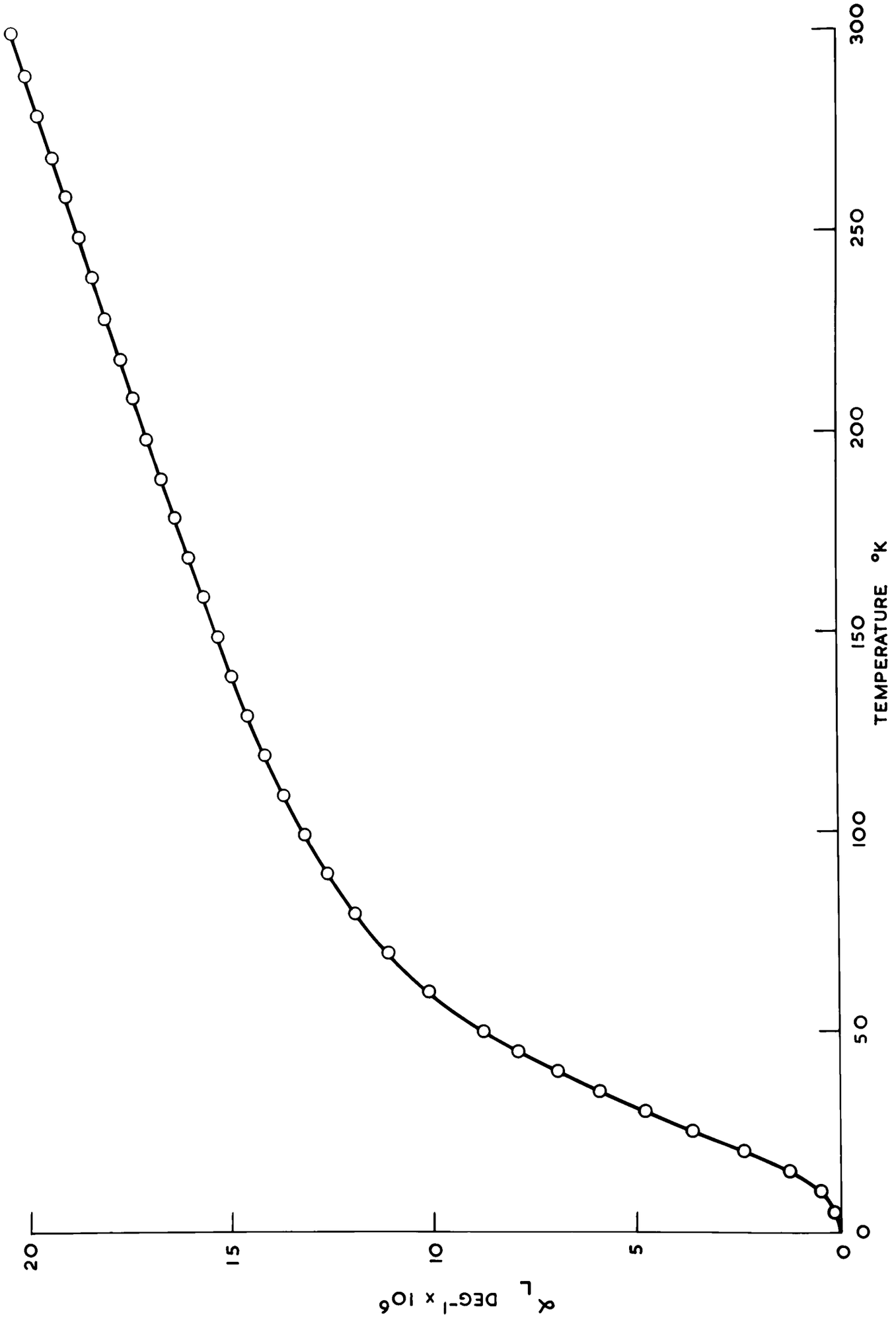


FIG. 3·4 LINEAR EXPANSION COEFFICIENT (α_L) OF α-Np.

interval 20 - 275°C being available (Zachariasen (1952)).

The expansion coefficient, α_L, was therefore measured for α-neptunium by the same technique as used for α-Pu. In the case of Np however owing to the small amount of metal available, the length of the specimen was only ~ 0.2". The errors in α_L were therefore further increased to ~ ± 20 - 25% below 100°K and ~ ± 10% above. The smoothed values obtained from several runs are shown in Figure 3.4, showing the expansion coefficient rises to a value of ~ 20 x 10^{-6} per deg. at 300°K. A Grüneisen constant, γ, value of ~ 1.8 at 300°K is indicated from the present α_L value and the bulk modulus value described in the next section.

The expansion coefficient of α-Np is considerably less than that of α-Pu and consequently the Grüneisen gamma is nearer to the expected value.

In the case of plutonium carbide no expansion coefficient data has been published below room temperature. Three authors, Pallmer (1962), Kruger (1962), and Ogard, Land and Leary (1965) quote average values of α_L between 20 - ~ 850 °C, for carbon compositions in the range 45.8 - 50.4 at/o, and show reasonable agreement between 10.0 - 11.0 x 10^{-6} per deg. Only the last reference quotes a relation between length and

temperature from which a value of α_L at room temperature can be calculated. This is 8.4×10^{-6} per deg. for a carbon composition of 45.8 at/c.

3.3. 2 Elastic Constants

The bulk modulus (K) values required for the calculation of $(C_p - C_v)$ are obtained from the published values of Youngs Modulus (E) and Rigidity Modulus (G), using the well-known relations between the elastic constants :-

$$\sigma = 1 - \frac{E}{2G} \; ; \quad K = \frac{E}{3(1-2\sigma)} \; ; \quad E = \frac{9KG}{G + 3K} \qquad 3.11$$

where σ is Poisson's ratio.

The only published data on the elastic moduli of α-Pu below room temperature are by Lallement (1963) and Linford (1964). The former gives values of E in the range 10 - 300°K (E = 9.4 at 300°K) and the single value of σ, by dispersion, of ~ 0.23 at 300°K; no density or purity figures are quoted. Linford quotes E between 20 - 300°K (E = 9.99 at 300°K) and values of σ, again by dispersion, of 0.18 at 300°K and ~ 0.17 at 78°K, on a plutonium sample of density 19.65 gm/c.c. Apart from the $\sim 5\%$ difference in values of E, (comparable

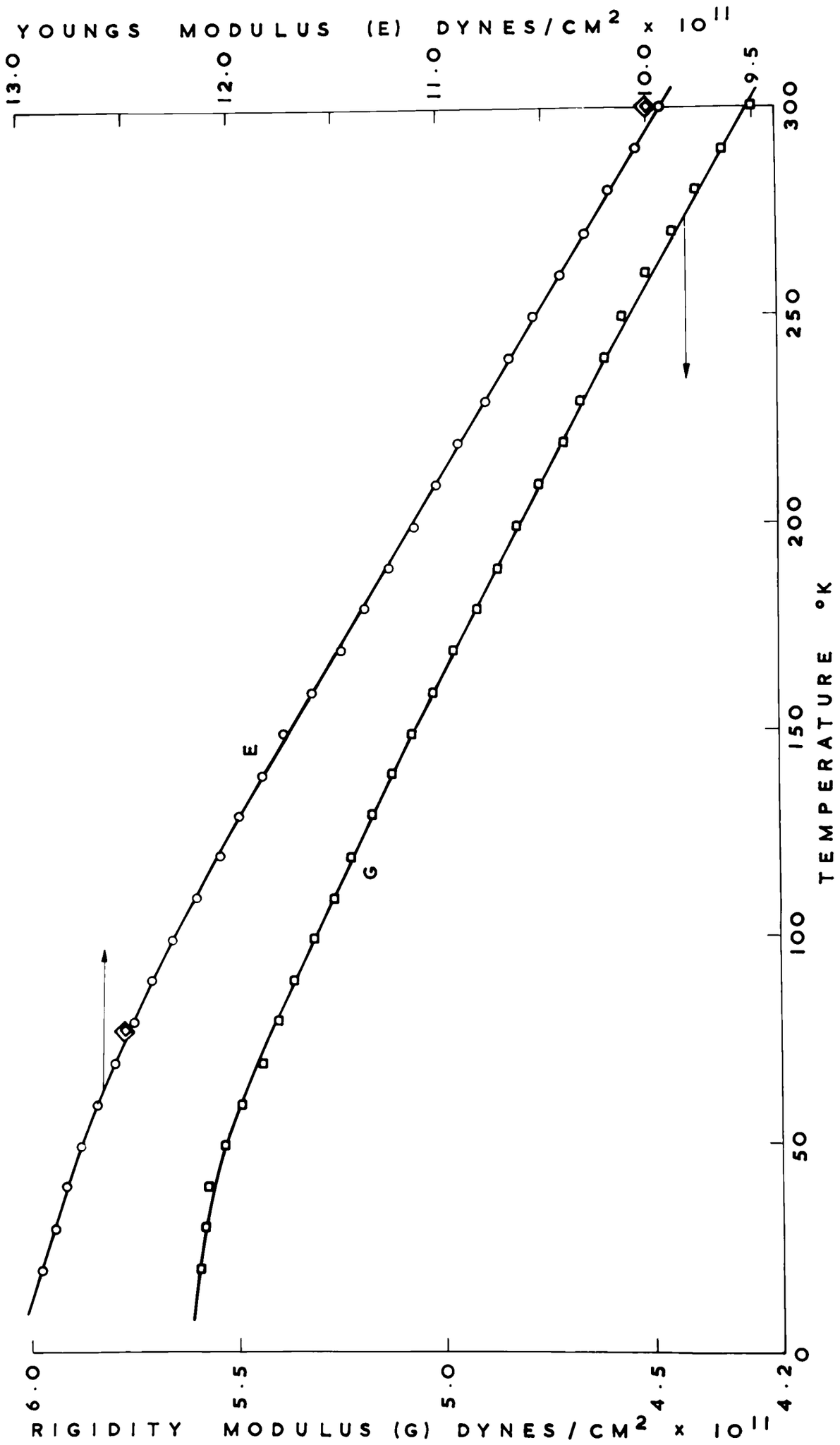


FIG. 3.5 ELASTIC MODULI OF α - PLUTONIUM

differences have been reported by Kay and Linford (1960) in room temperature values for specimens of differing densities) the most striking difference in these two determinations is that whereas Linford obtains a smooth temperature variation of E, Lallement sees a marked minimum of $\sim 3\%$ between 50 and 60°K.

Despite the possible correspondence between this minimum and the small excess seen in the present work on specific heat at $\sim 60^{\circ}K$, the work of Linford has been used to calculate $(C_p - C_v)$ for the following reasons :-

a) a 3% minimum in $(C_p - C_v)$ at 60°K would only produce a 0.03% maximum in the derivations of C_v since $C_p - C_v$ is only $\sim 1\%$ of C_p at this temperature.

b) Linford's work is on material of comparable density to all our α-Pu samples.

c) a private communication (Linford (1968)) for which we are greatly indebted, contained more recent and accurate values of E together with values of the rigidity modulus, G (previously unpublished) over the range 20 - 300°K. These values are plotted in Figure 3.5, and again show smooth temperature variations. Figure 3.6 shows the values of bulk modulus (K) and Poisson's ratio (σ), derived from the E and G values

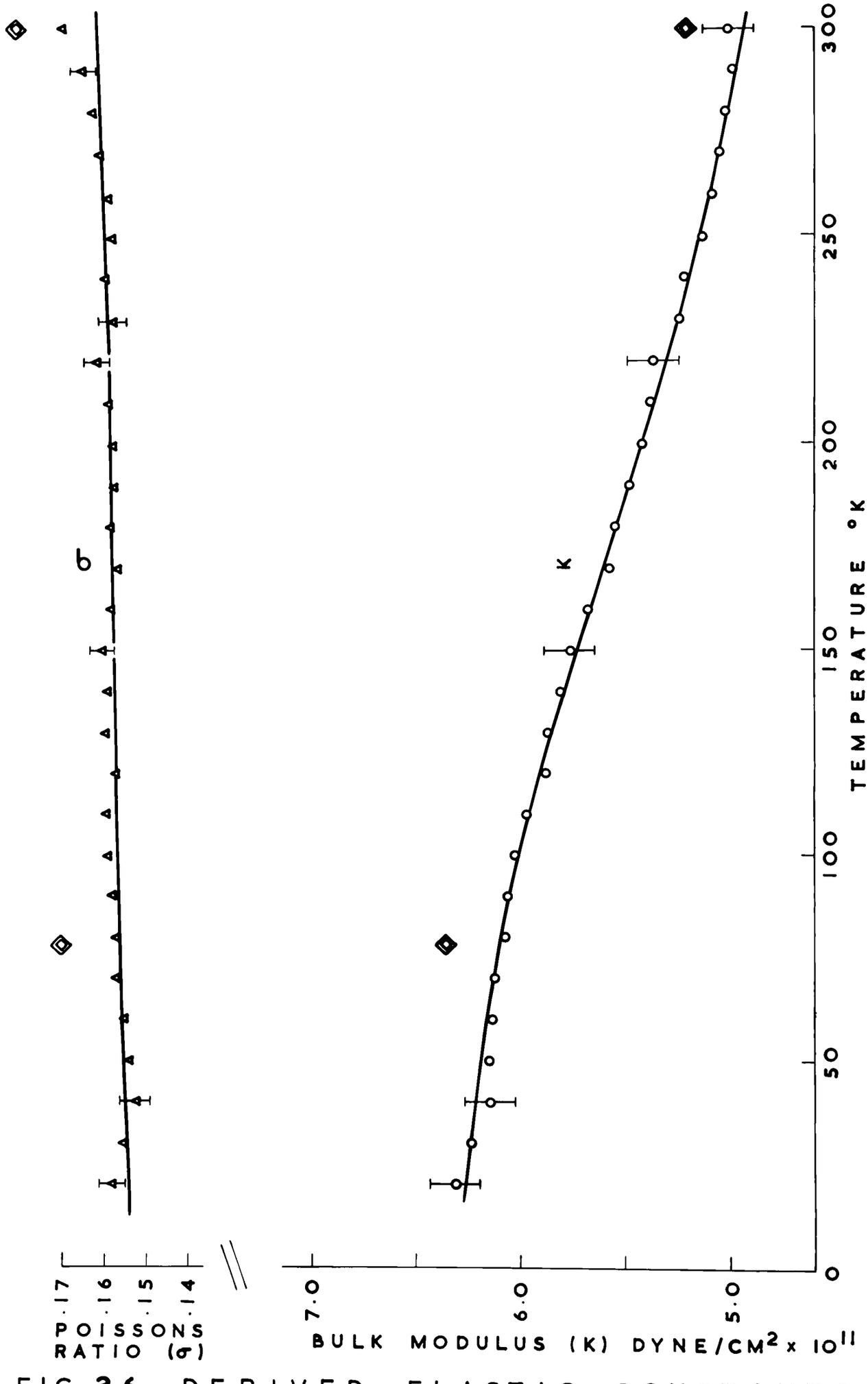


FIG. 3.6 DERIVED ELASTIC CONSTANTS OF α-PLUTONIUM

of Figure 3.5, by means of equations 3.11. The points shown by the "double-diamond" symbol on both Figures 3.5 and 3.6 are those derived from the published work of Linford (1964).

The difference in K is almost entirely due to the different value of σ used in the two cases; one is determined by dispersion and used with E to calculate K; the other is derived from the determined values of E and G.

The accuracy of the derived values of K (and of σ) are estimated by Linford to be about ± 2%.

The extensive temperature variation of the elastic constants of α-Pu allow the Debye theta corresponding to the elastic constants to be calculated and to obtain a reasonable extrapolation to absolute zero. According to lattice theories this should be identical to Θ_D derived from the thermal data as $T \rightarrow 0$.

From the Debye treatment of a lattice, that it is analogous to a continuous, isotropic and elastic solid, in so far as the distributions of frequencies, which result from the propagation of sound waves of permitted wavelengths, is concerned, the cut-off frequency, $_D$, is given by :-

$$\frac{4\pi V}{3}\left(\frac{1}{c_L^3}+\frac{2}{c_T^3}\right)\ _D^3 = 3N$$

where c_L and c_T are the velocities of longitudinal and transverse sound waves.

Since $k\,\theta_D = h\,\nu_D$, then

$$\theta_D = \frac{h}{k}\left[\frac{4\pi V}{9N}\left(\frac{1}{c_L^3} + \frac{2}{c_T^3}\right)\right]^{-1/3}$$

Now c_L and c_T can be expressed in terms of the adiabatic bulk modulus (K_S) and Poisson's ratio (σ) in the form :-

$$c_L^2 = \frac{3(1-\sigma)\,K_S}{(1+\sigma)\,\rho} \quad \text{and} \quad c_T^2 = \frac{3(1-\sigma)\,K_S}{2(1+\sigma)\,\rho}$$

Thus θ_D can be expressed in the form :-

$$\theta_D = \frac{3.626 \times 10^{-3} \times K_S^{1/2}}{A^{1/3} \times \rho^{1/6} \times [f(\sigma)]^{1/3}} \qquad 3.12$$

where $f(\sigma) = 2\left[\frac{2(1+\sigma)}{3(1-2\sigma)}\right]^{3/2} + \left[\frac{1+\sigma}{3(1-\sigma)}\right]^{3/2}$

and A is the atomic weight, and ρ the density.

Using the values of K_S and σ for α-Pu shown in Figure 3.6, in equation 3.12, the Debye theta, corresponding to the elastic constants (θ_{EL}), results in an approximately linear

variation in θ_{EL} from a value of 180 at 300°K to 200 at 100°K, becoming less temperature dependent below 100°K, and extrapolating to a value of 206 at 0°K.

The elastic constants data available on plutonium carbide and neptunium is considerably less extensive.

No data at all could be found on plutonium carbide even at room temperature or above. A suggestion of the values of E and σ can possibly be gained from the work of the most closely related and iso-structural carbide, uranium carbide.

Graham and Chang (1964) found that with single crystals of UC, K has the value of 16.36 (± .04) x 10^{11} dynes/cm^2 and σ is 0.287 (± 0.010). Hall (1967) on polycrystalline samples found that E was in the range 15.28 - 18.81 x 10^{11} dynes/cm^2 for samples of different carbon composition and porosity. Also for a carbon content of 48.4 at/o, K was equal to 15.52 x 10^{11} dynes/cm^2 and σ = 0.297.

In the case of neptunium, the only published data is from the high pressure work of Stephens (1966), which gives the single value of the isothermal compressibility (at room temperature) at 1 atmosphere of 0.00136 kb^{-1}. This is equivalent to a bulk modulus of 7.46 x 10^{11} dynes/cm^2.

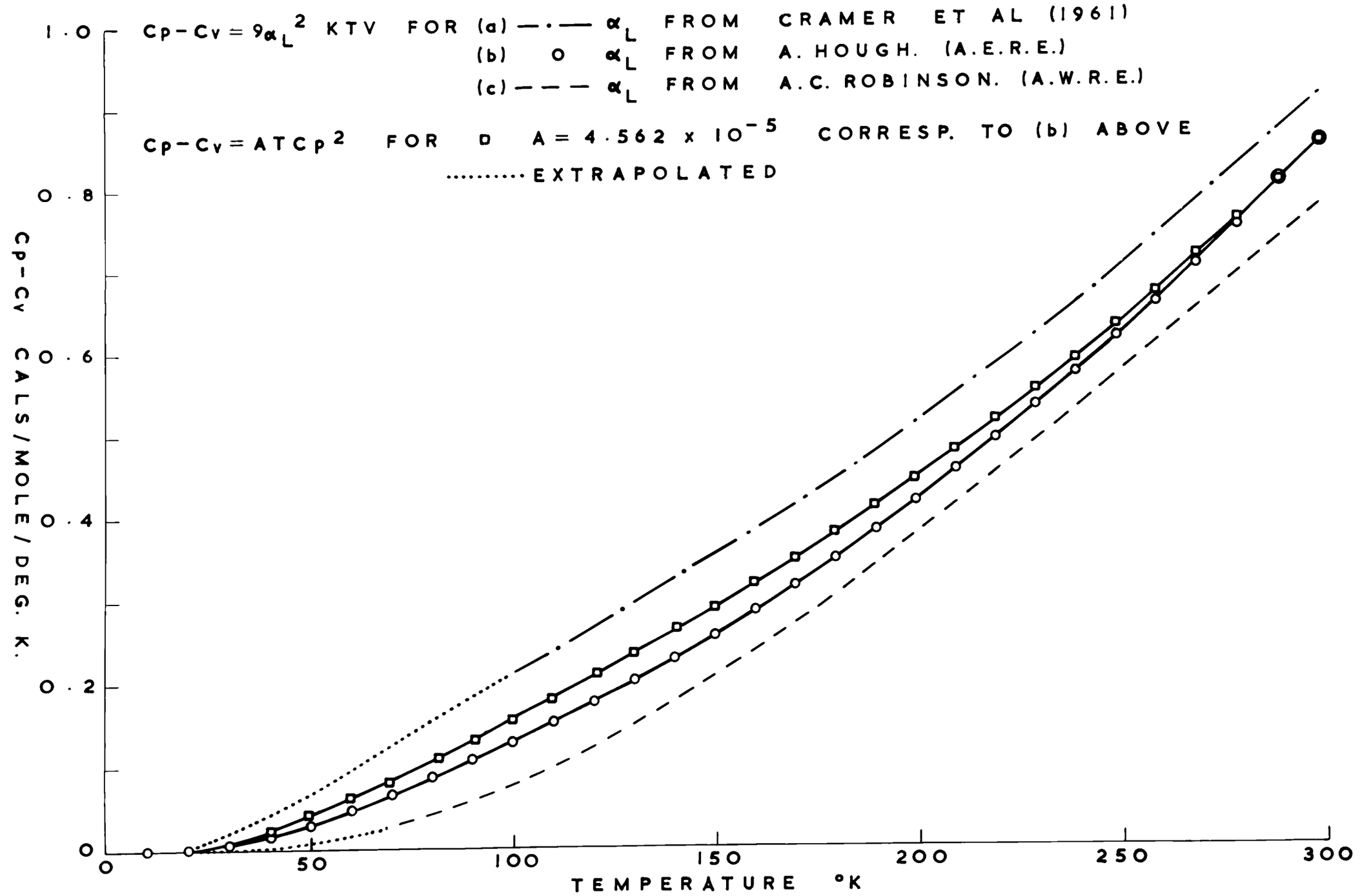


FIG. 3.7 DILATION TERM ($C_p - C_v$) FOR α-Pu

3.3.3 Dilation Term

For α-Pu the dilation term ($C_P - C_V$) has been calculated from 20 - 300°K, from equation 3.7 using the expansion coefficients (a_L) and isothermal bulk modulus (K_T), corrected from K_S by equation 3.9, described in the last two sections. The experimentally determined density was used in the molar volume corrected for expansion, since this was the value corresponding to the determined a_L and K_T.

The values of $C_P - C_V$ so calculated are shown in Figure 3.7, corresponding to the three sets of data for a_L shown in Figure 3.2. $C_P - C_V$ is in general high and rises to a value of $\sim$ 0.85 cals/mole/°K at 300°K. At 100, 200 and 300 °K, $C_P - C_V$ contributes $\sim$ 2.5, 6 and 11% respectively to C_P.

Also shown in Figure 3.7 are the values of $C_P - C_V$ obtained using equation 3.10, where A has the value 4.562×10^{-5} and was determined using the a_L at room temperature from the present work.

For plutonium carbide it is not possible to determine $C_P - C_V$ because of the lack of data on the bulk modulus. If PuC is assumed to have a value of K_S similar to UC, namely $\sim 16 \times 10^{11}$ dynes/cm^2, the resulting value of $C_P - C_V$ at 300°K is $\sim$ 0.14 cals/mole/°K, using the room temperature a_L.

Since the mechanical properties undoubtedly differ, this must necessarily only be a crude estimation. It however is much smaller than for α-Pu, due mainly to the much smaller expansion coefficient and forms approximately 1% of the C_p value at 300°K.

For neptunium, the value of $C_p - C_v$ at 300°K is $\sim 0.22_4$ cals./mole/°K, using the present value of α_L and the single available value of bulk modulus at room temperature. This is $\sim 3\%$ of C_p at 300°K and the resulting value of A in the expression $C_p - C_v = A\ T\ C_p^2$ is $1.33_9 \times 10^{-5}$.

3.4 Estimation of Errors in Relation to Method of Evaluation

Some mention has been made during Chapter 2 of the accuracies of various components of the equipment but a summary of their combined effect of the measurement of specific heat has been left until after the further contributing factors of the calculation of self heat and calorimeter thermal capacity determination were discussed.

Consider first the errors in the rate of rise of temperature. The measuring system provides approximately

100 thermocouple voltage readings for each degree rise in temperature, and each voltage can be measured to an absolute accuracy of $\pm$ .05 μV ahd has a relative scatter of $\pm$ .03 μV. The large number of voltage readings enables a number ($\sim$ 10) of values of the increment in thermocouple voltage, corresponding to approximately one degree intervals, to be taken, each increment having the same mid-point value. The effect of the relative scatter is thus reduced by a factor of $\sim 1/\sqrt{10}$ and the accuracy of measurement of such increments, which vary between $\sim$ 10 and 50 μV over the range of measurement, is $\pm$ 0.2% under the worst conditions. Change in absolute accuracy should not be appreciable over the time taken for such increments, though it still determines the accuracy of the mid-point value. The error in the time interval between voltage readings is insignificant, and so the rate of rise in thermocouple voltage has the same accuracy of $\pm$ 0.2%.

The thermocouple calibration was found to have an average deviation from a smooth power series curve of $\pm$ 0.05°K to 0.02°K over the temperature range 10 - 300°K, and the smooth curve is probably within $\pm$ 0.02°K of the thermodynamic scale. Smoothed thermoelectric power values from the calibration are smooth to within $\pm$ 0.2% and a value at the mid-

point of the increments considered above should have an absolute accuracy of ± 0.5%, under the worst conditions. Thus conversion of rates of rise of thermocouple voltage to rates of rise of temperature results in an absolute error in dT/dt of $\sim \pm$ 0.7% and a relative accuracy of ± 0.4% at the lowest temperatures, which falls by a factor of 2 above about 40°K. The rates of rise are mean values over approximately one degree intervals, and the temperature of the midpoint of such intervals, which corresponds to the temperature of the resulting mean specific heat has however only an absolute accuracy of $\sim \pm$ .05°K.

The error in the self heat has been discussed fully in Section 3.1 and can vary by $\sim$ 0.9% depending on the value of Pu^{239} self heat used. We feel justified in using the higher value, as will be seen in the next chapter but this must still be retained in the absolute accuracy. Relative accuracy is not affected since it is a constant factor throughout. Additional heat accuracies, when they are used are small, $\sim$ 0.1 - 0.2%.

The resulting total thermal capacity values have thus an absolute accuracy of $\sim \pm$ 1.5% falling to ± 0.75% above about 40°K. The corresponding point to point accuracy is $\sim$ 0.4% falling to 0.2%. The contributions of the specimens

to the total thermal capacities were between ~ 50 - 60% for Pu and PuC samples, but only about 40% for Np. All specific heat results presented in the next chapter have therefore a probable absolute accuracy of ~ ± 3% below ~ 40°K and ± 1.5% above, the smaller Np sample being balanced by a more precise power value. The corresponding point to point accuracy is ~ ± 1.0% and ± 0.5%.

The experimental scatter of the specific heat points will be seen to be comparable to this relative accuracy except in the range covered by a nitrogen run. Here the small fluctuations in refrigerant temperature produce short term variations in the thermocouple reference junction, which was not accounted for in the above discussion and leads to a slightly higher scatter of ~ ± 1%. Slow drift or difference in temperature of different liquid nitrogen samples are accounted for by measurement of refrigerant temperature.

Corrections for curvature of Cp, due to the finite temperature interval method are small compared with the other sources of error, since a 1°K temperature interval was used throughout the range 10 to 300°K. Such corrections were not made.

Heat loss corrections were reduced eventually to a similar small level, and agreement between results from

successive refrigerant runs, within the above scatter, justified their neglect.

REFERENCES

Asaro, F., (1953): Thesis, University of California, also Report No. UCRL - 2180.

Asaro, F. and Perlman, I., (1952): Phys. Rev., 88, 828.

Asaro, F. and Perlman, I., (1954): Phys. Rev., 94, 381.

Asaro, F. and Perlman, I., (1954a): Phys. Rev., 93, 1423.

Baranov, S.A., Kulakov, V.M., Samoilov, P.S., Zelenkov, A.G. and Rodionov, Y.F., (1962): Sov. Phys. J.E.T.P. 14, 1232.

Baranov, S.A., Kulakov, V.M. and Belenky, S.N., (1963): Nucl. Phys. 41, 95.

Baranov, S.A., Kulakov, V.M. and Shatinsky, V.M., (1964): Nucl. Phys. 56, 252.

Baranov, S.A., Gadzhiev, M.K., Kulakov, V.M. and Matinsky, V.M., (1965): J. Nucl. Phys. (U.S.S.R.), 1, 397.

Barron, T.H.K., (1957): Ann. Physics, 1, 77.

Bijl, D. and Pullan, H., (1955): Physica, 21, 285.

Brauer, F.P., Stromatt, R.W., Ludwick, J.D., Roberts, F.P. and Lyon, W.L., (1960): J. Inorg. Nucl. Chem. 12, 234.

Brown, F., George, G.G., Green, D.E. and Watt, D.E., (1960); J. Inorg. Nucl. Chem. 13, 192.

Butler, J.P., Eastwood, T.A., Collins, T.L., Jones, M.E., Rowke, F.M. and Schuman, R.P. (1956): Phys. Rev., 83, 1249.

Butler (1956a): Phys. Rev., 103, 634.

Butler, J.P., Lounsbury, M. and Merritt, J.S., (1956): Canad. J. Chem. 34, 253.

Chamberlain, O., Gofman, J.W., Segre, E. and Wahl, A.C., (1947): Phys. Rev., 71, 529.

Chin-Fan Leang (1962): Compt. Rend. 255, 3155.

Corruccini, R.J. and Gniewek, J.J., (1960): Specific Heats and Enthalpies of Technical Solids at Low Temperatures. N.B.S. Monograph 21.

Cramer, E.M., Hawes, L.L., Miner, W.N. and Schonfeld, F.W. (1961): The Metal Plutonium, Univ. of Chicago Press, p. 212.

Dokuchaev, Y.P., (1959): Atomnaya Energ. 6, 74.

Eichelberger, J.F., Grove, C.R. and Jones, L.V., (1963): Mound Lab. Progress Report No. MLM-1177.

Farwell, J.E., Roberts, J.E. and Wahl, A.C., (1954): Phys. Rev., 94, 363.

Freedman, M.S., Wagner, F. Jnr. and Engelkemeir, D.W., (1952): Phys. Rev., 88, 1155.

Goldin, L.L., Tretyakov, E.F. and Novikova, G.I., (1955): Conference of Academy of Sciences of U.S.S.R. on Peaceful Uses of Atomic Energy, Phys., Maths. and Sc., p. 167.

Graham, L.J. and Chang, R., (1964): Compounds of Interest in Nuclear Reactor Technology, Eds. Waber, Chiotti and Miner, I.M.D. Special Report 13, Met. Soc., A.I.M.E., p. 409.

Hall, A.R., (1967): A.E.R.E., Harwell, Report No. AERE-R-5650.

Hall, G.R. and Markin, T.L., (1956): J. Inorg. Nucl. Chem. 2, 202.

Hall, G.R. and Markin, T.L., (1957): J. Inorg. Nucl. Chem. 4, 137.

Harvey, B.G., (1952): Phys. Rev., 85, 482.

Hoffman, D.C., Ford, G.P. and Lawrence, F.O., (1957): J. Inorg. Nucl. Chem. 5, 6.

Hough, A., Marples, J.A.C., Mortimer, M.J. and Lee, J.A. (1968): Phys. Letters 27A, 222.

Hummell, J.P., (1956): Thesis, Univ. of California, also Report No. UCRL-3456.

Inghram, M.G., Hess, D.C., Fields, P.R. and Pyle, G.L., (1951): Phys. Rev., 83, 1250.

Jaffey, A.H. and Lerner, J., (1950): Argonne Nat. Lab. Classified Report No. ANL-4411 (Unpublished).

Jaffey, A.H. and Magnusson, L.B., (1949): National Nuclear Energy Series, IV - 14B p, 978, McGraw-Hill, N.Y..

Johnson, V.J., (1961, Ed.): A Compendium of the Properties of Materials at Low Temperatures (Phase 1), Pergamon Press.

Kay, A. and Linford, P.F.T., (1960): Plutonium 1960. Clever-Hume Press, London (1961), p. 51.

Kondratev, L.N., Novikova, G.I., Vorobev, A.M. and Goldin, L.L., (1956): Bull. Acad. Sci. (U.S.S.R.) Phys. Series 20, 795.

Kruger, O.L., (1962): J. Nucl. Mat., 7, 142.

Lallement, R., (1963): Phys. Letts., 5, 182.

Landholt and Börnstein (1961): Zahlenwerte und Funktionen. 2, (4) Springer-Verlag, Berlin.

Lederer, C.M., Hollander, J.M. and Perlman, I., (1967): Table of Isotopes, 6th Edition, Wiley, N.Y..

Linford, P.F.T., (1964): Cryogenics, 4, 395.

Linford, P.F.T., (1968): A.W.R.E. Aldermaston, Private Communication.

MacKenzie, D.R., Lounsbury, M. and Boyd, A.W., (1953): Phys. Rev., 90, 327.

Magnusson, L.B., Engelkemeir, D.W., Freedman, M.S., Porter, F.T. and Wagner, F. Jnr. (1955): Phys. Rev., 100, 1237A.

Magnusson, L.B. and La Chapelle, T.J., (1948): J. Am. Chem. Soc., 70, 3534.

Markin, T.L., (1959): J. Inorg. Nucl. Chem. 9, 320.

Mech, J., Diamond, H., Studier, M.H., Fields, P.R., Hirsch, A., Stevens, C.M., Barnes, R.F., Henderson, D.J. and Huizenga, J.R., (1956): Phys. Rev., 103, 340.

Mott, N.F., and Jones, H., (1936): The Theory of the Properties of Metals and Alloys, Clarendon Press, Oxford.

Oetting, F.L., (1965): J. Inorg. Nucl. Chem. 27, 2151.

Oetting, F.L. and Gunn, S.R., (1967): J. Inorg. Nucl. Chem. 29, 2659.

Ogard, A.E., Land, C.C. and Leary, J.A., (1965): J. Nucl. Mat. 15, 43.

Pallmer, P.G., (1962): Hanford (U.S.A.) Report No. HW-72245.

Robinson, A.C., (1964): A.W.R.E., Aldermaston, unpublished.

Rose, B. and Milstead, J., (1956): J. Nucl. Energy, 2, 264.

Rosenblum, C., Valaderes, M. and Milstead, J., (1957); J. Phys. Rad., Paris, 18, 609.

Rothschild (1958): Nature, 182, 790.

Rytz, A., (1960): C.R. Acad. Sc., Paris, 250, 3156.

Seaborg, G.T., James, R.A. and Ghiorso, A., (1949): N.N.E.S. IV - 14B, 1554.

Sliagin, K.N., (1956): Sov. Phys. J.E.T.P., 3, 663.

Sliagin, K.N., (1956A): Bull. Acad. Sci. (U.S.S.R.) Phys. Series, 20, 810.

Smith, A.L., (1961): J. Inorg. Nucl. Chem. 17, 178.

Stephens, D.R., (1966): J. Phys. Chem. Solids, 27, 120.

Stone, R.E. and Hulet, E.K., (1967): J. Inorg. Nucl. Chem. 20, 30.

Stout, J.W. and Jones, W.M., (1947): Phys. Rev., 71, 582.

Strominger, D., Hollander, J.M. and Seaborg, G.T., (1958): Rev. Mod. Phys., 30, 585.

Thompson, S.G., Street, K., Ghiorso, A. and Reynolds, F.L., (1950): Phys. Rev., 80, 1108.

Wallman, J.C., Graf, P. and Coda, L., (1958): J. Inorg. Nucl. Chem., 7, 199.

Westrum, E.F. Jnr. (1951): Phys. Rev., 83, 1249.

Westrum, E.F. Jnr., Hindman, J.C. and Greenlee, C., (1949): N.N.E.S., IV-14B, 1717.

Zachariasen, W.H., (1952): Acta Cryst., 5, 660.

CHAPTER 4

EXPERIMENTAL RESULTS

The experimental data obtained on the metals α-plutonium, α-neptunium and the metallic compound plutonium monocarbide, will be presented in this chapter, together with some analysis and discussion of the results.* Further analysis on α-plutonium in particular, and discussion in relation to other low temperature properties will be held in Chapter 5.

Some preliminary experiments were performed on a high purity copper sample in order to test some of the components of the apparatus. Since it was considered unlikely that the experimental conditions which would exist with a highly radioactive material such as α-plutonium, could be reproduced with a dummy specimen, further development of the system was carried out using a specimen of α-Pu. The apparatus and experimental procedure described in Chapter 2, are the final result of such developments, and a certain amount of this

---

* Some of the data presented here have been published by
Lee, Mendelssohn and Sutcliffe (1965);
Lee, Marples, Mendelssohn and Sutcliffe (1965);
Griffin, Mendelssohn, Sutcliffe et al. (1966).



MAG. X250

PLATE 4·1 (a).

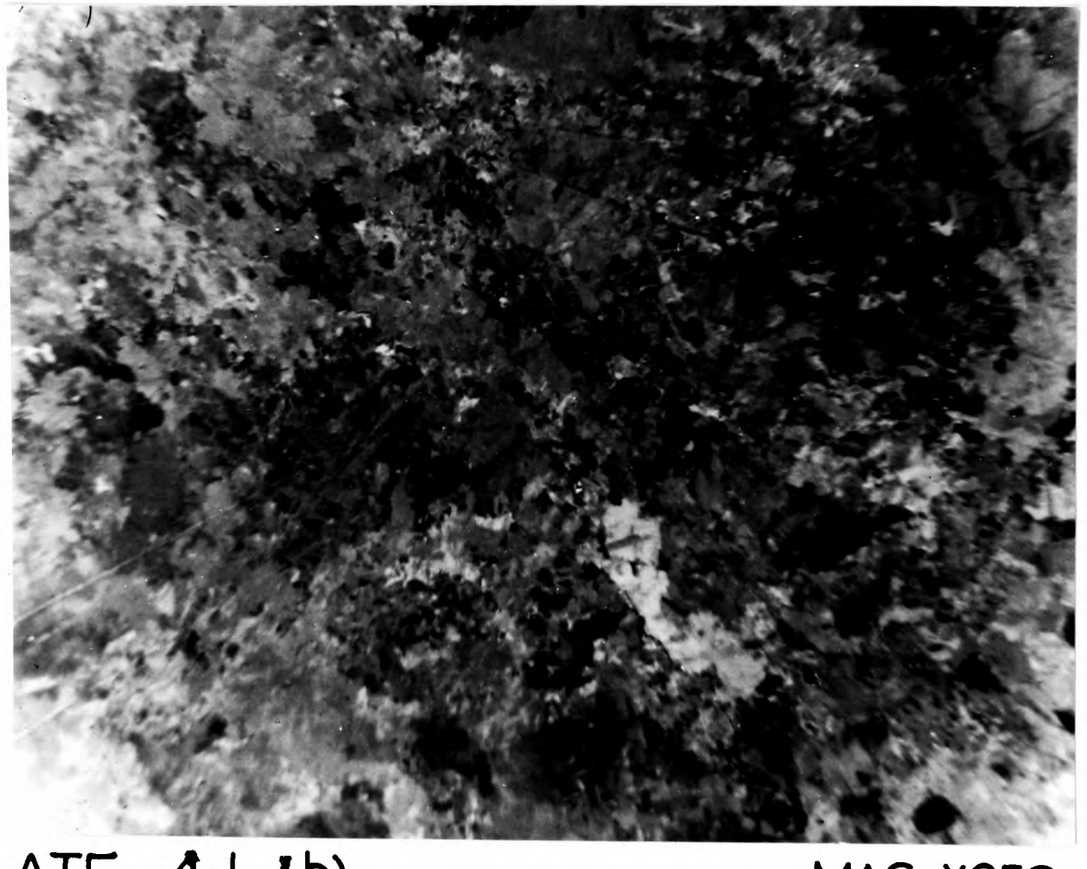


PLATE 4·1 (b).

MAG. X250

chapter is devoted to a description of how the final system was evolved.

4.1 Plutonium.

Plutonium is unique among metals in having six different allotropic modifications between room temperature and its low melting point of ~ 640°C. The stable phase below ~ 120°C, α-plutonium, has a monoclinic crystal structure.

Three samples of α-plutonium were investigated and are designated Pu3, Pu4 and Pu6.

4.1. 1. Pu3.

The sample, Pu3, was from electrorefined high purity plutonium prepared by U.S.A.E.C.. Spectrographic, chemical and isotopic analyses are given in Table 4.1. Maximum impurity level including detection limits is ~ 400 ppm; true level is probably ~ 300 ppm. Metallographic examination was also carried out. Inclusion levels can be seen from Plate 4.1(a) to be very small, and grain size (Plate 4.1(b)) is approximately 25 μcrons max. The density was 19.61_6 gm/c.c. which compares favourably with a theoretical value for Pu^{239} of 19.82.

TABLE 4.1

Pu3

Spectrographic Analysis. Results in ppm by weight							
Ag	< .5	Cr	10	Pb	<1	W	<25
Al	25	Co	1	Pd	< 2.5	Zn	<10
As	<10	Ga	12	Sb	< 2.5	Cl	5.3
Au	< 1	In	< .5	Si	16		
B	< 1	K	1	Sn	3		
Ba	< .1	Mg	3	Sr	< .5	Gas Analysis	
Be	< .025	Mn	6	Ts	<25		
Bi	<1	Mo	1	Th	<50	N_2	= 0
Ca	<25	Ni	11	Ti	5	O_2	= 4.3
Cd	<2.5	P	<100	V	.5	H_2	= 1.7

Chemical Analysis (ppm)		Isotopic Analysis (Wt/O)	
Am	20	Pu^{238}	- .003
C	11	Pu^{239}	- 97.537
Fe	10	Pu^{240}	- 2.349
		Pu^{241}	- .080
		Pu^{242}	- .000

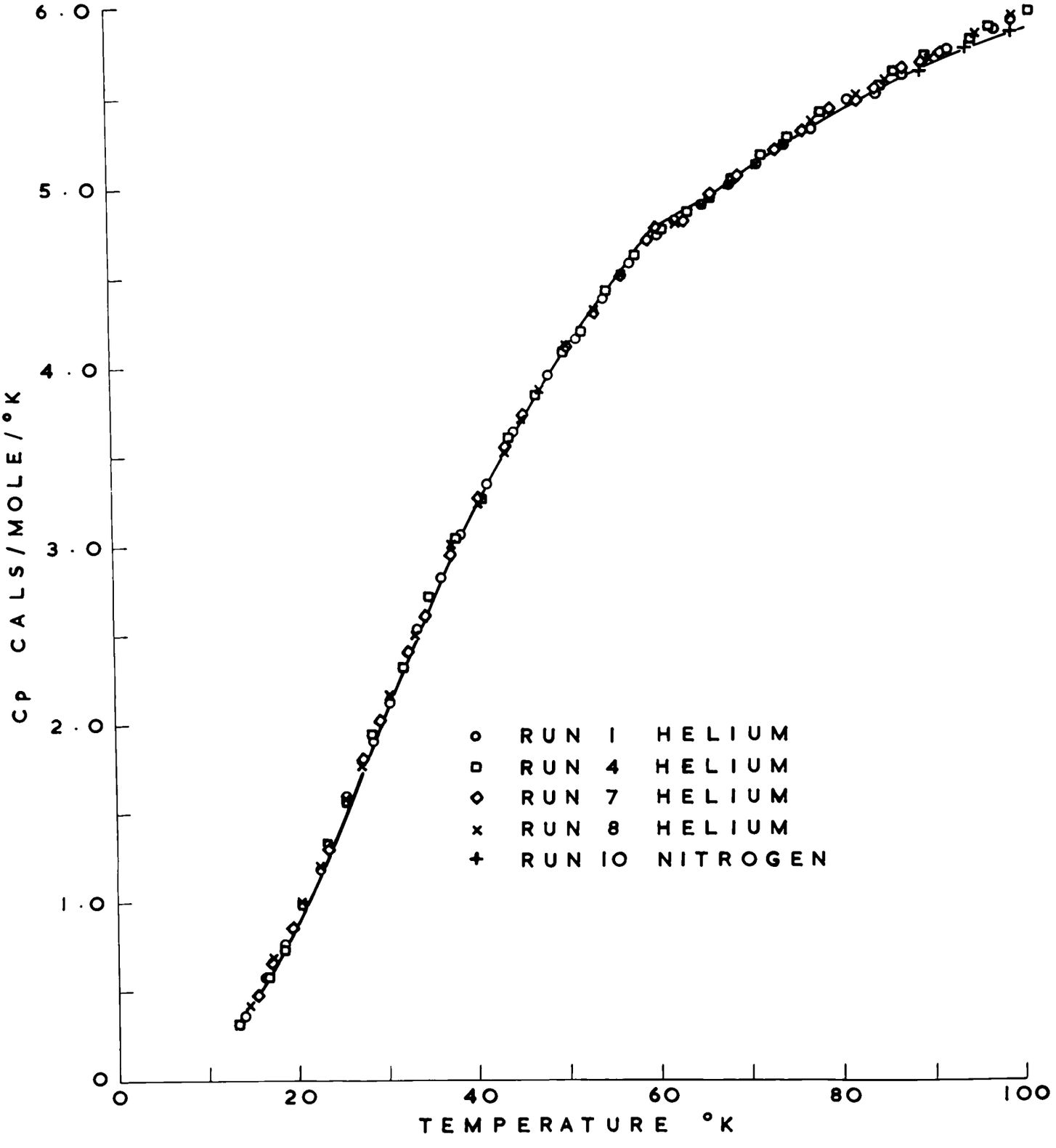


FIG. 4.1 SPECIFIC HEAT OF Pu3

The specimen was machined directly from the as-supplied material, to a shape described in Section 2.5, of outer diameter 1.0 cm. and height 1.5 cm.. The weight of the sample was 19.53_3 gm..

The isotopic analysis (at the time the measurements were taken) given in Table 4.1 and self heat values of Section 3.1 leads to a self heat/gm. of 2.0635 mwatts, and a total self heat of 40.306 mwatts.

Pu3 was canned in a high purity copper calorimeter and several helium and nitrogen runs were carried out. The results of some of these runs in the temperature range ~ 14°K to 100°K, are shown in Fig. 4.1. In general C_p values are high, reaching a value of almost 3R cals./mole/°K at only ~ 100°K; they were reproducible, compare the agreement between helium runs 1, 4, 7 and 8; and show a smooth temperature dependence except for the temperature range 50 - 70°K where a small 'excess' occurs of ~ 2%. The excess is not large enough to produce a maximum, only a deviation from a smooth curve. (The line drawn in Fig. 4.1 is not supposed to represent the best line through the points plotted, but corresponds to the sp.ht. values determined on Pu6, which will be referred to later.)

The extent of the 'excess' is more clearly seen from

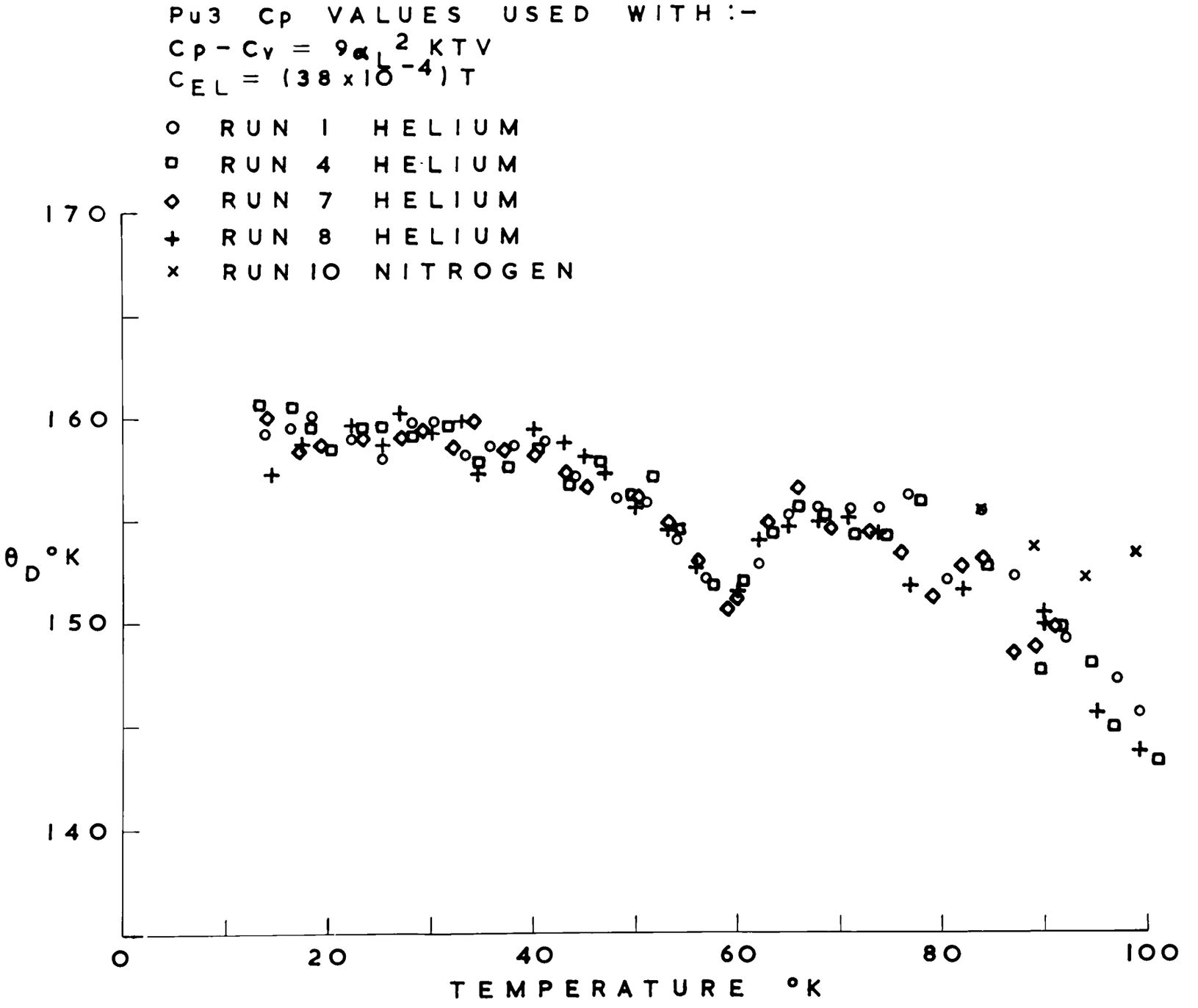


FIG. 4.2 DEBYE THETA (θ_D) VALUES FOR Pu3

Fig. 4.2 where the C_p values of Fig. 4.1 are interpreted in terms of an effective Debye theta, using the dilation term ($C_p - C_v = 9\alpha_v^2 KTV$), discussed in Chapter 3, and an electronic coefficient γ of 38×10^{-4} cals./mole/deg.^{2} (the reason for which will be seen later), a quite marked dip in θ_D ($\sim 6^\circ K$) appears centred around a temperature of $59 - 60^\circ K$.

What also became apparent from this early set of runs was that above $\sim 75^\circ K$ the C_p values obtained from a helium run began to rise above those obtained from a nitrogen run, and at higher temperatures the helium values began to turn upwards quite markedly. Similarly the nitrogen values began to deviate from the normal expected extension of the lower temperature curves at $\sim 110 - 115^\circ K$. The conclusion reached was that conditions must be far from adiabatic as the temperature excess of the calorimeter above the refrigerant became excessive. Heat loss from the calorimeter produced an effective C_p, calculated on zero heat loss, which was too high. Any such heat loss must be an increasing function of the temperature excess, and therefore could not account for the shape of the excess centred at $60^\circ K$, although complete faith in its existence, and any analysis of its shape must await confirmation and attainment of satisfactory results at higher temperatures.

At the time of the measurements on Pu3, the question of obtaining reliable specific heat values at all on plutonium, was in doubt (see comparison with earlier work in Section 4.1. 3), and also the temperature region of most interest from other low temperature properties (see Chapter 5), appeared to be in the region of 50 - 60°K or certainly below 100°K, where radiation losses are not usually excessive. As a consequence a relatively crude system was employed in so far as elimination of all heat losses was concerned. It differed from that described in Chapter 2 and illustrated in Fig. 2.2(b) in the following respects.

The calorimeter was suspended at a fixed height, such that the extension clamped between the heat switch jaws was always outside the radiation shield. The emissivities of the surfaces of calorimeter, radiation shield and vacuum can were probably all fairly high. A number of spare leads terminating inside the radiation shield produced a greater heat loss from the shield and no additional conical shield existed inside the shield.

4.1. 2. Pu4.

On arrival of a further billet of high-purity plutonium from U.S.A.E.C., it was decided to make measurements on a new

specimen, in order to confirm or otherwise the existence of the 'excess' centred at ~ 60°K, to investigate the temperature distribution within the calorimeter, and to improve adiabatic conditions at the higher temperatures.

The specimen was again machined from as-received material, the analyses for which are given in Table 4.2. Impurity and inclusion levels, and grain size were very comparable to Pu3, and the density was 19.65 gm/c.c.. Dimensions were almost identical, and specimen weight was 19.496 gms, giving a total self heat of 40.94_9 mwatts.

The new calorimeter again of high-purity copper was used which had the additional feature of two constantan heaters of equal resistance, one in the centre of the centre pin, and the other wound on the outer cylindrical surface. (The calorimeter used for Pu4 was shown in Fig. 2.4(a) except that the outer heater has been omitted.)

Variation of the heating rate is a time-honoured test for investigation of possible temperature gradients within a calorimeter. Despite the finding of West (1963) that no change in heat capacity values for different heating rates is not a sufficient condition that there are no temperature gradients, it must remain a necessary condition.

The volume-generated self-heat obviously is advantageous

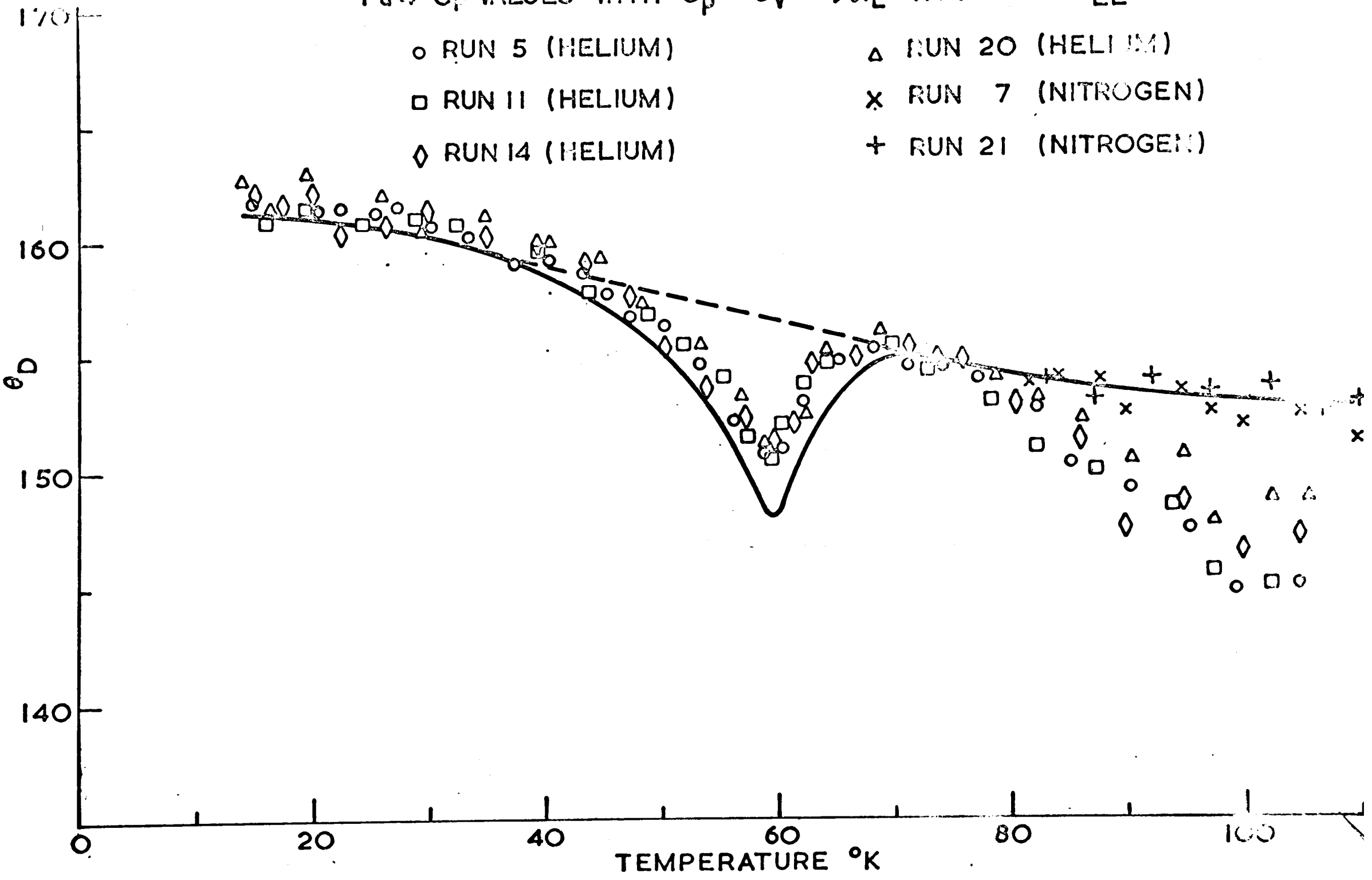
TABLE 4.2

PuH

Spectrographical Analysis (ppm by weight)							
Ag	2	Cd	< 2.5	Ni	13	Th	< 1
Al	15	Cr	5	P	< 100	Ti	< 1
As	< 10	Cu	1	Pb	1	V	< 0.5
Au	< 1	Ga	< 1	Pd	< 2.5	W	56
B	< 1	In	< 0.5	Sb	< 2.5	Zn	< 10
Ba	< 0.1	K	2	Si		Gas Analysis	
Be	< 0.025	Mg	3	Sn	< 2	N_2 =	< 1
Bi	< 1	Mn	11	Sr	< 1	O_2 =	17
Ca	< 25	Mo	2	Ta	19	H_2 =	6

Chemical Analysis (ppm)		Isotopic Analysis (Wt/O)	
Am	5	Pu^{238}	.004
C	14	Pu^{239}	96.970
Fe	15	Pu^{240}	2.880
U	20	Pu^{241}	0.111
		Pu^{242}	0.000

FIG. 4.3 DEBYE THETA (θ_D) VALUES FOR Pu 4.



in reducing temperature gradients within the specimen although its magnitude and the poor thermal conductivity of α-plutonium (~ 20 - 30 mwatts/deg./cm. at ~ 100°K) are both factors on the debit side. Possible temperature gradients between specimen and measuring thermocouple must be affected differently by the dissipation of additional heat to the centre heater, than to the outer heater. This results not only from the different thermal paths between the two heaters and the thermocouple junction, but also from the different thermal paths between heaters and specimen. The centre heater has probably a low thermal resistance to the specimen, since the specimen shrinks on to the centre pin of the calorimeter on decreasing the temperature.

In order to investigate whether such temperature gradients were significant, several helium runs were carried out on PuI_4 both with and without additional heat. During the runs in which additional heat was used differing amounts of heat and dissipation in either or both of the heaters was employed.

Helium, nitrogen, CO_2 and ice runs were also done without additional heat to investigate the excess at ~ 60°K on a second specimen, and to extend the range of measurement up to room temperature.

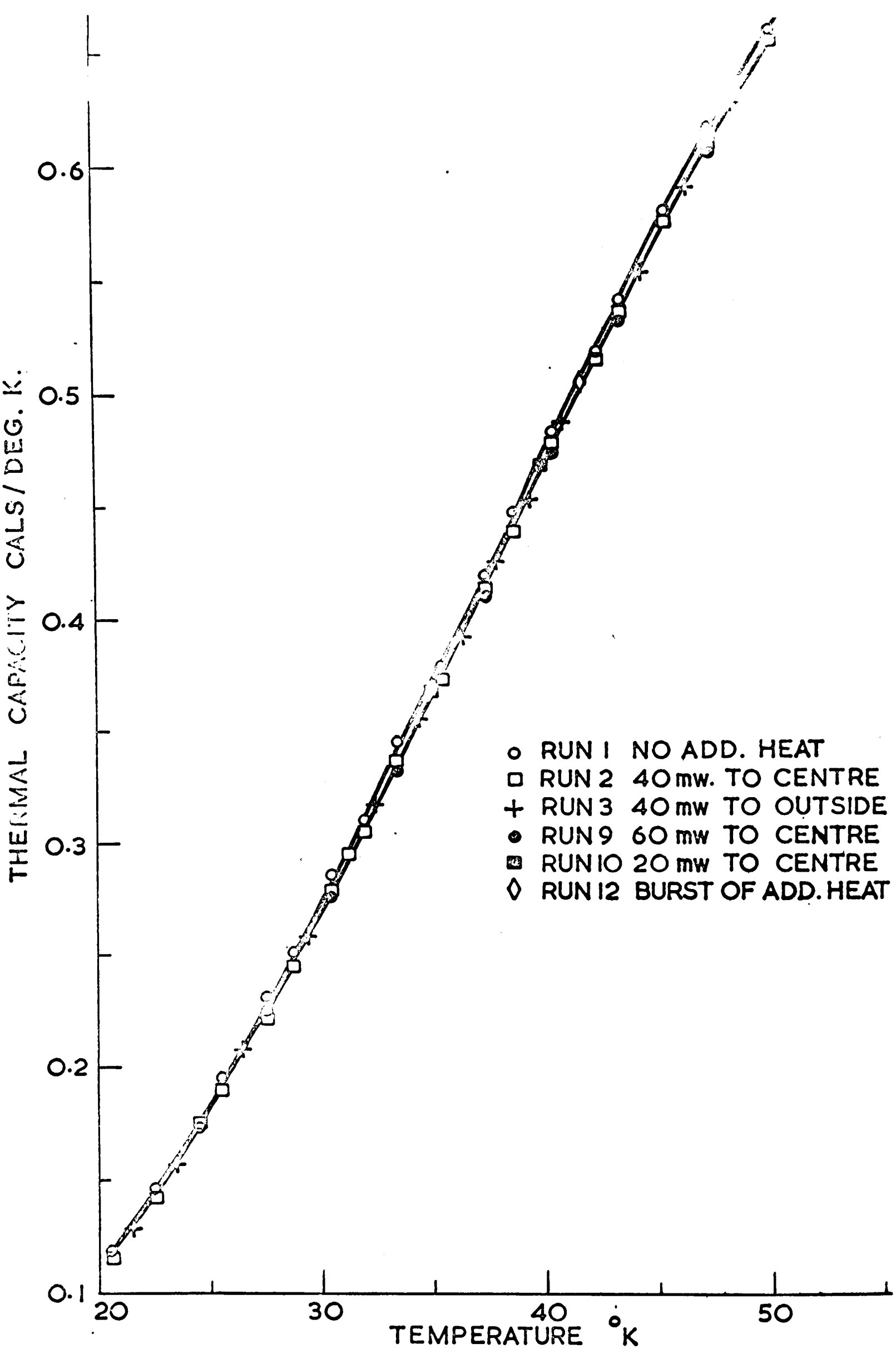


FIG 4.4 ADDITIONAL HEAT RUNS ON Pu 4.

Helium and nitrogen runs without additional heat confirmed the specific heat values obtained for Pu3, below $\sim 100^{\circ}K$. Magnitude of C_p for Pu4 was within 2% below $\sim 40^{\circ}K$, and 1% between 40 and $100^{\circ}K$. Slight differences can best be seen by a comparison of θ_D values obtained using the same dilation and electronic terms in both cases. Those for Pu4 are shown in Fig. 4.3, showing θ_D values slightly higher than Pu3 below $\sim 40^{\circ}K$, the difference being $\sim 2.5^{\circ}K$ in θ_D at a temperature of $15^{\circ}K$. Again there is a marked dip in θ_D centred at 59 - $60^{\circ}K$ which is of the same magnitude $\sim 6^{\circ}K$.

The additional heat runs are discussed now before considering the higher temperatures above $100^{\circ}K$. Figure 4.4 shows some of the helium additional heat runs, total thermal capacities being plotted for the temperature range 20 - $50^{\circ}K$. The results showed a displacement which increased as the additional power increased, being of the order of 1% for 40 mwatts of additional heat. However the two runs (2 and 3) with the same amount of additional heat (40 mw) in one case to the centre heater and the other to the outer heater showed good agreement ($< 0.5\%$) within the experimental scatter.

It was then realised that due to the restriction of small space available for the centre heater ($\sim$ 3 mm diam.), the resistance of the heater leads contributed a significant

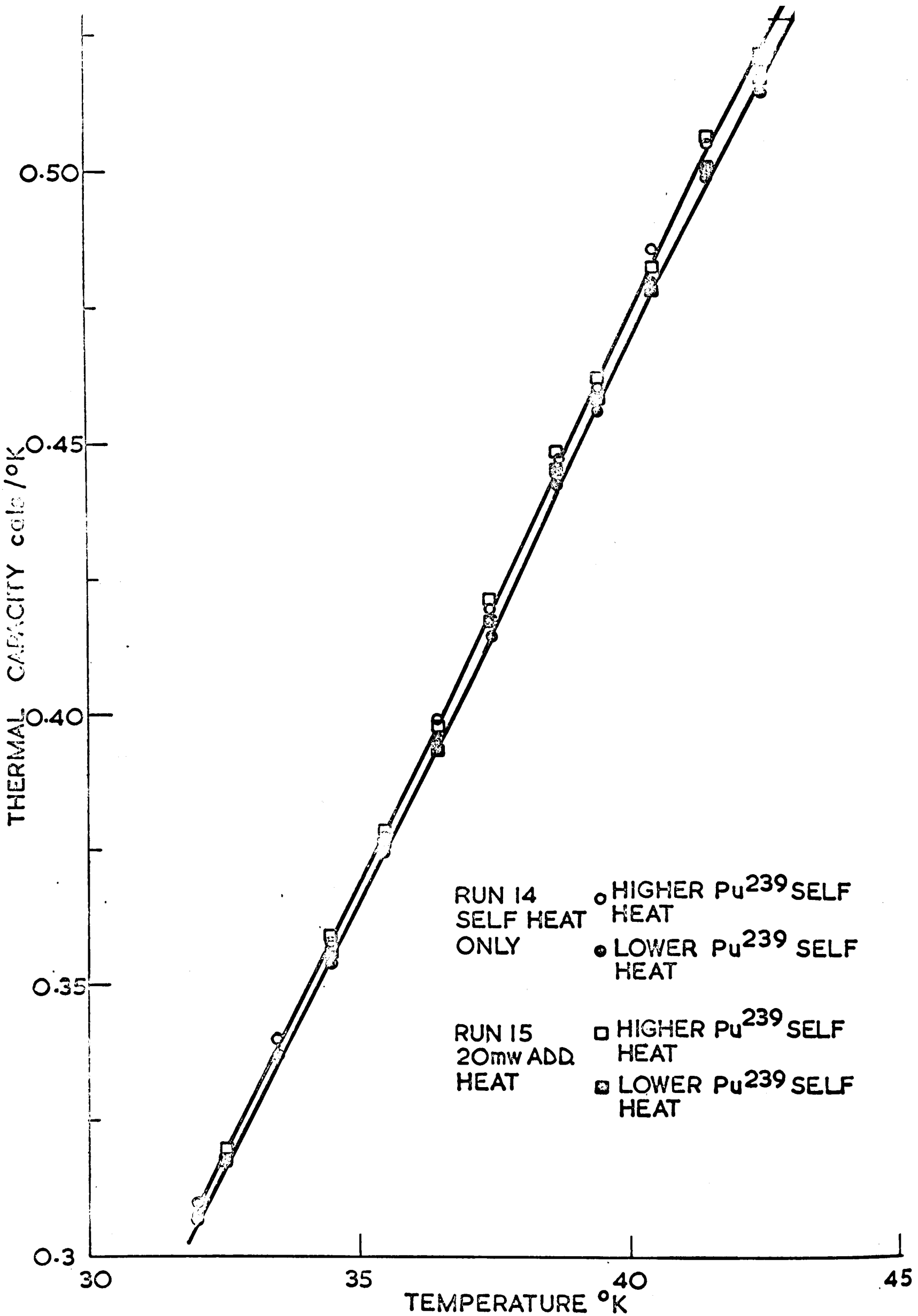


FIG.4.5 VARIATION OF Pu^{239} SELF HEAT.

fraction (~ 2%) of the heater resistance. A correction for this could not entirely account for the displacement shown in Fig. 4.4. This was reduced to ~ 0.1% by replacing the constantan leads with copper. There still remained however ~ 0.5% discrepancy.

The reason for this did not become apparent until the work of Oetting (1965) on the self heat of Pu^{239} (described in Section 3.1) came to notice. Accurate calorimetric work suggested a self heat for the isotope Pu^{239} almost 1% higher than the previously accepted value. Using his higher value accounted for the 0.5% discrepancy mentioned above. This is illustrated in Fig. 4.5 and comparison is to be made between the relative agreement between open circles and squares, and closed circles and squares. See also Fig. 4.12 for a similar plot for a section of a nitrogen run on Pu6.

Considering the small displacements produced once copper heater leads were used for rates of rise of temperature of more than double the self heat only rates, and the good agreement between the same heat to centre and outer heater, we feel justified in using the larger Pu^{239} self heat value. This higher value has been used in the calculation of the C_p values and the resulting θ_D values of Pu3 and Pu4 shown in Figs. 4.1, 4.2 and 4.3.

Turning our attention now to the temperature range above

THE NUMBERS IN CIRCLES REFER TO RUN NUMBER OF Pu4 REFERRED TO IN TEXT.

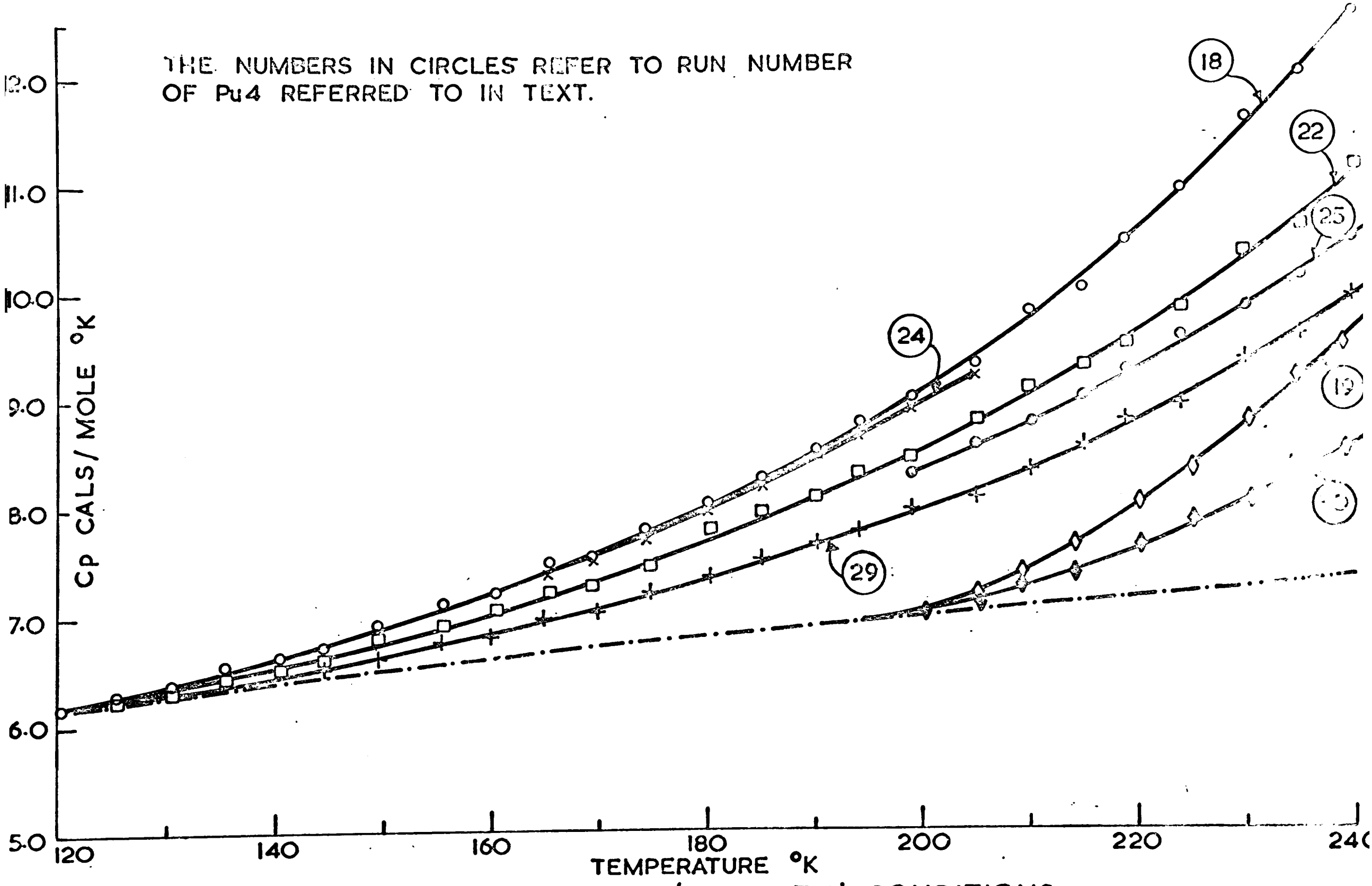


FIG. 4.6 ATTEMPTS TO IMPROVE 'ADIABATIC' CONDITIONS.

100°K, Fig. 4.6 shows the C_p values obtained for nitrogen (run number 18) and CO_2 (19) runs made on PuI_4. The deviation from a normal specific heat curve (dotted line), obtained by extrapolating between the points of small or zero temperature excess between calorimeter and refrigerant, could not be analysed into a simple T^4 (radiation) or $T + T^4$ (conduction + radiation) form. The resulting power of T was ~ 3, and it was therefore considered that the heat loss was probably some combination of radiation and conduction losses, though not necessarily to a fixed temperature.

The magnitude of heat loss to account for the deviation is $\sim$ 5 mwatts at $\sim$ 200°K with nitrogen as refrigerant. Consideration of the various possible sources of heat loss, suggested that radiation loss from the part of the calorimeter protruding out of the top of the shield could certainly account for a portion of this, and that temperature inequalities over the radiation shield of the order of a few degrees were needed to account for most of it. Uncertainties in the emissivities of the various surfaces however make accurate estimates difficult. Similarly conduction losses by the electrical leads would require either very inefficient thermal anchoring inside the shield or enormous temperature differences between calorimeter and shield to account for a significant part of

the total heat loss. Conduction along the nylon suspension was negligible compared with the other possible heat losses.

The first step towards improving 'adiabatic' conditions was made by supporting the calorimeter from the heat switch mechanism, such that it dropped inside the shield on opening the heat switch. The small radiation disc linked to the shield closed the hole in the shield completely and also reduced the conduction along the suspension, which was now much shorter. A nitrogen run, number 22, of Fig. 4.6, shows that the heat loss was reduced as a result by about a quarter.

To investigate possible temperature inequalities in the shield, the differential thermocouple was replaced with a thermopile with three junctions, one on the lid of the shield, one on the side, and one on the bottom. The nitrogen runs numbers 24 and 25 are with the thermopile, the difference being that run 24 is with the shield controller controlling to zero indicated difference (as all previous runs have been) and that run 25 was controlled such that $T_{shield} < T_{cal.}$, the difference being $2/3^{o}K$. These are to be compared with run 18, as temporary difficulties of the nylon suspension breaking, prior to introducing a small spring in its length, caused the reversion to the fixed height suspension of the calorimeter. It can be seen that temperature differences of the order of

$2^{o}K$ can indeed account for most of the heat loss.

Several further improvements were in that the leads anchored to the shield were shielded from the calorimeter by an inner conical shield; thermal anchoring of leads inside the shield was improved, and any superfluous leads were cut out; and the shield heater was extended and wound around the electrical leads immediately prior to them entering the shield. The improvements as a result of these, with control now back to zero temperature difference, is shown by run 29 with nitrogen and run 30, with CO_2. Similar improvements were also evident on ice runs (not shown).

The conclusions reached were that the remaining heat loss was due to radiation loss from the calorimeter to those parts of the shield which were also excessively cooled by heat loss from shield to surrounding vacuum can at refrigerant temperature. Since additional heat runs had shown satisfactory temperature distributions within the calorimeter, the outer heater could be dispensed with, enabling a highly polished surface to be achieved over the majority of the calorimeter.

A further billet of even higher purity plutonium had by this time arrived, and this is described in the next section.

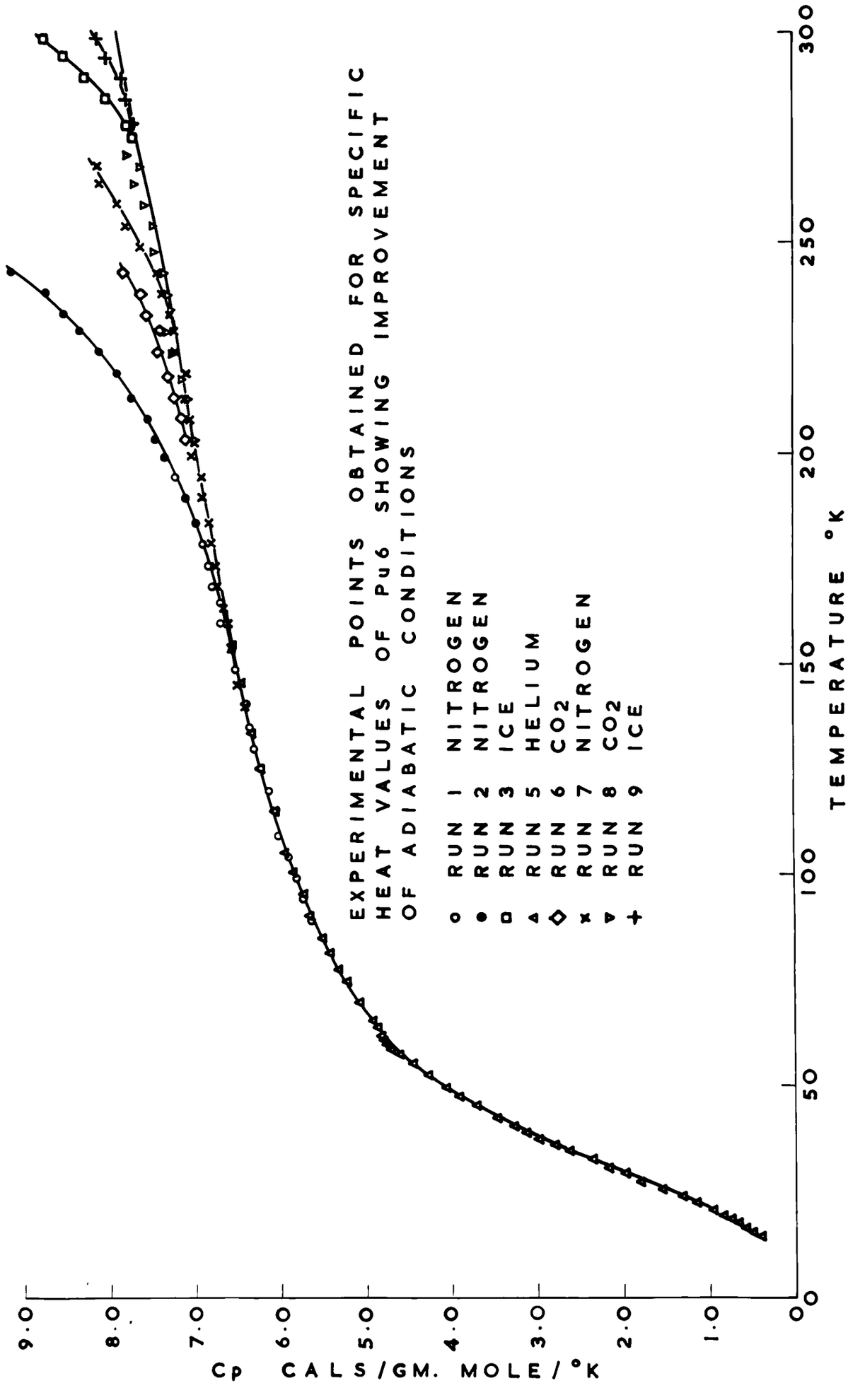


FIG. 47. SPECIFIC HEAT OF Pu 6

4.1. 3. Pu6.

The analyses for Pu6 are shown in Table 4.3. Maximum impurity levels are ~ 100 ppm, the actual impurity level being probably ~ 50 ppm. Metallographic examination revealed even less inclusion level and probably comparable grain size ~~(Plate 4.1(a) and (b))~~. Weight of the sample was 19.306_2 gms leading to a self heat of 2.052_8 mw/gm and a total self heat of 39.63_2 mwatts.

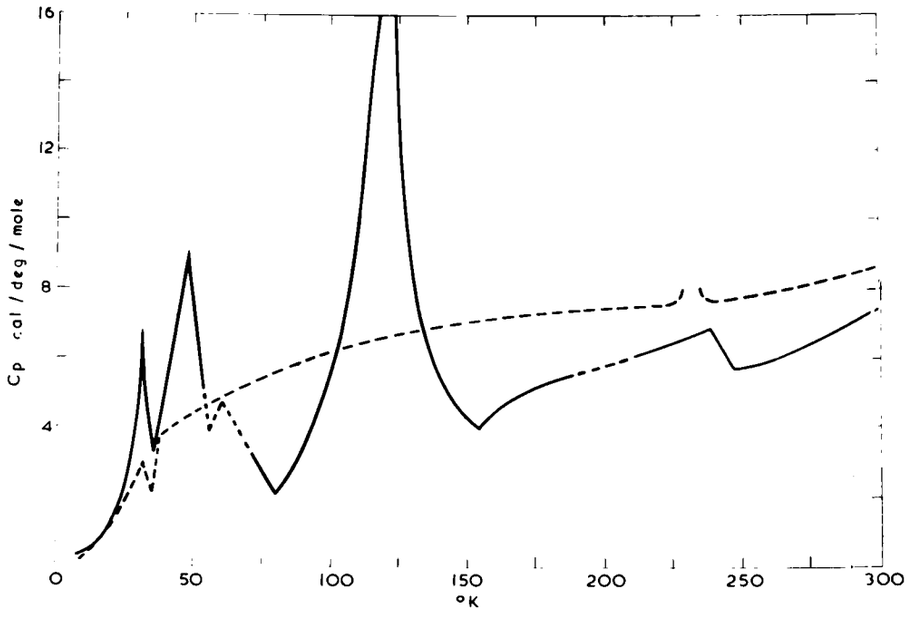
Pu6 was canned in a high purity silver calorimeter (shown in Fig. 2.4(b)), and series of helium, nitrogen, CO_2 and ice runs were carried out. These are shown by runs 1, 2, 3, 5 and 6 of Fig. 4.7. The effect of the highly polished surface of the calorimeter can be seen from the higher temperature region. Deviation from the expected curve has been reduced by a factor of two. The further step of coating the radiation shield with 0.001" aluminised melinex produced the result shown by runs 7, 8 and 9, of Fig. 4.7. It can now be seen that satisfactory agreement was obtained between the top end of a nitrogen run (200 - 230°K) with the beginning of the CO_2 run, and similarly between CO_2 and ice runs in the region of 270°K. Because of the agreement between various runs with different refrigerants, it was considered justifiable that heat loss from the calorimeter had been reduced to an

TABLE 4.3

Pu6

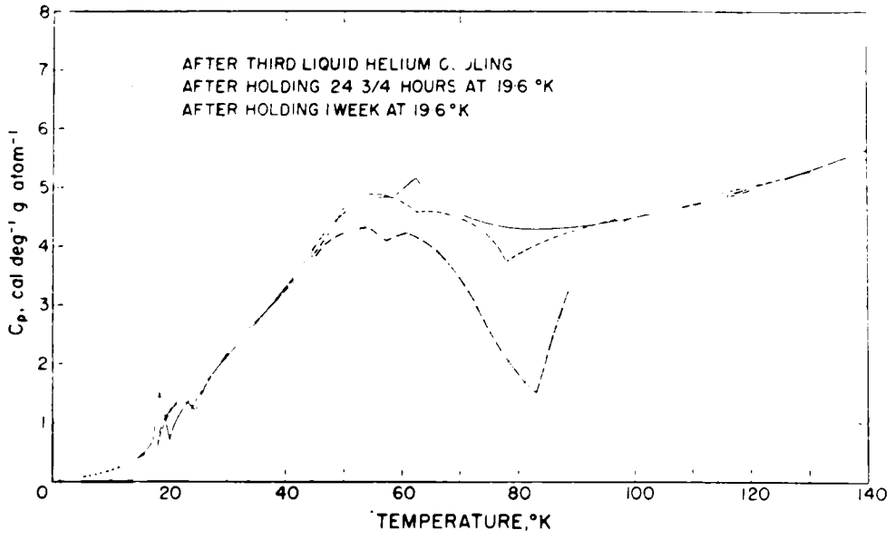
Spectrographic Analysis (ppm by weight)							
Al	< 0.5	Ga	< 1	Pb	< 1	Y	< 1
B	< 0.5	Hf	< 1	Re	< 1	Zn	< 10
Ba	< 0.5	La	< 1	Si	< 2	Zr	< 1
Be	< 0.001	Li	< 0.005	Sn	< 1		
Bi	< 1	K	< 0.5	Sr	< 0.5		
Ca	< 4	Mg	2	Ta	6		
Cd	< 1	Mn	< 0.5	Th	< 0.5	Gas Analysis	
Co	< 1	Mo	< 1	Ti	< 0.5	N	2.9
Cr	< 0.5	Na	< 1	V	< 0.5	H	< 5
Cu	< 0.5	Ni	< 0.5	W	2.5		

Chemical Analysis ppm		Isotopic Analysis (Wt/O)	
Am	14	Pu^{238}	0.005
C	10	Pu^{239}	98.022
Fe	5	Pu^{240}	1.938
U	11	Pu^{241}	0.034
		Pu^{242}	0.001



[redacted] SPECIFIC HEAT OF PLUTONIUM
(ACCORDING TO SANDENAW, OLSEN, AND GIBNEY)

FIG. 4·8 (a)



[redacted]: Heat capacity curves for an electro-refined plutonium specimen showing effects of various holding times in boiling liquid helium and boiling liquid hydrogen.

FIG. 4·8 (b)

insignificant level and almost true adiabatic conditions existed. Some deviation still occurred if runs with any refrigerant were extended much above a small overlap region with the next refrigerant but this was reduced even further by silverplating the inside of the outer vacuum can (the effect of this can be seen from any later specific heat runs).

Genuine specific heat values have thus been obtained up to a temperature of almost 300°K. Comparison with Pu3 and Pu4 shows that good agreement exists below 100°K, both in respect of absolute values and of confirmation of the small excess in the region of 60°K. We are now in a position also to compare the present work with previous determinations of specific heat of α-plutonium.

The only specific heat work below room temperature published prior to commencing this work was that of Sandenaw, Olsen and Gibney (1961) and Sandenaw (1962), the results of which are shown in Figs. 4.8(a) and (b) respectively. The earlier work suggested a probable C_p curve shown by the dotted line of 4.8(a) for a normal purity sample of α-Pu. However the appearance of numerous irreproducible peaks on a sample of higher purity shown by the predominately solid line, meant that little weight could be placed on the reliability of any C_p values. This early work did however suggest

the importance of cooling rates and storage times at temperatures below $\sim 80^{\circ}K$ and also possibly the importance of good thermal contact between specimen and calorimeter. Later work, Sandenaw (1962), shown below $100^{\circ}K$ in Fig. 4.8(b) produced more reproducible values, but still suggested the presence of a broad maximum at $\sim 60^{\circ}K$ and a small peak at $\sim 20^{\circ}K$ shown by the solid line. (Dotted lines are for different storage times at $19.6^{\circ}K$ which will be mentioned later). No evidence of the small peak at $20^{\circ}K$ can be found from the present work, and the hump at $\sim 60^{\circ}K$ is considerably smaller. Absolute values of C_p are in reasonable agreement at $\sim 40^{\circ}K$ and at room temperature, but at $100^{\circ}K$ Sandenaw's values are $\sim$ 20% lower than ours, and $\sim$ 10% lower at $200^{\circ}K$.

During the course of this work, further low temperature C_p measurements of α-plutonium were published by Taylor, Loasby, Dean and Linford (1965) using a continuous heating isothermal technique, in which heat losses were calculated. When allowance is made for the smaller self heat value of Pu^{239}, their values agree remarkably well ($< \pm 1\%$) with the present work over the whole temperature range, except that they see no evidence of the small excess at $60^{\circ}K$.

Further comparisons with our present work will be made during the following analysis of the specific heat results. Because of the existence of the small excess at $60^{\circ}K$ in our

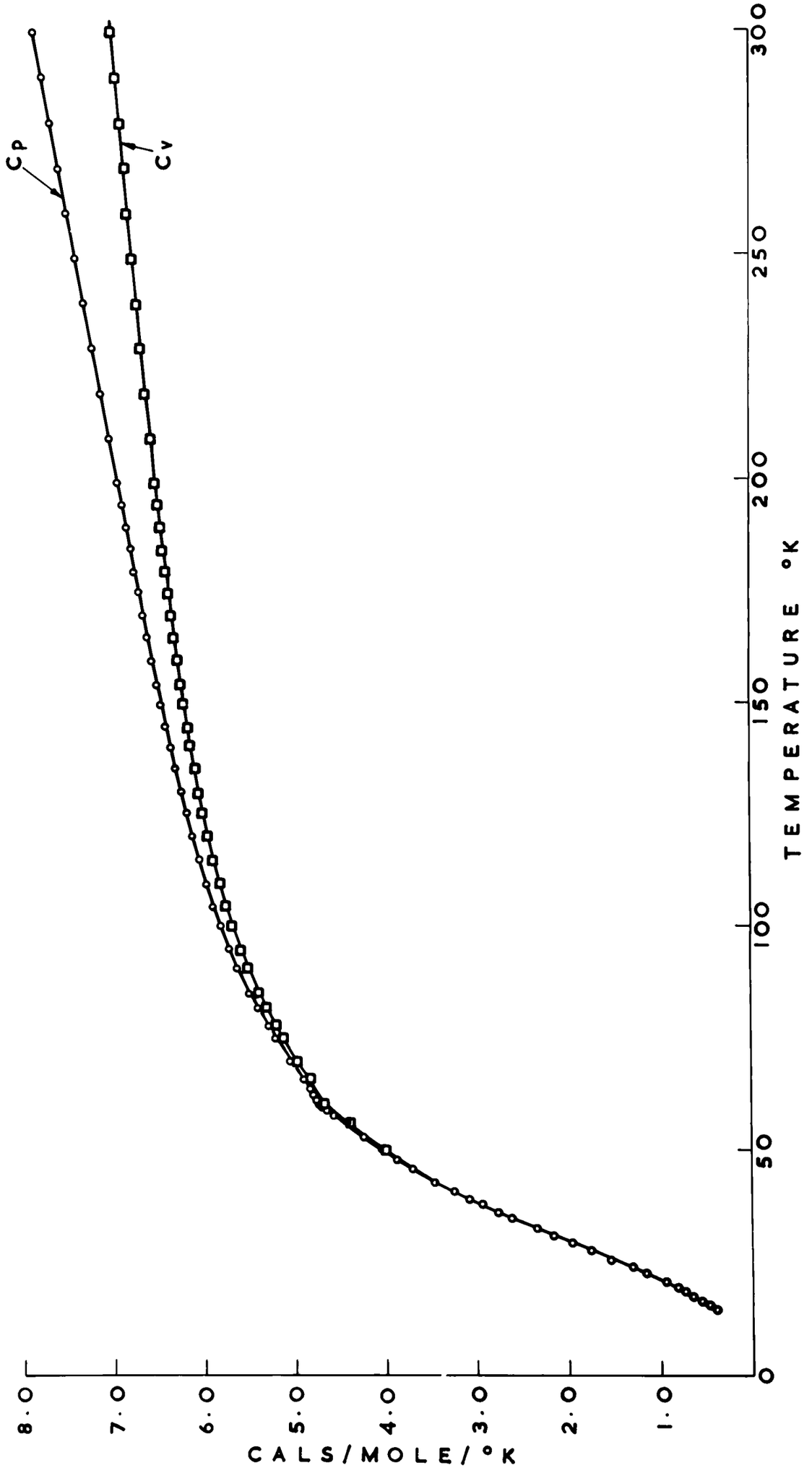


FIG. 4·9. Cp AND Cv OF Pu 6

present work actual experimental C_p values have been used in the analysis below $\sim 100^{\circ}K$ and smoothed values above $100^{\circ}K$. These are shown in Fig. 4.9 together with C_V values derived using the dilation term, discussed in Section 3.3. 3, using the relation

$$C_P - C_V = 9 \alpha_L^2 K T V$$

with our present values for α_L.

Resolution of C_V into lattice and electronic terms is dependent upon a knowledge of the electronic coefficient γ. A plot of C_V/T v. T^2 at the lowest experimental temperatures, $\sim 14 - 20^{\circ}K$, still shows curvature and the normal method of extracting γ from the intercept of such a plot cannot be made. The lowest points suggested an upper limit of $\gamma = 50 \times 10^{-4}$ cals./mole/deg.^{2} and so the C_V values were analysed in terms of an effective θ_D variation with temperature for various γ values below 50×10^{-4}. The resulting θ_D values are shown in Fig. 4.10 for the range of γ's between 37 and 40×10^{-4}. The only method available to us for an estimation of the true γ is to select that value which gave the least temperature dependent θ_D variation in the range $T > \frac{\theta_D}{2}$ where most metals show an almost constant value of θ_D.

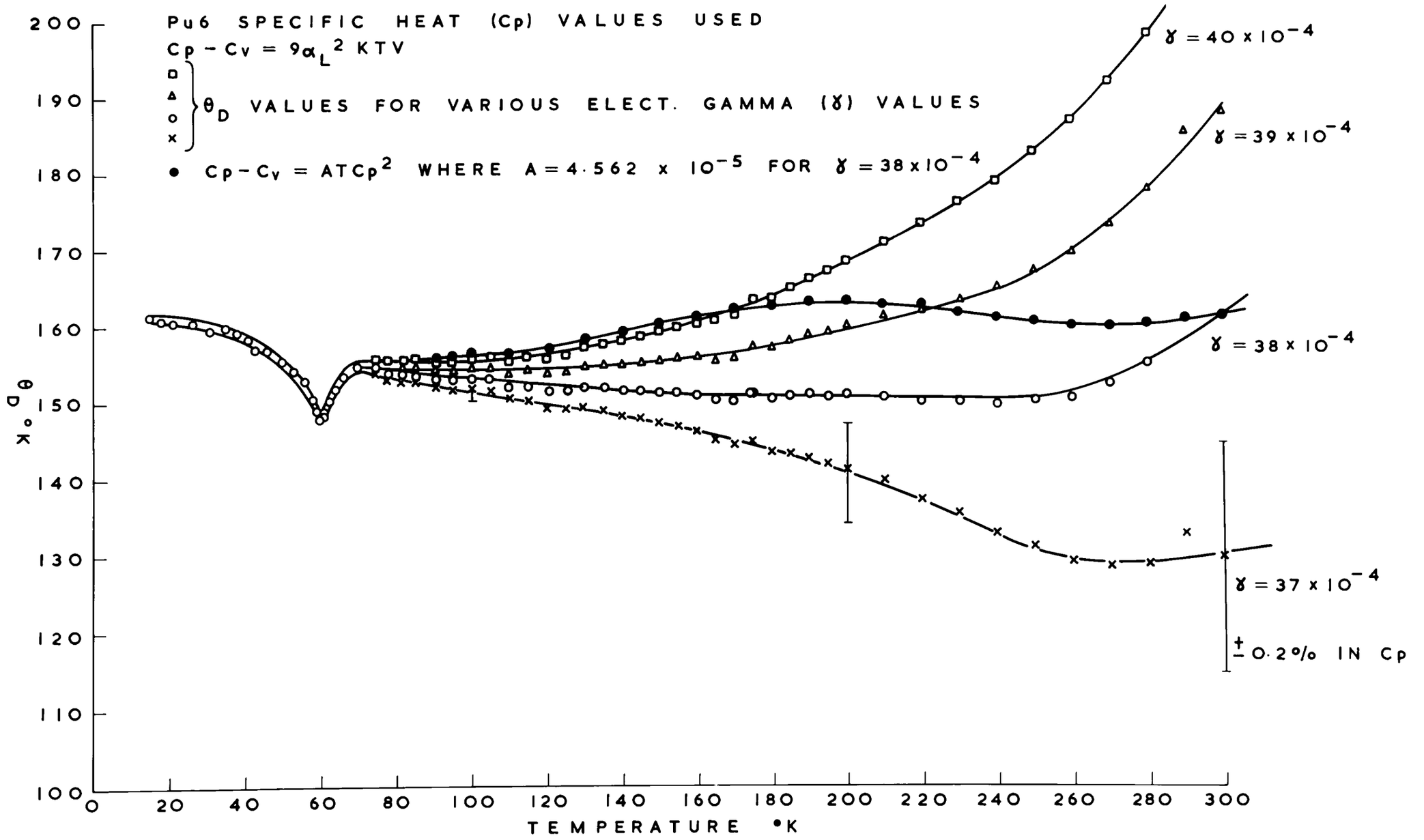


FIG. 4·10. θD VARIATION OF Pu6

The increasing sensitivity of θ_D as the temperature is raised together with the neglect of any additional contributions to other than C_L and C_e, such as possible anharmonic terms (see Foreman (1962)), must necessarily make the choice of $\gamma = 38 \times 10^{-4}$ (and the θ_D values at the higher temperatures) open to considerable uncertainty. Further the large value of $C_P - C_V$ for α-Pu due to the magnitude of a_L, also means that uncertainty in a_L and $C_P - C_V$, has a marked effect upon the choice of γ. For comparison, also shown in Fig. 4.10 is the θ_D variation for $C_P - C_V = ATC_P^2$ where $A = 4.562 \times 10^{-5}$ and $\gamma = 38 \times 10^{-4}$. Also Fig. 4.11 shows the effect of various a_L values discussed in Section 3.3. 1.

The work of Taylor et al. (1965) would result in comparable values for γ and θ_D, if the higher self heat of Pu^{239} is used and a similar method of analysis is adopted. They suggest γ is between 28.5 and 35×10^{-4} cals./mole/$^oK^2$ dependent upon the method of analysis, but use of the higher self heat would alter these to $\sim$ 31.5 and 38×10^{-4}. Sandenaw (1962) however suggests radically different values of $\sim 196 \times 10^{-4}$ cals./mole/$^oK^2$ for γ and θ_D values $\sim 200^oK$, determined by a least squares $C_P = \gamma T + \beta T^3$ fit in the temperature range 11 - 31^oK. This exceptionally high value of γ must be regarded with some suspicion considering the temperature range from which it was derived and the occurrence

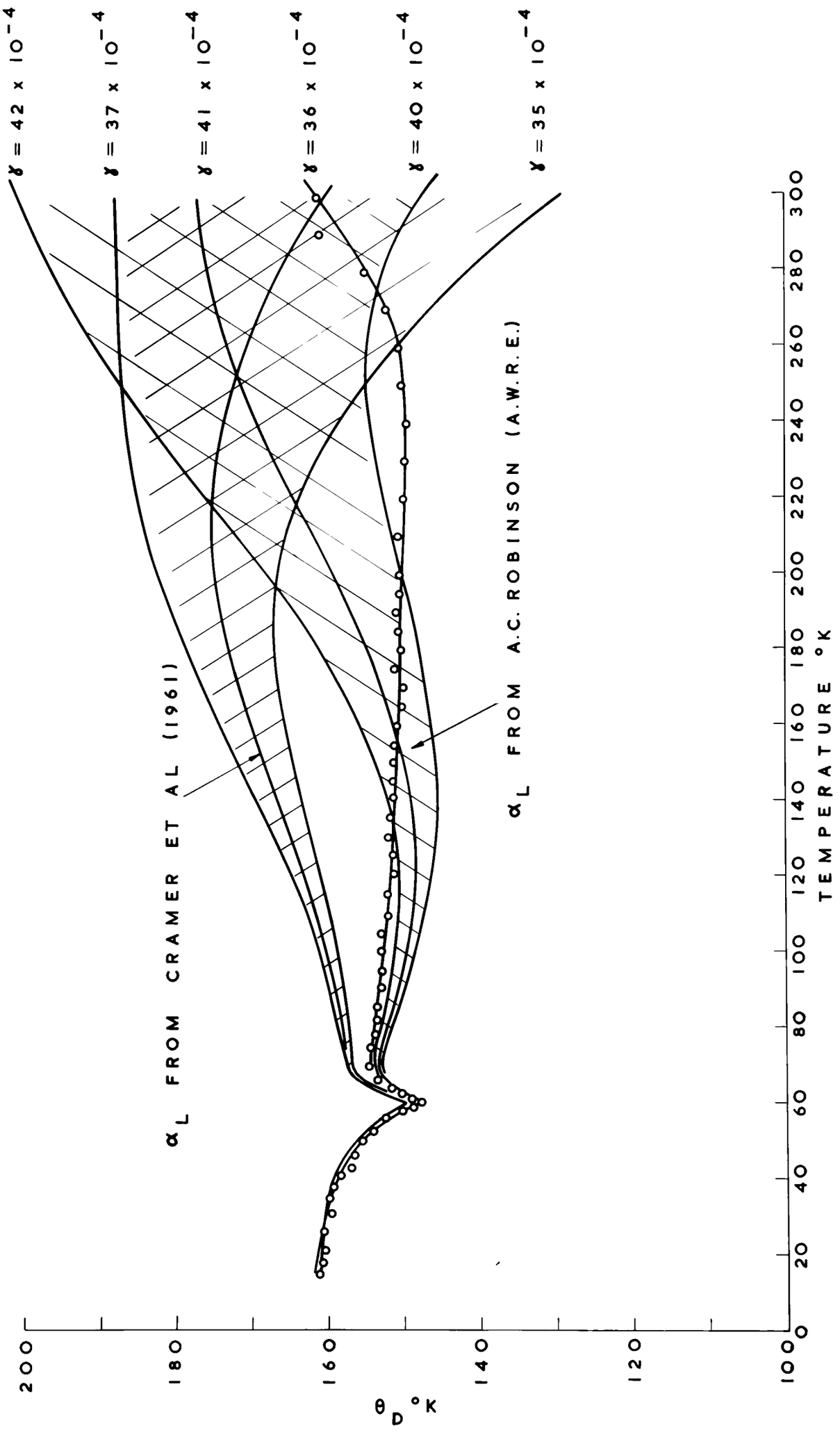


FIG. 4·11. θ_D VARIATION FOR DIFFERENT α_L VALUES

of a peak in some runs in the centre of it (at $\sim 20^{\circ}K$).

The choice of $\gamma = 38 \times 10^{-4}$ however has little effect on the θ_D values below $\sim 80^{\circ}K$ and the distinct minimum in θ_D is again evident. It has a depth of $8.5^{\circ}K$ compared with $\sim 6^{\circ}K$ for both Pu3 and Pu4. The minimum is quite different from the normal θ_D variation due to deficiencies of the simple Debye model to represent true lattice conditions in that it occurs at $\sim \frac{\theta_D}{3}$ compared to the normal temperature range of $\frac{\theta_D}{10}$ to $\frac{\theta_D}{12}$, and is much sharper. The increase in θ_D to a constant value in the region of $\frac{\theta_D}{50}$, could still occur in α-plutonium since the lowest temperature attainable in this work is only $\sim 14^{\circ}K$ ($\sim \frac{\theta_D}{12}$). The apparent levelling off of θ_D to a value of $\sim 161^{\circ}K$ is quite probably followed by an increase at lower temperatures, particularly as the θ_o value suggested by elastic constants measurement is considerably higher $\sim 206^{\circ}K$ (see Section 3.3. 2).

θ values calculated from elastic constants (θ_e) data at higher temperatures, or from Einstein compressibility (θ_E) and Lindeman's melting point formula (θ_m) (see e.g., Mott and Jones) should not necessarily agree with the calorimetric θ_D, but in many metals they often prove to be quite similar, (Blackman (1951)). For α-plutonium, $\theta_e = 180^{\circ}K$ (at $300^{\circ}K$), $\theta_E = 127^{\circ}K$ and $\theta_m = 135^{\circ}K$, which compare favourably with the calorimetric θ_D of 150 - $160^{\circ}K$. Estimation of θ from

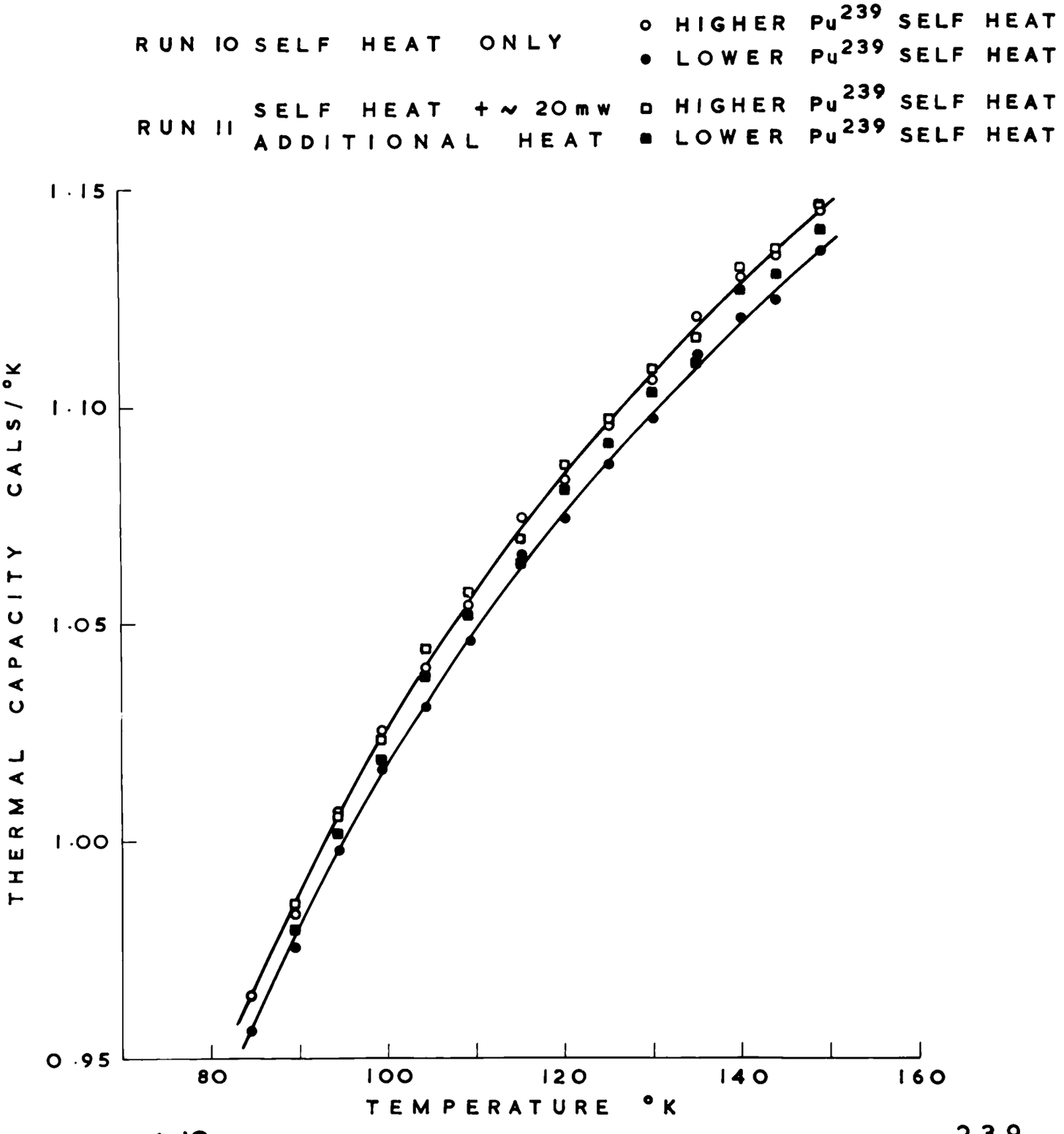


FIG. 4·12. EFFECT OF VARIATION OF Pu^{239} SELF HEAT VALUE

electrical resistivity data from the Grüneisen-Bloch relation is not applicable to α-Pu because of its exceedingly anomalous resistivity curve (see next chapter).

Returning to the minimum in θ_D caused by the small excess in C_p, it would appear on the basis of this work, that despite its smallness it is genuine, since it was found on all three α-plutonium specimens and not on any subsequent materials investigated; that it is caused by some contribution to the total specific heat other than the lattice or conduction electrons. A further analysis of its shape and magnitude and also its relation to other anomalous low temperature properties is deferred until the next chapter.

Further runs on Pu6 were carried out to investigate Pu^{239} self heat contribution discussed in the previous section. Figure 4.12 shows a section of a nitrogen run on Pu6 and is to be compared with Fig. 4.5. In addition the effect on C_p of storage at low temperatures was looked into.

Defects in the lattice of α-plutonium due to its radioactive decay, can remain in equilibrium with their surroundings at low temperatures. They accumulate if the temperature is kept low, but anneal out at various annealing temperatures as the temperature is increased depending upon the type of defects stored. The annealing is accompanied by a release of

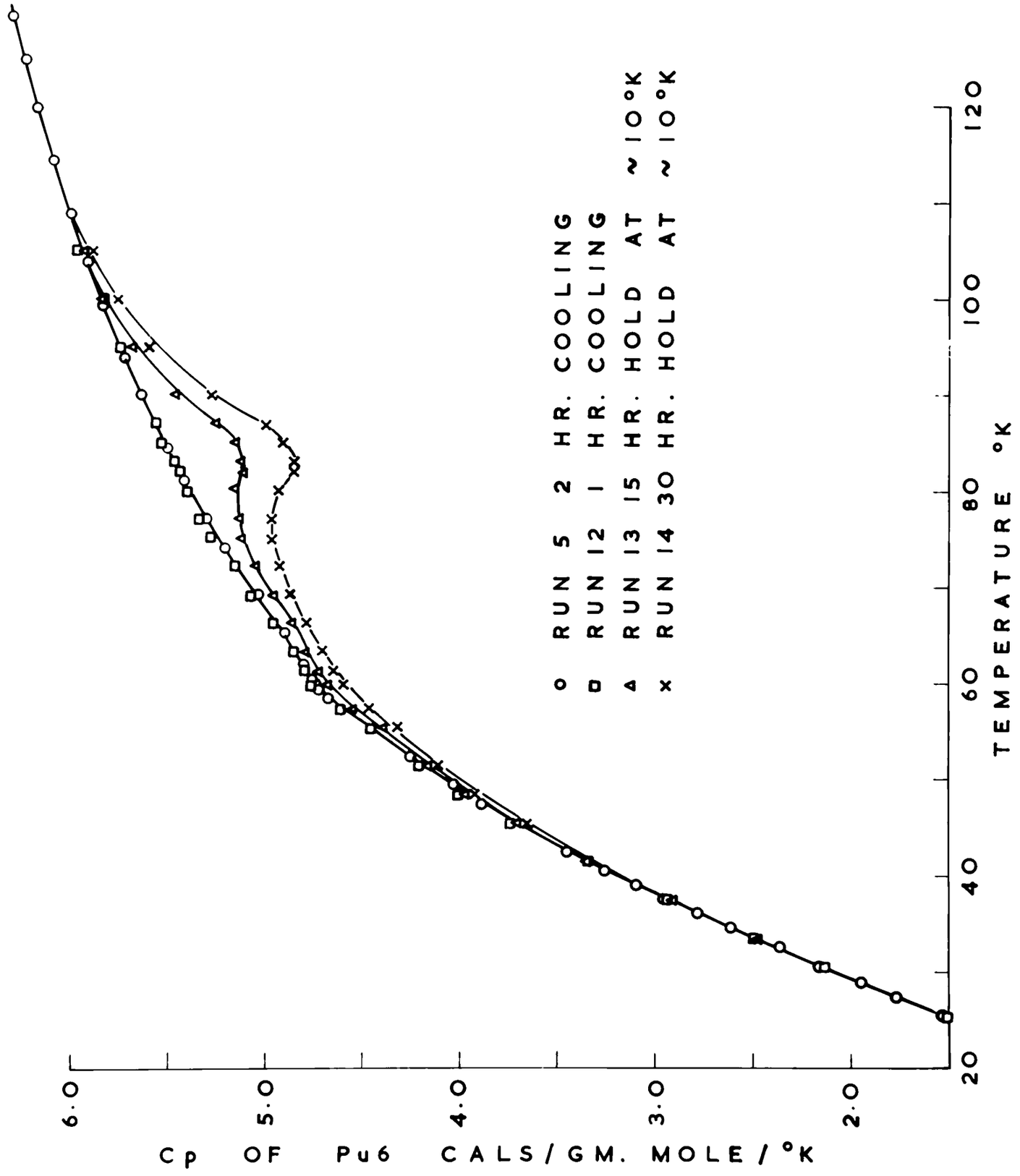


FIG. 4·13. SHORT TERM DAMAGE OF Pu6 WHEN HELD AT ~10°K

energy, which will therefore affect the specific heat values in the region of an annealing stage. Some of the irreproducibility of the early specific heat values of α-Pu was attributed to this cause. Long storage times were not possible with the present equipment, and therefore holds for only 15 and 30 hours at $\sim 10^{\circ}K$ were attempted. Normal cooling times for previous runs was $\sim$ 2 hours below room temperature with less than 1 hour below $\sim 80^{\circ}K$. A fast cool down (maximum 1 hour below room temperature) was also carried out to compare with the normal cools. These are all shown in Fig. 4.13. It can be seen that there is good agreement between 1 and 2 hour cools both in the size of the excess at $\sim 60^{\circ}K$ and in the absence of any minimum at $\sim 83^{\circ}K$. The holding curves begin to fall below the normal curve, at $\sim 30^{\circ}K$, reach a minimum at $\sim 83^{\circ}K$, corresponding to a maximum rate of annealing, and return almost to the normal curve by $\sim$ 100 - 110°K. The difference between the 1 hour cool C_p values ($C_{UNDAM.}$) and stored runs ($C_{DAM.}$) is shown in Fig. 4.14. The area under difference curves represents the total release of stored energy and was found to be 0.487 cals./mole/hr. for the 15-hour hold at $\sim 10^{\circ}K$ and 0.485 cals./mole/hr. for the 30-hour hold. This compares with values of 0.38 cals./mole/hr. when stored at $\sim 20^{\circ}K$ by Sandenaw (1962) and 0.40 cals./mole/deg. by

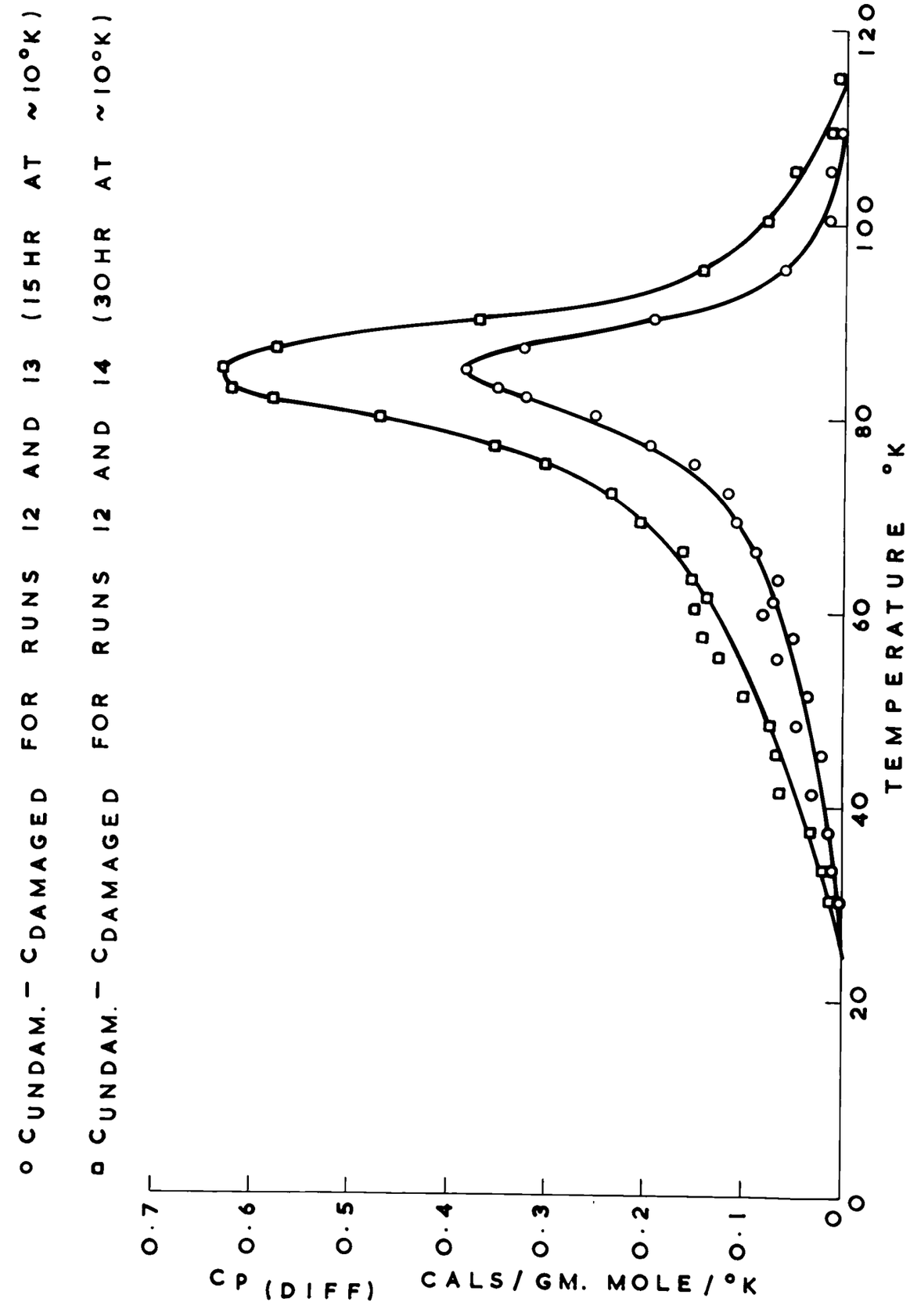


FIG. 4·14. SPECIFIC HEAT DIFFERENCE BETWEEN UNDAMAGED AND DAMAGED RUNS

Taylor et al. (1965) for storage at $\sim 10^{\circ}K$. Vineyard (1961) on the basis of radiation damage theory, assuming ≈ 1800 Frenkel pairs are produced per disintegration, estimates the stored energy to be ~ 0.64 cals/mole/hour. Wigley (1963) has extensively investigated self-irradiation damage effects using electrical resistivity as measuring parameter, and the annealing stage found in the present work, corresponds to his first major stage, starting at $\sim 40^{\circ}K$ and showing a maximum rate at $\sim 80^{\circ}K$. A second smaller annealing stage starting at $\sim 120^{\circ}K$ is not seen on the less precise specific heat work. Exact comparisons are not possible since the resistivity work was a true isochromal anneal which could not be done with the specific heat measurements.

The effect of short-term self irradiation damage on the magnitude of the excess at $60^{\circ}K$ of C_p is unfortunately masked by the fact that annealing commences at $\sim 30^{\circ}K$. The θ_D analysis shown in Fig. 4.15, of the undamaged and damaged runs of Fig. 4.13, shows that the minimum in θ_D has almost disappeared on the 30-hour storage run.

The standard thermodynamic functions, entropy, enthalpy, and Gibbs free energy, of α-Pu were calculated by a computer programme and application of the trapezoidal rule for small

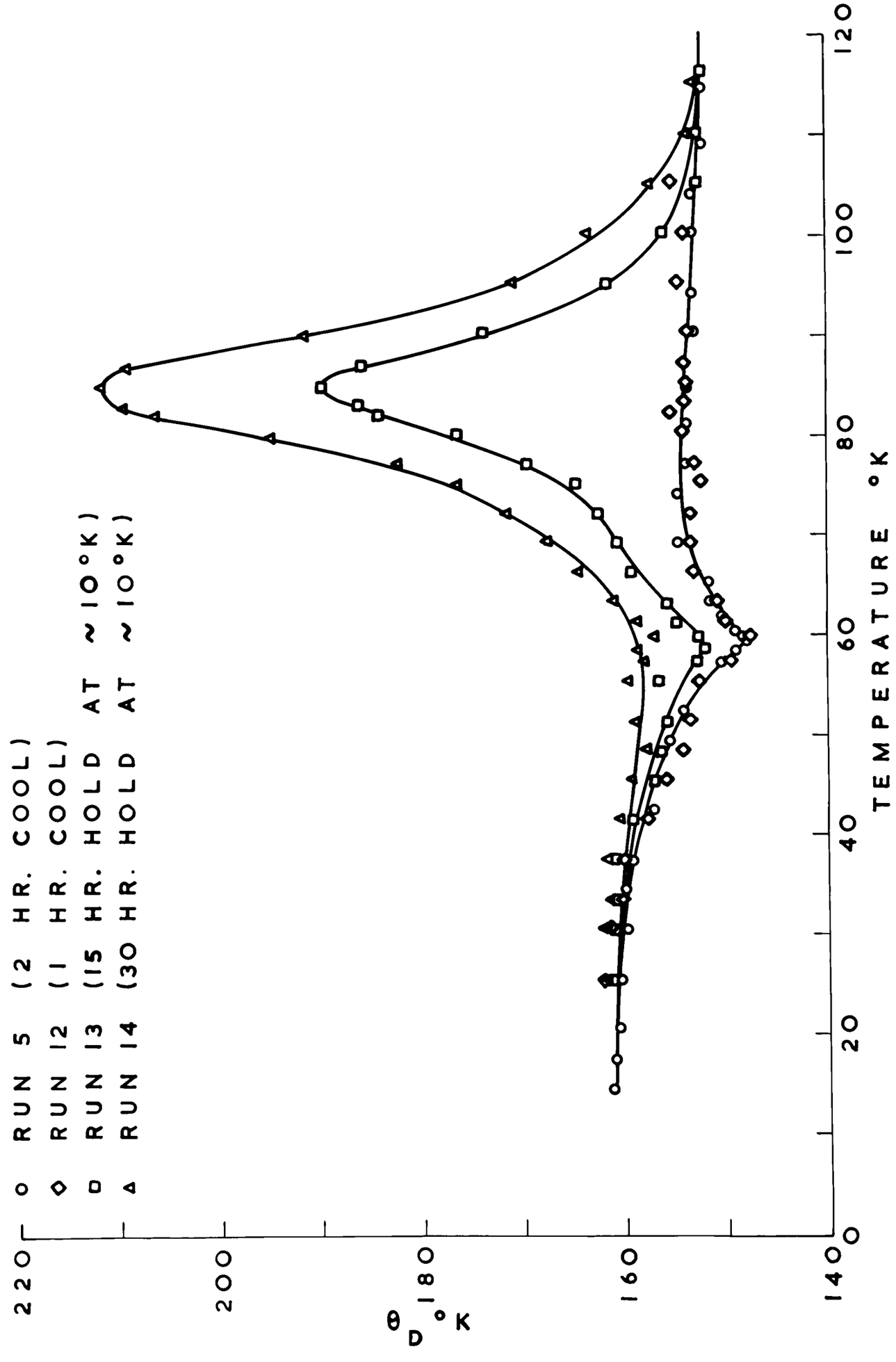


FIG. 4·15. θ_D VARIATION FOR SHORT TERM DAMAGE ON Pu 6

temperature intervals up to 300°K. Smoothed C_p values were used and those below the range of measurement (14 - 300°K) were obtained by graphical extrapolation of the θ_D temperature variation from Fig. 4.10. The contribution to the total entropy and enthalpy due to the extrapolation below 15°K is only 0.176 and 1.86 cals./mole/(deg) respectively. The values of S_{298} and $H^\circ_{298} - H^\circ_o$ so derived for α-Pu are 13.31 (± .05) and 1728.8 (± 10) cals./mole/(deg) respectively. These compare with 13.18 (± .04) and 1687 (± 50) derived from Taylor's work and 12.30 (± 0.12) and 1543 (± 25) from Sandenaw (1962). A full table of molar thermodynamic functions are given in Appendix I, together with the smoothed C_p values used.

4.2 Neptunium

Neptunium exists in three allotropic modifications below its melting point of ~ 640°C. The stable form below ~ 280°C is the α-phase which has an orthorhombic crystal structure. It is still only available in limited quantities, and a small amount of neptuniun oxide was received from U.S.A.E.C.. This was converted to fluoride (NpF_4) at Windscale and then reduced to metal at Harwell by means of a calcium reduction technique in the presence of iodine. We are indebted to A. Hough for the reduction and for casting

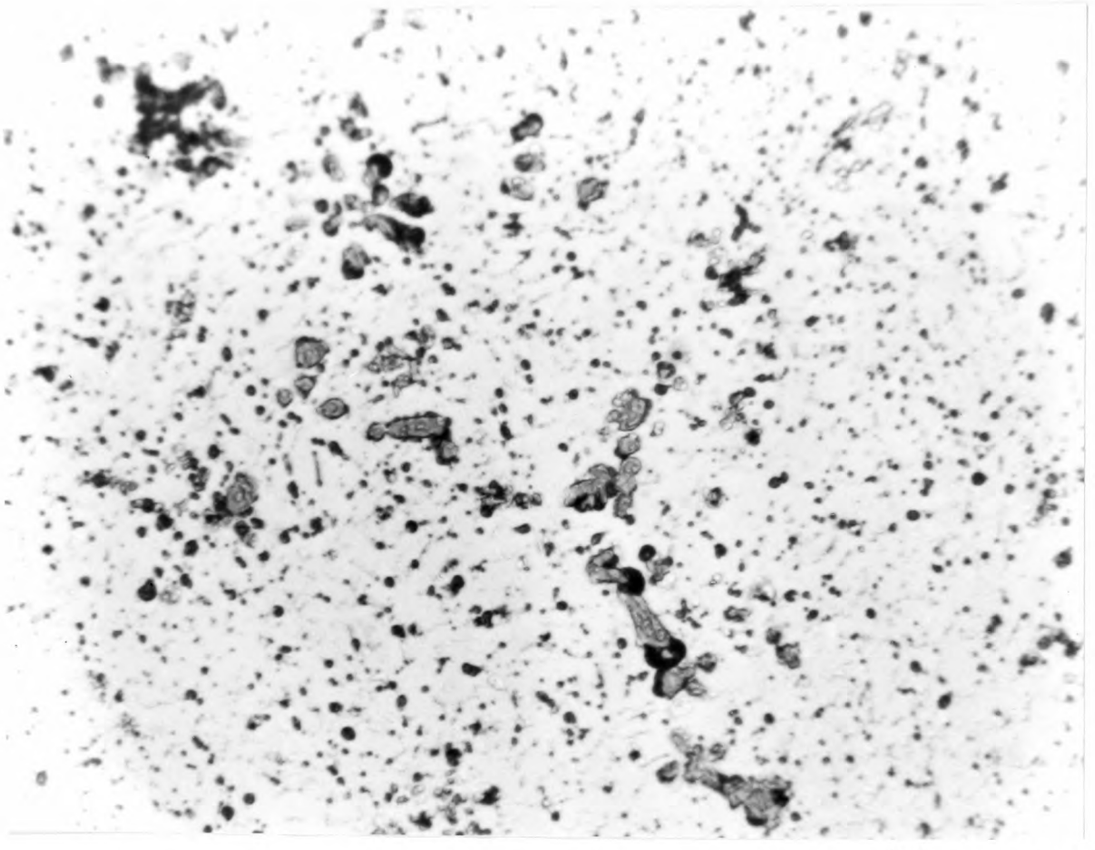


PLATE 4·3 (a).

MAG. X 1000

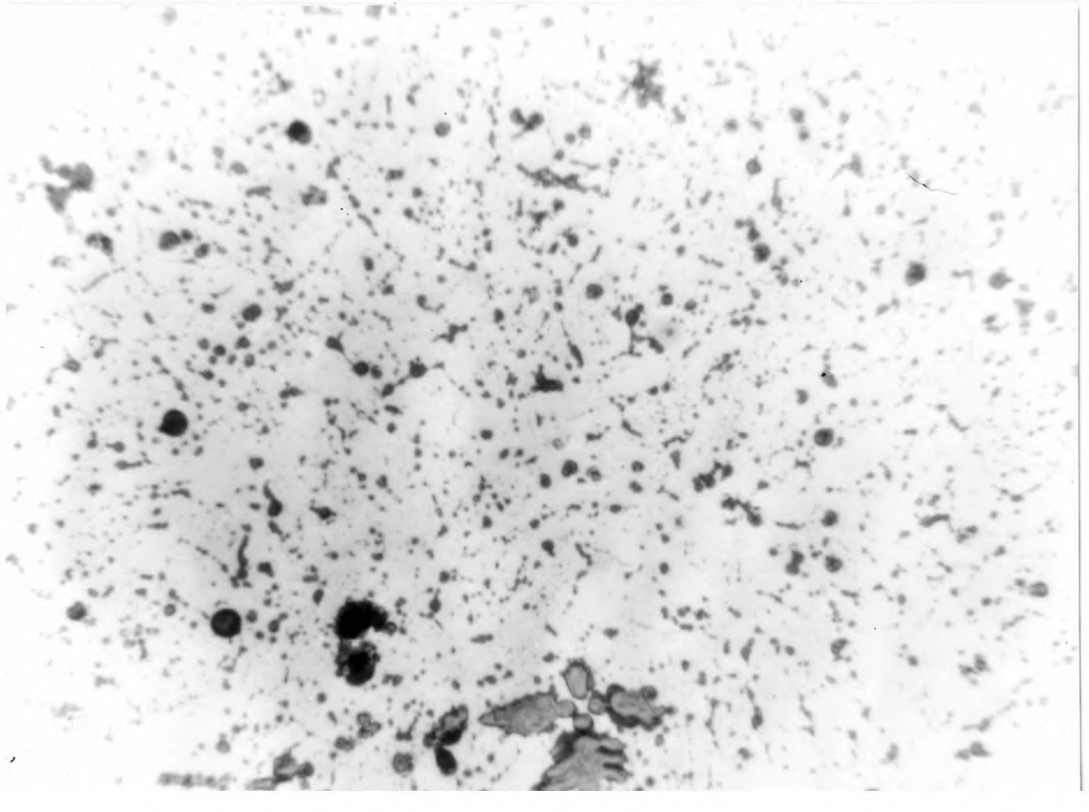


PLATE 4·3 (b).

MAG. X1000

into cylindrical shape. It was then machined to size, and the centre hole drilled and tapered. Since the weight available was only a few grams a special small scale calorimeter was constructed of high purity silver.

The analyses shown in Table 4.4 revealed that the purity of the neptunium was only 99.10%, which was confirmed by the high inclusion level shown on metallographic examination. Plate 4.3(a) and (b) show two different areas of the specimen, and the grain size can be seen to be ~ 10 μcrons, from the accumulation of inclusions in the grain boundaries.

Due to the low value of the self heat of neptunium, the small amount of radioactive plutonium and americium impurities (total of 0.146 wt/o) contribute approximately 20% of the total self heat of 0.0256_7 mwatts/gm. The weight of the specimen was only 3.139_8 gms giving a total self heat of 0.0799_9 mwatts. The accuracy of the neptunium analysis is considerably less than similar plutonium analyses. Also even the small quantities of Pu^{238} present contribute 10% to the total self heat, and the analysis of this isotope in particular was somewhat uncertain. For this reason and because the system of measurement had been designed to deal with considerably higher self heats and hence higher rates of rise of temperature, amounts of additional heat varying

TABLE 4.4

α-Np

Spectrographic Analysis

Following Detected (Wt/O) :-

Si - 0.052:	Fe - 0.12:	Mg - 0.07:	Cr - 0.01:
Ni - 0.11 :	Al - 0.07:	Cu - 0.14:	Na - 0.10.

Following not detected :-

Sb : Pb : V : Be : Nb : Mo : P : Ag : Ge : Tl : Sn :
In : La : Pd : Y : Ti : Pt : Mn : Co : Sc : Sr : Ba :
Au : Ta : Bi : Ga : Zn : Dy : Yb : Eu : W : Hg : As :
Os : Ir : Zr.

Gas Analysis (Wt/O)

O_2	0.042
N_2	0.014

Isotopic Analysis (Wt/O)

Np^{237}	99.10
Am^{241}	.000061
Pu^{238}	.000407
Pu^{239}	.1399
Pu^{240}	.00516
Pu^{241}	.00026

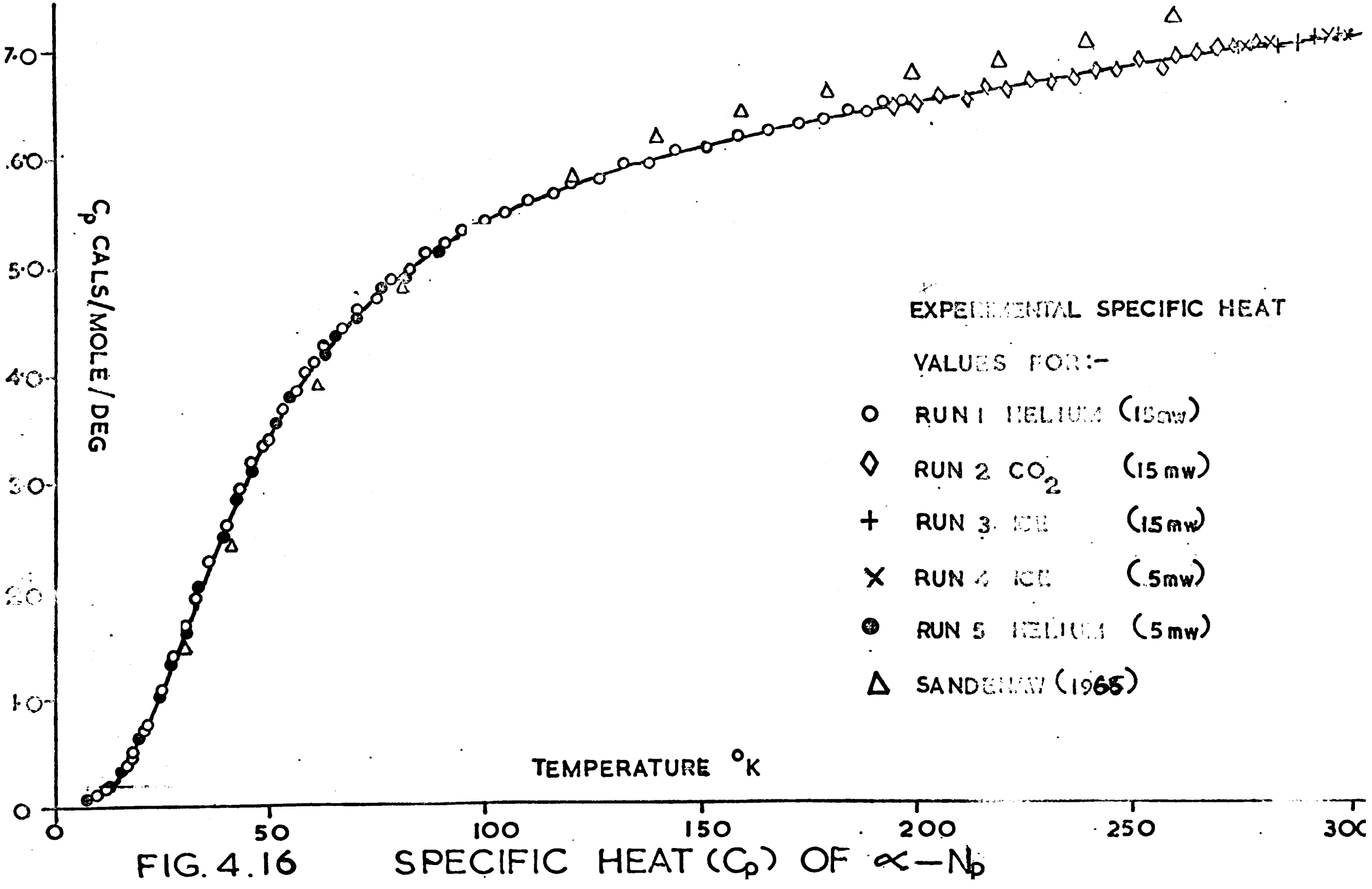


FIG. 4.16 SPECIFIC HEAT (C_p) OF α—Nb

between 2.5 and 15 mwatts were used.

The results of several of the specific heat runs (with additional heat levels of 5 - 15 mwatts) are shown in Fig. 4.16. Good agreement was obtained between runs of differing additional heat levels and between runs using different refrigerants.

In general the C_p values, like plutonium, are high reaching a value of $\sim$ 3R by $\sim$ 140°K and $\sim$ 7.1 cals./mole/deg. at 300°K.

The only other specific heat determination below room temperature on α-Np was by Sandenaw (1965), and some of his quoted values are also shown in Fig. 4.16. Considerable differences can be seen in the values of C_p, our present work giving values $\sim$ 10% higher in the region of 50°K, and $\sim$ 5% lower at 200°K and $\sim$ 12% lower at room temperature. Sandenaw also observed some unusual effects; a small peak at $\sim$ 85°K, increased scatter, by a factor of 2 or 3, in the temperature range 75 - 140°K and a change of slope at $\sim$ 240°K. None of these were observed by us. No total impurity content is given by Sandenaw, but it is described as impure Np, and it is possible that these small effects are due to impurities and not truly representative of neptunium. However since the purity of our sample leaves

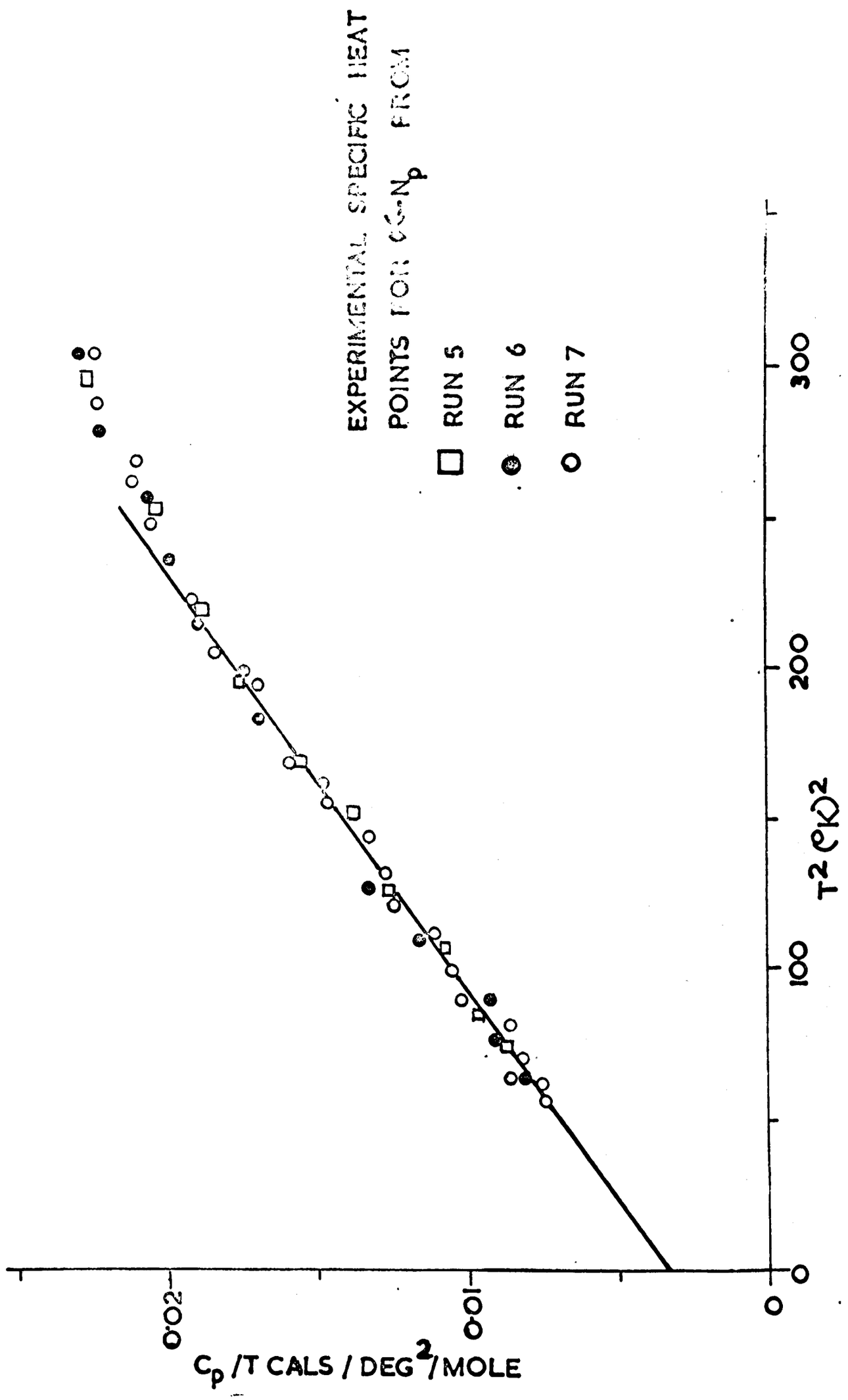


FIG. 4.17 $C_p/Tv.T^2$ PLOT FOR α–Np.

a lot to be desired, confirmation of the correct absolute values of C_p must await the availability of high purity material. It is interesting to note however that our room temperature value is within 2% of an extrapolated value from the work of Evans and Mardon (1959) between 60 and 210°C.

The use of additional heat levels of ~ 2.5 mwatts (runs 6 and 7) enabled the lowest temperature at which C_p values could be evaluated to be ~ 7.5°K. The resulting C_p/T v. T^2 plot for the temperature range 7.5 to 17.5 is shown in Fig. 4.17, and can be seen to be linear below ~ 15°K. The intercept and gradient of the least squares deviation line drawn in Fig. 4.17 yield from equation 1.13 and equation 1.7 an electronic-contribution coefficient $\gamma = 34 \times 10^{-4}$ cals./mole/deg.^{2} and θ_D of 187.5 °K. These compare favourably with Sandenaw's values of $\gamma = 33 \times 10^{-4}$ and $\theta_D = 190$°K.

Using the value of $\gamma = 34 \times 10^{-4}$ the smoothed specific heat curve shown in Fig. 4.16 has been analysed in terms of effective θ_D values and its temperature variation is shown in Fig. 4.18. θ_D is remarkably temperature independent by only about 5%. The minimum at ~ $\theta_D/5$ is perhaps a little high compared to the normal ~ $\theta_D/10$, but its smooth variation leads us to conclude that the specimen of α-Np investigated displays a fairly normal C_p curve which can be

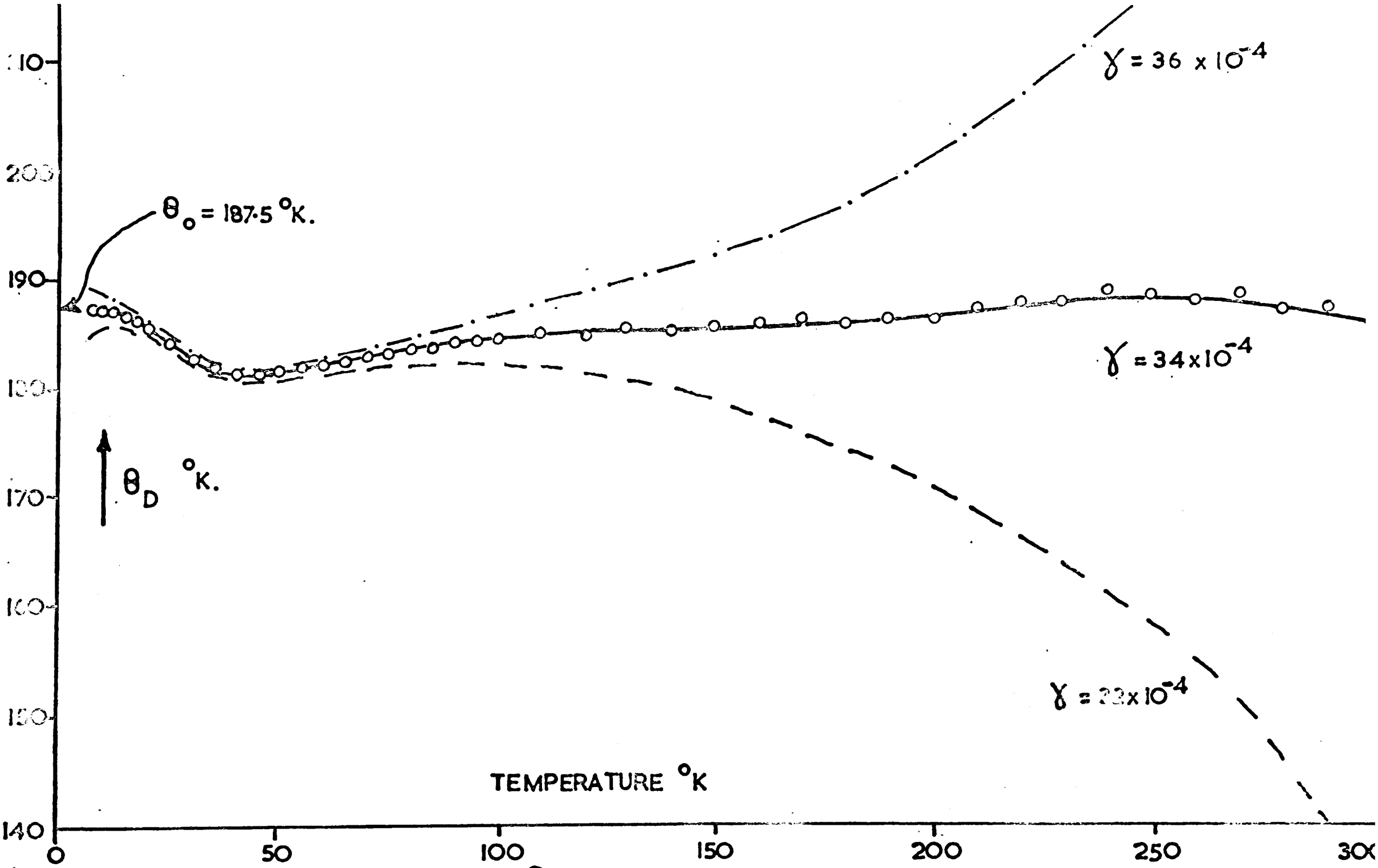
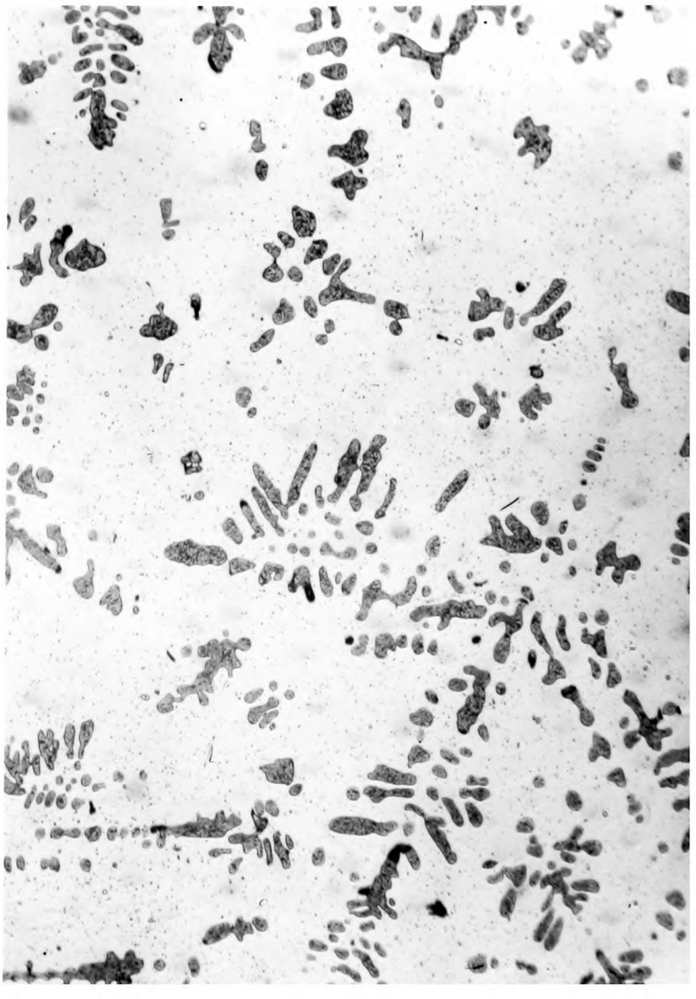


FIG. 4.18 VARIATION IN θ_D FOR α-N_p.

accounted for on the basis of lattice and conduction electron contributions only. Variation in Θ_D for slightly differing γ values are also shown in Fig. 4.18 as a comparison with α-Pu, where γ was estimated from the least temperature dependent Θ_D curve.

The only values of Θ available from other properties of α-Np are a value of $\Theta_m = 137^\circ K$ from Lindeman's melting point formula and $\Theta_R = 137^\circ K$ from the resistivity curve, although the latter value is only applicable in the range 17 - 35°K.

The standard thermodynamic properties have been evaluated from the smoothed C_p values and are tabulated in Appendix II. Below 7.5°K, C_p values have been extrapolated using the C_p/T v. T^2 plot, and the contribution to the total entropy and enthalpy at higher temperatures, due to this extrapolation below 7.5°K is only 0.032 and 0.159 respectively. The values of S_{298} and $H^\circ_{298} - H^\circ_o$ are 12.10 (± 0.10) cals./mole/deg. and 1591.8 (± 20) cals./mole respectively. Despite the differences in C_p values observed between this work and that of Sandenaw, the entropy and enthalpy values compare quite well, his values being 12.03 and 1622.



MAG. X100

PLATE 4·4.

4.3 Plutonium Monocarbide

Plutonium monocarbide is one of four carbides formed in the plutonium-carbon system. It is non-stoichiometric with an approximate composition of $PuC_{0.85}$, and has a face-centred cubic (NaCl type) structure.

Full spectrographic analysis was not carried out but the probable impurity level is ~ 1 - 2000 ppm. Isotopic analysis gave the following in wt/o of total carbide:-

Pu^{238}	Pu^{239}	Pu^{240}	Pu^{241}	Pu^{242}	Am^{241}
0.0067	90.96_9	4.02_6	0.250	0.010	0.038

and carbon analysis, 4.60 wt/o. This gives a self heat of 2.122_9 mwatts/gm, which for the sample weight of 13.323 gm, leads to a total self heat of 28.28_4 mwatts.

Metallographic examination (see Plate 4.4) revealed the presence of a higher carbide phase, Pu_2C_3, but little free carbon. Lineal counting estimated the sesquicarbide composition to be 12.70 volume per cent.

The specific heat values that were determined on this sample of monocarbide were evaluated in terms of two possible compositions. In the first the 4.60 wt/o carbon and 95.26 wt/o plutonium were considered as forming a 'monocarbide'

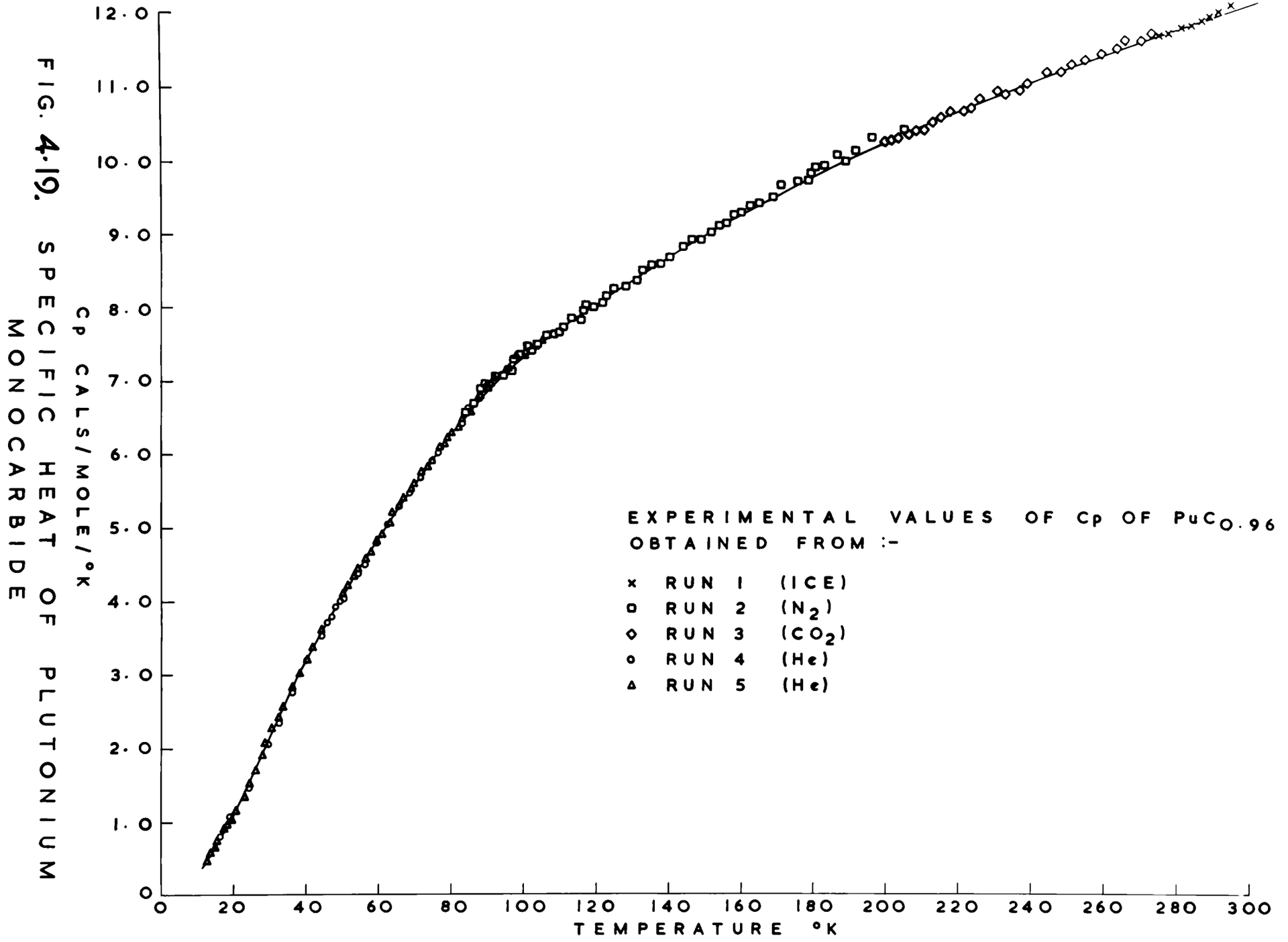


FIG. 4.19. SPECIFIC HEAT OF PLUTONIUM MONOCARBIDE

of composition $PuC_{0.96}$ having a molecular weight of 250.59. Because of the lack of data on Pu_2C_3 this is strictly the only way in which the specific heat values can be interpreted. However if it is assumed that the specific heat of Pu_2C_3 is comparable with U_2C_3, whose specific heat is well known (see e.g., Andon, Counsell, Martin and Hedger (1964), then subtraction from the total thermal capacity, an amount corresponding to 12.14 wt/o, U_2C_3 (and hence Pu_2C_3) results in the remainder corresponding to a composition of $PuC_{0.87}$ having a molecular weight 249.50. Even if the specific heats of U_2C_3 and Pu_2C_3 differ by as much as 10%, such a correction will only introduce an error of just over 1% in the values for $PuC_{0.87}$, always provided however that the various contributions to the total specific heat of the monocarbide are independent of carbon composition. This assumption will be discussed further in the next chapter.

A series of helium, nitrogen, CO_2 and ice runs were carried out and the experimental points obtained between 12.5°K and room temperature is shown in Fig. 4.19 for the $PuC_{0.96}$ composition. Other low temperature properties of plutonium monocarbide (discussed fully in the next chapter) have suggested the existence of a magnetic transition in the region of 100°K. The temperature range 80 - 120°K was

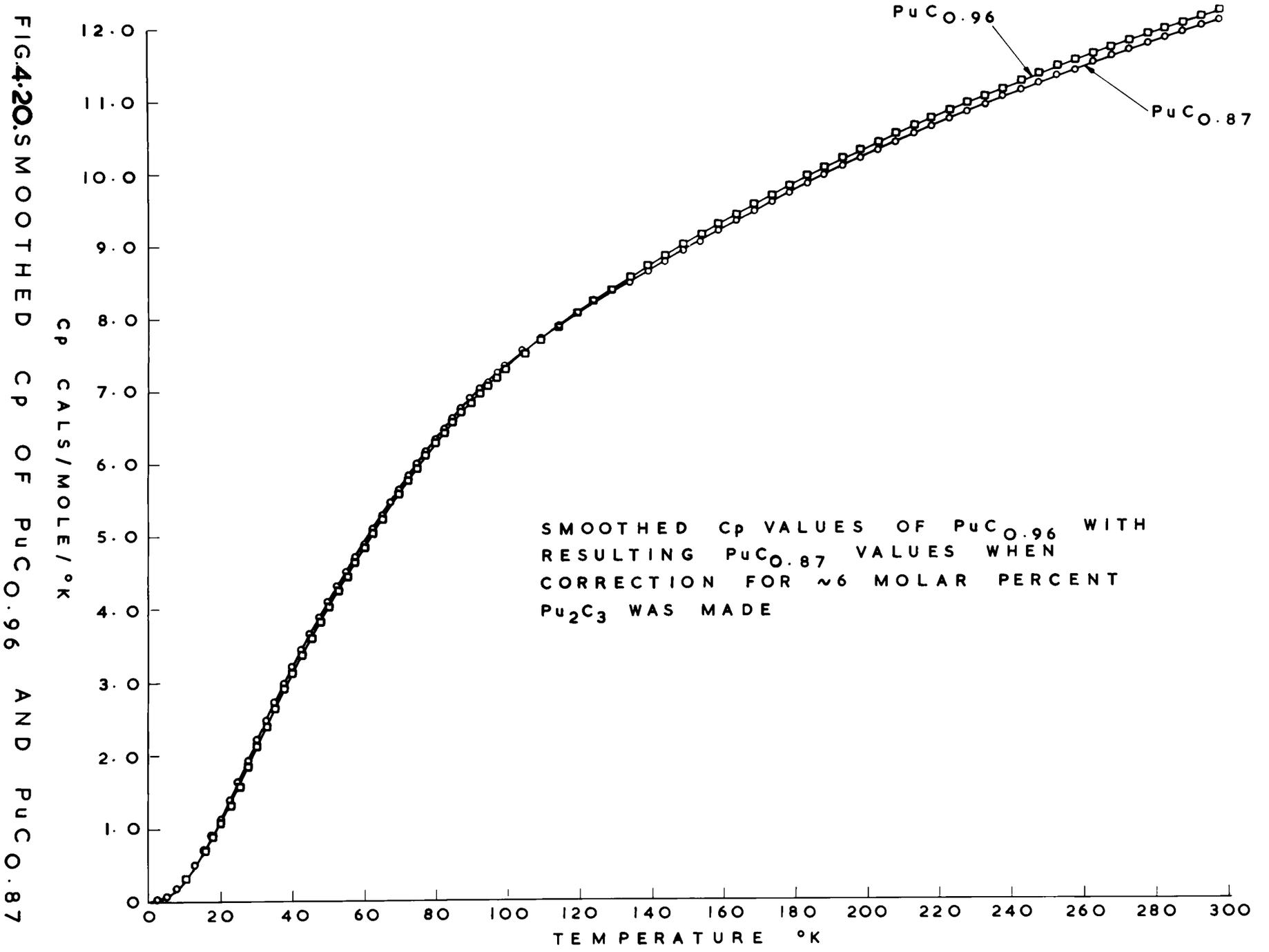


FIG. 4.20. SMOOTHED Cp OF $PuC_{0.96}$ AND $PuC_{0.87}$

therefore studied with considerable care. The large number of points in this region, combined with the slightly higher scatter from the nitrogen points results in an apparent widening of the experimental scatter but all are within ~ ± 1%. We conclude therefore that for the sample investigated C_p lies on a smooth curve within the limits of ~ ±1%, and rises to a value of ~ 12.17 cals./mole/deg.

The smooth curve of Fig. 4.19 was then corrected for the higher carbide composition as described and a comparison of the resulting C_p values for $PuC_{0.96}$ and $PuC_{0.87}$ is shown in Fig. 4.20. The difference is only ~ 2.5% at ~ 40°K and ~ 1% at 300°K, the two curves crossing at ~115°K.

No other specific heat work is available on the monocarbide below room temperature and the only work above, is by a drop calorimeter technique between 425 and 1925°C for a sample of composition $PuC_{0.87}$ by Kruger and Savage (1964). Their work leads to an extrapolated value at 300°K of ~ 11.3 cals./mole/deg., which is ~ 7% lower than this work. Such a difference seems excessive to be accounted for solely by the different compositions of the samples investigated. It must be noted that high and low temperature methods have quite often led to discrepancies, and in particular, a similar situation arose in the case of uranium monocarbide between

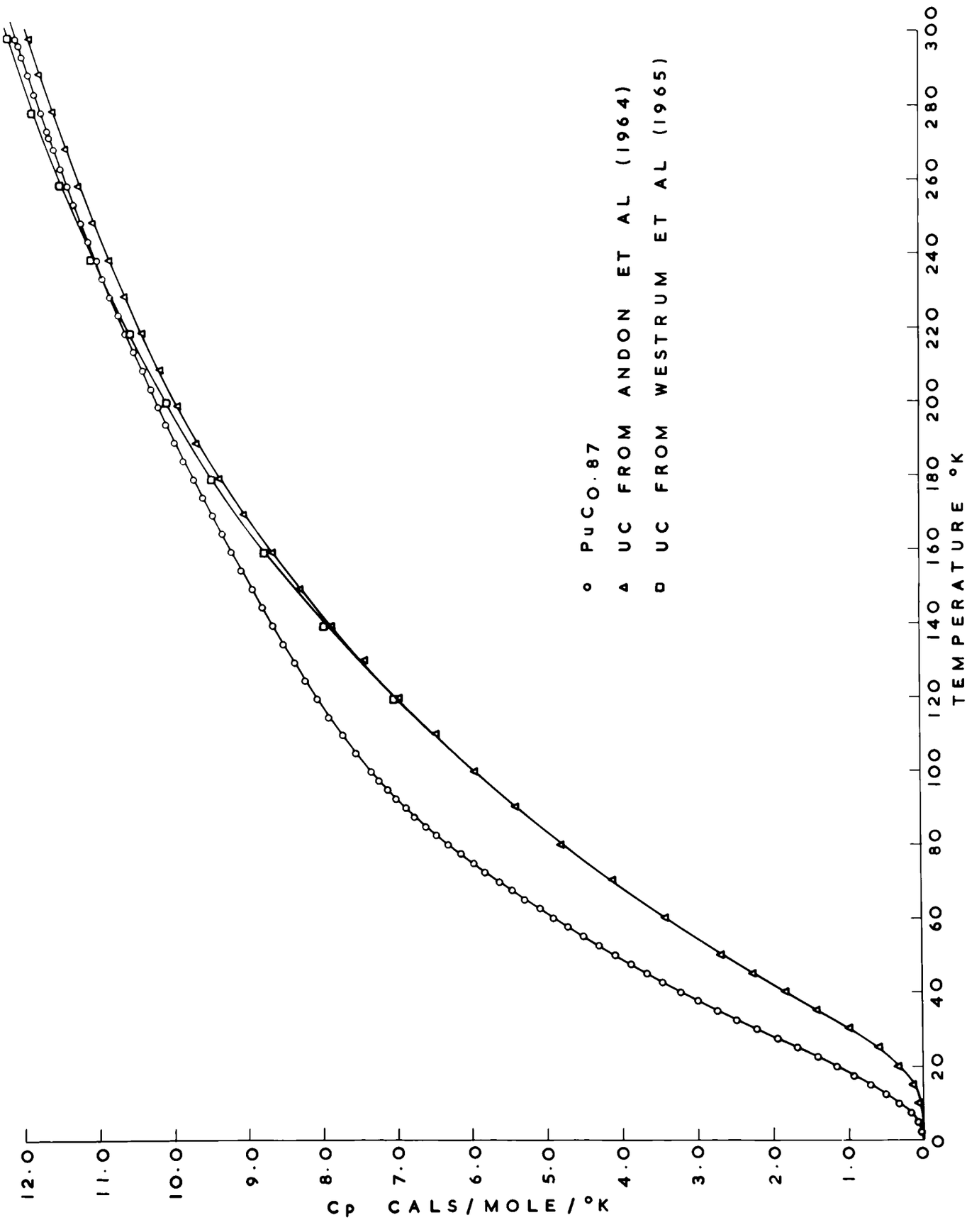


FIG. 4-21. COMPARISON OF Cp OF PuC AND UC

1962 and 1965 until the higher temperature data was found to be in error.

A comparison of our present results of plutonium monocarbides and the published data on uranium monocarbide from Andon, Counsell, Martin and Hedger (1964) and Westrum, Suits and Londsdale (1965) is shown in Fig. 4.21. Although C_p values are comparable at room temperature, the 'PuC' curve is considerably higher over most of the temperature range up to 200°K, and leads, as it will be seen, to significantly higher entropy values.

The monocarbides of transition and rare-earth metals and also of uranium and thorium have been found to have many metallic properties. In particular that their low temperature specific heats follow a $\beta T^3 + \gamma T$ relation. Our present work on 'PuC' down to 12.5°K, results in a C_p/T v. T^2 plot which is still slightly curved at $\sim$ 12.5°K. Extrapolation from the lowest points would suggest anupper limit for γ of $\sim 120 \times 10^{-4}$ cals./mole/deg.^{2} A high value is not too surprising when compared with uranium carbide which has a value ($\sim 45 \times 10^{-4}$) which is almost twice that of the metal uranium ($\sim 26 \times 10^{-4}$).

Estimation of γ from an analysis similar to that adopted

for α-plutonium is not too successful for 'PuC'. In the first place it is not possible to evaluate the dilation term although an estimate based on UC would suggest it is small. Secondly θ_D values are strongly temperature dependent despite considerable variation in the value of γ. Suffice it to say that θ_D from the basic C_p values varies from $\sim$ 200°K at $\sim$ 20°K, to a broad maximum of $\sim$ 350°K in the region of $\sim$ 150°K and falls below 200°K at $\sim$ 270°K. Analysis of the UC results, even with a knowledge of γ from very low temperature determinations (see Harness, Matthews and Morton (1964)) results in a similar strongly dependent θ_D variation.

The thermodynamic functions, entropy and enthalpy and Gibbs free energy are tabulated in Appendices III and IV for the compositions $PuC_{0.96}$ and $PuC_{0.87}$. Extrapolation below 12.5°K was obtained by fitting the C_p values between 12.5°K and 25°K to a function of the form $0.75F(\theta_D)$, where $F(\theta_D)$ is the Debye function. The choice of the factor 0.75 was selected to give an almost constant value of θ_D in this region, and this value was used below 12.5°K. The contribution to the entropy and enthalpy at higher temperatures resulting from this extrapolation is 0.23 cals./deg./mole and 1.9 cals./mole respectively. The values of S_{298} and $H^o_{298} - H^o_o$

for $PuC_{0.96}$ are 17.25 (± 0.15) and 2379 (± 40) and for $PuC_{0.87}$ are 17.33 and 2370 respectively.

Rand (1968) using the best smooth curve through the present C_p values and the high temperature data, and a value of S_{298} of 17.3 obtains excellent agreement for the entropy of formation at 1600°K with that obtained from high temperature vaporization measurements.

REFERENCES

Andon, R.J.L., Counsell, J.F., Martin, J.F. and Hedger, H.J., (1964): Trans. Far. Soc., 60, 1030.

Blackman, M., (1951): Proc. Phys. Soc., 64A, 681.

Evans, J.P. and Mardon, P.G., (1959): J. Phys. Chem. Solids, 10, 311.

Foreman, A.J.E., (1962): Proc. Phys. Soc., (Lond.), 79, 1124.

Harness, J.B., Matthews, J.C. and Morton, N., (1964): Brit. J. Appl. Phys. 15, 963.

Kruger, O.L. and Savage, H., (1964): J. Chem. Phys., 40, 3324.

Lee, J.A., Marples, J.A.C., Mendelssohn, K. and Sutcliffe, P.W., (1965): Plutonium 1965, Chapman and Hall, London (1967), p. 189.

Lee, J.A., Mendelssohn, K. and Sutcliffe, P.W., (1965): Cryogenics, 5, 227.

Griffin, C.S., Mendelssohn, K., Sutcliffe, P.W., Wigley, D.A., Hall, R.O.A., Lee, J.A. and Marples, J.A.C. (1966): Int. Conf. Low Temp. Phys., 10th, Moscow, 4, 117.

Oetting, F.L., (1965): J. Inorg. Nucl. Chem. 27, 2151.

Rand, M.H., (1968):'Thermochemical Assessment of Pu-C System', to be discussed at a panel meeting,

Sept. 1968, IAEA, Vienna.

Sandenaw, T.A., (1962): J. Phys. Chem. Solids, 23, 1241.

Sandenaw, T.A., (1965): J. Phys. Chem. Solids, 26, 1075.

Sandenaw, T.A., Olsen, C.E., and Gibney, R.B., (1960): Plutonium 1960, Cleaver-Hulme Press, London (1961), p. 66.

Taylor, J.C., Loasby, R.G., Dean, D.J. and Linford, P.F., (1965): Plutonium 1965, Chapman and Hall, London, (1967), p. 162.

Vineyard, G.H., (1961): Unpublished.

West, E.D., (1963): NBS J. of Res. 67A, 331.

Westrum, E.F., Suits, E. and Lonsdale, H.K. (1965): Symp. Thermophys. Props., Papers, 3rd, Lafayette, Ind. p. 156.

Wigley, D.A., (1963): Thesis, Univ. of Oxford.

CHAPTER 5

DISCUSSION OF RESULTS

The purpose of this chapter is to discuss the results of this investigation into the specific heats of plutonium, neptunium and plutonium monocarbide, not only in their relation to their low temperature properties in general but, also in the case of Pu and Np, in the broader context as members of the actinide series.

The transition lanthanide and actinide metals all possess the common feature of incompletely filled inner shells. With the transition metals of the 1st, 2nd and 3rd long periods it is the 3d, 4d and 5d shells, respectively, that are incomplete whereas with the rare earths it is the 4f shell that is progressively filled on passing along the series. Although the earlier members of the actinide series actinium, thorium, protoactinium and possibly uranium show many properties similar to transition metals, it is found that as one passes along the series between U, Np and Pu the metals are found to become less transition-like and more lanthanide-like. Americium, curium, etc. certainly as far as their chemical properties are concerned almost wholly resemble the

lanthanides. The gradual change may well be the cause of some of the unusual properties of the metals situated in the 'in between' region and in this respect the 5f electrons must play an important role.

For this reason it is necessary to review the present state of understanding of the band structure of the better-known earlier members, Th and U in relation to their physical properties before progressing to Np and Pu.

5.1 Thorium

Thorium has four electrons outside the radon core $\{1s^2, 2s^2 \ldots\ldots 5d^{10}, 6s^2, 6p^6\}$ of closed sheels. Spectroscopic data suggests that the outer electron configuration of the free atom is $6d^2\ 7s^2$. Spin-orbit interactions split the 5f and 6d levels of the free atom and on forming the solid, these levels are spread out into bands. The 7s levels form a broad band that is raised in energy by several eV, the 6d levels form broad overlapping bands, while the 5f levels form much narrower split bands as a consequence of the more limited spatial extension of the 5f electronic wave functions. Lehman (1956) has obtained an energy band scheme for f.c.c. Th, which is the stable α-phase below $\sim$ 1400^{o}C, and shows the Fermi level to be in the broad 6d

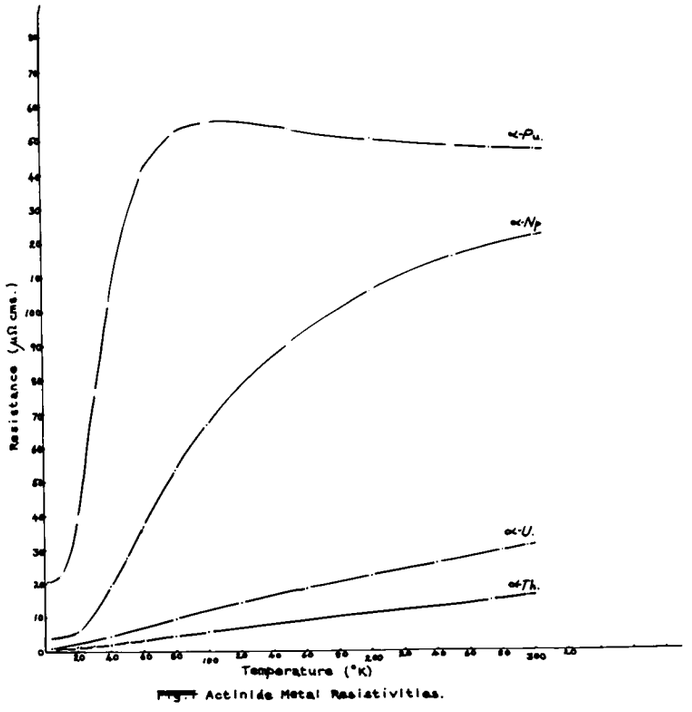
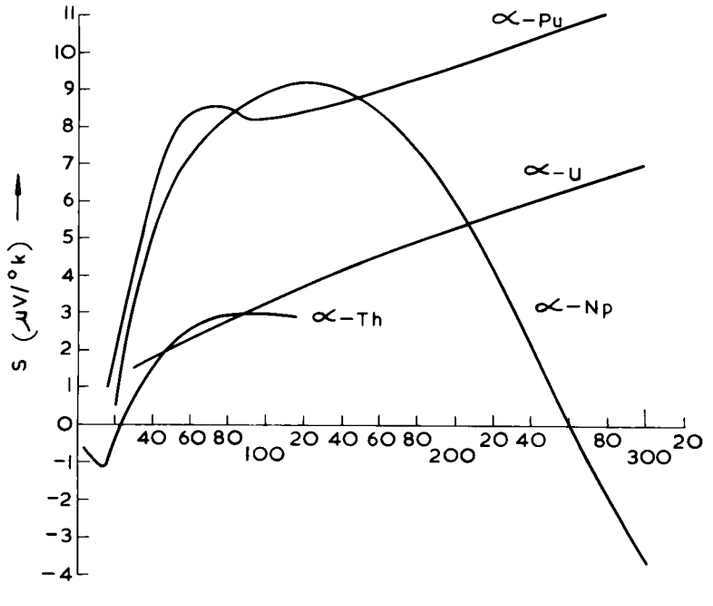


Fig. 1 Actinide Metal Resistivities.

FIG. 5·1 (a).



ABSOLUTE THERMOELECTRIC POWERS

FIG. 5·1 (b).

bands, below the bottom of the 5f bands, above which the 7s band starts.

Evidence that the 5f and 7s states are unimportant in Th and that the 6d states are thus the conduction states comes from the lack of an unusually large electronic specific heat (C_e) and a low electrical resistivity (ρ) (compared with the later actinides), both of which are proportional to the density of states at the Fermi level ($n(\epsilon_F)$). Smith and Wolcott (1955) found the electronic coefficient γ to be 11.2×10^{-4} cals./mole/deg.^{2} from specific heat measurement between 1 and 20°K, and Meaden (1961) (from which the resistivity curve of Fig. 5.1 (a) is taken) and later Haen and Meaden (1965) found room temperature resistivities of between 15 - 25 μΩcm. The magnetic susceptibilities (χ) determined by Smith and Greiner (1959) and Lam, Nevitt, Ross and Mitchell (1965) showing $\chi = 0.4 \times 10^{-6}$ emu/gm at 300°K, and very little temperature dependence down to 4.2°K, suggest small values of $n(\epsilon_F)$ compared to the later actinides.

The low values of thermo-electric power (S), as shown in Fig. 5.1 (b) (again taken from Meaden (1961)) suggests that in comparison the slope of $n(\epsilon_F)$ is smaller, providing further evidence that ϵ_F is below the narrow 5f bands.

No low temperature anomalies have been reported for

α-Th, any deviation from the behaviour of an 'ideal' metal can be attributed to it being either a 6d transition metal, or probably more correctly, an actinide without any 5f electrons. In this respect its ideal electrical resistivity (ρ_i) deviates from the Grüneisen-Bloch behaviour at low temperatures, yielding an index of T between 2.6 - 3.1 as compared with an ideal metal of 5.

The thermal conductivity (Haen and Meaden (1965)) is linear at low temperatures, but larger than expected due possibly to a lattice contribution, which is also found in three 'homologues of Th in the 4A group'. The lattice contribution is also present up to room temperature and above, in common with the later actinides.

For comparison the calorimetric Θ_D of α-Th is 170°K at zero °K (Smith and Wolcott (1955)) and falls rapidly to a minimum of 138°K at ~ 14°K and then rises to a value of 140°K at ~20°K. Above 20°K, Θ_D is between 140 and 160°K (Griffel and Skochdopole (1953)). Elastic constants Θ_E is 164.2 °K at zero °K (Alers and Neighbour (1959)) and ~158°K at room temperature. Lindemann's melting point formula gives Θ_m = 151°K and the electrical resistivity Θ_R is between 113 and 168°K for various reported values of ρ.

Thorium is also a superconductor with a fairly low

transition temperature of 1.37°K.

5.2 Uranium

The spectroscopic data of Keiss, Humphreys and Laun (1946) suggest the electronic configuration of the six electrons outside the radon core is $5f^3$ 6d $7s^2$. Quantitative treatment of the band structure of uranium is limited to the high temperature b.c.c. γ-phase, since the lower α- and β-phases are of the less amenable orthorhombic and tetragonal structures.

Ridley (1958) using a Wigner-Seitz method found that the very broad 7s band lies too high in energy, as in Th, to be occupied at all in the metal; the broad 6d band has a width of $\sim$ 6 eV and the fairly narrow 5f band of width 0.6 to 1.2 eV has about the same energy as the 6d band, causing the 6d and 5f bands to overlap with about 3 electrons in each. Lehman (1959 and 1960) solving the Dirac equation for a statistically derived potential found similar energies, band widths which were slightly wider, and also the spin-orbit splitting of the 5f band to be of the order of the band width. The Fermi energy now appears in the region of a minimum in the centre of the $5f_{5/2}$ band.

That the occupied region of the 6d band probably overlaps at least to some extent into the 5f band of α-uranium, is suggested by the very much higher density of states at the Fermi level, that is indicated by the various experimental data.

The electronic contribution is large, γ having a value between 26.1×10^{-4} cals./mole/deg.^{2} (Smith and Wolcott (1955)) and 23.7 (Flotow and Osborne (1966)). The electrical resistivity is also considerably larger than thorium (Fig. 5.1(a), but more important it is not exactly linear in T. From as low as 100°K, the temperature coefficient decreases with increasing temperature. This can be interpreted (see Meaden (1961)) in terms of a two band model and using the Mott-Jones formula for resistivity (Mott (1936): Jones (1956)) :-

$$\rho(T) = \rho(\epsilon_{F_0}, T)\left[1-\frac{\pi^2 k^2 T^2}{6}\left\{3\left(\frac{1}{n(\epsilon)}\frac{d(n(\epsilon))}{d\epsilon}\right)^2-\frac{1}{n(\epsilon)}\cdot\frac{d^2 n(\epsilon)}{d\epsilon^2}\right\}_{\epsilon=\epsilon_F}\right] \qquad 5.1$$

where $n(\epsilon)$ is the density of states in a narrow high f-type band, which overlaps a broad low conduction band. Thus the deviation from linearity is determined by the density of states and its derivative with respect to energy evaluated at the Fermi level. In a high narrow band, $n(\epsilon)$ will alter sharply

with a change in energy, or Fermi level, and hence the dependence of ϵ_F on temperature can qualitatively explain the general form of the resistivity curve of α-U although exact comparison is not possible without more knowledge of the parameters involved.

Blatt (1961) extended equation 5.1 and found that the thermoelectric power is given by

$$S = -\frac{\pi^2 k^2 T}{3e}\left[\frac{1}{n(\epsilon)} \cdot \frac{d(n(\epsilon))}{d\epsilon}\right]_{\epsilon=\epsilon_F} \qquad 5.2$$

for a simple two band model. The experimentally determined positive S for α-U(shown in Fig. 5.1(b)) points to a positive value of the slope of $n(\epsilon)$ at the Fermi level, which agrees with the band structures discussed.

Low temperature resistivities give $\rho_i \propto T^n$ where $n = 3.1$ for α-U, very comparable with α-Th, despite the almost ideal behaviour of Th above $\sim \theta/4$, where ρ is proportional to T.

Although the two band model and a temperature dependent Fermi level provides a crude qualitative explanation of some of the electronic properties of α-U, a closer inspection of

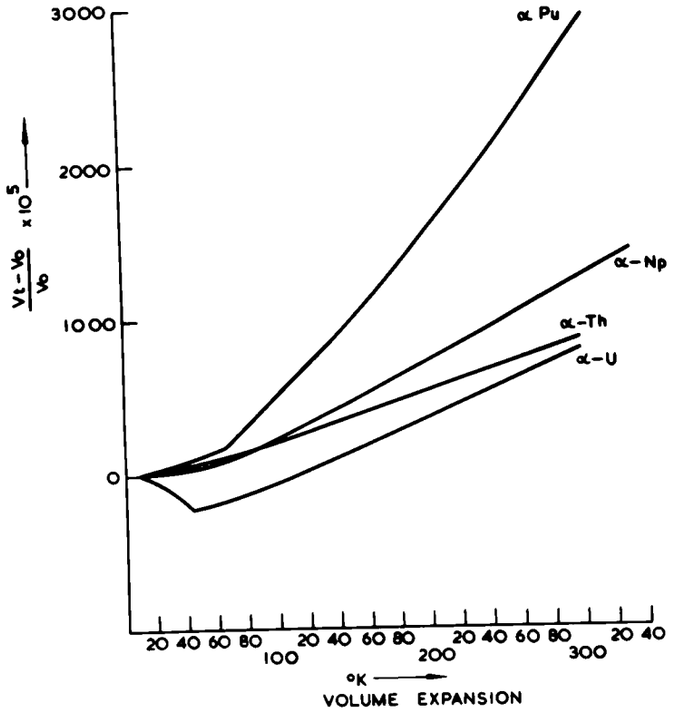

3000
2000
1000
0
α Pu
α-Np
α-Th
α-U
$\frac{V_t - V_0}{V_0} \times 10^5$
20 40 60 80 100 20 40 60 80 200 20 40 60 80 300 20 40
°K
VOLUME EXPANSION

FIG. 5·2.

many of its properties in the region of 43°K reveals that the situation in U is a little more complex. Large anomalies occur in the elastic constants at ~ 43°K (Fisher and McSkimin (1961) and Fisher and Dever (1968)); the volume expansion coefficient is negative below 43°K (Barret, Mueller and Hitterman (1963)) shown in Fig. 5.2, and a marked drop in Hall coefficient occurs at ~ 35 - 40°K (Berlincourt (1959)).

Small anomalies have also been seen in the region of 43°K on electrical resistivity (Meaden (1961), Arajs and Colvin (1964)), thermal conductivity (Hall (1968)) and thermoelectric power (Meaden (1961)) and magnetic susceptibility (Lam et al. (1968)). Nothing has so far been published on any unusual effect on the specific heat or neutron diffraction near 43°K.

In addition the enormous positive pressure dependence of the superconducting transition temperature, and the pressure induced bulk superconductivity are considered to be integrally connected with the '43°K transformation' (Smith and Gardner (1965) and (1967)).

The situation is by no means understood as can be evidenced from the variety of possible explanations put forward.

ranging from a structural phase change, electron transfer to a virtual bound 5f state, or formation of a spin density wave. Space limits any further discussion of α-U except for a brief mention of characteristic temperatures.

Calorimetric θ_D values at zero ^oK range between 200^oK (Smith and Wolcott (1955)) and 222^oK (Flotow and Osborne (1966)). The various values arise from not only differences in the magnitude of C_P but from the fact that even at 4^oK θ_D has not attained a constant value. θ_D falls sharply above 4^oK falling to a value of $\sim$ 170^oK at 25^oK. The anomalies in elastic constant and expansion coefficient lead via the unusual dilation term, to a further decrease in θ_D to a value of $\sim$ 163^oK at $\sim$ 45^oK, before increasing to $\sim$ 180^oK at 80^oK, followed by further increase to $\sim$ 300^oK at room temperature.

The most recent elastic constants data of Fisher and Dever (1968) yield θ_e at zero ^oK of 248.2^oK which is $\sim$ 12% higher than the highest and most recent calorimetric θ_D value at 0^oK. Fisher and Dever suggest that this may also be connected with the 43^oK transformation, or possibly due to the contribution of defects in the lattice vibrational heat capacity (Rosenstock (1959)). The resistivity θ_R is not applicable due to nonlinear variation of ρ with T and θ_m = 143^oK.

5.3 Neptunium

Neptunium has 7 electrons outside the radon core and the outer electron configuration is probably $5f^4$ 6d $7s^2$ in the neutral atom.

No theoretical treatment of the band structure of orthorhombic α-Np has been attempted nor indeed of either of its higher phases. One can only infer that it is probably similar to that of uranium with a broad low conduction band overlapped near the Fermi surface by a narrow high density of states f-type band, which could be based on either 5f electrons or mixed 5f and 6d.

Comprehensive understanding of the properties of α-Np is hindered not only by the limited properties investigated but also by the fact that the work that has been done has had to be carried out on considerably impure material.

The placing of the Fermi level of α-Np within the high density f-band certainly seems justified from the high electronic specific heat, the extremely high electrical resistivity and the high paramagnetic susceptibility. Consider these three in turn.

The high electronic coefficient $\gamma = 34 \times 10^{-4}$ cals./mole/deg.^{2}, determined in the present work, is extremely high

compared with values of 11.2 for Th and ~ 24 for U. Few metals in fact have higher γ-values and of those that do, praseodymium, holmium, thulium and cerium are all antiferromagnetic, (holmium is also ferromagnetic and cerium exhibits a large effect due to electron promotion), with large additional contributions to their specific heats at the transition temperatures. Plutonium is the only other metal with a larger γ than Np and it too is possibly antiferromagnetic (see next section). By inference then Np may also be magnetic, though the complete lack of any anomalous contribution would seem to eliminate such a possibility within the range 7.5°K to 300°K. The small anomalies of Sandenaw referred to in the last chapter must probably be attributed to impurities since they are not confirmed here.

The high electrical resistivity can be seen from Fig. 5.1(a). At room temperature it is almost four times that of U, and again is amongst the highest found. Furthermore the decrease in temperature coefficient of resistance with increasing temperature is even more striking. The same mechanism as discussed for uranium due to the temperature dependence of the Fermi surface may also be operating in Np (Meaden (1961)) to account for the decreasing temperature coefficient, since the necessary conditions of $n(\epsilon_F)$ and probably

$dn(\epsilon_F)/d\epsilon$ being large are also satisfied. Meaden also suggests that the band structure itself might be temperature dependent giving rise to an anomalous variation of density of states with temperature or possibly to the promotion of electrons into the conduction band. It is not possible to distinguish the variation in γ produced by these two without additional information of the correct lattice contribution.

Small anomalies have also been noticed on the electrical resistivity at $\sim 155^{\circ}K$ and $\sim 273^{\circ}K$ by King (unpublished) and Meaden (1961). These however were not reproducible from sample to sample and are attributed by Meaden to magnetic impurities. The index of T from the low temperature ideal resistance again produced a value of ~ 3 comparable to Th and U but in contrast Np was not found to be superconducting down to $0.75^{\circ}K$.

The thermoelectric power also measured by Meaden showed large but smooth changes in magnitude and a change of sign. The extreme sensitivity of S to impurities allied to the fact that small discrepancies were found compared to the work above room temperature of Lee, Evans, Hall and King (1959) limit the reliance of any conclusions from the thermoelectric power measurements. Similarly the large differences in Hall coefficient, equally sensitive to impurities, found by Brodsky

(1967) in two different samples must also await confirmation from better purity material.

Magnetic susceptibility measurements have also been carried out on α-Np. W.E. Gardner (unpublished) showed changes of slope characteristic of ferromagnetic impurity on one sample of suspected magnetic impurity and normal paramagnetic behaviour on a second sample. The lack of any large temperature variation was confirmed by Brodsky (1967) showing values of $\chi = 6 \times 10^{-6}$ emu/gm at $\sim 10^{\circ}K$ falling to $\sim 3 \times 10^{-6}$ at room temperature. This is about 7 times higher than Th and despite the impurity uncertainty and the uncertainty of subtraction of the diamagnetic contributions would suggest a considerably higher value of $n(\epsilon_F)$. The lack of any marked change of slope in χ of Np does not totally exclude the presence of a magnetic transition (cf. α-Mn discussed in the next section).

Self-irradiation damage experiments have also been conducted on α-Np (Griffin, Mendelssohn, King, et al. (1965)) and the increase in resistivity at low temperatures would seem to fit into the picture of increasing deviation (from U to Np to Pu) from normal behaviour (Griffin, Mendelssohn and Mortimer (1968)). Conclusions that the additional resistivity deviates from Matthieson's Rule (as certainly is the

case in Pu) cannot be made since the additional resistivity begins to anneal out almost immediately on raising the temperature above 4.2°K.

Mössbauer studies have been made by Stone (1967) on Np at 4.2°K and no signs of magnetic splitting were found.

The complete absence of any lattice dynamic calculations on Np, nor in fact on any actinides (due to their complex structures and incomplete investigation) make it difficult to decide whether the variation of Θ_D shown in the last chapter is due to any additional phenomenon apart from the deficiencies of the Debye model. The gradual nature of the minimum in Θ_D, despite the minimum appearing at slightly higher temperatures than normally found, together with the small percentage changes in the magnitude of Θ_D would suggest not. The magnitude of Θ_D is comparable with the other actinides Th, U and also Pu, though it is not possible to make any statements concerning possible trends in the actinides (cf. Gschneider (1964)) without more complete studies.

On the evidence to date it would then appear that neptunium is probably not magnetic although any final conclusion must await the availability of high purity material. On this

assumption then the resistivity must be explicable in terms of the change in Fermi level with temperature or some temperature dependence of the density of states at the Fermi surface. Any resulting changes in electronic specific heat, which are probably gradual ones considering the resistivity curve, cannot be distinguished without more knowledge of the lattice term.

5.4 Plutonium

The spectroscopic data of Van der Berg and Klinkenberg (1954) suggest that the ground state of the neutral Pu atom is probably $5f^5\ 6d\ 7s^2$. Later work suggests that it might be slightly different somewhere between $5f^6\ 7s^2$ and $5f^4\ 6d^2\ 7s^2$.

Intuitive extension of the band structure calculations of Th and U led Lee and Hall (1959) to suggest a similar pattern of narrow spin-orbit split 5f bands overlapping a broad 6d conduction band, with again the 7s level too high in energy to be occupied. In the case of Pu however Lee and Hall suggest that since the 5f charge distribution contracts with increasing atomic number, the width of the 5f bands should be narrower than in uranium. The Fermi level is probably in the $5f_{5/2}$ band, holding about 5 electrons and the remaining three contained in the conduction band. Once again

the very high electronic specific heat, paramagnetic susceptibility and room temperature electrical resistivity would confirm a high density of states at the Fermi level resulting from such a band structure.

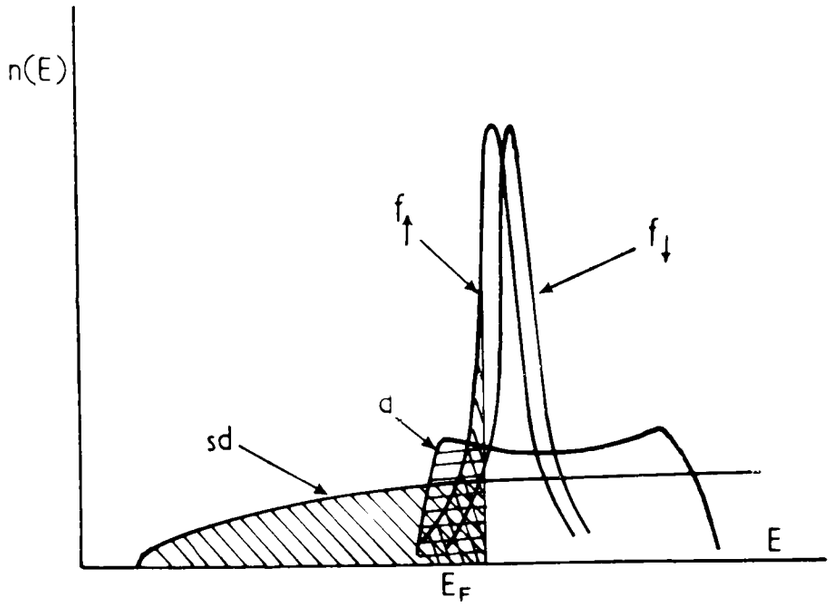
A considerable amount of effort has recently been directed towards band structure calculations of the f.c.c. δ-phase of Pu (see Kmetko (1965) and Kmetko and Waber (1965)). The results of such calculations, though differing slightly and dependent upon the method used (rigid multiple band, tight binding and Augmented Plane Wave), confirm the qualitative picture already outlined and are also successful in accounting for some of the high temperature properties of the δ-phase. The low temperature properties however are extremely sensitive to the 5f band shape, and hence present a much more difficult problem.

In fact the extremely unusual nature of the low temperature properties of in particular α-Pu has led to considerable conflict in their explanations. They are essentially divided into two; on the one hand explanation of particularly the electronic transport properties is in terms an extension of the ideas of change in Fermi level with temperature; and on the other hand the postulation of a paramagnetic → antiferromagnetic transition is made.

Lee, Hall, King and Meaden (1960) first made the qualitative suggestion that equation 5.1 may account for the negative slope of the resistivity of α-Pu above $\sim 105^{\circ}K$ (see Fig. 5.1(a)) and also that of δ-stabilised alloys of Pu. Smoluchowski (1962) extended this by considering a simple parabolic shape of the 5f band, and found some quantitative agreement. In order to explain the resistivity maximum, followed at low temperatures by a sharp fall, Smoluchowski, following Wilson (1938), assumes that the number of phonons available for interband scattering is drastically reduced at low temperatures by quantum selection rules. This phonon cut off should lead to an exponential temperature dependence of the resistivity at low temperatures which however has not been observed (see Meaden (1961), Wigley (1963)), an index of T in $\rho_i \propto T^n$ of between $\sim 2 - 2.8$ results.

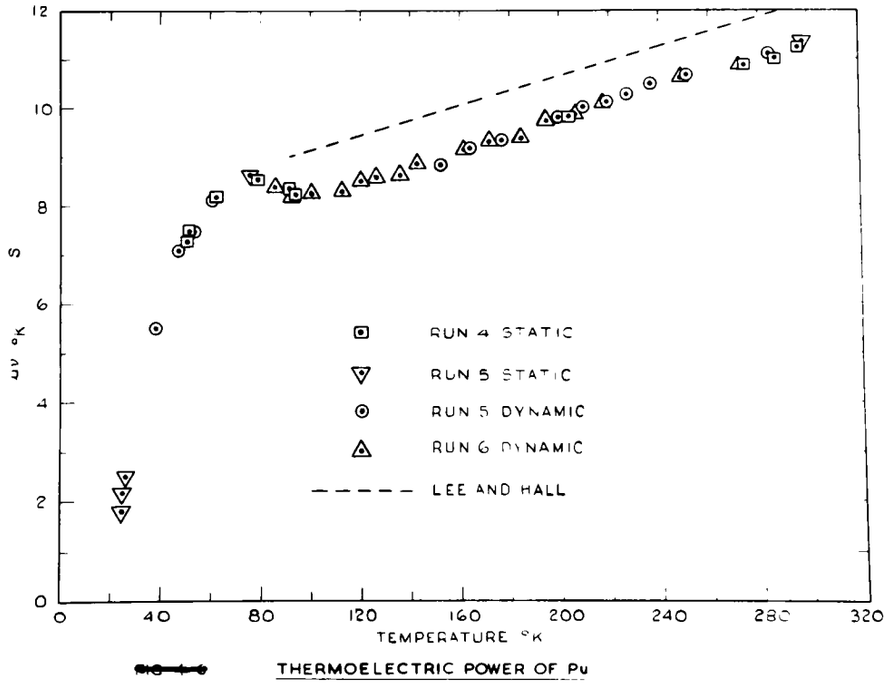
The criticisms of the explanation of the negative temperature coefficient are that although change of Fermi level with temperature may be a contributory factor, as has been seen possible in the earlier actinides, it is unlikely to be the major factor (Meaden (1963)).

The alternative magnetic transition hypothesis suggested by several authors (Sandenaw and Gibney (1958), Sandenaw and Olsen (1960) and Lee, Meaden and Mendelssohn (1960)) was



Structure de bande proposée pour le plutonium α.

FIG. 5.3(a)



THERMOELECTRIC POWER OF Pu

FIG. 5.3(b)

based on the unusual resistivity curve and, in the last named, the close parallel between α-Pu and α-Mn (considered in more detail by Meaden (1961)). Rocher and Friedel (1961) and Rocher (1962) treated the problem theoretically, and by assuming that the 5f level contracts onto the nucleus with a consequent weakening of the interactions between neighbouring atoms, virtual bound states are supposed to exist. Exchange decoupling splits these 5f states into two sub-levels of opposite spin with a difference in population of ~ 0.3 electrons, and a resultant magnetic moment of 0.3 μB. Rocher supposes that this magnetic moment is sufficient to give magnetic ordering at low temperatures. The band structure for this model is shown in Fig. 5.3(a) and in support of his choice of $\sim 65^{\circ}K$ as the Neél point, Rocher cites Meaden's thermoelectric power results shown in Fig. 5.3(b), the change of slope at $65^{\circ}K$ indicating the Neél point. Friedel (1965) suggests that some of the details of Rocher's analysis should be revised, but the main conclusions should remain and in-particular if the magnetic moments are in 5f shells in resonance with other valence electrons then the relatively small magnetic moments could explain large resistivity effects observed near T_N.

The lack of direct proof of the existence of magnetic order at low temperatures from in particular neutron

diffraction work has caused many workers to compare the various properties with that of known antiferromagnets such as α-Mn (T_N = 95-100°K) to which there are many similarities. Until such positive proof (or otherwise) can be given this comparison method must remain, and has been adopted here as supporting evidence to what we will show is the removal of one possible stumbling block to the magnetic order argument, namely the lack of a specific heat anomaly at T_N. Consider then the properties that are in support.

The electrical resistivity temperature variation (Meaden (1961), Wigley (1963)) can be explained. Well below T_N the resistive component due to the interaction between conduction electron spins and the ordered spins of localised electrons will be small, but will rise rapidly as the ordered spins are thermally disordered, as T_N is approached. At T_N = $\sim$ 55 - 60°K, all such long range order is destroyed, and the existence of short range order above T_N is then assumed capable of giving a maximum and a subsequent decrease in resistivity. Similarly the high residual resistivities and the large variation of residual resistivity for different specimens exhibiting very small differences in room temperature resistivity, can be explained by the fact that a certain

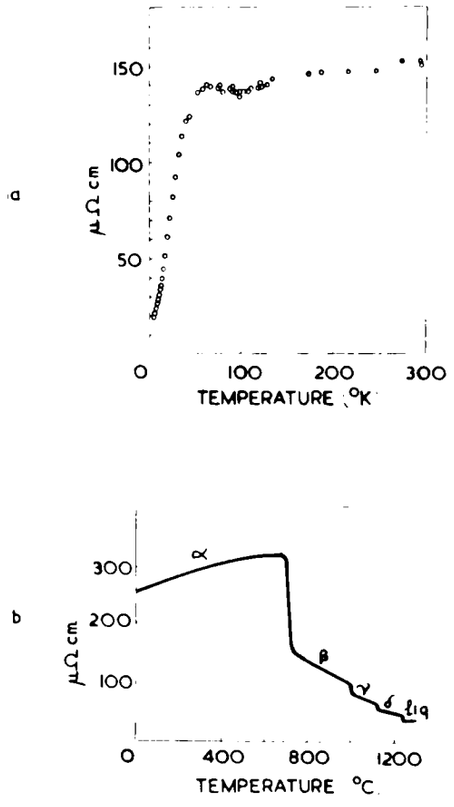
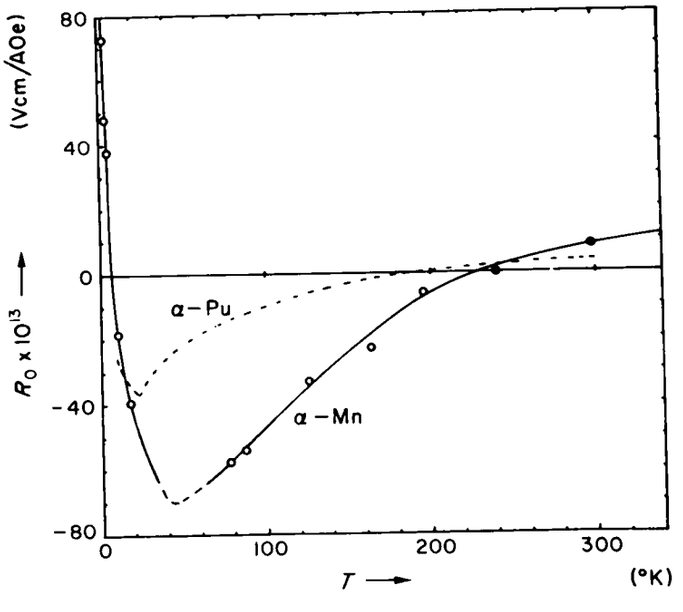


FIG 5·4 ELECTRICAL RESISTIVITY OF MANGANESE
a) AFTER WHITE AND WOODS 1957
b) AFTER GRUBE AND SPEIDAL 1940



The Hall effect of α-manganese as a function of temperature. The point at 240° K refers to a second specimen and the point at 297° K is due to Foner. Brodsky's Hall curve for α-plutonium is also indicated

FIG. 5·4 (c).

percentage of spins are prevented from ordering by the presence of chemical or physical impurities. The anomalous resistance of α-Mn had been similarly explained in terms of spin-disorder by Coles (1958). Figures 5.4(a) and 5.1(a) show how similar the resistivity curves of α-Mn and α-Pu are, although in α-Mn the short range order term has ceased by $\sim 100^{\circ}K$ and the resistivity increases with a positive coefficient. Higher phases of Mn however shown in Fig. 5.4(b) show negative coefficients in common with some of the higher phases of α-Pu. An even sharper maximum at $\sim 20^{\circ}K$ appears on the resistivity-temperature curve of β-Pu stabilised by quenching (King and Lee (1963)) and a similar mechanism must also be proposed for this phase too.

While on the topic of electrical resistivity, strong additional support of an antiferromagnetic transition in α-Pu is provided by the self-irradiation damage effect due to storage at low temperatures (Wigley (1963)). The temperature dependence of the accumulated resistivity due to self-damage deviates strongly from a simple additive resistance obeying Matthiesen's rule. An increase in resistivity occurs below T_N, while a decrease occurs above T_N in the region of the maximum, resulting eventually in an almost temperature

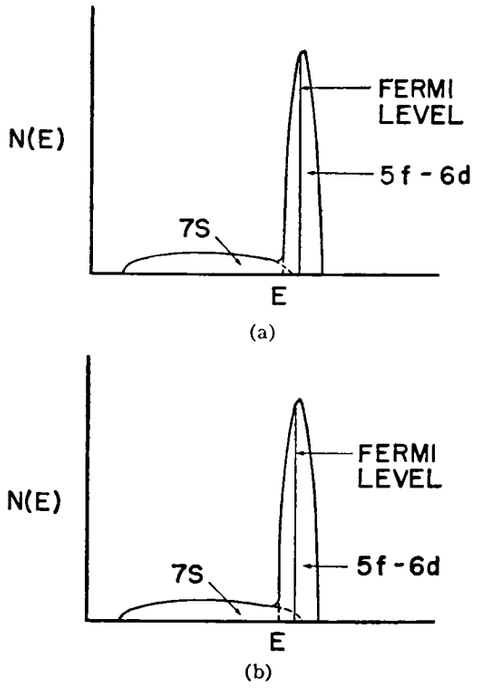


FIG. 5.5(a)

FIG. 5.5 Proposed band overlap (schematic) with increasing temperature for plutonium; (a)below 190°K, (b) above 190°K.

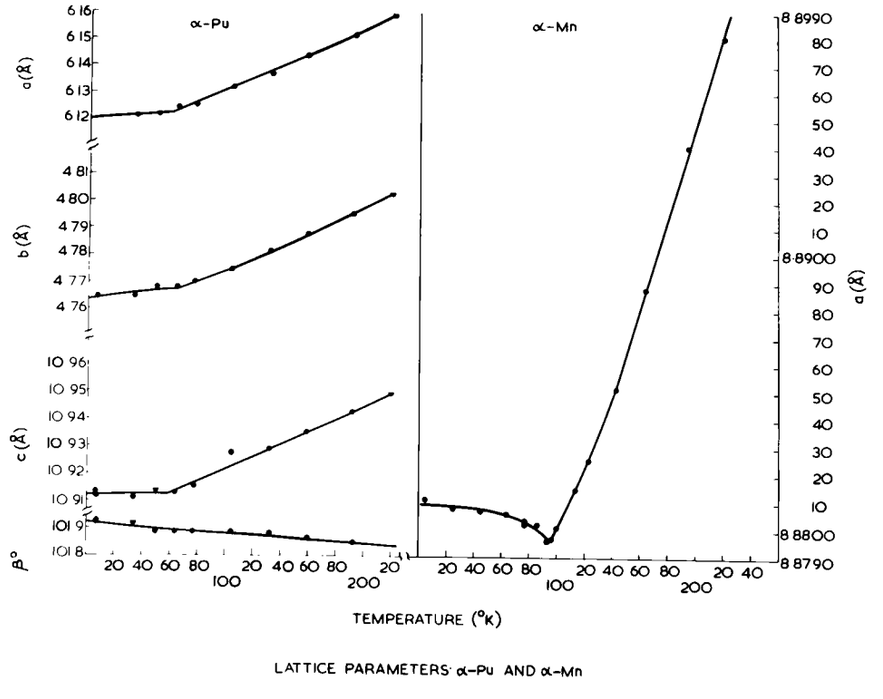


FIG. 5.5(b)

independent resistivity. Such deviations are difficult to explain, on anything other than the destruction of magnetic order, the simple defects that are considered to occur acting in the same way as chemical and physical impurities affect the residual resistivity. Similar behaviour is also seen in β-Pu (King, Lee, Mendelssohn and Wigley (1965) and also in proton-irradiated α-Mn (Mendelssohn and Wigley (1966)).

Another property supporting a magnetic-transition is the Hall effect. A comparison of the marked changes that occur in the Hall coefficients of both α-Pu (Brodsky (1965) and α-Mn (Meaden and Pelloux Gervais (1967)) is shown in Fig. 5.4(c). The marked similarity and the occurrence of the minimum in α-Mn at $\sim 40^{\circ}K$, well below $T_N = 95^{\circ}K$, should be noted since Brodsky's value of $T_N = 23^{\circ}K$ is taken from the position of the minimum.

Transverse magnetoresistivity measurements (also by Brodsky (1967)), indicate a similar low temperature magnetic transition with a $T_N = 20 - 30^{\circ}K$ for α-Pu, from the occurrence of negative magnetoresistivities below $\sim 27^{\circ}K$.

Both Hall coefficient and transverse magneto resistivity data at room temperature lead Brodsky to the band structure shown in Fig. 5.5(a), where the top of the broad 7s band is

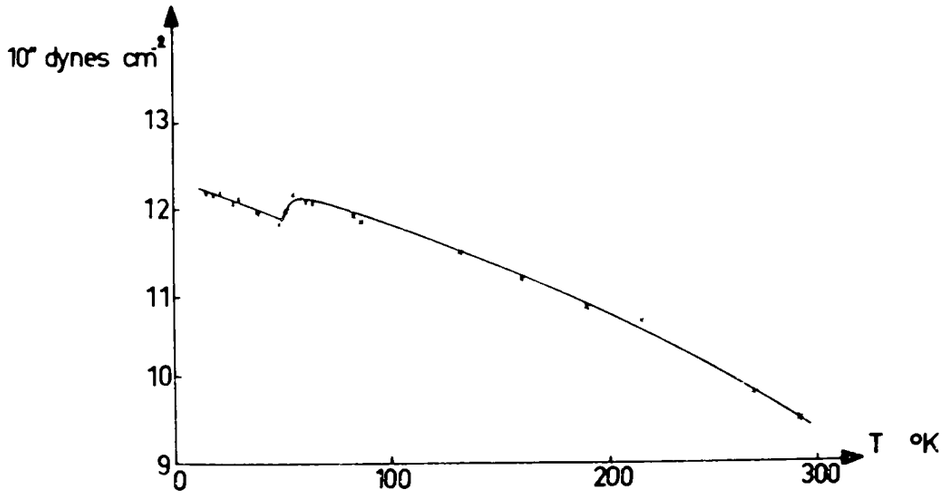


Fig. 1. Module d'Young du plutonium alpha.

FIG. 5.6 (a)

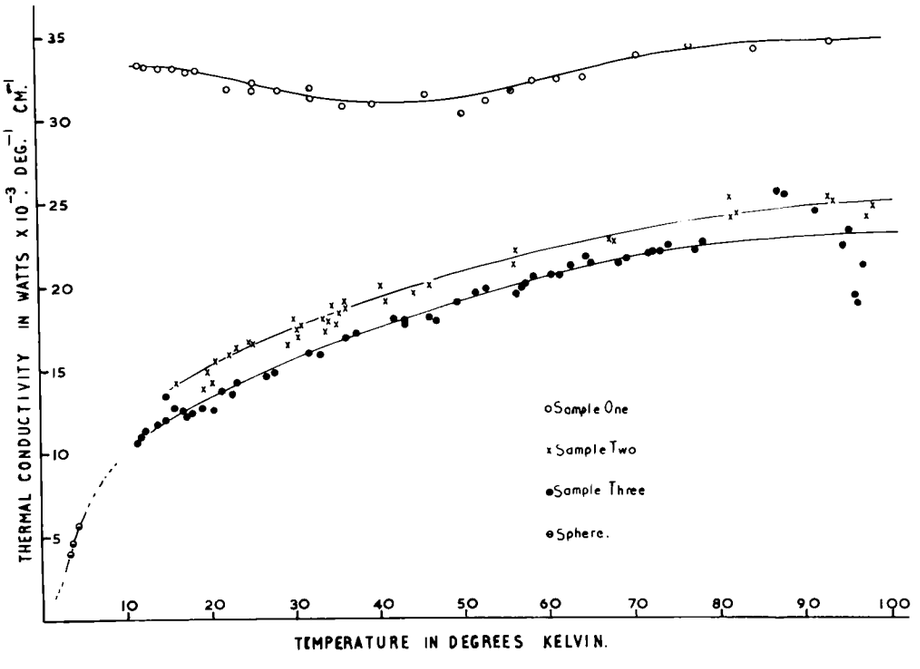
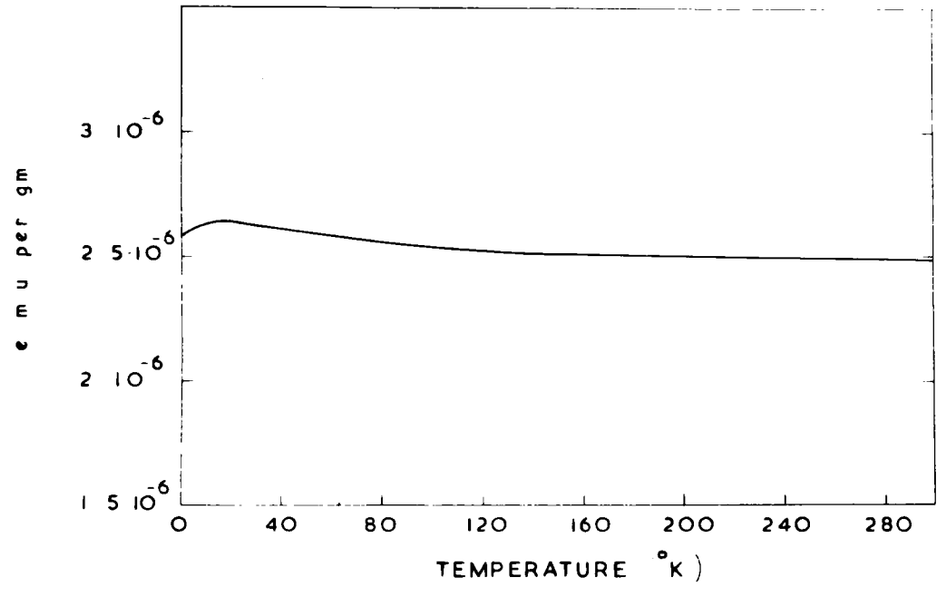


FIG. 5.6 (b)

in the region of the middle of the 5f-6d narrow band and is just below and just above the Fermi level at temperatures below and above 190°K respectively. Since similar band schemes emerge from consideration of Th, U and Np, and Th is definitely not magnetic, the simple two band model on which such schemes are based is probably not strictly applicable to the complex actinides.

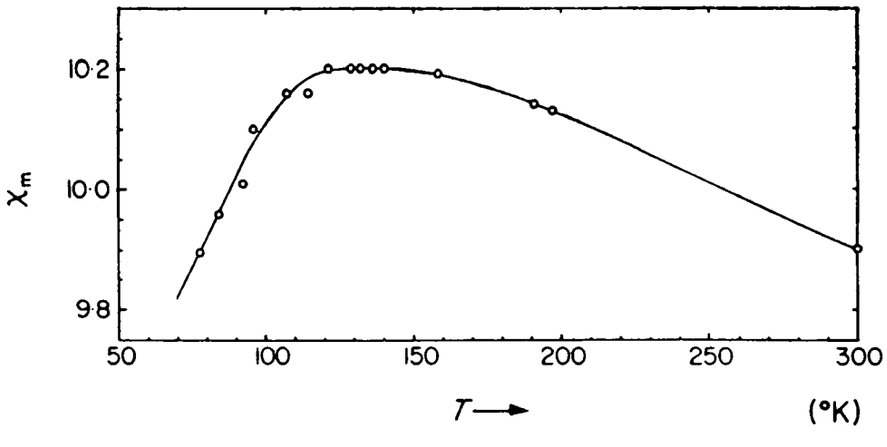
Thermal expansion anomalies have also been observed by Lallement and Solent (1965) and by Lee, Marples, Mendelssohn and Sutcliffe (1965), the latter data can be seen in Fig. 5.2 and Fig. 5.5(b) showing volume expansion and lattice parameters respectively. Figure 5.5(b) also shows the 'a' parameter of α-Mn for comparison. The marked negative expansion of α-Mn and the small negative contribution to α-Pu can be seen both starting at their respective T_N's, but it must be said that we saw no confirmation of this on the expansion coefficient work described in Chapter 3.

The anomaly on Young's Modulus seen by Lallement (1963) shown in Fig. 5.6(a), must be treated with some reserve since it has not been reproduced by either Linford (1964) or by a recent communication from Rosen, Erez and Shtrickman (1968). The latter work however finds an anomaly in the longitudinal attenuation coefficient of α-Pu which he describes by means



~~FIG. 5-6~~ SUSCEPTIBILITY OF Pu (WEIL et al. 1960)

FIG 5.7(a)



The magnetic susceptibility of α-manganese as a function of temperature

FIG 5.7(b)

co-operative electronic transition but few details are given. The behaviour of α-Pu however is in marked contrast to similar work on α-Mn (Rosen (1968)) which shows anomalies on Young's Modulus and compressibility at $\sim 96^{\circ}K$, and also both attenuation coefficients.

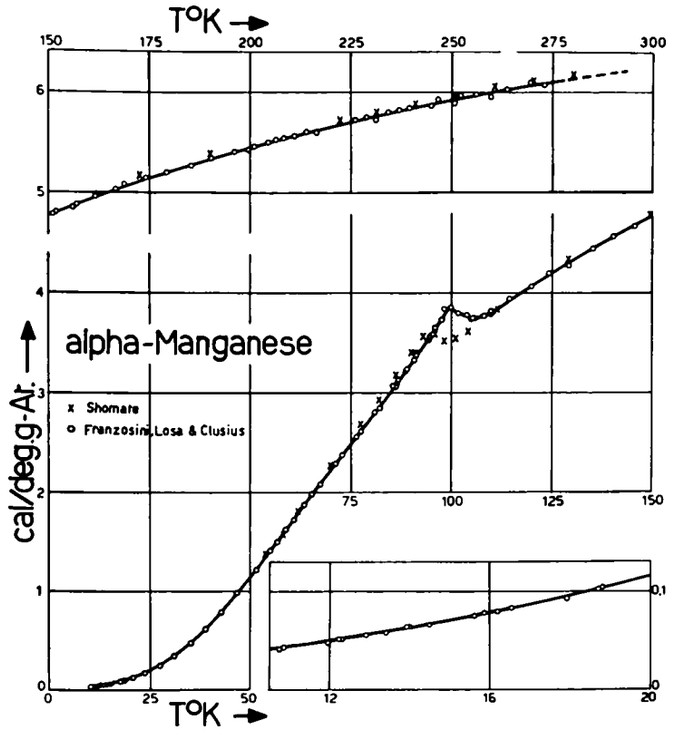
Thermal conductivity measurements on α-Pu (Hall (1968)) shown in Fig. 5.6(b) have been extended down to $\sim 7.5^{\circ}K$ for the high purity material (top curve) and show a maximum which one would normally associate with a purity peak. However self-irradiation damage work shows that this peak is damaged far quicker than the corresponding electronic term resulting from the resistivity by means of the Wiederman-Franz relation, and must therefore be attributed to something other than the usual electronic and possible lattice terms.

Turning to the debit side, as far as a magnetic transition is concerned, the magnetic susceptibility of α-Pu (Weil, Quezel, Cohen and Pascard (1960) shown in Fig. 5.7(a)) shows little temperature dependence but possibly a small maximum at $\sim 20^{\circ}K$. More recent work of Brodsky (1967) on purer material shows a slight increase in χ at $\sim 40^{\circ}K$. Large changes of slope at an antiferromagnetic transition do not however occur in α-Mn (Meaden and Pelloux-Gervais (1967)) as

shown in Fig. 5.7(b). A flat maximum is seen between 120 - 170°K which is considerably above T_N. Thus the lack of any striking effect on χ of α-Pu, may not necessarily rule out the antiferromagnetic hypothesis.

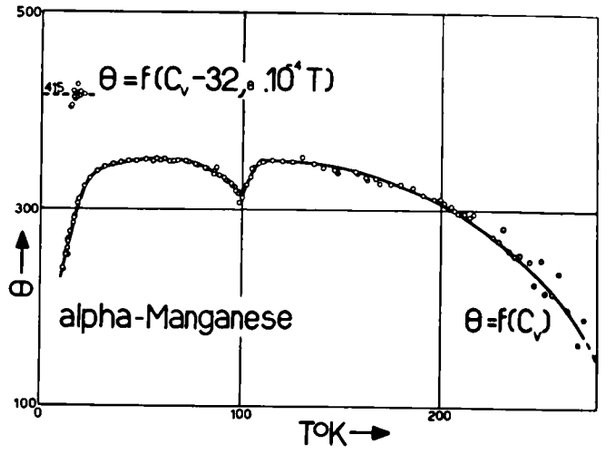
There are also some reservations concerning the major evidence against a magnetic transition namely neutron diffraction work. Early work at Harwell was on δ stabilised Pu, and Los Alamos only extended their measurements down to ~23°K. Later work by Roof (1963) on fairly impure α-Pu suggests negative results but the properties of α-Pu^{239} do not make such a determination easy. α-Pu has a monoclinic structure which produces a many peaked complex diffraction pattern in which a few small lines of the magnetic superlattice may well be lost. Further the high thermal fission cross section of Pu^{239} results in unfavourable peak to background ratios and the high absorption cross section results in a loss in intensity of all diffracted peaks. Complete disproof of the existence of magnetic order must await experiments on other isotopes of Pu such as Pu^{240} or Pu^{242} which would produce much more favourable conditions.

A hint of further negative results comes from recent Mössbauer work (Blow (1968)) on Pu_6Fe, which shows a resistivity curve that is qualitatively similar to α-Pu, but which



Atomic heat C_p vs. temperature for alpha-manganese between 10 and 273 °K; in the lower right hand corner the region between ~ 10 and 20 °K is magnified. Circles: this paper; crosses: SHOMATE.

FIG. 5·8 (d).



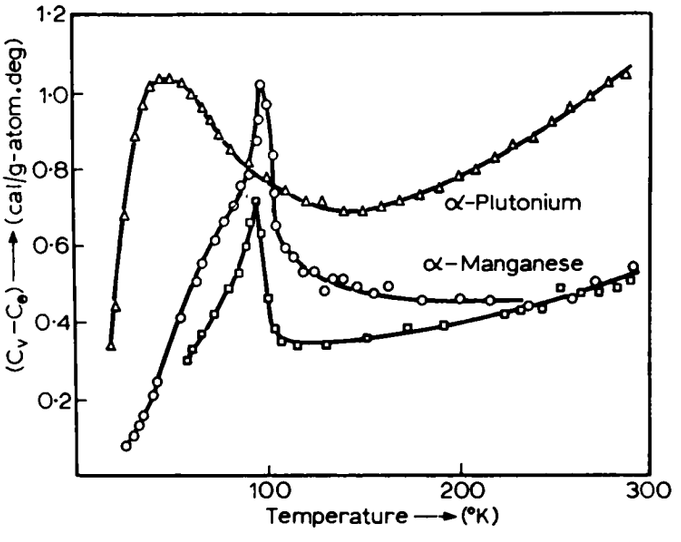
The continuous curve shows the characteristic DEBYE temperatur $\Theta = f(C_v)$ for alpha-manganese when the observed C_v values are used in the calculation. We also report (for $10° < T < 21$ °K) the values of Θ^*, which may be calculated after deducting the quantities $C_e = 32{,}_8 \cdot 10^{-4} \cdot T$ from the above C_v values.

FIG. 5·8 (b).

shows no splitting or line broadening with experimental error at temperatures down to $\sim 16^{o}K$. These results are not wholly satisfactory and some doubt exists about the true characterisation of the different samples used for resistivity and Mössbauer experiments. Confirmation must await further work, or preferably work on the metal itself.

We will now consider how the present specific heat results fit into this pattern of anomalous properties and how they compare with α-Mn.

The specific heat of α-Mn has been investigated by Schomate (1945) and Franzosini, Losa and Clusius (1964) and both are shown in Fig. 5.8(a). Both show a maxm., the former at $\sim 95^{o}K$ and the latter at $\sim 100^{o}K$, although its size is considerably smaller than the normal peak seen in the rare-earth antiferromagnet transitions but only just over twice that seen in α-Pu. On analysis in terms of θ_D, a minimum is seen shown in Fig. 5.8(b) which although larger in depth is not dissimilar in shape to that of α-Pu (compare Figs. 4.2, 4.3 and 4.10). The fact that in Fig. 5.8(b) θ_D is plotted as a function of C_V without subtraction of the electronic term makes little difference to the shape or size of the minimum, but does, of course, result in changes in θ_D at high



△ Data of Taylor . ○ Data of Franzosini □ Data of Shomate

[redacted]. Specific heats ($C_v - C_\theta$) of α-plutonium and α-manganese versus temperature

FIG. 5·9.

and low temperature. However on subtracting $C_e = \gamma T$ for $\gamma = 32.8 \times 10^{-4}$ a considerably larger temperature variation in θ_D results than was deduced for α-Pu. θ_D for α-Mn rises to $\sim 550^{\circ}K$ at $300^{\circ}K$. This together with the selection of the value of θ_D at $0^{\circ}K$ has a crucial bearing on the various analyses of C_p of α-Mn that have appeared in the literature.

Consider the analysis of Taylor and Linford (1967) first. From Taylor's smooth C_p of α-Pu, he subtracts the dilation term, and also a lattice term derived from the low temperature elastic constants θ_o of $204^{\circ}K$, assuming that θ_o is temperature independent. The resulting curve is shown in Fig. 5.9. For comparison he carried out a similar analysis for the C_p values of α-Mn of the above authors but uses a different θ_o in each case. For the data Franzosini et al. he uses $\theta_o = 415^{\circ}K$, which was the low temperature θ_D they found from their specific heat values between 10 and $21^{\circ}K$; but for Shomata's data he uses θ_o of $392^{\circ}K$ from the calorimetric data of Booth, Hoare and Murphy (1955) also determined between 11 - $20^{\circ}K$. These curves for $(C_V - C_{e_o})$ are also shown in Fig. 5.9 taken from Taylor's paper. Taylor concludes from the considerable difference in shape of these curves since the α-Pu curve is steeper on the lower temperature side, and is not λ-shaped, compared with both α-Mn curves, that there

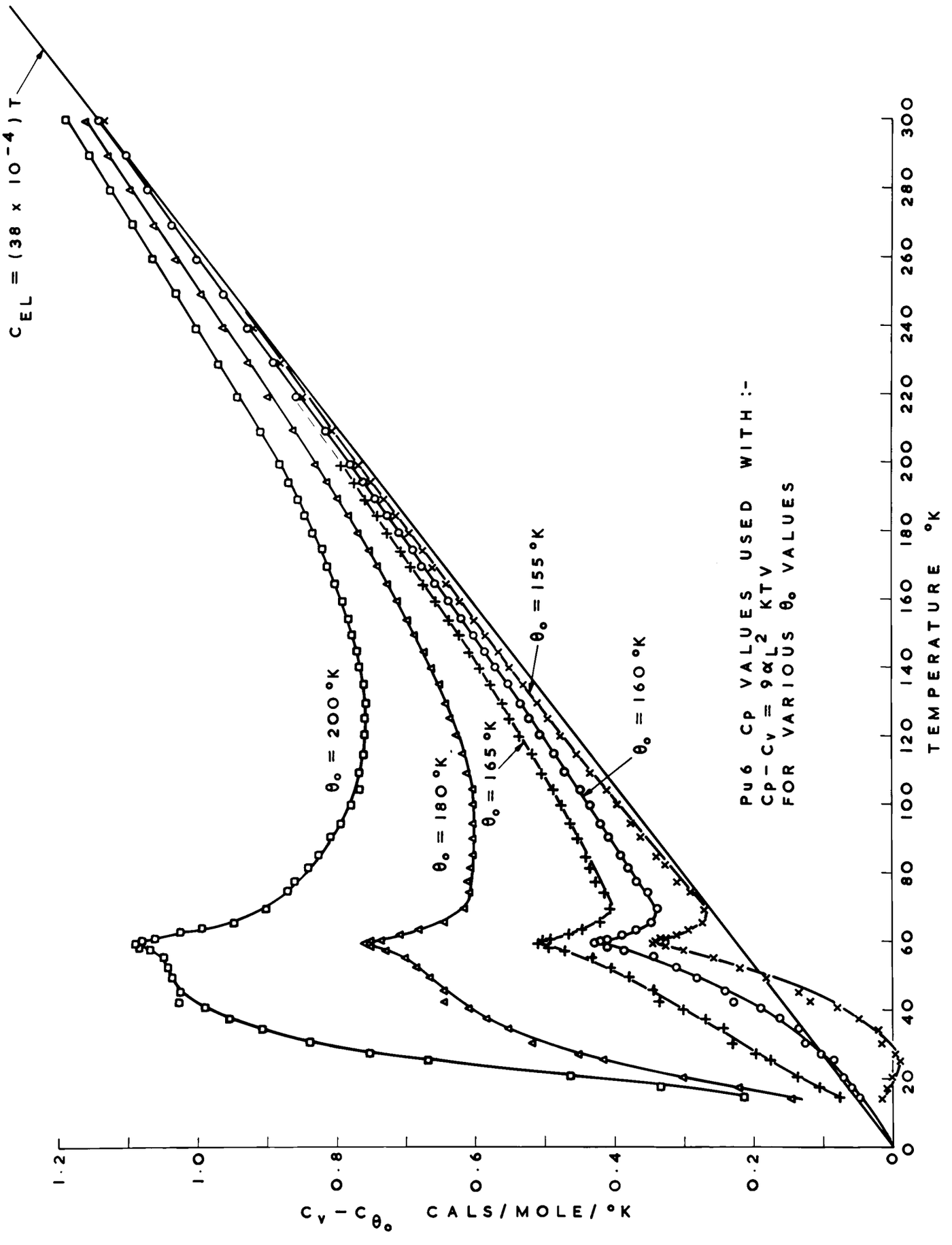
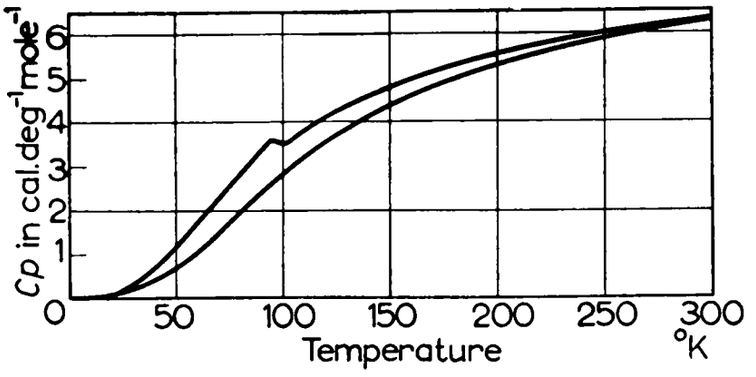


FIG. 5.10 MAGNETIC AND ELECTRONIC CONTRIBUTIONS TO C_v OF Pu6

is no support for a magnetic ordering transition in α-Pu, of the type found in α-Mn.

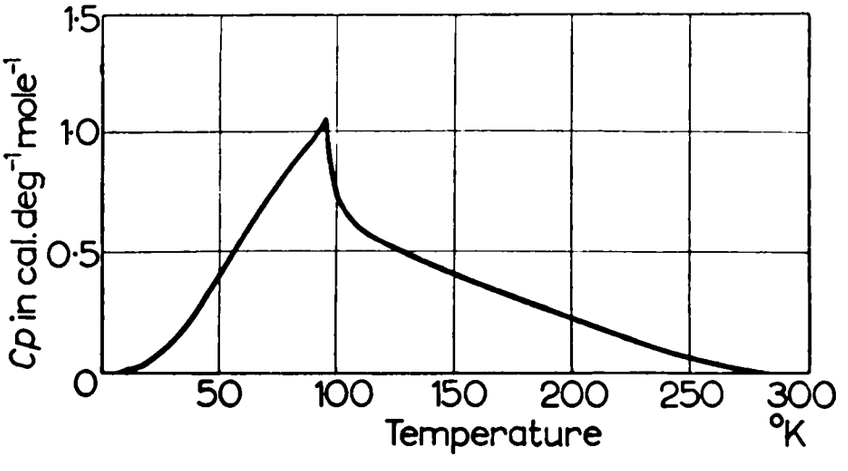
If now a similar analysis is carried out on the present work on α-Pu, and further that θ_o values are chosen between 205°K and 155°K, the series of curves shown in Fig. 5.10 results. Here we have a small peak superimposed on the shape of Taylor's α-Pu curve for a similar θ_o value which in fact is comparable to the shape of the α-Mn curves of Fig. 5.9, for somewhat smaller values of θ_o. Further it can now be seen that the difference between the two α-Mn curves of Fig. 5.9 is almost entirely due to the different θ_D values used. The Franzosini curve is also a small λ-peak superimposed on a smoother curve similar to the α-Pu curve of Taylor. In other words such an analysis, when performed on our present work, does in fact emphasise the similarity of α-Pu and α-Mn. Further the recent work of Rosen (1968) gives an elastic constants θ value at 0°K of 485°K, considerably higher than the calorimetric θ_D. Thus the α-Mn curves of Fig. 5.9 correspond to θ_o values (415°K and 392°K) much less than the elastic constants θ_o, and should therefore be compared with an α-Pu curve of Fig. 4.10 which has a value much less than the elastic constants θ_D.

Tauer and Weiss (1957) have analysed the C_p data of



Measured specific heat of α-Mn (upper curve) and theoretical lattice plus electronic specific heats (lower curve).

FIG. 5·11 (a).



The separated magnetic specific heat of α-Mn.

FIG. 5·11 (b).

Shomate in an attempt to separate the magnetic term, following the method of Hofman, Paskin, Tauer and Weiss (1956). This had been used with considerable success on several ferromagnetic metals and antiferromagnetic salts, yielding quite satisfactory entropy and energy values corresponding to the magnetic transition, as outlined in Chapter 1. Their method is to reduce the C_P values of C_V by means of the dilation term (or rather an approximation to the dilation term) and then to subtract an electronic term using γ from the low temperature region ($\theta_D/50$). The magnetic term (C_{MAG}) is then separated by using a lattice term with a constant θ_D the θ_D being selected from a region other than where its value is affected by the magnetic contribution, i.e., at a temperature low enough such that C_{MAG} is negligible but not too low that it will not represent the lattice term in the region of C_{MAG} (preferably therefore $> \theta_D/10$) or from a temperature well above the transition temperature. Tauer and Weiss chose $\theta_D = 460^{\circ}K$ (from the temperature region of $300^{\circ}K$) and the resulting C_{MAG} can be seen from Figs. 5.11(a) and 5.11(b), to have an enormous high temperature tail. By integration of C_{MAG} the entropy (S) and energy (W) associated with the transition were 1.07 cal./mole/deg. and 95 cals/mole/deg. These were found to give good agreement with the values

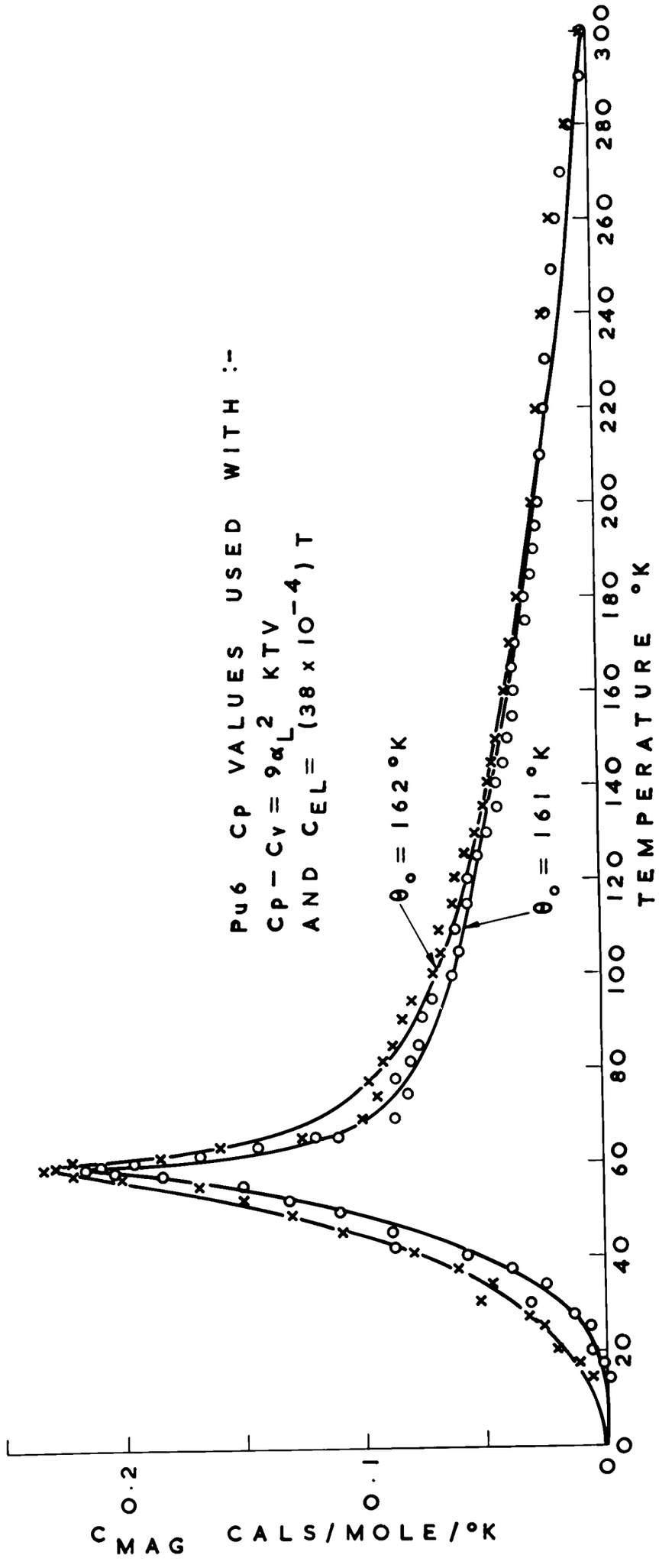


FIG. 5.12 MAGNETIC CONTRIBUTION TO SPECIFIC HEAT OF Pu6

expected using equations 1.15 and 1.16 from the magnetic moments predicted from the neutron diffraction work of Schull and Wilkinson (1953) and Kasper and Roberts (1956).

A later paper by Gazzara, Middleton and Weiss (1964) used a θ_o value of 390°K derived from X-ray intensity measurement and gave a value of S = 0.25 cal./mole/deg. which is down by a factor of 4. Shomate's original estimates of S and W, from a smooth curve extrapolation over the region of T_N, were 0.48 and 18.3 respectively.

The difficulty is obviously the estimation of the lattice term, the effect of which is exaggerated by a strongly temperature dependent θ_D.

We have carried out a similar analysis for α-Pu. The choice of θ_D is made easier by the comparative temperature independent variation of θ_D as shown by Fig. 4.10, but the smallness of C_{MAG} means that even a small change in θ_D or the θ_o value chosen to represent θ_D, affects the entropy and energy markedly. We have used the value of $\gamma = 38 \times 10^{-4}$, resulting from the straight line portion of Fig. 5.10 and a value of θ_o of 161°K such that C_{MAG} remains positive in the region of 20°K. The difference C_{MAG} is shown in Fig.5.12

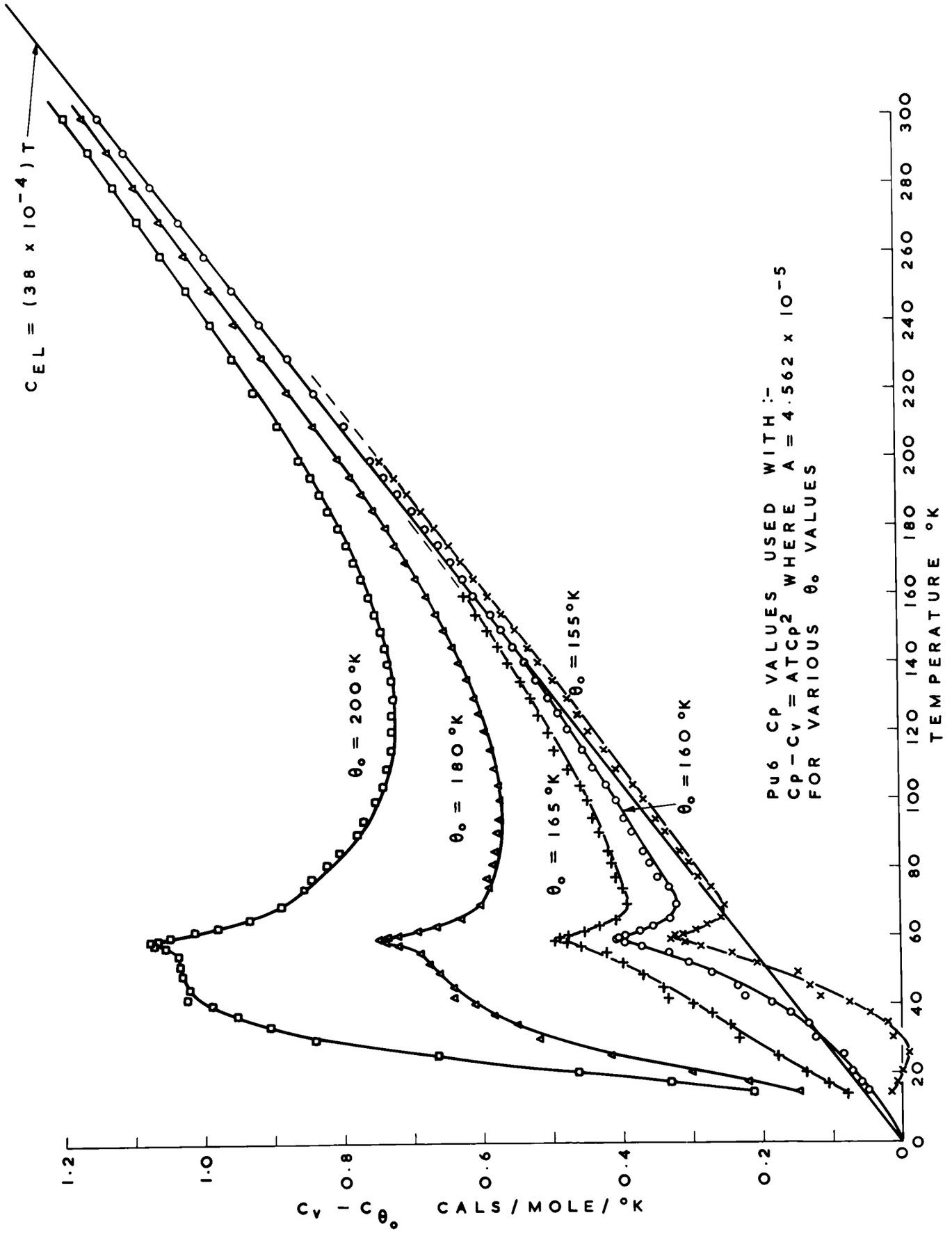


FIG. 5.13 MAGNETIC AND ELECTRONIC CONTRIBUTIONS TO C_v OF Pu6

(where the curve using $\theta_o = 162^oK$ has also been shown). A long tail is also evident and the entropy and energy values shown below result :-

θ_o	$W = \int C_{MAG}\, dT$	$S = \int \frac{C_{MAG}}{T}\, dT$
^oK	cals./mole	cals./mole/deg.
161	11.98	0.145
162	13.84	0.182

If instead of the dilation term $C_p - C_V = 9\, \alpha_L^2\, K\, T\, V$ used in the above, the approximate form of $C_p - C_V = A\, T\, C_p^2$ where $A = 4.562 \times 10^{-5}$ for α-Pu is used, θ_D variation is even less temperature dependent and similar analysis yields Figs. 5.13 and 5.14. C_{MAG} now has a much smaller tail and S and W, using again $\gamma = 38 \times 10^{-4}$ and $\theta_o = 161$ and 162 are :-

θ_o	W	S
161	6.44	0.164
162	8.13	0.140

The values of S and W can be seen to vary considerably, but

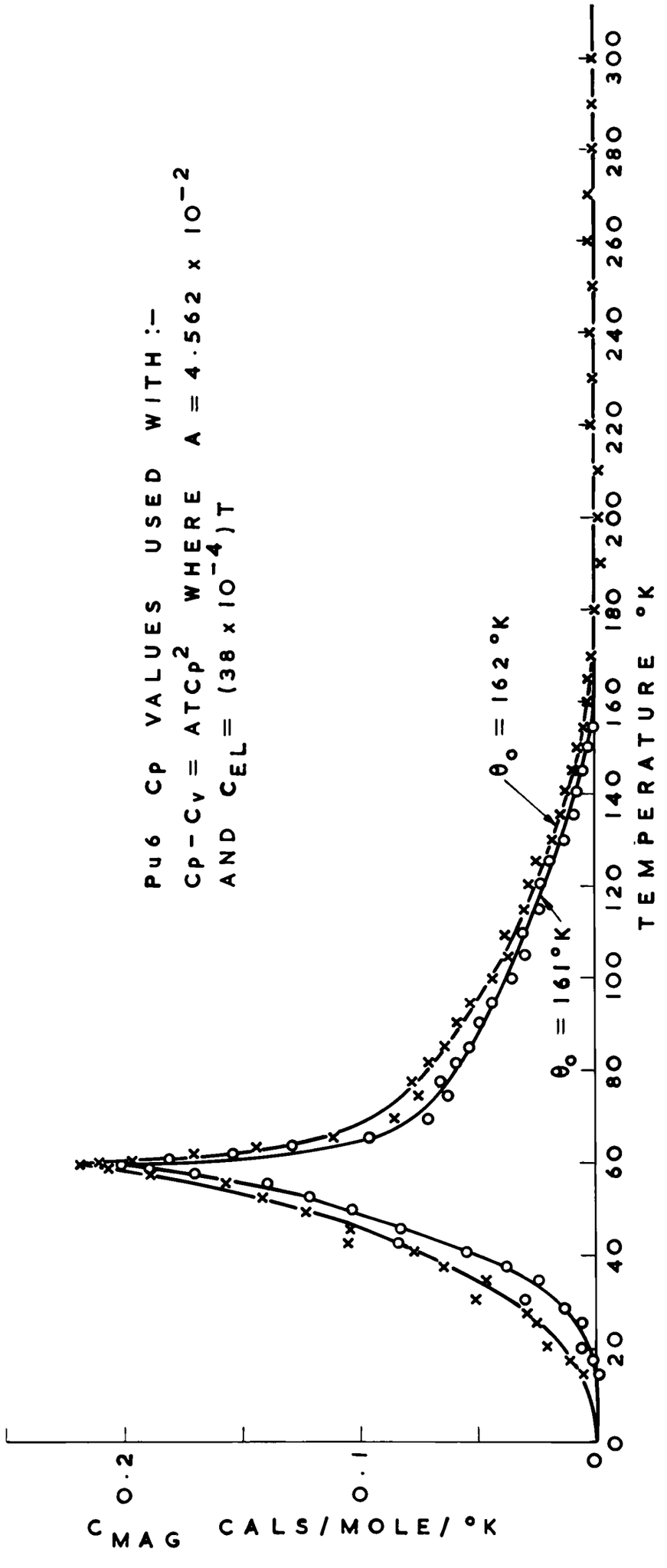


FIG. 5.14 MAGNETIC CONTRIBUTION TO SPECIFIC HEAT OF Pu 6

what does emerge is that they are generally smaller than the corresponding values of α-Mn. This apart there are marked similarities between the relative shapes of C_{MAG} for α-Mn and α-Pu which leads us to postulate that a magnetic transition does exist in α-Pu. Possible further evidence is that the temperature dependence of C_{MAG} is between 2 and 4 below T_N of 59.5°K and a high temperature tail does appear which is comparable to the $1/T^2$ tail resulting from statistical theory of magnetic transitions discussed in Chapter 1. The certainty with which we can estimate the powers of T particularly the $1/T^2$ tail with such a small magnitude of the whole transition is, of course, somewhat limited but the shape is conducive to a co-operative transition which could well be antiferromagnetic. The magnitude of the spin magnetic moment resulting from equation 1.16, however is small ($\sim$ s = 0.05) and critically dependent upon the choice of the value of S. Further equation 1.16 is only strictly valid for half integral spins, the smallest value of which s = $\frac{1}{2}$, leads to an entropy of 1.39 cals./mole/deg. For any non-half-integral spin values equation 1.16, must be replaced by

$$S = R \sum_i A_i \log_e (2s_i + 1)$$

where A_i is the fraction of atoms having spin s_i.

It is possible that the low entropy values found in α-Pu are due inpart to the fact that a number of the atoms have zero spin. Different spin values for different atomic positions are not unlikely in the complex monoclinic structure of α-Pu. A further possibility to account for the small entropy is that possibly complete ordering has not been achieved by $\sim 14^{\circ}K$ at which the lowest specific heat values were obtained. In this case the T^3 low temperature tail of the transition could have been lost in the assumed lattice term, which is approaching T^3. Complete ordering would be hindered by the small purity levels still present or by any small amount of self-irradiation damage defects present. This as it has been seen can account for the residual resistivity of α-Pu.

The significant difference in the size of the dip in θ_D mentioned in the last chapter, for the different purity samples, might also support this purity effect. Pu3 and Pu4 of similar purities ($\sim$ 300 ppm) gave dips of $\sim 6^{\circ}K$ in θ_D at $\sim 60^{\circ}K$ whereas for Pu6 ($\sim$ 50 ppm), the dip was $\sim 8.5^{\circ}K$. This can be seen from Fig. 4.3, where the full line corresponds to Pu6. Further the absence of any observable effect on Taylor's specific heat of α-Pu, since his purities were of the order of several thousand ppm, might thus be explained.

The small effective value of s from the present work, and the value of ~ 0.3 from Rocher's theoretical treatment (though this may be altered, by revisions to Rocher's analysis, it would still probably be small) may also explain the lack of any significant effect on the magnetic susceptibility, any small change being masked by the large paramagnetic contribution.

In summary then it appears that the specific heat work would confirm the hypothesis of a magnetic transition, and that this is possibly of the antiferromagnetic type, and is at $\sim 60^{\circ}K$. The limitations in the analysis caused by the lack of both an accurate γ from very low temperature measurements and of any additional information on the lattice term, allied to the small magnitude of the 'excess' on C_p, must make some of the predictions somewhat tentative, but the co-operative nature of the effect seems beyond doubt. Although there is some discrepancy between values of T_N suggested by the many supporting anomalies discussed earlier, the dangers of predicting T_N from electronic transport properties in particular have been shown by the anology with α-Mn. Real confirmation of the magnetic hypothesis however can only come from neutron diffraction measurements. One can only hope that the availability of either Pu^{240} or Pu^{242} or the

production of single crystals of plutonium will make these measurements more satisfactory in the near future.

5.5 Plutonium Monocarbide

All the actinides so far discussed form monocarbides which belong to a family of f.c.c. carbides (NaCl type) consisting of many from the transition metal and rare earth series.

The abundant experimental evidence that the bonding in the actinide carbides is not entirely of ionic character has led to the interpretation of their characteristic behaviour in terms of the collective band theory. Bates and Unstead (1964) have deduced a band structure for ThC and UC that is similar to the band models proposed for Th and U. Similarly Kimetko and Waber (1965) have shown that the band structure of PuC probably contains a very narrow 5f band. In general the electronic properties of these three actinide carbides are in agreement with such interpretations.

Costa and Lallement (1964) have reported a high resistivity ($\sim$ 100 $\mu\Omega$cm at 300°K) of sintered ThC, an almost linear resistivity temperature dependence and a superconducting transition temperature of $\sim 9^{\circ}$K. They also measured the

thermoelectric power which was found to be negative varying between $\sim$ -1 and - 10 $\mu V/^{o}K$ in the range $20^{o}K$ to $300^{o}K$. Arc-melted material however has been found to have considerably lower resistivities, $\sim$25 $\mu\Omega$cm at $300^{o}K$ (Kempter (1962)) and it is therefore probably true to say that the Fermi level in ThC is below any narrow 5f bands, being comparable with a transition metal carbide. Further evidence to support the placing of the Fermi surface in a fairly broad d-band, is provided by the electronic specific heat coefficient of $\gamma = 6.9 \times 10^{-4}$ cals./mole/deg. (Harness, Matthews and Morton (1964)).

UC however has an enormous electronic coefficient, reported as 48.6×10^{-4} by Combarieu, Costa and Michel (1963) and 44.7×10^{-4} by Harness et al.. A large, but not so large, density of states at the Fermi surface is also suggested from the magnetic susceptibility of UC (Lam, Nevitt, Ross and Mitchell (1965)) of $\sim 4 \times 10^{-6}$ emu/gm, but its absence of temperature dependence would suggest a small value of $dn(\epsilon_p)/d\epsilon$. In this respect it would agree with Bates and Unstead's prediction of the Fermi surface being in the region of a shallow minimum between associated with two overlapping but spin-orbit split 5f bands. Resistivity of UC (Costa and

Lallement (1964) shows fairly normal behaviour being linear above 100°K and rising to a room temperature value of 50 μΩcm., from a residual of 10 μΩcm. The thermoelectric power is extremely large, rising to a max m. of 75 μV/°K at 200°K before falling to a small value at 100°K and below.

The first evidence of typical rare-earth behaviour in actinide carbides is provided by NpC, Lam and Ross (1967) found a peak in the magnetic susceptibility of NpC at 310°K suggesting a paramagnetic - antiferromagnetic transition, and on further reducing the temperature, ferromagnetic behaviour occurs below 200°K. Little else however appears to have been published on NpC, but the occurrence of such magnetic behaviour would suggest a large density of states at the Fermi surface, and highly localised f electrons by analogy with the rare-earth carbides.

Many properties of PuC also would suggest that it also was magnetic, an antiferromagnetic transition being suggested at 100°K, but the range of stoichiometry that PuC exhibits has been found to markedly affect the transition temperature.

Costa and Lallement (1964) found for a carbon composition of 47.5 at/o resistivities (250 μΩcm) which was almost

temperature independent above 100°K. However below 100°K it was found to increase reaching a value of almost 350 μΩcm at ~ 10°K. The thermoelectric power was also large and is ~ + 5 μV/°K above 100°K. At 100°K there is a change of slope and S then falls rapidly, being zero at ~ 60°K, falling to a minimum value of ~ -5 μV/°K at ~ 25°K. Costa and Lallement also cite magnetic susceptibility work of Cohen, which shows pronounced deviation from Curie-Weiss behaviour below 100°K. On the basis of these, Costa and Lallement suggest that PuC undergoes an antiferromagnetic transition at ~ 100°K, explaining the unusual resistivity increase as being due to a superexchange mechanism via the carbon vacancies.

Later work on the magnetic susceptibility (Lam, Nevitt, Ross and Mitchell (1965)) showed similar strong temperature dependence of χ above 100°K, but below 100°K, χ rose to a sharp maximum at ~ 20°K. Three samples of differing carbon contents, 45, 46 and 47 at/o showed some differences in the shape of the χ curves between 20 - 50°K, and some unexplained time dependencies were seen below 50°K on two of the specimens. A Curie-Weiss plot yielded a positive value of the Curie-Weiss constant θ (normally negative for antiferromagnetism) for the composition nearest to stoichiometry.

A recent private communication from Lallement shows considerable shifts in the temperature of χ maximum for relatively small changes in composition.

Neutron diffraction work (Green, Arnold, Leary and Nereson (1967)) found four small, but well defined lines appeared in the diffraction pattern below 100°K on a monocarbide sample of carbon composition 47.6 at/o, made from highly enriched Pu^{240}. A later communication suggested an antiferromagnetic structure with planes of constant spin perpendicular to the 100 planes of magnitude 0.67 μB.

The specific heat results on a PuC sample of 49.0 at/o carbon presented in this thesis are however in opposition to this what now would appear strong evidence in favour of an antiferromagnetic transition. No specific heat anomalies (within ± 1%) were seen in the range 12.5°K to 300°K, C_p showing a smooth variation with temperature throughout this range. It must be emphasised that the single specimen investigated was one of rather high carbon composition and ~ 6 volume/o sesquicarbide (Pu_2C_3) was present. This carbon composition is considerably higher than those of the results discussed above, and Lallement's recent work has stressed the sensitivity of the susceptibility maximum to carbon content. Unfortunately

it appears that T_N increases in temperature with increasing carbon content and the argument that it has been depressed below 12.5°K does not hold. Since it would seem unlikely to elevate T_N anywhere near to exceeding 300°K, the contradiction remains puzzling.

Lam, Nevitt, Ross and Mitchell have considered their susceptibility results on the alternate hypothesis of PuC being ionic, the ions being noninteracting except for crystalline field effects. Their results could be explained on the ionic basis with Γ_1 as the lowest energy state of the Pu^{+4} ion. The large electronic specific heat contribution however suggested from our work, (though we can only strictly put an upper limit of $\sim 100 \times 10^{-4}$ cals/mole/deg^2 from the nonlinear C_p/T v. T^2 plot, the slope of C_p (and probably C_v) at the high temperatures would suggest a high γ) would make the ionic nature of PuC difficult to imagine. The anomalies in resistivity and thermoelectric power and the neutron diffraction work however make it eminently more difficult to provide an alternative explanation.

Further discussion must however await more specific heat work on a variety of carbon positions, particularly nearer to the suggested stoichiometric composition than the present sample, and in addition it would be preferable to

have more results on the effect of variation of carbon content on other properties besides the susceptibility.

REFERENCES

Alers, G.A. and Neighbours, J.R., (1959): Rev. Mod. Phys. 31, 675.

Arajs, S. and Colvin, R.V., (1964): J. Less Common Metals. 7, 54.

Barrett, C.S., Mueller, M.H. and Hitterman, P.L., (1963): Phys. Rev., 129, 625.

Bates, L.F. and Unstead, P.B., (1964): Brit. J. Appl. Phys. 15, 543.

Berlincourt, T.G., (1959): Phys. Rev., 114, 969.

Blatt, F.J., (1961): J. Phys. Chem. Solids., 17, 177.

Blow, S., (1968): Thesis, Oxford University.

Booth, G.L., Hoare, F.E. and Murphy, B.T., (1965): Proc. Phys. Soc. Lond. 68B, 830.

Brodsky, M.B., (1967): Priv. Comm.

Brodsky, M.B., (1965): Phys. Rev., 137A, 1423.

Coles, B.R., (1958): Adv. Phys. 7, 40.

de Combarieu, A., Costa, P. and Michel, J.C., (1963): Compt. rend. 256, 5518.

Costa, P. and Lallement, R., (1964): J. Phys. Chem. Solids. 25, 559.

Fisher, E.S. and McSkimin, H.J., (1961): Phys. Rev., 124, 67.

Fisher, E.S. and Dever, D., (1968): Priv. Comm.

Flotow, H.E. and Osborne, D.W., (1966): Phys. Rev., 151, 564.

Franzosini, P., Losa, G.G. and Clusius, K., (1964): Z. Naturforsch. 19a, 1348.

Friedel, J., (1965): 'Plutonium 1965'. Chapman and Hall, London (1967), p. 244.

Gazzara, C.P., Middleton, R.M. and Weiss, R.J., (1964): Phys. Letters, 10, 257.

Green, J.L., Arnold, G.P., Leary, J.A. and Hereson, N.G., (1967): J. Nucl. Mat. 23, 231.

Griffel, M. and Skochdopole, R.E., (1953): J. Amer. Chem. Phys. 20, 695.

Griffin, C.S., Mendelssohn, K., King, E., Lee, J.A., Rand, M.H. and Street, R.S., (1965): Plutonium 1965, p. 189.

Griffin, C.S., Mendelssohn, K. and Mortimer, M.J., (1968): Cryogenics, 8, 110.

Grube, G. and Speidal, H., (1940): Z. Electrochem. 16, 233.

Gschneider, K.A., (1964): Solid State Phys. 16, 275.

Haen, P. and Meaden, G.T., (1965): Cryogenics, 5, 194.

Hall, R.O.A., (1968); Priv. Comm.

Harness, J.B., Matthews, J.C. and Morton, N., (1964): Brit. J. Appl. Phys. 15, 963.

Hofman, J.A., Paskin, A., Tauer, K.J. and Weiss, R.J., (1956):
J. Phys. Chem. Solids, 1, 45.

Jones, H., (1956): Handbuch der Physik, A247, 199.

Kasper, J.S. and Roberts, B.W., (1956): Phys. Rev., 101, 537.

Keiss, C.C., Humphreys, C.J. and Laun, D.D., (1946):
J. Res. N.B.S., 37, 57.

Kempter, C.P., (1962): J. Less Comm. Metals, 4, 244.

Kimetko, E.A., (1965): Plutonium 1965, p. 222.

Kimetko, E.A. and Waber, J.T., (1965): Plutonium 1965, p. 244.

King, E. and Lee, J.A., (1963): Cryogenics, 3, 117.

King, E., Lee, J.A., Mendelssohn, K. and Wigley, D.A., (1965):
Proc. Roy. Soc., A284, 325.

Lallement, R. (1963): Phys. Letters, 5, 182.

Lallement, R. and Solente, P., (1965): Plutonium 1965, p. 147.

Lam, D.J., Nevitt, M.V., Ross, J.W. and Mitchell, A.W., (1965):
Plutonium 1965, p. 274.

Lam, D.J. and Ross, J.W., (1968): Phys. Rev., 165, 617.

Lee, J.A., Evans, J.P., Hall, H.O.A. and King, E., (1959):
J. Phys. Chem. Solids, 11, 278.

Lee, J.A. and Hall, H.O.A., (1959): J. Less Comm. Metals,
1, 356.

Lee, J.A., Hall, R.O.A., King, E. and Meaden, G.T., (1960): Plutonium 1960, Cleaver Hume Press, London (1961), p. 38.

Lee, J.A., Meaden, G.T. and Mendelssohn, K., (1960); Cryogenics, 1, 52.

Lee, J.A., Marples, J.A.C., Mendelssohn, K. and Sutcliffe, P.W., (1965): Plutonium 1965, p. 176.

Lehman, G.W., (1956): U.S.A.E.C. Report NAA-SR-1659.

Lehman, G.W., (1959): Phys. Rev., 116, 846.

Lehman, G.W., (1960): Phys. Rev., 117, 1493.

Meaden, G.T., (1961): Thesis, Oxford University.

Meaden, G.T., (1963): Proc. Roy. Soc., 276, 553.

Meaden, G.T. and Pelloux-Gervais, P. (1967): Cryogenics, 7, 161.

Mendelssohn, K. and Wigley, D.A., (1966): Phys. Letters, 20, 483.

Mott, N.F., (1936): Proc. Roy. Soc., 153A, 699.

Ridley, E.C., (1958): Proc. Roy. Soc., 247A, 199.

Rocher, Y.A., (1962): Advan. Phys., 11, 233.

Rocher, Y.A. and Friedel, J., (1961): J. Phys. Chem. Solids, 18, 196.

Roof, R.B., (1963): Los Alamos Report. No.LA 2912 (unpublished).

Rosen, M., (1968): Phys. Rev., 165, 357.

Rosen, M., Erez, G. and Shtrickman, S., (1968): Phys. Rev., Letters, 21, 430.

Rosenstock, H.B., (1959): J. Phys. Chem. Solids, 12, 41.

Sandenaw, T.A. and Gibney, R.B., (1958): J. Phys. Chem. Solids, 6, 81.

Sandenaw, T.A. and Olsen, C.E., (1960): Plutonium 1960, p. 59.

Schull, G.G. and Wilkinson, M.K., (1953): Rev. Mod. Phys., 25, 100.

Shomate, C.H. (1945): J. Chem. Phys., 13, 326.

Smith, T.F. and Gardner, W.E., (1965): Phys. Rev., 140, A1620.

Smith, T.F. and Gardner, W.E., (1967): Phys. Rev., 154, 309.

Smith, J.F. and Greiner, J.D., (1959): Phys. Rev., 115, 884.

Smith, P.L. and Wolcott, N.M., (1955): Annexe 1955-3, Bull. Inst. Int Froid, p. 103.

Smoluchowski, R., (1962): Phys. Rev., 125, 1577.

Stone, J.A., (1967): Priv. Comm.

Tauer, K.J. and Weiss, R.J., (1957): J. Phys. Chem. Solids, 2, 237.

Taylor, J.C. and Linford, P.F.T., (1967): Cryogenics, 7, 305.

Van der Berg, M. and Klinkenberg, P.F.A., (1954): Physica, 20, 161.

Weil, L., Quezel, G., Cohen, J. and Pascard, R., (1960); Plutonium 1960, p. 104.

Wigley, D.A., (1963): Thesis, Oxford University.

Wilson, A.H., (1938): Proc. Roy. Soc., 167, 580.

White, G.K. and Woods, S.B. (1957): Can. J. Phys., 35, 346.

APPENDIX I

MOLAR THERMODYNAMIC FUNCTIONS FOR ALPHA-PU

T °K	C_p Cal./Deg.	S Cal./Deg.	$H^\circ - H^\circ_o$ Cal./Deg.	$-(G-H^\circ_o)/T$ Cal./Deg.
12.5	0.263	0.114	0.994	0.035
15.0	0.429	0.176	1.860	0.053
17.5	0.638	0.258	3.194	0.075
20.0	0.881	0.359	5.094	0.104
22.5	1.135	0.477	7.614	0.138
25.0	1.456	0.613	10.85	0.178
27.5	1.770	0.766	14.89	0.224
30.0	2.087	0.933	19.71	0.276
32.5	2.350	1.111	25.25	0.334
35.0	2.663	1.296	31.52	0.395
37.5	2.940	1.489	38.52	0.462
40.0	3.196	1.687	46.19	0.532
42.5	3.460	1.889	54.51	0.606
45.0	3.668	2.092	63.42	0.683
47.5	3.885	2.296	72.86	0.762
50.0	4.067	2.500	82.80	0.844
52.5	4.250	2.703	93.20	0.928
55.0	4.417	2.905	104.03	1.013
57.5	4.595	3.105	115.30	1.100
60.0	4.750	3.304	126.98	1.188
62.5	4.821	3.499	138.94	1.276
65.0	4.891	3.690	151.08	1.365
67.5	4.972	3.876	163.41	1.455
70.0	5.057	4.058	175.95	1.545
72.5	5.142	4.237	188.70	1.634
75.0	5.227	4.413	201.66	1.724
77.5	5.310	4.586	214.83	1.814
80.0	5.380	4.755	228.19	1.903
82.5	5.447	4.922	241.73	1.992
85.0	5.510	5.086	255.42	2.081
87.5	5.569	5.246	269.27	2.169
90.0	5.628	5.404	283.27	2.257
92.5	5.681	5.559	297.40	2.344
95.0	5.732	5.711	311.67	2.430
97.5	5.779	5.861	326.06	2.516
100.0	5.825	6.007	340.56	2.602

APPENDIX I continued

T °K	C_p Cal./Deg.	S Cal./Deg.	$H^\circ - H^\circ_o$ Cal./Deg.	$-(G-H^\circ_o)/T$ Cal./Deg.
105.0	5.912	6.294	369.91	2.771
110.0	5.997	6.571	399.68	2.937
115.0	6.070	6.839	429.84	3.101
120.0	6.143	7.099	460.38	3.263
125.0	6.208	7.351	491.25	3.421
130.0	6.268	7.596	522.44	3.577
135.0	6.327	7.834	553.93	3.730
140.0	6.385	8.065	585.71	3.881
145.0	6.440	8.290	617.77	4.029
150.0	6.493	8.509	650.11	4.175
155.0	6.544	8.723	682.70	4.318
160.0	6.595	8.931	715.55	4.459
165.0	6.646	9.135	748.65	4.598
170.0	6.695	9.334	782.00	4.734
175.0	6.740	9.529	815.59	4.869
180.0	6.788	9.720	849.41	5.001
185.0	6.835	9.906	883.47	5.131
190.0	6.880	10.089	917.75	5.259
195.0	6.926	10.269	952.27	5.385
200.0	6.971	10.444	987.01	5.509
205.0	7.016	10.617	1022.0	5.632
210.0	7.062	10.787	1057.2	5.753
215.0	7.108	10.954	1092.6	5.872
220.0	7.155	11.117	1128.2	5.989
225.0	7.198	11.279	1664.2	6.105
230.0	7.241	11.437	1200.2	6.219
235.0	7.285	11.594	1236.5	6.332
240.0	7.330	11.748	1273.1	6.443
245.0	7.374	11.899	1309.8	6.553
250.0	7.418	12.049	1346.8	6.661
255.0	7.462	12.196	1384.0	6.768
260.0	7.507	12.341	1421.4	6.874
265.0	7.551	12.485	1459.1	6.979
270.0	7.595	12.626	1496.9	7.082
273.15	7.623	12.714	1521.0	7.140
275.0	7.639	12.766	1535.0	7.184
280.0	7.683	12.904	1573.3	7.285
285.0	7.727	13.040	1611.9	7.385
290.0	7.772	13.175	1650.6	7.483
295.0	7.817	13.308	1689.6	7.581
298.15	7.845	13.311	1714.3	7.642
300.0	7.862	13.440	1728.8	7.678

APPENDIX II

MOLAR THERMODYNAMIC FUNCTIONS FOR ALPHA-NP

T	C_p	S	$H^\circ - H^\circ_0$	$-(G-H^\circ_0)/T$
°K	Cal./Deg.	Cal./Deg.	Cal./Deg.	Cal./Deg.
7.5	0.055	0.032	0.159	0.011
10.0	0.105	0.054	0.359	0.018
12.5	0.181	0.086	0.717	0.028
15.0	0.288	0.128	1.304	0.041
17.5	0.439	0.183	2.212	0.057
20.0	0.625	0.254	3.543	0.076
22.5	0.861	0.340	5.401	0.100
25.0	1.097	0.443	7.848	0.129
27.5	1.370	0.560	10.93	0.163
30.0	1.643	0.691	14.70	0.201
32.5	1.928	0.834	19.16	0.244
35.0	2.185	0.986	24.30	0.291
37.5	2.437	1.145	30.08	0.343
40.0	2.688	1.310	36.49	0.398
42.5	2.912	1.480	43.49	0.457
45.0	3.135	1.653	51.05	0.518
47.5	3.328	1.826	59.12	0.583
50.0	3.520	2.003	67.68	0.649
52.5	3.685	2.179	76.69	0.718
55.0	3.849	2.354	86.11	0.788
57.5	3.970	2.528	95.89	0.860
60.0	4.108	2.700	106.00	0.933
62.5	4.245	2.870	116.44	1.007
65.0	4.382	3.040	127.23	1.082
67.5	4.488	3.207	138.31	1.158
70.0	4.594	3.372	149.67	1.234
72.5	4.688	3.535	161.27	1.311
75.0	4.782	3.696	173.11	1.387
77.5	4.864	3.854	185.16	1.464
80.0	4.946	4.009	197.43	1.542
82.5	5.019	4.163	209.88	1.619
85.0	5.092	4.314	222.52	1.696
87.5	5.156	4.462	235.33	1.773
90.0	5.219	4.608	248.30	1.849
92.5	5.278	4.752	261.42	1.926
95.0	5.337	4.894	274.69	2.002
97.5	5.390	5.033	288.10	2.078
100.0	5.442	5.170	301.64	2.154

APPENDIX II continued

T	C_P	S	$H^\circ - H^\circ_0$	$-(G-H^\circ_0)/T$
°K	Cal./Deg.	Cal./Deg.	Cal./Deg.	Cal./Deg.
105.0	5.532	5.438	329.07	2.304
110.0	5.621	5.697	356.96	2.452
115.0	5.699	5.949	385.26	2.599
120.0	5.776	6.193	413.94	2.744
125.0	5.842	6.430	442.99	2.887
130.0	5.908	6.661	472.36	3.027
135.0	5.967	6.885	502.05	3.166
140.0	6.025	7.103	532.03	3.303
145.0	6.077	7.315	562.28	3.438
150.0	6.128	7.522	592.80	3.570
155.0	6.174	7.724	623.55	3.701
160.0	6.220	7.921	654.54	3.830
165.0	6.261	8.113	685.74	3.957
170.0	6.302	8.300	717.15	4.082
175.0	6.342	8.484	748.76	4.205
180.0	6.381	8.663	780.56	4.446
185.0	6.417	8.838	812.56	4.446
190.0	6.453	9.010	844.73	4.564
195.0	6.488	9.178	877.09	4.680
200.0	6.523	9.343	909.61	4.795
205.0	6.555	9.504	942.31	4.908
210.0	6.587	9.663	975.16	5.019
215.0	6.617	9.818	1008.2	5.129
220.0	6.647	9.970	1041.3	5.237
225.0	6.677	10.120	1074.6	5.344
230.0	6.707	10.267	1108.1	5.449
235.0	6.737	10.412	1141.7	5.553
240.0	6.766	10.554	1175.5	5.656
245.0	6.794	10.694	1209.4	5.757
250.0	6.821	10.831	1243.4	5.858
255.0	6.872	10.967	1277.6	5.956
260.0	6.922	11.101	1312.1	6.054
265.0	6.928	11.233	1346.7	6.151
270.0	6.933	11.362	1381.4	6.246
273.15	6.950	11.443	1403.3	6.305
275.0	6.960	11.490	1416.1	6.340
280.0	6.987	11.615	1451.0	6.433
285.0	7.014	11.739	1486.0	6.525
290.0	7.040	11.861	1521.1	6.616
295.0	7.066	11.982	1556.4	6.706
298.15	7.082	12.057	1581.7	6.762
300.0	7.092	12.101	1591.8	6.795

APPENDIX III

THERMODYNAMIC FUNCTIONS FOR $PuC_{0.87}$

T °K	C_P Cal./Deg.	S Cal./Deg.	$H^\circ - H^\circ_o$ Cal./Deg.	$-(G-H^\circ_o)/T$ Cal./Deg.
12.5	(0.510)	(0.246)	(2.117)	(0.077)
15.0	0.718	0.357	3.652	0.114
17.5	0.931	0.483	5.714	0.157
20.0	1.161	0.622	8.329	0.206
22.5	1.405	0.773	11.54	0.260
25.0	1.669	0.935	15.38	0.319
27.5	1.940	1.106	19.89	0.383
30.0	2.217	1.287	25.09	0.451
32.5	2.486	1.475	30.96	0.522
35.0	2.737	1.668	37.49	0.597
37.5	2.980	1.865	44.64	0.675
40.0	3.218	2.065	52.39	0.755
42.5	3.450	2.267	60.72	0.838
45.0	3.671	2.471	69.62	0.923
47.5	3.886	2.675	79.07	1.010
50.0	4.098	2.880	89.05	1.099
52.5	4.307	3.085	99.56	1.188
55.0	4.514	3.290	110.6	1.279
57.5	4.715	3.495	122.1	1.371
60.0	4.913	3.700	134.1	1.464
62.5	5.106	3.904	146.7	1.557
65.0	5.290	4.108	159.7	1.651
67.5	5.472	4.311	173.1	1.746
70.0	5.644	4.513	187.0	1.841
72.5	5.824	4.714	201.4	1.937
75.0	5.982	4.914	216.1	2.033
77.5	6.162	5.114	231.3	2.129
80.0	6.323	5.312	246.9	2.225
82.5	6.476	5.509	262.9	2.322
85.0	6.623	5.704	279.3	2.419
87.5	6.763	5.898	296.0	2.515
90.0	6.892	6.090	313.1	2.612
92.5	7.016	6.281	330.5	2.709
95.0	7.134	6.470	348.1	2.805
97.5	7.245	6.656	366.1	2.901
100.0	7.351	6.841	384.4	2.998

APPENDIX III continued

T	C_P	S	$H^\circ - H^\circ_0$	$-(G-H^\circ_0)/T$
°K	Cal./Deg.	Cal./Deg.	Cal./Deg.	Cal./Deg.
105.0	7.547	7.205	421.6	3.189
110.0	7.731	7.560	459.8	3.380
115.0	7.905	7.908	498.9	3.569
120.0	8.070	8.248	538.8	3.757
125.0	8.226	8.580	579.6	3.944
130.0	8.373	8.906	621.1	4.128
135.0	8.518	9.225	663.3	4.311
140.0	8.663	9.537	706.2	4.492
145.0	8.806	9.844	749.9	4.672
150.0	8.946	10.144	794.3	4.849
155.0	9.084	10.440	839.4	5.025
160.0	9.218	10.731	885.1	5.199
165.0	9.350	11.016	931.5	5.371
170.0	9.480	11.297	978.6	5.541
175.0	9.608	11.574	1026.3	5.709
180.0	9.734	11.847	1074.7	5.876
185.0	9.856	12.115	1123.7	6.041
190.0	9.974	12.379	1173.2	6.204
195.0	10.090	12.640	1223.4	6.366
200.0	10.202	12.897	1274.1	6.526
205.0	10.312	13.150	1325.4	6.685
210.0	10.420	13.400	1377.2	6.842
215.0	10.526	13.646	1429.6	6.997
220.0	10.630	13.890	1482.5	7.151
225.0	10.732	14.130	1535.9	7.303
230.0	10.831	14.367	1589.8	7.454
235.0	10.928	14.600	1644.2	7.604
240.0	11.023	14.832	1699.1	7.752
245.0	11.117	15.060	1754.4	7.899
250.0	11.211	15.285	1810.3	8.044
255.0	11.304	15.508	1866.5	8.189
260.0	11.394	15.729	1923.3	8.331
265.0	11.482	15.947	1980.5	8.473
270.0	11.569	16.162	2038.1	8.613
273.15	11.623	16.296	2074.7	8.701
275.0	11.654	16.375	2096.2	8.753
280.0	11.737	16.586	2154.6	8.891
285.0	11.819	16.794	2213.5	9.027
290.0	11.900	17.001	2272.8	9.163
295.0	11.980	17.205	2332.5	9.298
298.15	12.030	17.332	2370.4	9.382
300.0	12.060	17.407	2392.5	9.431

APPENDIX IV

THERMODYNAMIC FUNCTIONS FOR $PuC_{0.96}$

T °K	C_P Cal./Deg.	S Cal./Deg.	$H^\circ - H^\circ_0$ Cal./Deg.	$-(G-H^\circ_0)/T$ Cal./Deg.
2.5	0.018	0.009	0.022	0.0
5.0	0.065	0.034	0.126	0.009
7.5	0.157	0.077	0.404	0.023
10.0	0.304	0.141	0.980	0.043
12.5	0.476	0.226	1.955	0.070
15.0	0.672	0.330	3.390	0.104
17.5	0.878	0.449	5.327	0.144
20.0	1.098	0.580	7.797	0.190
22.5	1.337	0.723	10.84	0.241
25.0	1.595	0.877	14.51	0.297
27.5	1.863	1.041	18.83	0.357
30.0	2.136	1.215	23.83	0.421
32.5	2.404	1.397	29.50	0.489
35.0	2.655	1.584	35.83	0.560
37.5	2.900	1.775	42.77	0.635
40.0	3.141	1.970	50.32	0.712
42.5	3.376	2.168	58.47	0.792
45.0	3.601	2.367	67.19	0.874
47.5	3.820	2.568	76.46	0.958
50.0	4.036	2.769	86.29	1.043
52.5	4.248	2.971	96.64	1.130
55.0	4.458	3.173	107.5	1.218
57.5	4.663	3.376	118.9	1.308
60.0	4.865	3.579	130.8	1.398
62.5	5.058	3.781	143.2	1.490
65.0	5.243	3.983	156.1	1.582
67.5	5.426	4.185	169.4	1.674
70.0	5.600	4.385	183.2	1.768
72.5	5.779	4.585	197.5	1.861
75.0	5.939	4.783	212.1	1.955
77.5	6.118	4.981	227.2	2.050
80.0	6.280	5.178	242.7	2.144
82.5	6.432	5.373	258.6	2.239
85.0	6.580	5.568	274.8	2.334
87.5	6.720	5.761	291.5	2.430
90.0	6.852	5.952	308.5	2.525
92.5	6.976	6.142	325.8	2.620
95.0	7.096	6.330	343.4	2.715
97.5	7.210	6.515	361.2	2.810
100.0	7.319	6.699	379.4	2.905

APPENDIX IV continued

T °K	C_p Cal./Deg.	S Cal./Deg.	$H^\circ - H^\circ_o$ Cal./Deg.	$-(G-H^\circ_o)/T$ Cal./Deg.
105.0	7.522	7.061	416.5	3.095
110.0	7.714	7.416	454.6	3.283
115.0	7.894	7.763	493.6	3.470
120.0	8.067	8.102	533.5	3.656
125.0	8.232	8.435	574.3	3.841
130.0	8.388	8.761	615.8	4.024
135.0	8.541	9.080	658.1	4.205
140.0	8.693	9.394	701.2	4.385
145.0	8.842	9.702	745.1	4.563
150.0	8.989	10.004	789.6	4.739
155.0	9.132	10.301	834.9	4.914
160.0	9.273	10.593	881.0	5.087
165.0	9.409	10.881	927.7	5.258
170.0	9.545	11.163	975.0	5.428
175.0	9.681	11.442	1023.1	5.596
180.0	9.816	11.717	1071.9	5.762
185.0	9.940	11.987	1121.2	5.927
190.0	10.060	12.254	1171.2	6.090
195.0	10.175	12.517	1221.8	6.251
200.0	10.286	12.776	1273.0	6.411
205.0	10.398	13.031	1324.7	6.569
210.0	10.507	13.283	1377.0	6.726
215.0	10.615	13.532	1429.8	6.882
220.0	10.720	13.777	1483.1	7.036
225.0	10.825	14.019	1537.0	7.188
230.0	10.926	14.258	1591.3	7.339
235.0	11.026	14.494	1646.2	7.489
240.0	11.125	14.727	1701.6	7.637
245.0	11.220	14.958	1757.5	7.784
250.0	11.315	15.185	1813.8	7.930
255.0	11.407	15.410	1870.6	8.075
260.0	11.495	15.633	1927.9	8.218
265.0	11.584	15.853	1985.5	8.360
270.0	11.672	16.070	2043.7	8.501
273.15	11.726	16.205	2080.6	8.589
275.0	11.758	16.285	2102.3	8.640
280.0	11.842	16.497	2161.3	8.779
285.0	11.926	16.708	2220.7	8.916
290.0	12.008	16.916	2280.5	9.052
295.0	12.090	17.122	2340.8	9.187
298.15	12.142	17.251	2379.0	9.271
300.0	12.173	17.326	2401.4	9.321